DOE/SF/10802-1

ECONOMIC ANALYSIS OF THE UNIFIED HELIOSTAT ARRAY

Final Technical Report

January 31, 1981

Work Performed Under Contract No. AC03-80SF10802

Veda Incorporated
Camarillo, California

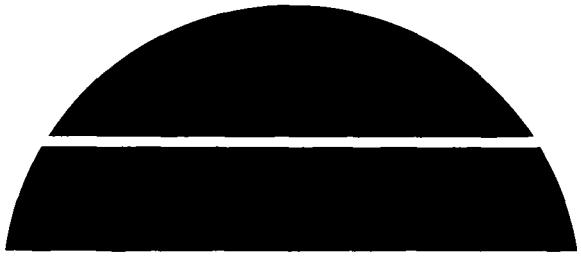

U.S. Department of Energy

Solar Energy

DISCLAIMER

Available from the National Technical Information Service, U. S. Department of Commerce, Springfield, Virginia 22161.

Price: Printed Copy A19
Microfiche A01

DOE/SF/10802-1
Distribution Category UC-62d

VEDA REPORT 43905-80U/P0069

ECONOMIC ANALYSIS OF THE UNIFIED HELIOSTAT ARRAY

Prepared by:

VEDA INCORPORATED
400 N. Mobil, Bldg. D
Camarillo, CA 93010

31 January 1981

Under Contract Number
DE-AC03-80SF10802

Prepared for:

Department of Energy
1333 Broadway
Oakland, CA 94612

TABLE OF CONTENTS

TABLE OF CONTENTS CONT'D

LIST OF ILLUSTRATIONS

LIST OF ILLUSTRATIONS CONT'D

LIST OF TABLES

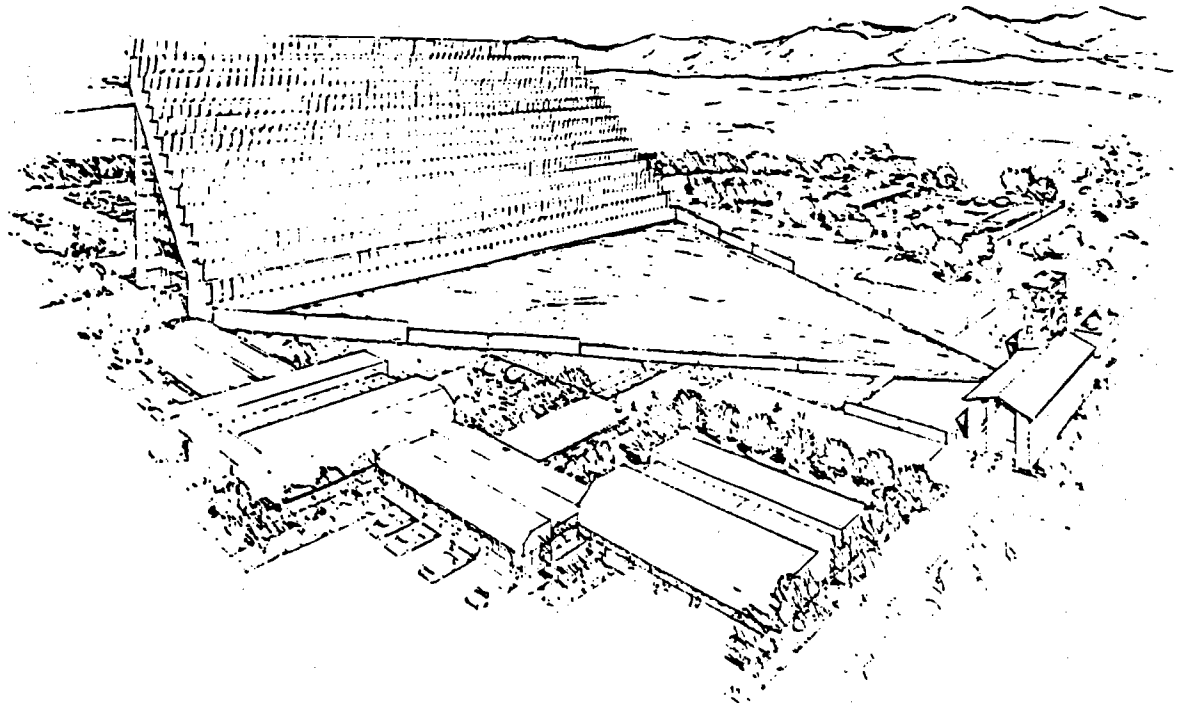

Figure 1-1. Typical Unified Heliostat Array (Artist's Concept).

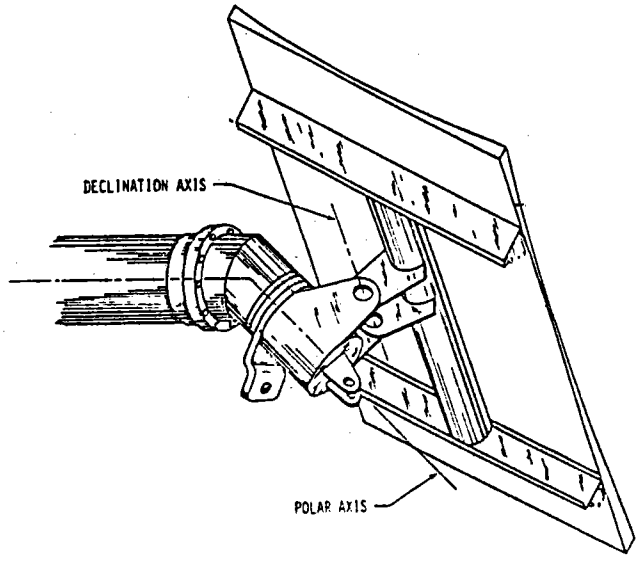

Figure 1-2. Veda Industrial Heliostat.

SECTION 1.0

EXECUTIVE SUMMARY

Title: Economic Analysis of the Unified Heliostat Array

Contract Number: DE-AC03-80-SF10802

Contract Price: $96,300

1.1 INTRODUCTION

The Unified Heliostat Array (UHA) is an arrangement of heliostats located on the south facing wall of a terraced structure. Previous investigations of heliostat fields have been devoted to the horizontal field arrangement. Whereas the horizontal field requires that the central receiver be located high above the heliostat field, the UHA configuration permits locating the central receiver at a lower height than most of the heliostats. Since locating an industrial process at the top of a tower, or transporting power down the tower to the process may not be feasible, the UHA concept extends central receiver technology to processes not previously considered candidates for solar thermal energy. The UHA concept is illustrated in Figure 1-1.

In addition to the UHA, Veda has introduced the concept of the Veda Industrial Heliostat (VIH). The VIH combines a toroidal mirror and an equatorial drive mechanism to minimize the daily and annual excursions of the tangential and sagittal foci at the central receiver aperture plane. By proper choice of radii of curvature and shape factor for the mirror, the same mirror configuration is used for all heliostats on a UHA designed for a given power level. The VIH provides a very uniform, relatively small, high intensity image at the receiver throughout the day and year. Use of the VIH further expands the

use of solar thermal technology to applications which require high temperature (above 1000°K) and high flux densities (greater than 1 MW/m^2). An artist's conception of the VIH is shown in Figure 1-2.

1.2 PROJECT DESCRIPTION

1.2.1 Purpose

The purpose of this project was to develop a first approximation of the cost of energy delivered to the aperture of a receiver located at the focal zone of the UHA. The cost of energy was evaluated in terms of a levelized charge over the UHA lifetime. In order to provide a data base, the costs were evaluated using a range of economic parameters, a range of working temperatures, three power levels and two types of heliostats.

1.2.2 Scope of Effort

This effort covered four major activities.

1. Development of a design specification for the UHA including operational environment, survivability criteria, size, heliostat loading and maximum deflection criteria.

2. Conceptual designs and capital cost for the UHA structure including engineering services, site preparation, materials, labor, maintenance, and structure salvage value.

3. Analysis of the optical performance of the heliostats mounted on the UHA including selection of spillage criteria and aperture size, distribution of the energy across the aperture and flux density contours, and energy collected for a nominal 330 day operational year.

4. Development of a levelized cost of energy and cost of usable energy at several working temperatures.

1.2.3 Limitations

Time and cost constraints of the project did not permit an analysis of a complete system. Specifically, the characteristics of the receiver and the plant or process were excluded from the analysis. The receiver was treated as a two-dimensional aperture and thermal losses were restricted to black body radiation losses from an area equivalent to that of the aperture at the assumed working temperature. Losses due to convection and conduction, which are present in any real receiver, were not considered.

The conceptual designs for the UHA structures were developed only for heliostat support within the design specification. Designs which allow other uses such as housing part of the process plant, warehouse space or office space, were beyond the scope of this study. Similarly, time and cost constraints of the project did not permit evaluation of more than one structural type. It is felt that less costly structural designs could be found to meet all of the requirements of the specification.

1.3 TECHNICAL APPROACH

1.3.1 Design Specification

The design of the UHA conceptual structures required the development of a design specification. In order to make maximum use of existing data, prior Department of Energy (DOE) specifications for central power project horizontal fields and heliostat characteristics were reviewed for applicability. Environmental conditions, including insolation data for Barstow, California, and soil characteristics prevalent at the solar facility in Albuquerque, New Mexico, were used. Industrial standards and building codes were also reviewed for their applicability.

The design specification related the location of heliostats, clearances required for operation, environmental considerations, the loads imposed by the heliostats on the UHA structural members, and the tolerances permissible in order to remain within the central receiver system horizontal collector field error budget.

1.3.2 Structural Design and Modeling

Bechtel National, Incorporated was charged with the design and cost evaluation of the UHA structures that best met the specification. Since the structures were not required to house any activity, but were solely for heliostat support, the choice of an open steel framework with concrete foundations was made as being the approach promising least cost. Based on a preliminary loads analysis, nine preconceptual designs for three power levels and three aspect ratios were developed to the extent that a relative cost determination could be made. Comparison with the performance calculations made by Veda Incorporated resulted in the choice of an array aspect ratio of 1:5, i.e., the height is one-fifth of the east-west length of the structure.

Once the aspect ratio had been chosen, more detailed evaluations were conducted. The simple design was modulated to evaluate cost effects of different distributions and sizes of structural members. The Structural Design Language (STRUDL) computer program was used for determining stresses and rotations. As a result, the preconceptual designs were modified to reduce cost. In three designs the VIH, an equatorially mounted heliostat having a mirror area of six square meters, was assumed. In the fourth design the 49 square meter repowering heliostat was assumed. Due to the difference in heliostat design, a different structural design plan was required.

1.3.3 Heliostat Performance Modeling

The optical performance of the UHA configurations was calculated by Veda Incorporated on a Data General Eclipse C/350 digital computer. The performance code, previously developed in-house by Veda, is a set of programs written in FORTRAN 5 which simulates the optical performance for any heliostat type and field geometry. The theory and methodology for these programs are detailed in Veda document 44112-80U/Q0401-3, "Methodology for Optical Performance Analysis," which is contained for reference purposes in Appendix C. For this study, the following assumptions were made: (1) the 1976 Barstow, California insolation data base applied; (2) mirror reflectivity was 0.9; (3) atmospheric transmittance was 0.99; (4) the receiver height was 8 meters; and (5) design point was local noon of the winter solstice. Design point, in current DOE practice, is the time of day and year when the highest efficiency of solar energy collection occurs. For the UHA, highest efficiency for the low receiver occurs at local noon of the winter solstice.

Preliminary computer runs were made to determine heliostat spacing such that shading and blocking were reasonably minimized without excessive enlargement of the structures. Based on this spacing, runs were made to determine the number of heliostats required to meet the power levels for the design point. The results of this analysis were used to size the UHA structures for the design specification. A second set of runs was then made to determine the effect of UHA aspect ratio on the amount of energy collected. The variation was only a few percent which, in conjunction with the preconceptual design costing values, led to the selection of the 1:5 aspect ratio for the detailed analysis.

Using the geometry for the 1:5 aspect ratio, detailed optical performance was calculated for each UHA. Cosine, shading, and blocking factors were developed for each heliostat. The energy delivered to the aperture was developed using a normal distribution of heliostat tracking error based on the maximum error of ± 3.0 milliradians. Flux density across the receiver face and flux contours were calculated each hour from 0700 to 1700 for equally spaced days at approximately two week intervals. The annualized energy was then developed assuming a nominal 330 day operational year.

1.3.4 Economic Analysis

The methodology of ERDA/JPL-1012 76/3 was used insofar as applicable. The intent of this methodology is to develop a levelized charge for the energy output over the system lifetime, including a return on investment to stockholders and creditors. Escalation rates of 6%, 8%, and 10%, and cost of capital rates of 8%, 10%, and 15% were used to develop a cost of energy matrix. The annualized energy charge divided by annualized energy entering the aperture is defined as cost of energy. The term "usable energy" has been used to describe recoverable energy at temperatures of 1000°K and above. Only reradiation losses were considered as these are essentially uncontrollable and dominate the losses at these temperatures. Annualized energy charge divided by usable energy is defined as cost of usable energy.

In this methodology a fixed charge rate to generate all expenses is developed. Earning rate of retained capital, equal to the cost of capital rate, helps to provide the funds for the Operations and Maintenance (O&M) expenditures over the system life. It is further provided that the fund established by this fixed charge will pay the return on investment and also recover the capital expended prior to first year of commercial operation.

Although this is a required methodology for public utilities, an industrial energy user would probably not use this approach. Instead, operation and maintenance costs would be added into the cost of the product during the period in which they were incurred. The amortization and cost of capital would be the same in either case. Where the utility charge would be constant, the industrial user charge would be variable, lower than the levelized charge amount at the outset and higher than that after some point in the system life.

The latter approach to analyzing the costs of usable energy was proposed as an additional effort. However, budget constraints did not permit this analysis under this contract. This type of analysis would be significant for the envisioned applications of the UHA.

1.4 RESULTS

1.4.1 Structural

An open frame steel truss and beam structure was designed to hold the heliostats. Concrete foundations were used. Mounting methods for the two heliostats were different, requiring two different support methods. The level of detail of the final conceptual designs included stairs, walkways, and wiring. Analysis showed that wind load survival considerations placed a greater stiffness requirement on the structure than that required to meet the heliostat deflection criteria when the VIH is used. Variations in internal bracing may result in nearly equalizing the loads resulting a lower cost structure. The repowering heliostat design may require additional structural material to meet deflection criteria. The designs are such that steel is essentially pre-cut

and fabricated at a factory and assembled on site. No unusual materials, processes, or skills are expected to be required. The longer and lower structure for a given power level is the least expensive of the designs investigated.

1.4.2 Optical Performance

Four UHA designs were analyzed. Three design point power levels of 1, 10, and 25 MWt were used with the Veda Industrial Heliostat (VIH) design. Only the 10 MWt design point power was analyzed with the repowering heliostats.

The VIH provides a very small, very uniform image at the aperture plane. Nearly half the power is supplied into a central zone where the flux is at least 70% of peak and whose area is about 25% of the design point aperture area. At the 10 MWt level, the largest image of the VIH system is smaller than the smallest image using the repowering heliostat. This results in lower reradiation losses and more usable energy at higher temperatures when the VIH is used, since the receiver aperture may be much smaller than that required in order to capture the same amount of energy when using the repowering heliostat.

Selecting aperture dimensions to meet design point criteria with minor spillage resulted in aperture sizes having about 2-3% annualized spillage for the VIH. Larger spillage, about 6%, was encountered with the aperture chosen for use with the repowering heliostat. Because of the diffuse image produced by the repowering heliostat, this large spillage was necessary in order to achieve reasonable high temperature efficiency. In order to reduce reradiation losses, apertures smaller than design point apertures were analyzed. Although the smaller apertures resulted in increased spillage, the dramatic

reduction in reradiation losses lowered the cost of usable energy in the high temperature region (above 1000°K). Since the image of the sun produced by the UHA is essentially circular and current receiver designs are often rectangular, both rectangular and circular apertures were investigated. While the circular aperture leads to a slight increase in spillage in order to capture only the high flux section of the image, it results in the minimum aperture area and the least reradiation loss for a given temperature. A multiple aperture receiver design, such as a receiver with concentric apertures which would utilize the added spillage to provide process preheating or steam, is suggested as an area for further investigation.

The high flux density achievable using the UHA and VIH, even in small collector fields, makes a significant percentage of the collected energy usable at temperatures above 1500°K. Even the 1 MWt UHA-VIH configuration produced average flux densities in excess of 1 MWt/m^2 within an aperture of 0.3 meters radius for a significant part the year. If a pressurized optical window is required on the receiver, this may be near the optimum module size. The 10 MWt UHA-VIH configuration performed similarly for an aperture of 1.3 meters radius, and the 25 MWt-VIH configuration provided the same performance within an aperture radius of 2 meters. By comparison, the 10 MWt UHA using the repowering heliostat was unable to achieve 1 MWt/m^2, even at peak intensity at the design point.

1.4.3 Cost of Energy

At temperatures below 811°K (1000°F) selective coatings may be used to reduce reradiation losses from receivers to a small percentage of that which would occur without such a surface preparation. It is assumed that any receiver

operating in this temperature range as a heat exchanger from radiant to thermal energy would have such a coating and reradiation could be neglected. No specific receiver was designed for this project and there is no large data bank on conductive and convective loss factors that would be suitable for estimating this type of loss for receivers suitable for use with the UHA. Therefore, there was no requirement for evaluating these losses. "Cost of Energy" thus refers to a lossless receiver operating at or below 811°K, and having an aperture capturing about 95-98% of the available energy from the heliostat arrays.

The cost of energy was determined by dividing the levelized annual charge by annual energy collected. The ratio of O&M costs to capital costs varies with the UHA selected and the escalation and cost of money rates. The extreme values of the cost of energy for each of the UHA designs is shown below in dollars per million BTU.

UHA	Heliostat	Low Cost of Energy	High Cost of Energy
1 MWt	VIH	42.54	60.55
10 MWt	VIH	28.81	48.15
10 MWt	Repowering	26.78	44.89
25 MWt	VIH	31.66	57.13

O&M costs dominate the cost of energy for the 1 MWt system, and costs of the structure associated with increasing height dominate the cost of energy for the 25 MWt design. The 10 MWt designs were the most cost effective. The configuration with the repowering heliostat was the least expensive due to a lower structural cost. However, this did not hold true at the higher temperatures.

1.4.4 Cost of Usable Energy

At temperatures where selective coatings are no longer effective, the term "usable energy" is used to express the amount of energy available for a process after considering reradiation losses. Since reradiation is a linear function of area and a fourth power function of temperature, operation at high temperatures implies large losses. To minimize losses, the size of the aperture must be kept as small as possible consistent with energy capture capability. For any particular working temperature there is a most cost effective aperture size for the given collector field.

For this part of the cost analysis both working temperature and aperture size were varied for each array. Because of the complex interactions of these variables with the cost parameters, no simple summary of the results is possible. In the body of the report there are graphs relating most cost effective aperture size for a given working temperature of the receiver. These graphs are derived by smoothing between the step wise changes in aperture size investigated. The table below uses preferred aperture sizes for the indicated temperature, and does not represent the performance of one particular aperture. For details on particular apertures, it is suggested that the reader use the data tables of Appendix E. Costs of usable energy are given in terms of dollars per million BTU at the indicated temperature.

UHA	Heliostat	Temperature in Degrees Kelvin			
		1000	1250	1500	1750
1 MWt	VIH	50.07	66.87	131.97	212.82
10 MWt	VIH	33.36	41.09	58.98	108.83
10 MWt	Repowering	32.22	46.72	75.12	258.35
25 MWt	VIH	36.12	44.09	62.50	115.80

The effect of diffuse imaging by the repowering heliostat is already apparent at 1000°K, although there is still a lower cost due to the lower initial capital cost of its supporting structure. As the working temperature increases to 1250°K, even the initial cost differential is overshadowed by the lower system efficiency. It is emphasized that this efficiency shift is due to the difference in heliostat characteristics.

1.5 CONCLUSIONS AND RECOMMENDATIONS

This study showed that the UHA concept can deliver solar thermal energy to a receiver conveniently located for most practical processes. This provides a potential expansion of central receiver technology to applications not previously considered candidates. This is particularly true for processes which involve large quantities of solid material, such as coal, where transporting the material to the top of a tower may be neither cost-effective nor even possible. In addition, supplying high power through a pressurized window will be more easily handled with the VIH. Optimization of window, process technology, and collector field will involve many tradeoffs to determine the best approach.

The structural concepts developed were shown to be cost-sensitive to site peculiar conditions, such as wind and soil, and heliostat type and spacing. Therefore, accurate costing for a particular application must include the specific environmental factors at the application site and an optimized spacing of the heliostats.

The UHA, in combination with the VIH, produces a solar image which is consistent in size, shape and flux distribution throughout the day and year.

Most of the power is delivered at a nearly constant flux density within a small central zone outside of which there ia a very rapid decay of flux density. In contrast, the repowering heliostat/UHA combination produces a distributed diffuse image which is highly variable in size and flux density throughout the day and year.

Because of its superior image quality, the UHA-VIH combination makes possible the utilization of a small aperture with high average flux for high temperature processes. The small aperture size results in high efficiency in the 1200°K to 2000°K temperature range. A substantial portion of the power from an array as small as the 1 MWt is usable in this range. These characteristics place the UHA concept in the power/temperature gap between the point focus tracker and the surround field and offer the potential expansion of solar thermal technology to applications previously not considered candidates. The findings of this study support the following specific recommendations for further study.

- Perform a heliostat spacing optimization study to determine the improvements in optical performance and assess potential cost reduction due to reduced land requirements and decrease in structure size.
- Conduct a structural study to determine expected cost deltas for upgrading structures, which are primarily designed for other purposes, to include supports for heliostats.
- Perform a study of several candidate processes that could benefit from central receiver technology and the type of high quality energy provided by the UHA-VIH system. The study would develop power/temperature/time profiles for the processes to assess the applicability of solar thermal power and potential fuel savings.

- Perform a detailed feasibility study to determine specific cost tradeoffs between various solar collection technologies for one of the industrial processes identified in the process profile study.

- Develop and field test a prototype of the Veda Industrial Heliostat to verify optical performance and production techniques.

SECTION 2.0

INTRODUCTION

2.1 BACKGROUND

It is well recognized that solar energy penetration of the market for high temperature process heat is extremely difficult. In this market, high temperatures generally go hand-in-hand with high heat rates. Although the tracking parabolic solar energy collector is capable of providing the highest temperatures, it is heat rate limited by the mechanical constraints of the individual collectors. Use of the tracking parabolic concentrator also requires the thermal load to move with the concentrator causing a constant change in orientation which presents serious technical problems for many high temperature processes. Additionally, for very high temperatures, piping material and joint technology preclude the transfer of heat to a fixed process location. These considerations place severe restrictions on the adaptation of this technology to the current marketplace.

An alternative concept is a fixed central receiver located at the focal zone of a heliostat array. A typical configuration is illustrated in Figure 2-1. While the central receiver concept has a lower peak temperature capability than the parabolic concentrator, it provides significantly higher heat rates to a central load. The characteristics of a specific application will dictate which concept is most efficient, but, in general, DOE studies have shown that the central receiver is the best candidate for current industrial applications in the 10 MWt region and higher. However, the central receiver concept does have limitations that restrict its use for a number of potential applications.

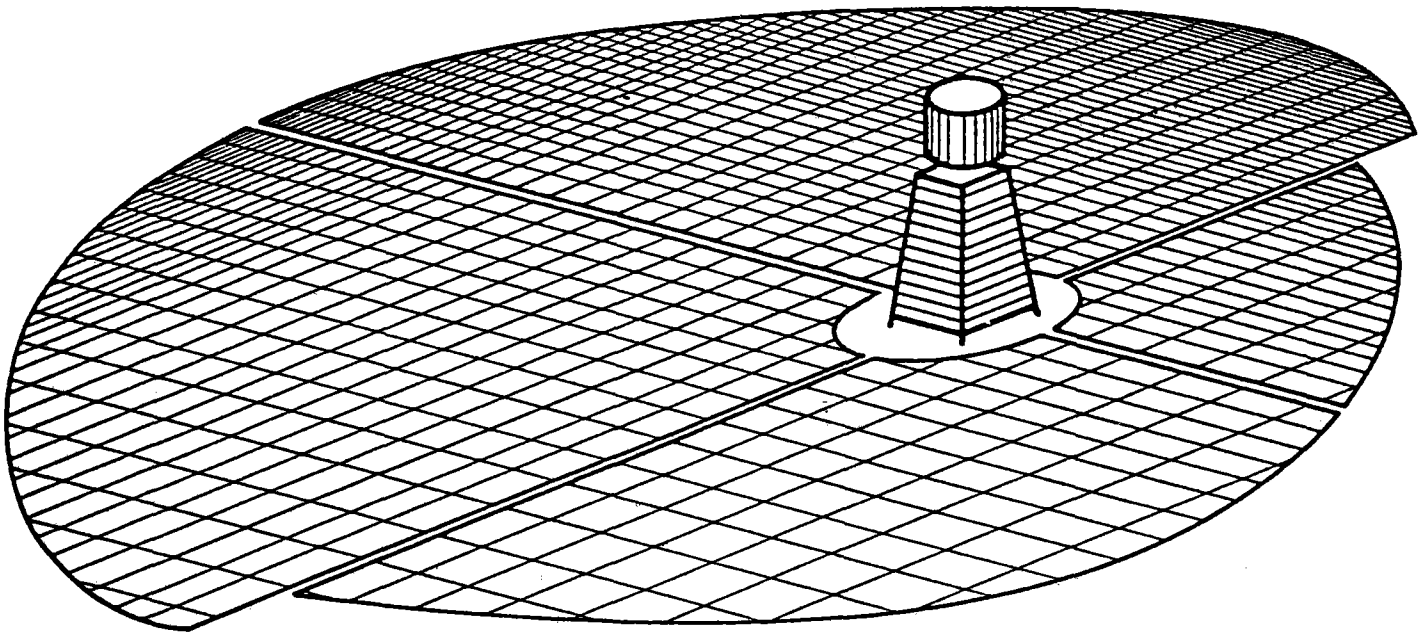

Figure 2-1. Typical Horizontal Field Configuration.

Most of the limitations are related to the size of the heliostat field, the height of the receiver, and uniformity of image size throughout the day and year. Present central receiver designs require the dedication of large land parcels for the heliostat field. The quantity of land required, and its geometry with respect to the receiver location, pose severe obstacles for incorporating the system into urban or suburban areas where the majority of potential industrial users are currently located. In the current system, the focal zone is located above the heliostat field. This requires that the receiver be located at the top of a tower. It is difficult and expensive to operate most industrial processes at such a location or to transport the heat through an intermediate medium to ground level. It would be better to operate the process at a convenient location and move the focal zone to that process. To alleviate the problems of dedicated land usage, receiver height, and improved quality of the solar image, Veda has introduced the concept of the Unified Heliostat Array.

2.1.1 Unified Heliostat Array

The Unified Heliostat Array (UHA) is comprised of conventional two-axis heliostats mounted on a terraced south facing wall of a single structure. The terraces are aligned in an east-west direction and the heliostats are affixed to the terraces by pedestal mounts. In the earth's north latitudes, the terrace steps are upward towards the north and the receiver is situated south of the structure. The UHA concept is illustrated in Figure 2-2.

The arrangement of heliostats on the array is chosen to eliminate or control the degree of inter-heliostat shading and blocking. Shading and blocking, the width of the terrace step, the height of the terrace riser, and

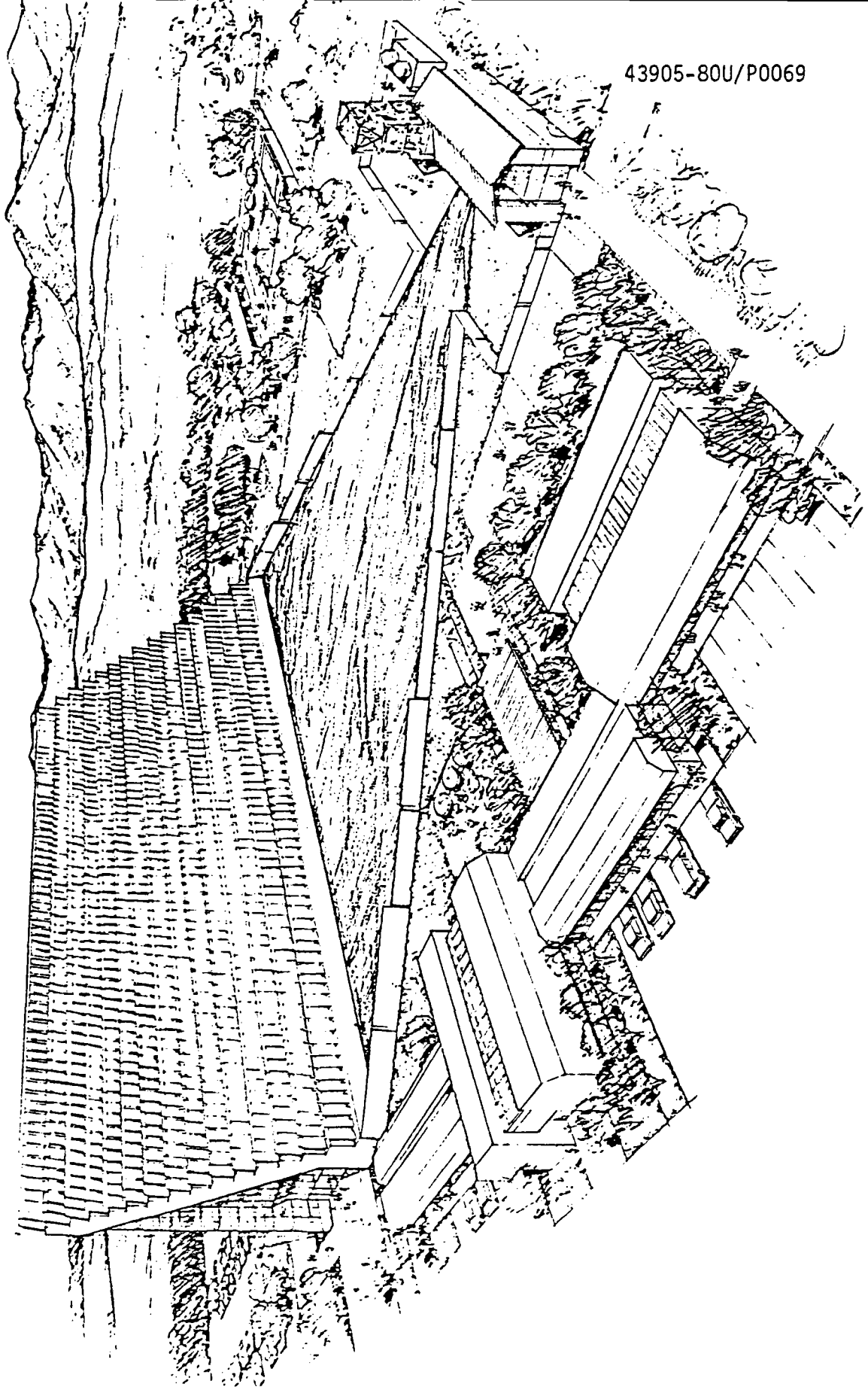

Figure 2-2. Typical Unified Heliostat Array (Artist's Concept).

the spacing of heliostats along the terrace, are a function of heliostat size and drive mechanism. The mounting pedestal may be either vertical or horizontal. Precision alignment of the heliostat is done at each individual pedestal. By allowing moderate early morning and late evening shading, a heliostat density of about 0.6 will allow the UHA to collect 2 MWt power for each acre of land used.

At latitude 35° the sun altitude angle is less than 15° for more than one hour after sunrise and for more than one hour prior to sunset. At a sun altitude angle of 15° the horizontal field is still partially shaded. Thus, the working day of the horizontal field at winter solstice is limited to about six hours, but extends to about ten hours at the equinox and to twelve hours at summer solstice. By comparison, early morning and late afternoon shading of the UHA is worst between equinoxes and summer solstice, but at winter solstice, shading and blocking losses are essentially zero whenever the sun is above the horizon. At times of the year near winter solstice, while the sun is still below 10° altitude, the power delivered to the receiver aperture by the UHA is greater than 50% of the power delivered to the aperture at local noon. Thus, the working day of the UHA, almost ten hours in length at winter solstice, varies only a few tenths of an hour between winter and summer solstices.

For an industrial process heat user the constant length day is an advantage in the form of personnel and process scheduling. Since the UHA can be designed to provide a nearly constant energy collection for any clear day throughout the year, the industrial user can plan on a nearly uniform process flow.

For remote locations, the potential hazards posed by the UHA would be no greater than those associated with the horizontal field. However, constructing a UHA in an urban environment would require a safety analysis. A receiver at ground level will require shielding to protect structures and activity in the near vicinity. Actual safety requirements would be very site specific and would have to be addressed as part of a particular applications study.

The reflected energy may be directed to any location above, below, or to either side of the UHA north-south centerline. Its versatility permits a single UHA to provide energy to one or more receivers appropriately located to meet the users needs. This array is readily adapted to a range of processes and brings the benefits of central receiver technology to a wide variety of industrial applications.

2.1.2 Veda Industrial Heliostat

While the UHA is capable of supporting any heliostat type, Veda has introduced a new heliostat design to improve overall system efficiency. The UHA naturally lends itself to a north facing receiver. The efficiency of such receivers can be increased by reducing the area through which thermal losses occur. Since most thermal losses occur at the aperture through which, or onto which, the solar energy enters the receiver, efficiency is most readily increased by minimizing the aperture size. The limiting factor in reducing aperture size and maintaining an acceptable spillage level is related to the optical concentration capability of the individual heliostats in the collector field. Increasing the optical concentration of a heliostat requires that a focusing mirror unit be used.

Heliostats for central receiver systems must track to large off-axis angles of sun position. Under these conditions the formation of a solar image at the normal focal distance of a spherical or parabolic mirror is a rarity, rather than a normal occurrence. Instead of a circular spot, two elliptical images are formed at foci which separate in opposite directions from the on-axis focal distance as the off-axis tracking angle increases. These image aberrations, due to the sagittal and tangential foci shifts, have been studied experimentally (c.f. Ref. 1) and are illustrated in Figures 2-3 and 2-4.

In Figures 2-3 and 2-4, the "Chief Ray" is the central ray of a bundle of parallel rays emanating from a point source. This ray forms an angle "a" with the mirror normal. The angle a is the off-axis tracking angle. In Figure 2-3, the sagittal focal line is perpendicular to the sagittal ray fan and is formed at a distance from the mirror surface that is proportional to F/cos a, where F is the on-axis focal distance. In Figure 2-4, the tangential focal line is perpendicular to the tangential ray fan and is formed at a distance from the mirror surface that is proportional to F cos a. Thus, when a = 0°, the distance from the mirror surface at which these two images are formed are the same. As a increases in magnitude the two images diverge. This divergence can be controlled by changing the value of F for mutually perpendicular directions on the mirror surface.

The shift in the two foci results in an image size and shape at the aperture plane which fluctuates as a function of time of day and time of year. To minimize this effect, and thus minimize the required aperture size, it is necessary to cause the excursion of each focused solar image to center around the receiver distance. Since the sagittal and tangential

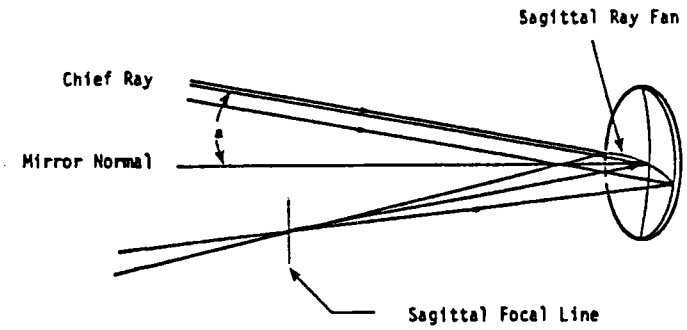

Figure 2-3. Sagittal Focus.

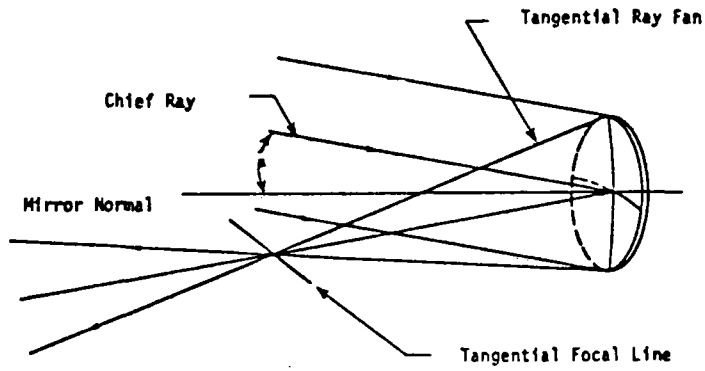

Figure 2-4. Tangential Focus.

images are formed at right angles to each other, it is possible to choose two orthogonal radii of curvature for the mirror surface to achieve this effect. The resultant surface is that of an outer segment of a toroid. This surface is shown in Figure 2-5.

A secondary effect of off-axis tracking is that the two images rotate about the reflected ray vector as a function of the space orientation of the plane of the off-axis angle. In order to preserve the proper orientation of the mirror surface to the plane formed by the incident and reflected rays, and to minimize aberrations, an equatorial axis drive mechanism is used in place of the azimuth-elevation system encountered in other heliostat designs. As applied to a heliostat, the polar axis is inclined by the local latitude angle from the horizontal in the meridian plane. The declination axis is affixed to and rotates about the polar axial direction. The heliostat mirror element is affixed to and rotates about the declination axis. Thus, the mirror surface achieves two axis tracking while maintaining the proper orientation. This configuration is shown in Figure 2-6.

Another element of the heliostat to be considered is mirror size. The maximum image size, and hence aperture size, for a properly figured toroidal heliostat is controlled by two functions, solar angular diameter and heliostat dimensions. The mirror surface dimensions may be adjusted to make the maximum lengths of the tangential and sagittal images equal to the same value. This results in the smallest image obtainable from a given heliostat which, in turn, results in the smallest aperture.

These elements of heliostat design: toroidal segment, equatorial mount, and optimized mirror dimension ratio have been combined by Veda to

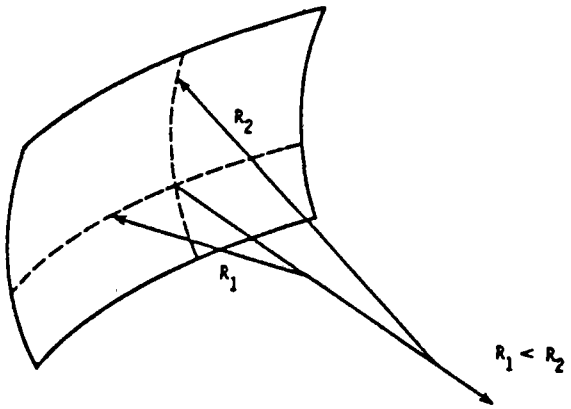

Figure 2-5. Toroidal Segment Mirror Surface.

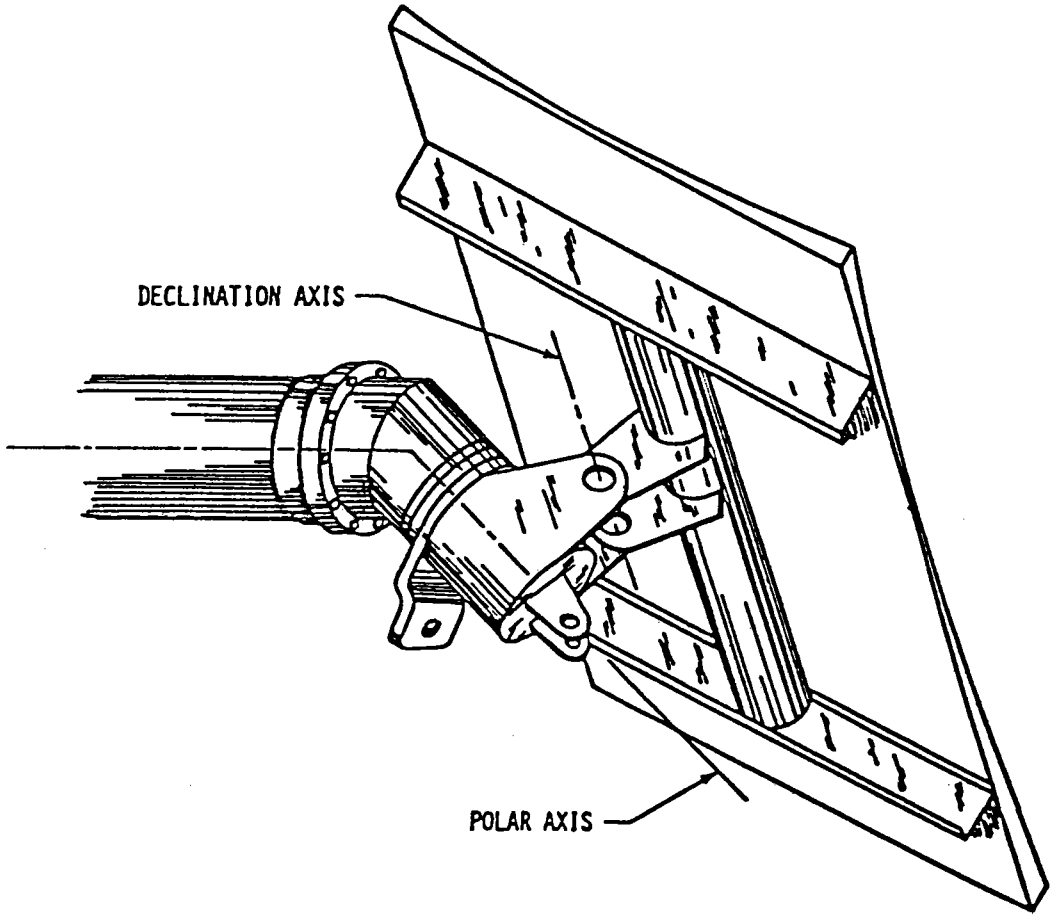

Figure 2-6. Veda Industrial Heliostat.

form a unique heliostat design. This design is the Veda Industrial Heliostat (VIH). The VIH produces an average flux density at the receiver aperture that is greater than that produced by any other heliostat currently under study for horizontal fields, and permits the use of the smallest aperture for a given amount of energy collected.

2.2 PROJECT OVERVIEW

2.2.1 Purpose

The heliostat field described above as the Unified Heliostat Array (UHA) is one of the class of heliostat fields applicable to central receiver projects. There has been no prior cost analysis made of this type of field. The purpose of this project is to develop a first approximation to the cost of energy delivered to the aperture of a receiver located at the focal zone of the UHA. The cost of energy will be evaluated in terms of a levelized charge over the UHA lifetime. In order to provide a data base permitting meaningful comparisons within a system context, the costs are evaluated in terms of both quantity and quality of the energy at the central receiver aperture for three power levels and two types of heliostats.

2.2.2 Scope of Effort

This effort covered four major activities:

1. Development of a design specification for the UHA including operational environment, survivability criteria, size, heliostat loading, and maximum deflection criteria.

2. Conceptual designs and capital cost for the UHA structure, including engineering services, site preparation, materials, labor, maintenance, and structure salvage value.

3. Analysis of the optical performance of the heliostats mounted on the UHA, including total energy delivered to

an aperture, selection of spillage criteria and aperture size, distribution of the energy across the aperture and flux density contours, and energy collected for a nominal 330-day operational year.

4. Development of a levelized cost of energy and cost of usable energy at several working temperatures, including capital costs of the structure and heliostats, maintenance cost, salvage value, and annualized energy collected.

2.2.3 Limitations

For electric utilities, it is desirable to evaluate the cost of energy in terms of a levelized charge over the system lifetime. This approach is used, but time and cost constraints of the project did not permit an analysis of a complete system. Specifically, the characteristics of the receiver and the plant or process that it drives are excluded from the analysis. The industrial user will probably not use a levelized cost methodology. The receiver is treated as a two dimensional aperture. Thermal losses are restricted to black body radiation losses from an area equivalent to that of the aperture at the assumed working temperature. Losses due to convection and conduction, which are present in any real receiver, are not considered.

The conceptual designs for the UHA structures were developed only for heliostat support within the design specification. Designs which allow other uses, such as housing part of the process plant, warehouse, or office space, are beyond the scope of this study. Likewise, due to budget constraints, other structural designs, which would result in different quantities of material and labor, were not investigated. The resultant costs of the system are, therefore, not minimized, nor is the optical performance maximized, both of which would reduce the price of the solar energy delivered.

SECTION 3.0

PROJECT DESCRIPTION

3.1 PROJECT ORGANIZATION

The project was divided into six technical tasks. This facilitated the management of the overall project and the orderly progression from UHA design specification, through several parametric designs, to the development of cost of energy for the final designs. The optical analysis and cost of energy tasks were performed by Veda Incorporated. The structure design tasks were performed by Bechtel National, Incorporated. These tasks are described in this section.

3.2 UHA DESIGN REQUIREMENTS

In order to develop structural concepts and preconceptual structure designs for the UHA, the design requirements had to be developed. These requirements were translated into a design specification which satisfied both general and site specific criteria for the conceptual designs of the parametric UHA cases. The criteria included:

- Geographic site, soil conditions, and seismic zone
- Insolation
- Wind and wind rise rates for operation and survivability
- Temperature
- Lightning
- Rain and hail
- Snow and ice loadings
- Structure dimensions

- o Heliostat weight, dimensions and aerodynamic loading
- o Allowable heliostat deflections

The estimates included heliostat spacing and quantities required. Appropriate materials and manufacturing standards and building codes were included by reference to form the specification.

3.3 PRECONCEPTUAL DESIGNS

Using the design specification as a basis, UHA candidate designs were developed. A variety of design concepts and materials were examined for suitability and cost. A low cost approach using open steel beam and truss construction was selected for the preconceptual UHA parametric designs. Candidate designs were developed for three power levels corresponding to peak winter design point power levels at the aperture of the receiver of 1, 10, and 25 MWt. For each power level three structures were designed with height to length aspect ratios of 1:1, 1:3, and 1:5. This resulted in nine preconceptual UHA designs.

The nine structures were designed to support the VIH. Additionally, for the 10 MWt structure, the designs were modified to support the 49 m^2 repowering heliostat developed by McDonnell Douglas.

Relative cost estimates for the nine preconceptual designs were developed for the purpose of establishing the effect of aspect ratio on total structure cost. The elements considered at this level of design were direct field and indirect field costs. The direct field cost encompassed materials, excluding wiring and auxiliaries, fabrication and labor. The indirect costs were composed of temporary construction facilities, construction equipment and service, and field office cost.

3.4 PRELIMINARY OPTICAL PERFORMANCE

For each of the nine structural designs, the optical performance of the UHA was modeled. Calculations were made of the relative annual collected energy and of characteristics of the energy, in terms of spot size and flux density, for all nine cases using the VIH. Additionally, the three aspect ratios for the 10 MWt power level were calculated using the 49 m^2 repowering heliostat design.

The primary purpose of this effort was to determine the effect of aspect ratio on total energy collected. Using the results of the preliminary optical performance and the estimated structural capital costs, a single aspect ratio, showing the highest performance to cost ratio, was selected for more detailed analysis.

3.5 CONCEPTUAL DESIGNS

Using the preferred aspect ratio determined in the above analysis, detailed conceptual designs were developed to a level of detail to include site preparation, foundation, structure, heliostat support attachments, wiring, and essential auxiliaries, such as stairways and platforms.

Conceptual capital cost estimates for two 10 MWt structures were developed, one to support the VIH, the other to support the repowering heliostat. Life cycle maintenance costs and structure salvage value were also estimated. These results were then extrapolated to provide cost estimates for a 1 MWt and a 25 MWt structure supporting the VIH. This effort resulted in designs and cost estimates for a total of four UHAs.

3.6 DETAILED OPTICAL PERFORMANCE

In this part of the project a detailed modeling of the UHA optical performance for the final designs was performed. The subjects investigated included: cosine, shading, and blocking factors; detailed analysis of the solar image at the aperture plane; sizing, shape, and efficiency of the aperture; flux distribution, power, and energy delivered to the aperture plane and through the selected apertures; and radiation loss levels at temperatures of 1000°K and above. At temperatures of 1000°K and above the residual power after reradiation losses will be usable at a process operating temperature.

3.7 COST OF ENERGY

Cost of energy was divided into two categories. At receiver temperatures below 1000°K radiation control methods are effective in reducing losses. At temperatures above 1000°K radiation losses become large. On this basis, at temperatures below 1000°K the annualized energy delivered through the aperture was considered to be completely usable and the cost of energy was computed by the standard levelized charge method for several escalation and cost of capital rates. At temperatures of 1000°K and above the annualized excess input power, above the black body radiation loss, was termed "usable energy" at the chosen temperatures. The cost of this annualized usable energy was then computed by the same levelized charge methods.

SECTION 4.0

TECHNICAL APPROACH

4.1 SPECIFICATION DEVELOPMENT

The design of the UHA conceptual structures required the development of a design specification. This specification addressed environmental factors, uses of the structure, and loads and load combinations imposed on the structure. The survivability of the structure and the allowable deflections of the individual heliostats were of central importance in this study.

In order to make maximum use of existing data, the basic approach for the specification development was a review of previous studies. Prior DOE specifications for central power project horizontal fields and heliostat characteristics were reviewed for applicability. Environmental conditions, including insolation data, for Barstow, California, and soil characteristics prevalent at the solar facility in Albuquerque, New Mexico, were used. Previous in-house studies conducted by Veda Incorporated on UHA design factors were reviewed. Industrial standards and building codes were also reviewed for their applicability.

4.2 STRUCTURAL DESIGN AND MODELING

The design specification relates the location of heliostats, the clearances required for their operation, the environmental considerations for the UHA, the loads imposed by the heliostats on the structural members, and the rotational tolerances permissible in order to remain within the central power system collector field's error budget.

Bechtel National, Incorporated was charged with the design and evaluation of the UHA structure to best meet this specification.

The initial work included a literature review of modern structures having similar configurations. In general, these are human habitable structures. For this study, the UHA is not considered to be a human habitable structure, rather, it is only a common foundation for heliostats. The choice of a steel framework with concrete foundations was made as being the approach promising least cost. Based on a preliminary loads analysis, nine conceptual designs for the three power levels and the three aspect ratios proposed were developed to the extent that a relative cost determination could be made. Comparison with the optical performance calculations made by Veda resulted in the choice of an array aspect ratio of 1:5, i.e., the height is one-fifth of the east-west length of the structure.

Once the aspect ratio had been chosen, more detailed evaluations were conducted. The simple design was varied to evaluate cost effects of different distributions and sizes of structural members. The STRUDL computer program was used for determining stresses and rotations. As a result, the conceptual designs were modified to reduce cost.

In three designs, the VIH, an equatorially mounted heliostat having a mirror area of six square meters and a predicted weight of 434 pounds, was assumed. In the fourth design the 49 square meter repowering heliostat with a predicted weight of 3,214 pounds was assumed.

4.3 OPTICAL PERFORMANCE MODELING AND SIMULATION

There are several factors that influence the actual energy intercepted by a heliostat mirror and directed toward the aperture. Insolation

is measured in power per unit area normal to the solar direction. The effective area of a heliostat is less than the surface area of the mirror. The ratio of effective-to-actual mirror area is called the cosine factor. This is due to the fact that the normal to the mirror must be pointed to cause reflection toward the fixed focal zone and has an angular displacement relative to the sun's direction. The effective area is further reduced by shading of a given heliostat from neighboring mirrors; that is, the casting of shadows on the face of a heliostat by other heliostats. These two factors, taken with the appropriate insolation data, adequately model the mechanics of computing energy intercepted by a heliostat.

The factors affecting the reflected energy are the reflectance of the heliostat mirror, the atomospheric transmittance, and the blocking of mirrors by other mirrors. The model developed by Veda Incorporated, described in Reference 4-1, implements mirror reflectivity and atmospheric transmittance as constants. The blocking of a mirror from the receiver occurs when neighboring mirrors fall within the line of sight to the receiver, preventing some portion of the blocked mirror's reflected energy from reaching the receiver.

To support future analysis, quick access to items of interest such as heliostat positions, orientations, obscured areas, cosine factors, shading and blocking factors, and energy delivered to the aperture as a function of time is important. Since this information could be required on several array configurations simultaneously, the analysis program builds a data base containing this information.

Loading the data base initially is accomplished by means of a digital simulation. Building a general model allows analysis of varied configu-

rations of heliostats with a minimum of software conversion. Vector equations were used as much as possible to reduce dependence on coordinate systems and because of their inherent computational efficiency over trignometric methods. The specific task for this project was to model the UHA configurations and heliostat types as required in the design specification.

The basic variable included in the model was the apparent position of the sun as seen from the site of the collector field. To allow for a reasonable change of declination between samples, the number of samples taken during the year was chosen as 24, averaging about 15 days between samples. Insolation values were taken from the 1976 Barstow data base. If a selected day had either erratic or extended cloud cover, the nearest reasonably clear day's insolation data was substituted.

The daily rotational motion of the earth was modeled by changing the direction cosines of the sun by an amount equivalent to a 15° per hour rotation. The model was exercised for each of the 24 selected days on an hourly basis between 0700 and 1700 local sun time when the sun was far enough above the horizon to deliver energy to the south side of the UHA.

Each heliostat element of the subject UHA was modeled by first computing the spatial orientation required to reflect the sun's energy from the center of the heliostat to the center of the aperture. Shading and blocking of the heliostat by any neighboring heliostats was computed geometrically, using the simplifying assumption that each mirror was a rectangular flat plate. No contribution to shading or blocking from structural members was considered since the UHA structure lies below and north of the mirror plane when the sun has reached the required angular altitude.

Once the area of the heliostat actually reflecting sunlight was known, its contribution to the energy incident on the receiver was computed. The total energy for a given time was computed using:

$$E_t = \sum_{i=1}^{n} A \cdot F_{Ci} \cdot (F_{Si} + F_{Bi} - 1) \cdot F_R \cdot F_T \cdot I_t$$

Where E_t is power on receiver at time t,

A is area of heliostat,

A_B is unshaded blocked area of heliostat

A_S is shaded area of heliostat

F_{Ci} is cosine factor of ith heliostat,

F_{Si} is shading factor of ith heliostat

$$= \frac{A - A_S}{A}$$

F_R is the reflectivity of a heliostat

= 0.9 for this study,

F_{Bi} is the blocking factor of the ith heliostat

$$= \frac{A - A_B}{A}$$

F_T is the atmospheric transmittance

= 0.99 for this study,

I_t is the insolation for time t,

n is the number of heliostats in the array

Annualized energy at the receiver was computed by summing E_t over every hour 0700 to 1700 for each of the 24 days over the year, dividing by 24 to get average daily energy, then multiplying by 330 productive days in the average year. This allowed 35 days offline per year for whatever reason (inclement weather, repairs and maintenance, etc.).

To allow an assessment of the distribution of energy across the receiver, the model sums an image of the sun from each heliostat in the receiver plane. The sum was built by dividing each mirror into segments and computing the energy contributed by each as if all of it were concentrated into a solar image originating from the center of the segment. The normal to each mirror segment was derived from the slope of the toroid at the center of the segment.

The receiver was modeled as a grid of square "bins" with each bin accumulating the small increment of energy contributed by each solar image that overlaps the bin. Since the receiver plane normal is not parallel to the normal from each mirror segment, the model accounted for image distortion by projection techniques. The energies collected by each bin after summing over the heliostat array are stored for each selected time of day and year for further processing.

The receiver aperture is assumed to be a flat, perfectly conducting plate, insulated except where it is exposed to the concentrated solar energy. On the exposed area, it is assumed to act as a black body. Actual receivers in a real world environment will have a variety of loss factors. The only loss factor considered in this analysis is the reradiation loss for such

a flat plate, as this loss mechanism will predominate over convective heat transfer to the air in the temperature regions of interest for the envisioned applications.

On the basis of the assumption that the receiver aperture is a perfectly conducting plate, and considering only radiation losses, the usable energy at some temperature T is simply the difference between energy into the aperture and reradiated energy at the temperature T.

4.4 ECONOMIC ANALYSIS

4.4.1 Levelized Charge Methodology

The starting point for this methodology is ERDA/JPL-1012-76/3 (Reference 4-2). The basic principle of the methodology is that if the system were to produce exactly its expected output, and if that output were sold at a fixed unit price, the selling price must be such that the resultant revenue would exactly recover the full costs of the system over its lifetime. This includes a return on the investments of stockholders and creditors. The required revenue per unit is found as the minimum energy price consistent with recovering all costs and is the levelized charge for the energy produced by that system.

This study is only concerned with an energy collection subsystem. Hence, many of the considerations necessary for the full utility system are inapplicable. The following assumptions are made in consonance with the referenced document.

- Capital acquisition for the entire project occurs at one time. Unless expended, the net capital earns at the same rate as the cost of money. Once expended, it can only earn in the form of payback from the levelized charge during the operating lifetime of the system.

- The referenced document uses an average inflation rate of 0.06 and a cost of capital equal to internal earnings of 0.08. In this analysis, escalation rates of 6%, 8%, and 10% are used with cost of capital at 8%, 10%, and 15% to develop a family of cost numbers.

- The capital outlays for the collector consist of land, heliostats, the UHA structure and associated wiring, and a central controller. Operation and maintenance costs include routine cleaning, operations and maintenance labor, general and administrative expenses, and electrical power.

- A construction start date is assumed for 1981 and a first year of commercial operation for 1984. Capital equipment (including installation, engineering, etc.) purchases are spread over three years. Operating and maintenance expenses start in 1983, one year prior to commercial operation.

Once an expenditure is made prior to the end of 1983, it is no longer a source of revenue until 1984, at which point it starts to receive payback from the fixed charge on energy sold. In the meantime it accumulates an additional burden at a rate equal to the cost of money and compounded annually; e.g., $100,000 expended in 1981 at a cost of money = 8% would require revenues of $8,000 for 1982 and $8,640 for 1983, thus making its "present value" at the beginning of 1984 $116,640. Annual earnings at a rate equal to the cost of money will be required on the present value amount plus an amount to accumulate over the system life the present value of capital less salvage value of the system.

The cost of heliostats is a function of heliostat design, cumulative production quantity, and current production rate. The "repowering" heliostat is nominally 49 m^2 in area, comprised of several mirror elements. In order to define the image at the aperture plane of the UHA system a detailed description of mirror size and placement was obtained by telcon from the cognizant engineers

at Sandia Livermore (SNLL). The outer dimensions of the mirror assembly yield 49 m^2. The actual available reflective surface is 46.18 m^2. All calculations were performed using the 46.18 m^2 usable mirror area. Sandia quoted \$230/m^2 as the cost that should be used. It is Veda's understanding that this is the expected cost at a production level of 25,000 units per year having been achieved. Veda applied this cost factor to the actual 46.18 m^2 of mirror area. If this gross cost were translated to the nominal 49 m^2, the effective cost per active mirror area as used in this report would reduce to \$216.76/m^2.

In order to accurately portray similar costing, the costs for the VIH, as developed by Reflective Modules, Incorporated, are for the same production rate of 25,000 units per year. The derived cost of \$100.50/m^2 did not include the local electronics package. On this basis, Veda added \$25/m^2, \$150 per heliostat, to the cost, resulting in a cost of \$125.50/m^2 for use in the cost analysis.

Operating and maintenance costs for labor, materials, and electrical power were estimated as an educated guess which included consideration of the number of personnel required and the skill levels which they should possess. General and Administrative (G&A) expenses were estimated at 50% of direct labor, and contingencies at 5% of maintenance. These costs were assumed to be in effect for the last year of construction, just prior to the first year of commercial operation, in order to provide on-the-job training as part of the installation and checkout of the system. The total of these expenses for the first year is then subjected to escalation, and a present value of these expenses determined. From this present value the O&M component of the levelized charge will be determined. The methodology of Reference 4-2 assumes that

the cost of money is equal to the internal rate of return, and that retained earnings earn at this rate. Thus, the excess of income from the levelized charge, over expenses, incurred during the early years will earn at this rate to assist in payment of the expenses, in excess of income, during later years.

The salvage value of each of the larger sizes of the UHA was expected to exceed the cost of recovery. This value was entered into the equation at an appropriate point to determine its effect on levelized charge.

The annualized cost of energy is equal to the total cost divided by system life. The levelized charge is equal to the annualized cost divided by the annualized energy.

4.4.2 Cost of Usable Energy

At working temperatures below about 811°K (1000°F) reradiation, reflection, and absorption can be controlled by selective coatings. Above that temperature, conventional coatings generally become relatively ineffective, and the basic material used as the energy absorber determines these characteristics.

To enable a practical designer to evaluate his application, the performance of the receiver can be calculated by application of multipliers relating the proposed receiver characteristics to the characteristics of a black body. The receiver characteristics used in this study were those of a black body (i.e., reflectance equals zero, absorptivity equals emissivity equals one). The Stefan-Boltzmann Law then applies.

This idealized aperture assumes a constant temperature across a flat plate, equal in size to the aperture size, absorbing and reradiating energy from the side toward the heliostat field and perfectly insulated on

the other side. Convection losses were neglected in this approach since they rapidly become relatively small as the absolute temperature increases. Convection losses increase approximately linearly with temperature; reradiation losses increase as the fourth power of absolute temperature.

Based on these assumptions, the power incoming from the heliostat field is equal to the integral over the aperture of the product of radiant flux and increment of aperture area. The power reradiated is equal to the product of the black body reradiation flux and the aperture area. The incoming power must equal or exceed the reradiation power for the temperature to remain constant. When these power levels are equal no useful work may be done. The corresponding temperature is known as stagnation temperature. When the incoming power exceeds the reradiation at the aperture temperature, the temperature either increases or the difference, between incoming and reradiated power, must be withdrawn. It is this power that may be withdrawn that is herein called usable power, or, as accumulated over the year, usable energy. An example of a constant temperature withdrawal would be an endothermic chemical process. The process proceeds, when the working temperature is attained, at a rate dependent on the excess power input.

Usable energy is thus related to temperature. In this analysis several temperatures were chosen and the usable energy calculated. The annualized charge was then divided by the annualized usable energy to obtain the levelized cost. At stagnation temperature, where reradiation losses exactly equal input, there is no usable energy. Thus, as the temperature approaches stagnation temperature, the cost of usable energy approaches infinity.

SECTION 5.0

RESULTS

5.1 UHA SPECIFICATION

"Specification for the Unified Heliostat Array", Veda document 43342-80U/P0069, (Reference 5-1), was the basis for the analysis conducted under this project. The document is included as Appendix A to this report. The specification was developed as the result of a review of prior DOE specifications for central power project collector fields and heliostat characteristics, and extrapolation from prior UHA design studies performed by Veda Incorporated. Key elements in those specifications were considered as assumptions:

- The site location is at 35° North latitude.
- Soil conditions are equivalent to those specified for Albuquerque, New Mexico.
- The reflectance of the mirror elements is 0.9.
- Building codes are those applicable in the area of Barstow, California.
- Seismic zone 3 applies.
- The atmospheric transmittance between mirrors and receiver when averaged over the array of heliostats is equal to 0.99.

The basic field arrangement of the UHA is such that the largest angle seen looking north from the receiver between westerly and easterly heliostats is 60 degrees. The general arrangement is shown in Figure 5-1.

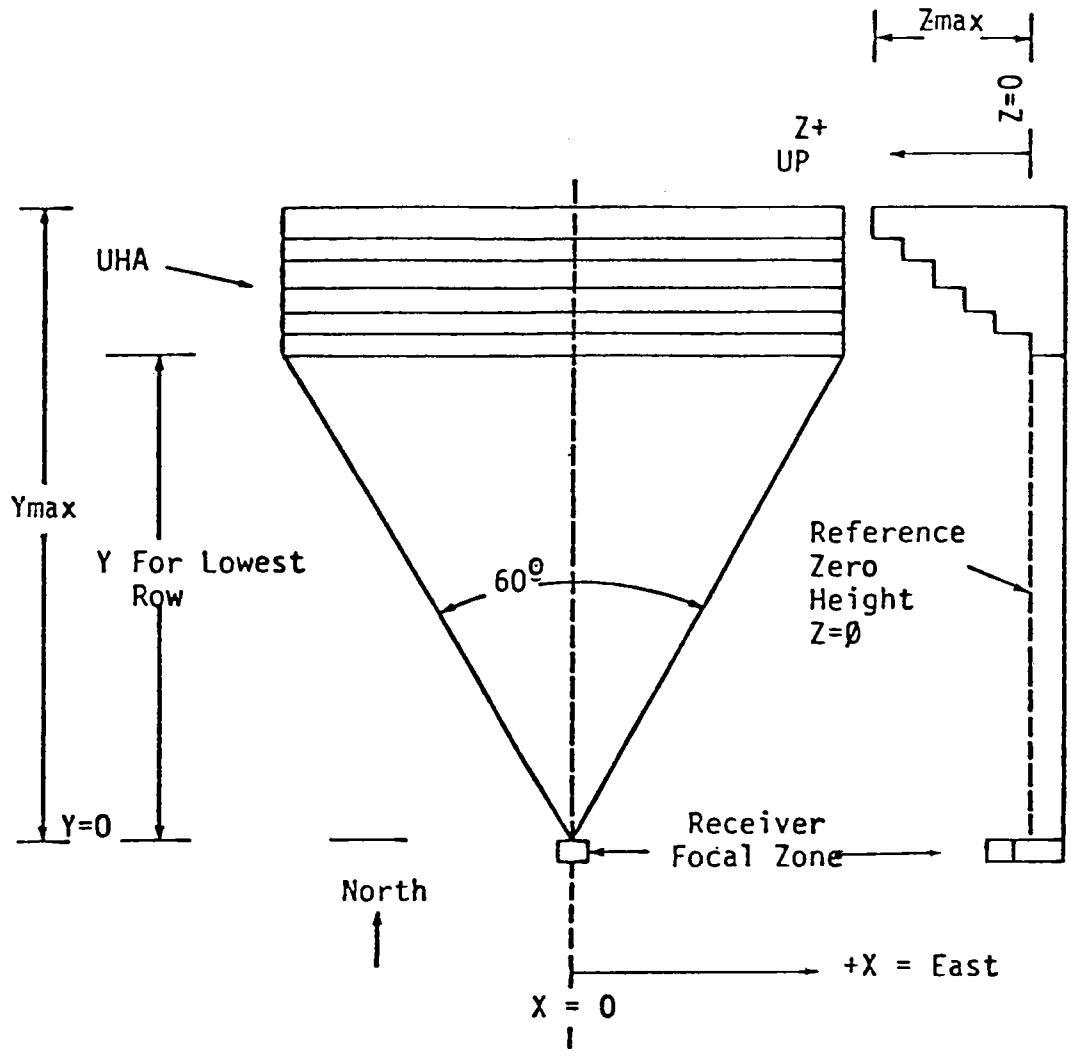

Array	±X	Ymax	Zmax	Note
1MWt	52.5m	111m	22m	Veda Heliostat
10MWt	170m	356.5m	68.2m	Veda Heliostat
10MWt	213m	410m	82.3m	Repowering Heliostat
25MWt	265m	559m	110m	Veda Heliostat
All	0.0m	0.0m	8.0m	Receiver Center

Figure 5-1. Layout of a UHA Central Power System.

The data for the repowering heliostat was obtained from Sandia Laboratory documents distributed by J. C. Gibson's letter dated November 6, 1979, Sandia document FSCM 14214, Issue C, and SAND-78-8180 (References 5-2 and 5-3). The conceptual design for the equatorially mounted heliostat was developed by Veda Incorporated. A preliminary design, costing, and loads analysis for this heliostat was performed by Reflective Modules, Incorporated.

5.2 PRECONCEPTUAL DESIGN AND COST

The intent of this task was to review structural materials and concepts applicable to the UHA and develop preconceptual designs which appeared to offer low cost construction. Once these designs had been developed to a sufficient level of detail, relative cost ratios were to be determined to aid in the selection of an array aspect ratio which offered the best tradeoff between performance and cost. The designs had to meet the criteria established in the specification.

The specification document described the UHA operational environment, the sizes of the required structures and the location and values of heliostat loads to be imposed on each of the twelve structural configurations. Bechtel National, Incorporated, using the specification as a basis, selected the appropriate materials and developed the preconceptual designs and relative costs. The results of this effort are contained in Appendix B, Sections 2 through 4. Highlights of that effort are presented here.

5.2.1 Review of Structural Concepts

The dimensions and spacings for the heliostats suggested that the supporting structure must have a slanting, terraced frame similar to that of

a stadium. The relative heights of the UHA structures ranged from that of a six story office building (1 MWt, aspect ratio 1:5) to that of the Transamerica Building in San Francisco (25 MWt, aspect ratio 1:1). The structure not only serves to support the heliostats against environmental forces, but also provides the proper orientation to maximize solar power collection.

A literature search was performed to find existing designs or structural concepts that served functions similar to the UHA concept and also represented major structures. The search encompassed general technical and trade literature such as proceedings papers, reports, govenment publications, and trade magazines. Computer searches were also performed on two engineering data bases, the Computer Engineering Index and the National Technical Information Service.

The literature search revealed one array structure identical to the UHA in function. It is a terraced array for holding heliostats currently under construction in Japan for a 1 MWe solar thermal pilot plant, (Reference 5-4). Other structures were also found that exhibited the terrace concept. Examples of these are New York's Shea stadium, the Hartford Jai-Alai Fronton and Harvard University's Gund Hall. A cross section of Gund Hall is illustrated in Figure 5-2.

No structures were found that directly compared with the UHA concept with respect to size, so structural configurations for this study had to be evolved from basic principles.

5.2.2 Structural Materials

Candidate materials considered in this study for the construction of the UHA included timber, concrete, and steel. Each was evaluated for its advantages and disadvantages from both a structural and a cost standpoint.

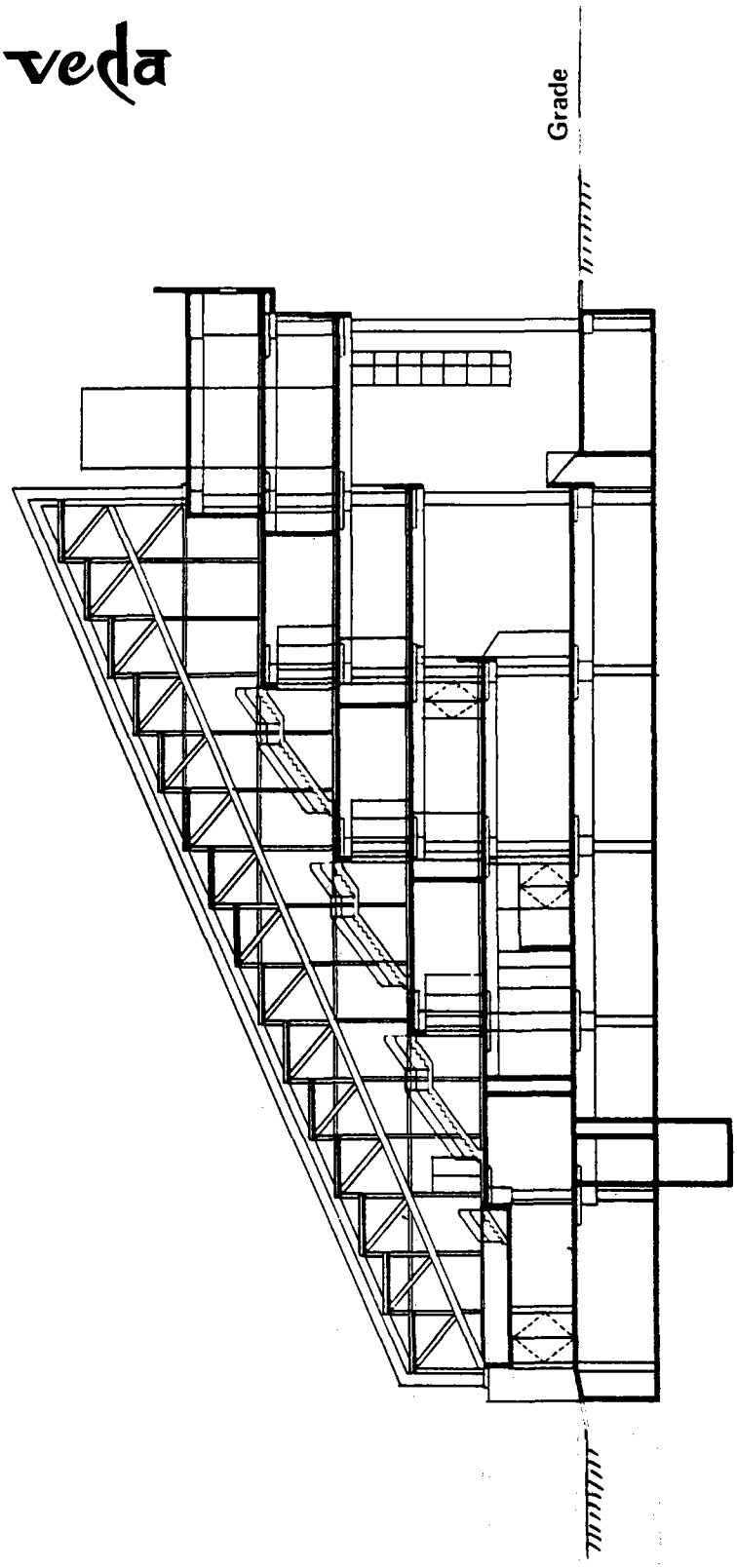

Figure 5-2. Cross Section of Gund Hall, Harvard University.

Timber was eliminated primarily for structural reasons. Concrete was eliminated primarily to minimize structural dead loads and to meet the required earthquake resistance for structural members, but was used for the UHA foundations. Steel was selected as the candidate material.

In addition to its structural properties, steel has the added economic advantages of availability in required sizes, potential for shop fabrication of standard pieces and reduced erection times which lowers construction costs.

5.2.3 Design Concept

After the reviews of structural concepts and materials, a steel beam and girder framing system was chosen for the preconceptual design. Each frame has a sloping main girder supported by equally spaced columns. The structure is braced against side sway in the longitudinal direction by east-west beams and the heliostat support beams. X-cable bracing is used to augment the overall structural stability. A typical structural configuration is shown in Figure 5-3.

In order to meet the heliostat pedestal rotational requirement of less than $\pm$ 1.5 mrad under operational winds of 12 m/s, a double support beam structure was used. Two parallel beams were used for each terrace of heliostats. The pedestal, as well as a removable handrail, clamps to the top flanges of the beams by U bolts. A metal grating, attached to the lower flange, provides bracing as well as a walkway for maintenance. A partial elevation showing the heliostats is given in Figure 5-4.

Poured concrete caissons were chosen for the foundation. This design was selected because it provides sufficient weight to resist uplift forces and

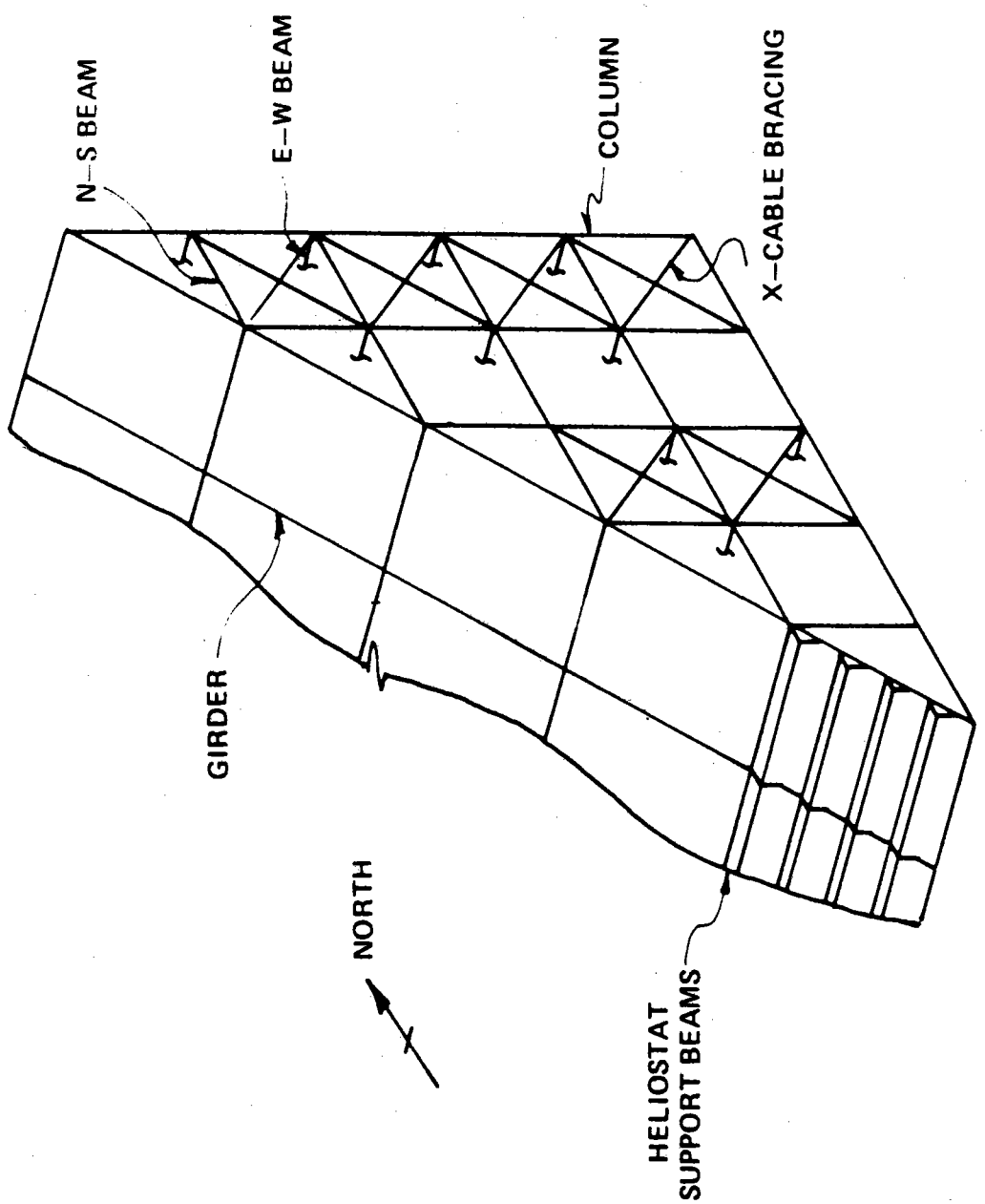

Figure 5-3. A Typical Unified Heliostat Array Structure.

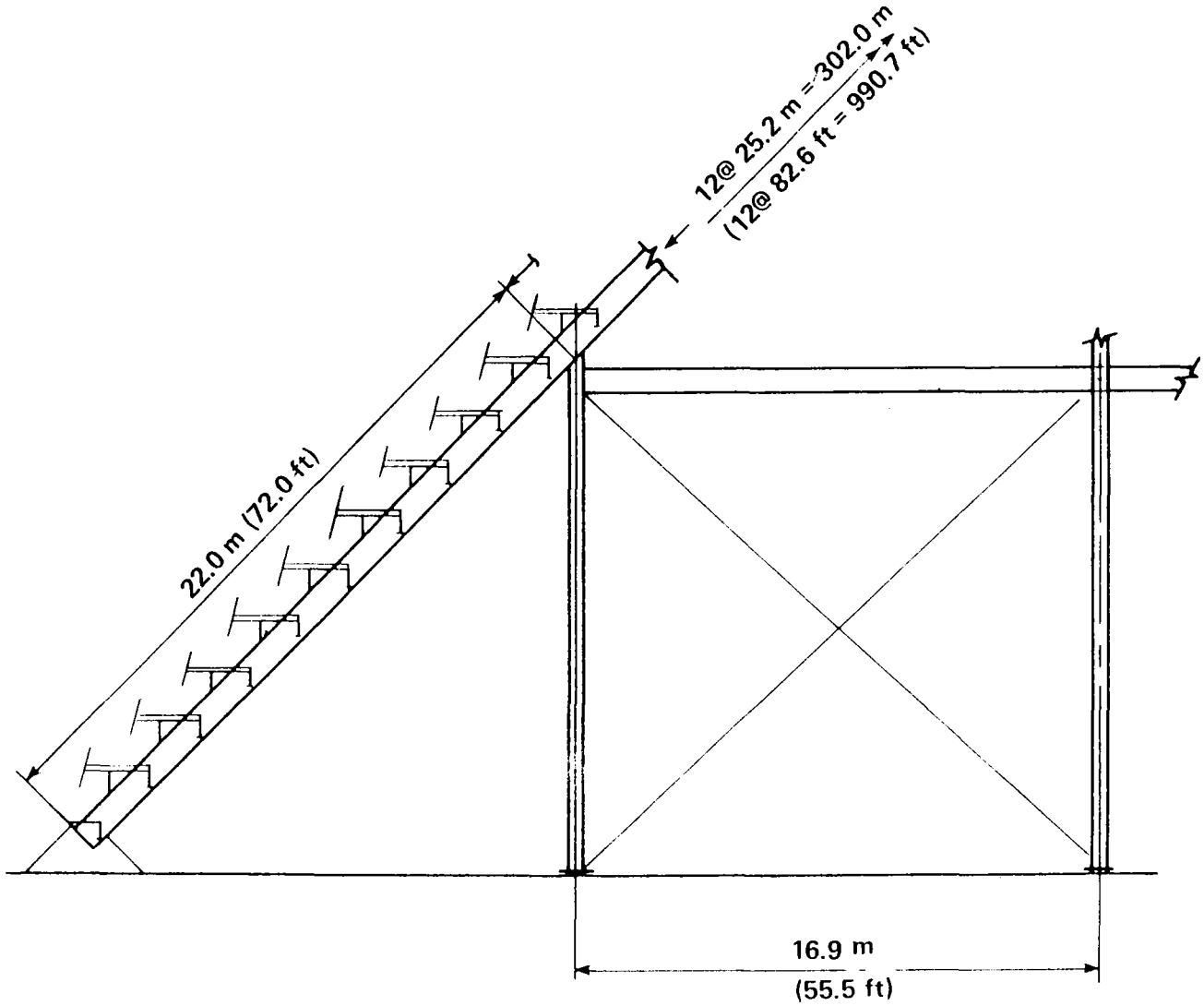

Figure 5-4. Partial Elevation of Typical UHA Showing Heliostats.

sliding, generally needs little or no forming and is rapidly installed in good soil conditions. Both of the latter reasons lead to reduced cost.

The significant aspect of the preconceptual designs is their extreme lightness for their size. Since the consideration of the structure for any purpose other than heliostat support was beyond the scope of this effort, very light structures which would not meet building codes for human habitation were conceived. Figure 5-5 compares the largest UHA, 25 MWt, to two large highrise buildings in terms of the amount of steel per unit volume of structure. As can be seen, the UHA is an order of magnitude lighter than the other structures.

5.2.4 Preconceptual Cost Ratios

The cost estimates for the preconceptual designs were an order-of-magnitude evaluation of the constructed costs. Material estimates for the designs are given in Tables 5-1 through 5-3. Table 5-4 presents the total estimates. Included are site preparation, material, labor, and indirect field costs. The material unit cost data and manhour data were based on Bechtel's experience and current project information. A detailed discussion of this information and the assumptions inherent in the estimates may be found in Appendix B.

The significant factor in these preliminary estimates is the dependence of cost on structure height. Greater height demands larger structural members which means an increase in both material and labor. For a given power level, an aspect ratio of 1:1 is approximately 1.7 times more expensive to construct than the 1:5 ratio. Taking the 1 MWt UHA with an aspect ratio of 1:5 as unity, the relative cost ratios for all the structures were calculated

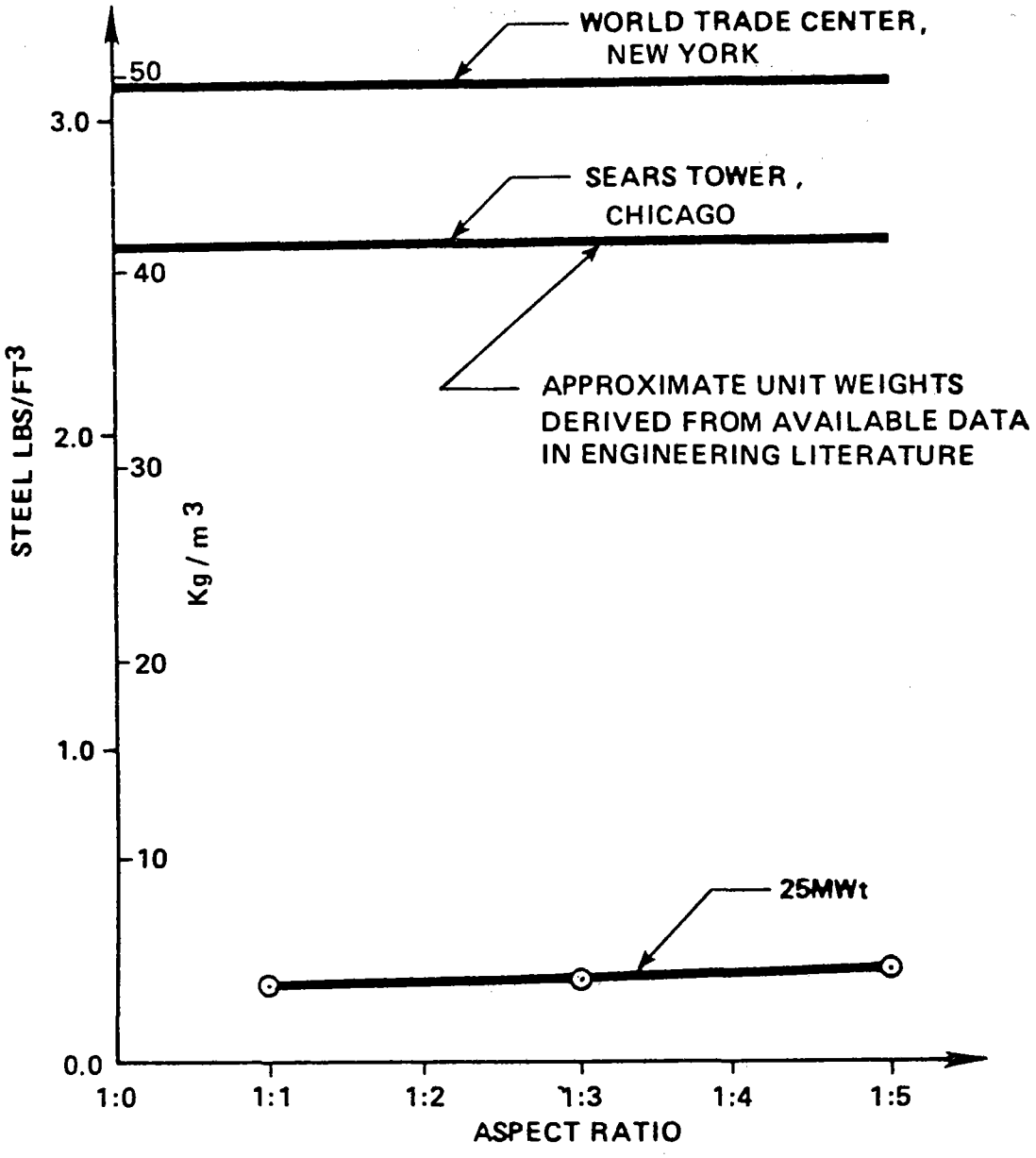

Figure 5-5. Steel Weight Comparisons.

Table 5-1. Material Quantities for 1 MWt Array.

Materials	Units	Aspect Ratio		
		1:5	1:3	1:1
Steel	ton	161	236	290
Concrete	cubic yard	122	117	120
Rebar	ton	2.4	2.4	2.4

Table 5-2. Material Quantities for 10 MWt Array.

Materials	Units	Aspect Ratio		
		1:5	1:3	1:1
Steel	ton	4493	5343	7827
Concrete	cubic yard	724	745	912
Rebar	ton	14	15	18

Table 5-3. Material Quantities for 25 MWt Array.

Materials	Units	Aspect Ratio		
		1:5	1:3	1:1
Steel	ton	14668	16875	27984
Concrete	cubic yard	1826	1970	3165
Rebar	ton	36	39	63

Table 5-4. Preconceptual Field Cost Estimates.

$ THOUSANDS -- SECOND QUARTER 1980

Configuration No.	1	2	3	4	5	6	7	8	9
Power Level	25 MWt	25 MWt	25 MWt	10 MWt	10 MWt	10 MWt	1 MWt	1 MWt	1 MWt
Aspect Ratio	1:1	1:3	1:5	1:1	1:3	1:5	1:1	1:3	1:5
Structure Height	794'	469'	361'	498'	296'	224'	159'	94'	72'
DIRECT FIELD COST									
Excavation	20	10	10	5	5	5	1	1	1
Concrete	250	150	140	70	60	60	10	10	10
Rebar	170	100	100	50	40	40	6	6	6
Formwork	510	320	300	150	120	120	20	20	20
Steel	64,500	38,900	33,800	18,100	12,300	10,350	670	540	370
DIRECT FIELD COST	65,450	39,480	34,350	18,375	12,525	10,575	707	577	407
INDIRECT FIELD COST*	13,550	8,520	7,650	3,925	2,675	2,225	153	123	93
FIELD COST	79,000	48,000	42,000	22,300	15,200	12,800	860	700	500
FIELD COST/MWt	3,160	1,920	1,680	2,230	1,520	1,280	860	700	500

*60% of Direct Labor Cost

Table 5-5. Total Field Cost Per MWt.

POWER LEVEL MWt	ASPECT RATIO		
	1:1	1:3	1:5
25	6.32	3.84	3.36
10	4.46	3.04	2.56
1	1.72	1.40	1.00

(Results normalized to lowest-unit cost ratio)

on a cost per megawatt basis. These results are summarized in Table 5-5 and were used in conjunction with the preliminary optical analysis to select the preferred aspect ratio for conceptual design.

5.3 PRELIMINARY OPTICAL ANALYSIS

The in-house work performed by Veda Incorporated prior to this contract formed the basis on which the location, size, and shape of the Veda heliostats were determined for the design specification. The preliminary optical analysis was concerned primarily with verification that this design information was adequate for a relative performance comparison assuming a uniform price per square meter for heliostats.

Each UHA aspect ratio was analyzed on a heliostat by heliostat basis each hour for the time interval of 0700 to 1700 for 24 evenly spaced days throughout the year. A circular earth orbit was assumed. Barstow 1976 insolation data was used. Clock time was assumed to be local sun time for determining insolation values to be used. Since a 330 day useful year was assumed

to account for poor insolation days as well as equipment outages, when a calculated day was non-typical of the seasonal insolation data the nearest nearly typical day insolation values were used. The annualized energy collection per unit of heliostat area was then evaluated to determine relative value of heliostats in each of the UHA configurations.

In performing the heliostat by heliostat analysis, cosine factor, shading factor, blocking factor, reflectance, and a fixed value of atmospheric transmittance were combined to develop an effectivity number for each heliostat. The average value of this number across the UHA field multiplied by the total heliostat area, multiplied by the insolation level, yielded the power delivered to the aperture. Daily symmetry about noon and annual symmetry about winter solstice were used in calculating the effectivity.

For the three UHA aspect ratios chosen for study under this contract, the annualized energy per unit area of heliostat was found to be least for the 1:1 aspect ratio and greatest for the 1:5 aspect ratio. This was due to the blocking of upper heliostats by the lower ones. As structure height increases, the look down angle becomes more severe and introduces the increased blocking.

Normalized Performance

Aspect Ratio	1:5	1:3	1:1
Relative Energy	1.08593	1.06018	1

A cursory computer run was made to study the performance of a 1:1 array in which the heliostats were staggered from one horizontal row to the next. That is, they were moved to the midpoint space location of those on the adjacent row. The shading and blocking improvement observed was normalized as

above to 1.04730. The design specification did not include this field arrangement. However, a staggered arrangement should be considered for future efforts.

The results of the preconceptual structural design study and performance analysis showed that, of the aspect ratios investigated, the preferred array dimensioning in terms of cost per unit energy is the 1:5 aspect ratio.

Although a staggered heliostat placement yields better performance, and the analysis indicated a possible performance improvement for total collected energy for aspect ratios beyond 1:5, investigation of these variables was beyond the scope of this contract.

5.4 CONCEPTUAL STRUCTURES DESIGN AND COST

With the selection of the 1:5 aspect ratio, the first step in the conceptual design process was a review of the preconceptual designs to identify areas where cost might be reduced. It was determined that reduction in the amount of steel used in the UHA structure was the primary factor that would lead to a cost reduction.

Table 5-6 gives the breakdown of the steel tonnages for the different structural components with the preferred aspect ratio of 1:5. This list of tonnages clearly indicated that the largest percentage of the total weight of the structure came from the support beams for the heliostats. Two different options were open to possibly reduce steel weights in the more detailed conceptual designs:

- Modify, by more detailed computer analyses, the existing preconceptual designs to determine if they meet the design criteria and then optimize the structure by varying the design parameters such as column and girder spacings.

- o Reduce the large percentage of steel in the support beams by using an alternate, more efficient supporting system for the heliostats and analyze the new system to check against the design criteria.

Table 5-6. Structural Steel Tonnage and Percentage Comparison.

UHA Aspect Ratio 1:5.

STRUCTURAL COMPONENT	THERMAL POWER LEVEL					
	1 MWt		10 MWt		25 MWt	
	TONS	%	TONS	%	TONS	%
Girders	40.8	25	809	18	2,066	14
E-W Beams	18.1	11	351	8	1,394	10
N-S Beams	12.7	8	346	8	1,462	10
Columns	23.8	15	974	21	4,580	31
Support Beams	66	41	2,013	45	5,165	35
Total Weight	161	100	4,493	100	14,667	100

After careful consideration the latter option was selected as a means of possibly reducing the total steel in the UHA structures.

5.4.1 Description of Modified Structural Concepts

The modified structural concept developed for the arrays consists of a series of frames, each of which are composed of a long sloping truss system supported by large diameter pipe columns. To meet the stringent rotation

criteria of ± 1.5 mrads, the heliostats are attached directly to each frame instead of on beams spanning between them. Thus, in all cases considered, the spacings of the sloping members for the different arrays are identical to the heliostat spacings. Similarly, the slope of the main trusses was determined by the choice of heliostat spacings.

Shown in Figure 5-6 are structural details of a typical interior frame of the arrays using the 6 m^2 heliostats. The truss system of this array has two W12x53 beams acting as the main chords with 5 inch (12.7 cm) square tubes used for vertical web members. W10x49 sections were selected for the horizontal web members of the truss and are located at the same elevations as the heliostats.

The pedestal of the heliostat is a 10 inch (25.4 cm) square tube shop welded to the exterior main chord of the truss. Gusset plates were used to transfer forces into the main frame from the pedestal and the horizontal web members. The heliostat units can be field bolted to the pedestals using this approach. Twenty-four inch diameter pipe sections, 1/2 inch thick, were selected for the columns. A Vierendeel truss, shown in Figure 5-7, is used to tie the main frames together longitudinally. The top of the rear column is stiffened with plates to which the slanting truss and longitudinal tie trusses are bolted.

For the structure of the 1 MWt array using the 6 m^2 heliostats, it was found that only one column per frame was needed to meet the design criteria. Two W12x22 beams were used as the main chords of the truss system with 5 inch (12.7 cm) square tubes being used for the vertical web members and W10x22

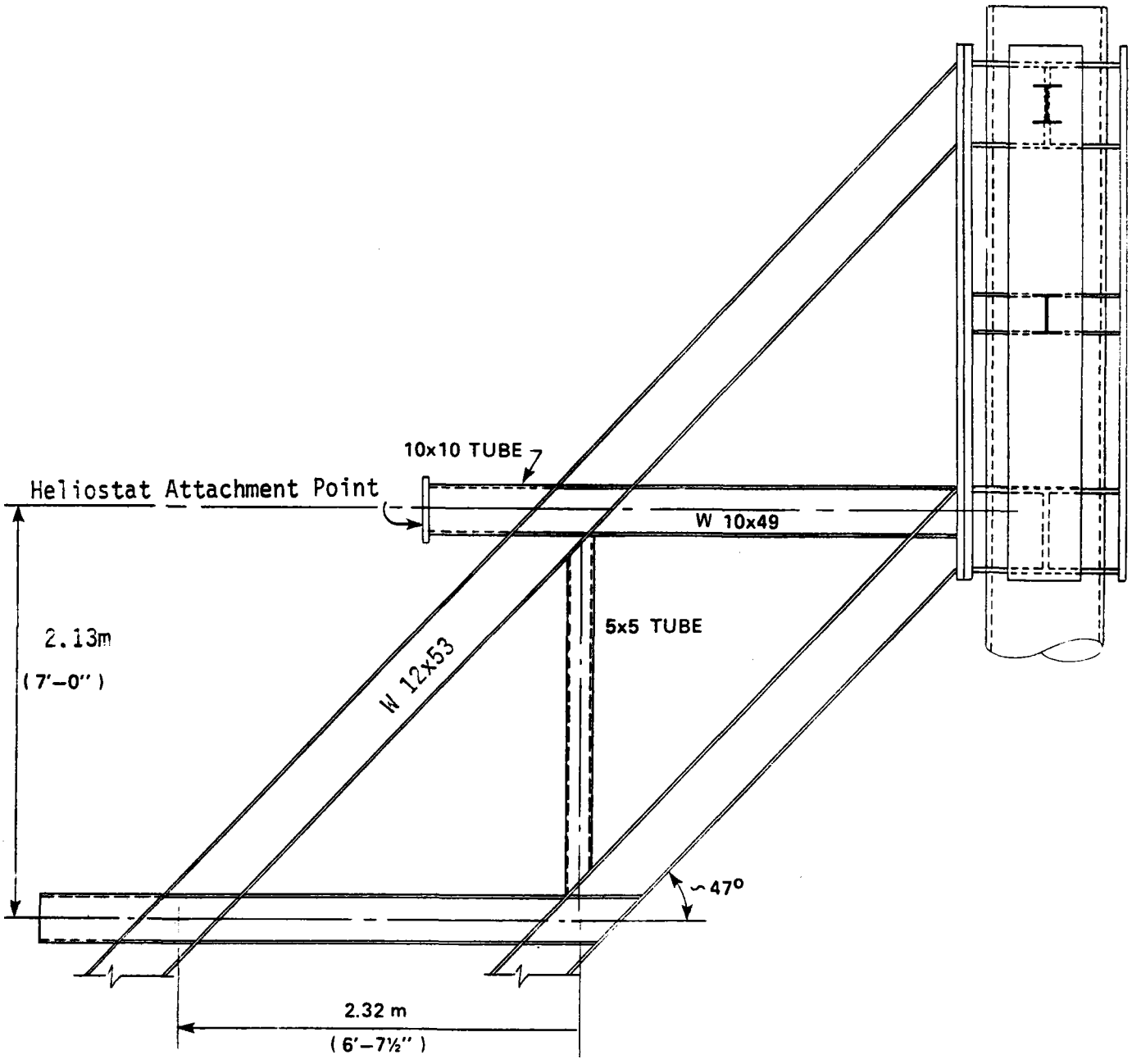

Figure 5-6. Detail for the 10 MWt Arrays with 6 m^2 Heliostats.

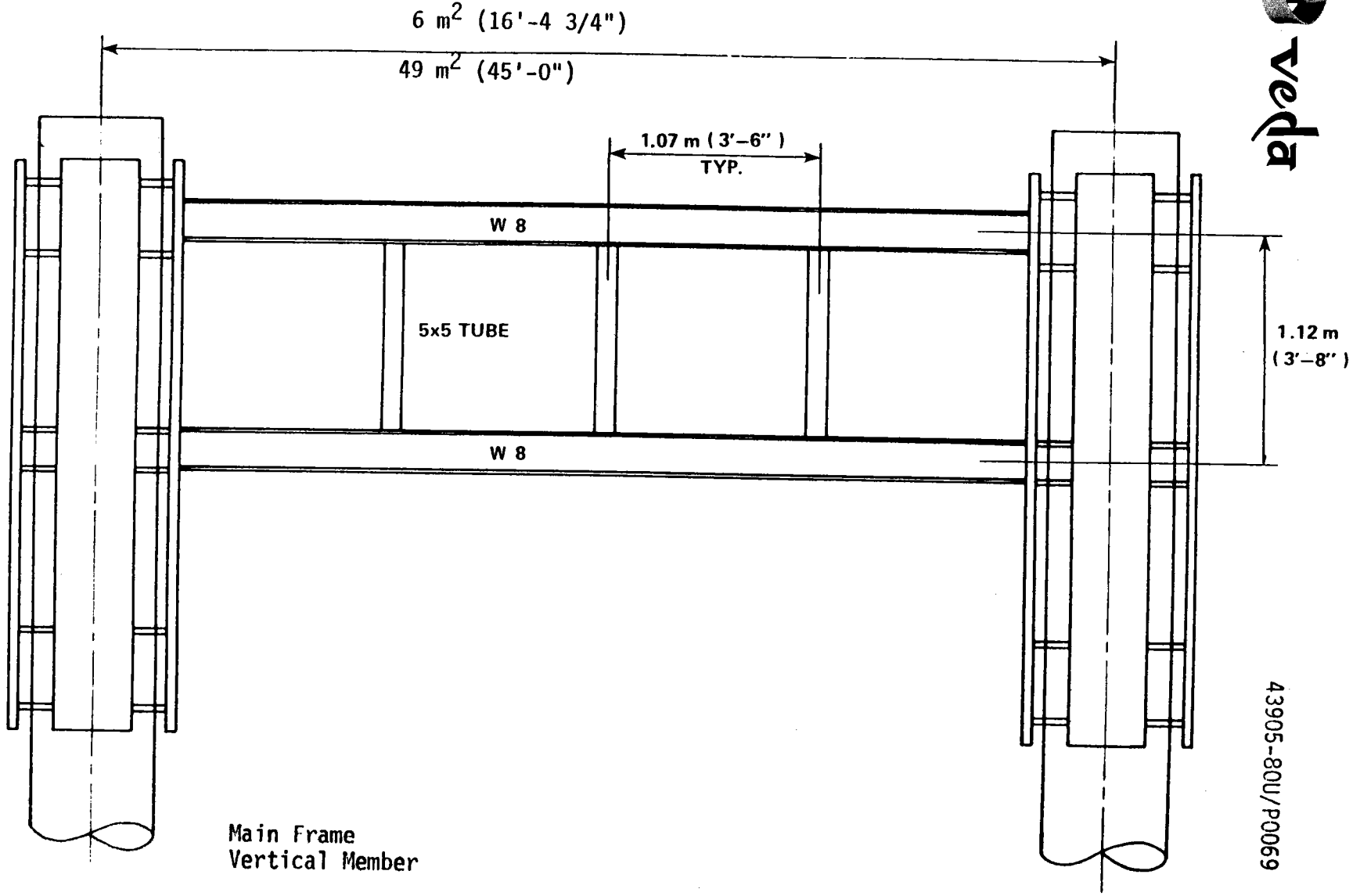

Figure 5-7. Vierendeel Tie-Truss Between Main Frames.

sections being selected for the horizontal web members. Fourteen inch diameter pipe sections, 3/8 inches thick, were chosen for the columns. The remaining structural details of the 1 MWt array are similar to the 10 MWt array.

The steel tonnages and foundation quantities of the 25 MWt structure were extrapolated from data of the nine preconceptual designs of the structures and the two modified detailed designs of the 1 and 10 MWt arrays.

For tall structures like the UHA, lateral forces due to wind might cause the structure to rock or rotate about its base. This rotation can cause uplift on the foundations and might be sufficiently large to overturn the structure. Therefore, for all three power levels the foundation designs had to provide sufficient mass to resist uplift. This fact, coupled with a need to provide resistance to sliding, and given the close spacing of columns, led to the decision to use a continuous strip footing with a caisson under each column. Primarily because of the overturning or uplift forces on the foundations, the amount of concrete and rebar used in the larger arrays increased over that given in the preliminary conceptual development by a factor of approximately three.

Shown in Figure 5-8 are structural details of a typical interior frame of the 10 MWt array using the 49 m^2 heliostats. Two W12x87 beams were selected as the main chords of the main sloping truss with 5 inch (12.7 cm) square tubes as web members. The columns and horizontal struts in the main frame consist of 18, 20, and 24 inch diameter pipe sections with varying thicknesses ranging from 3/8 to 1/2 inch.

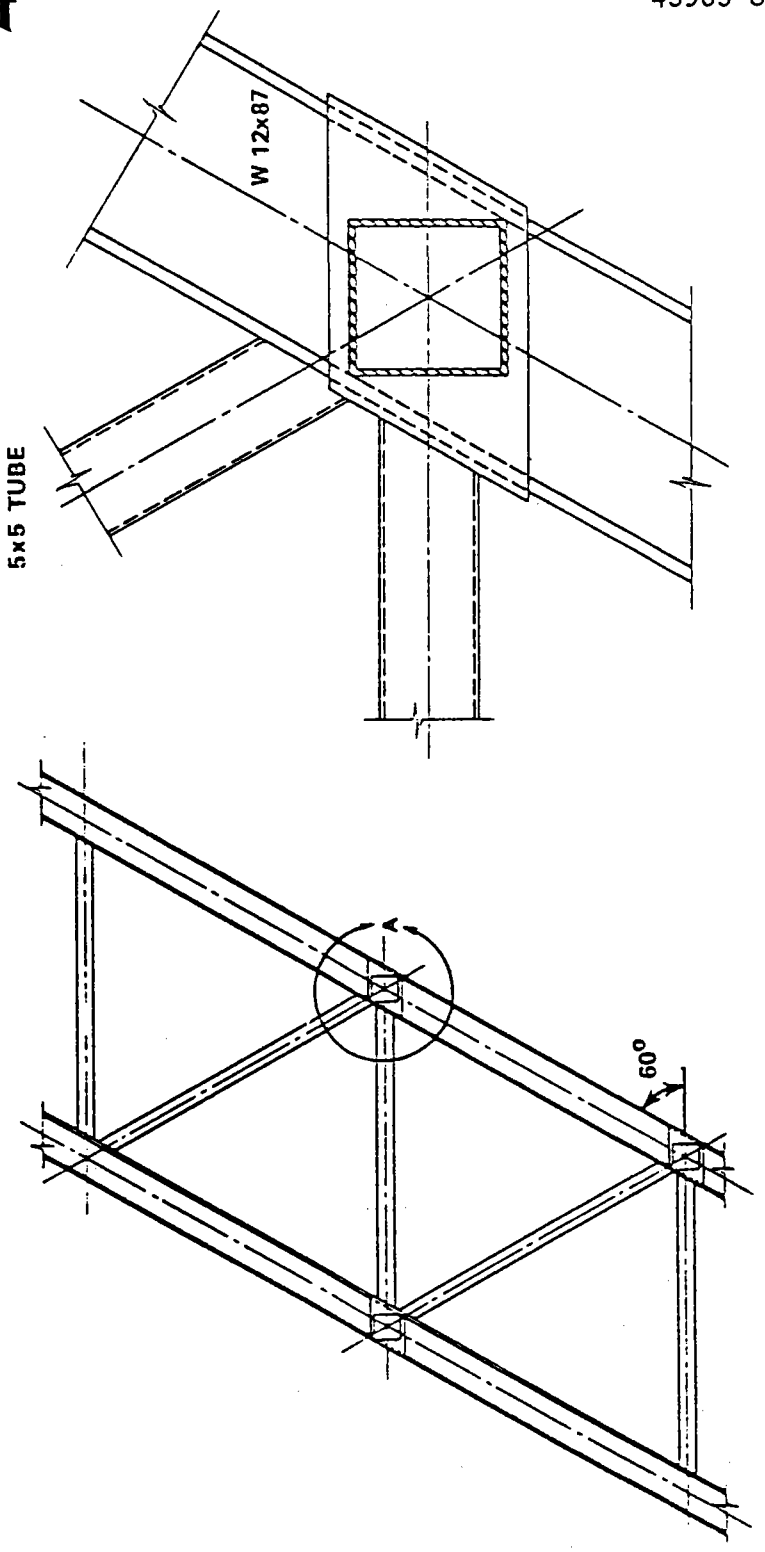

Figure 5-8. Detail for the 10 MWt Array with 40 m^2 Heliostats.

For this structure, however, the heliostat mirrors had problems in clearing the slanting truss system. For this reason, the heliostats were spaced between the main frames instead of attaching directly to the sloping truss.

To meet the rotation criteria of 1.5 mrads for the array using the larger 49 m^2 heliostat, a triangular shaped space frame, shown in Figure 5-9, was especially designed to span between the main frames. The space frame has three 8 inch (20.3 cm) square tubes which form the chords of the main longitudinal triangular shape. Each space frame has segments comprised of four 6 inch (15.2 cm) square tubes shop welded to the lower longitudinal member to form the vertex of an inverted tetrahedron. A rectangular flat plate is welded to the side members of the inverted tetrahedron to which the base of the vertical heliostat pedestal is attached.

The foundation design for this structural concept followed the same approach as was performed for the arrays with the 6 m^2 heliostats. Because of heliostat clearance and the resulting spacing, this structure is taller and steeper than the 6 m^2 arrays and, consequently is exposed to higher wind loads. However, the greater weight of steel supported by each individual column offsets the increased vertical component of the lateral wind loads. The end result is that this concept is not subject to uplift forces for the loading cases considered. Because of the increased distance between the main sloping truss members and support columns, it was decided to use individual augered caissons. The greater distance separating the main members and columns was also a reason the caissons were not connected together.

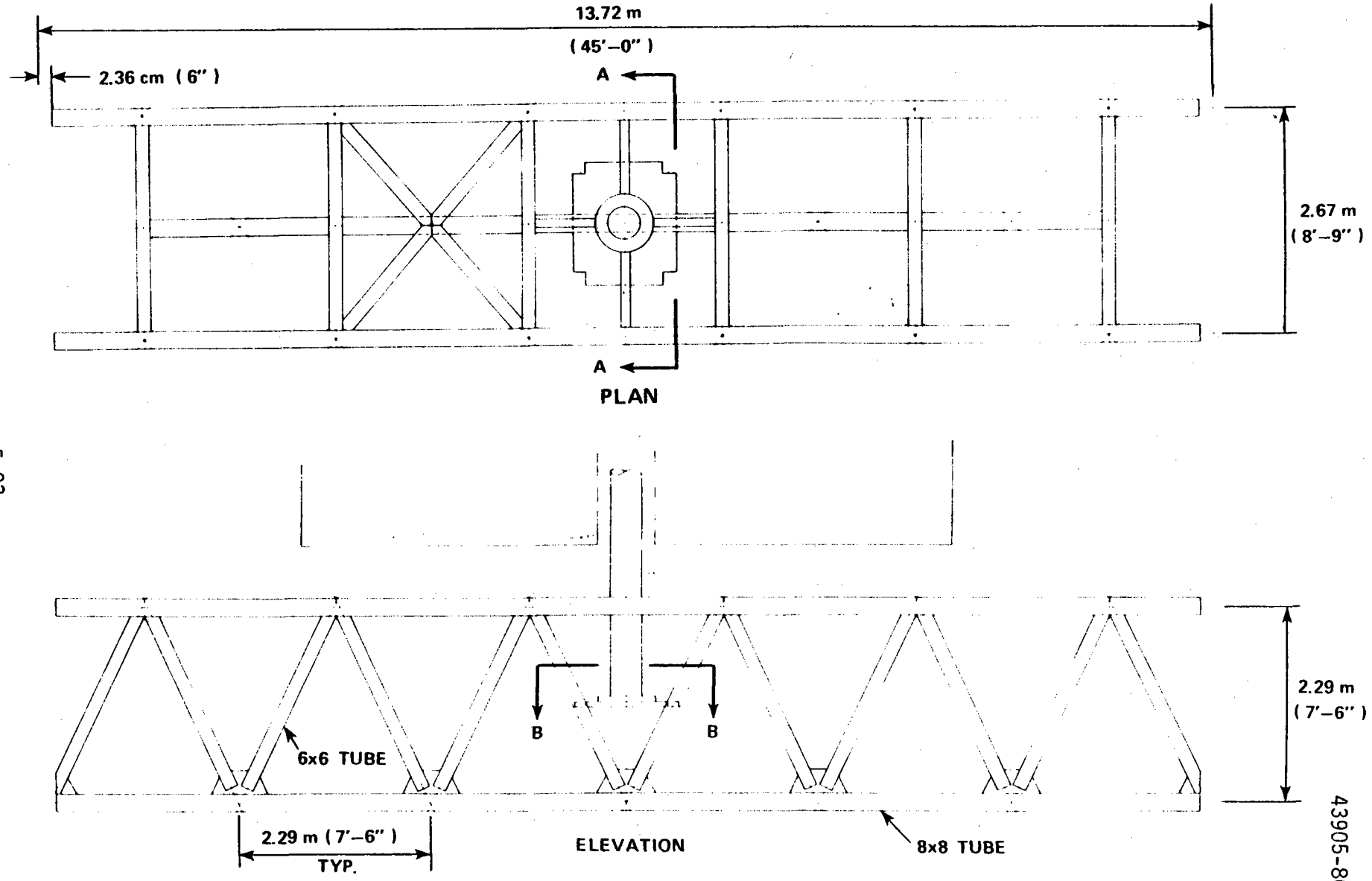

Figure 5-9. Triangular Space Frame Supporting 49 m^2 Heliostats.

43905-80U/P0069

5.4.2 Computer Analysis Procedure

The modified structural concepts of the arrays were analyzed by using the STRUDL computer program. STRUDL is an acronym for the Structural Design Language Program and consists of a series of computer programs for solving structural engineering problems. STRUDL can analyze continuous mechanics problems and framed structures, which is the case of the UHA concepts. Framed structures are defined as two or three-dimensional structures composed of slender, linear members, which can be represented by their structural properties along a centroidal axis. Such a structure is composed of many members connected together at joints or nodes.

All the structures analyzed by STRUDL for this study were run on the Bechtel in-house UNIVAC 1180 computer system.

For the STRUDL computer analyses, a typical interior frame of the UHA concept was modeled as a moment-resisting rigid frame. The large sloping truss which supports the heliostats was modeled as a beam with an equivalent bending stiffness. The columns and the struts were also modeled as line elements. Since the foundations are expected to be rather flexible, pinned supports were assumed.

Shown in Figure 5-10 is the idealized computer model of the 10 MWt array using the 6 m^2 heliostats. The slanting truss member of the array was modeled as a series of beams to obtain an accurate profile of the rotations along its length. The long columns and the horizontal struts of the array were also modeled as beams.

Shown in Figure 5-11 is an idealized computer model of the 10 MWt array using the 49 m^2 heliostats. Since this structure is higher and has a

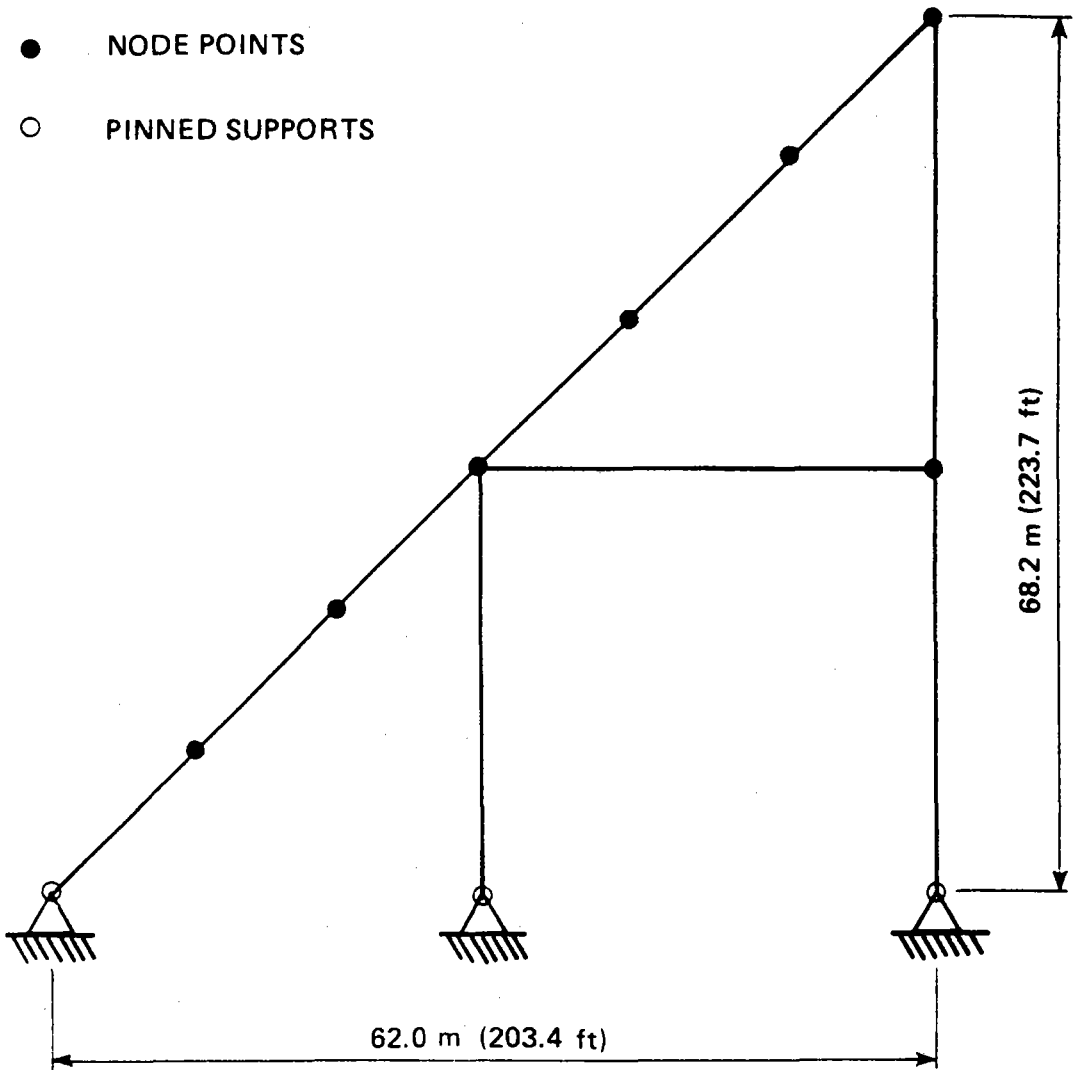

Figure 5-10. Idealized Model for the 10 MWt Array with 6 m^2 Heliostats.

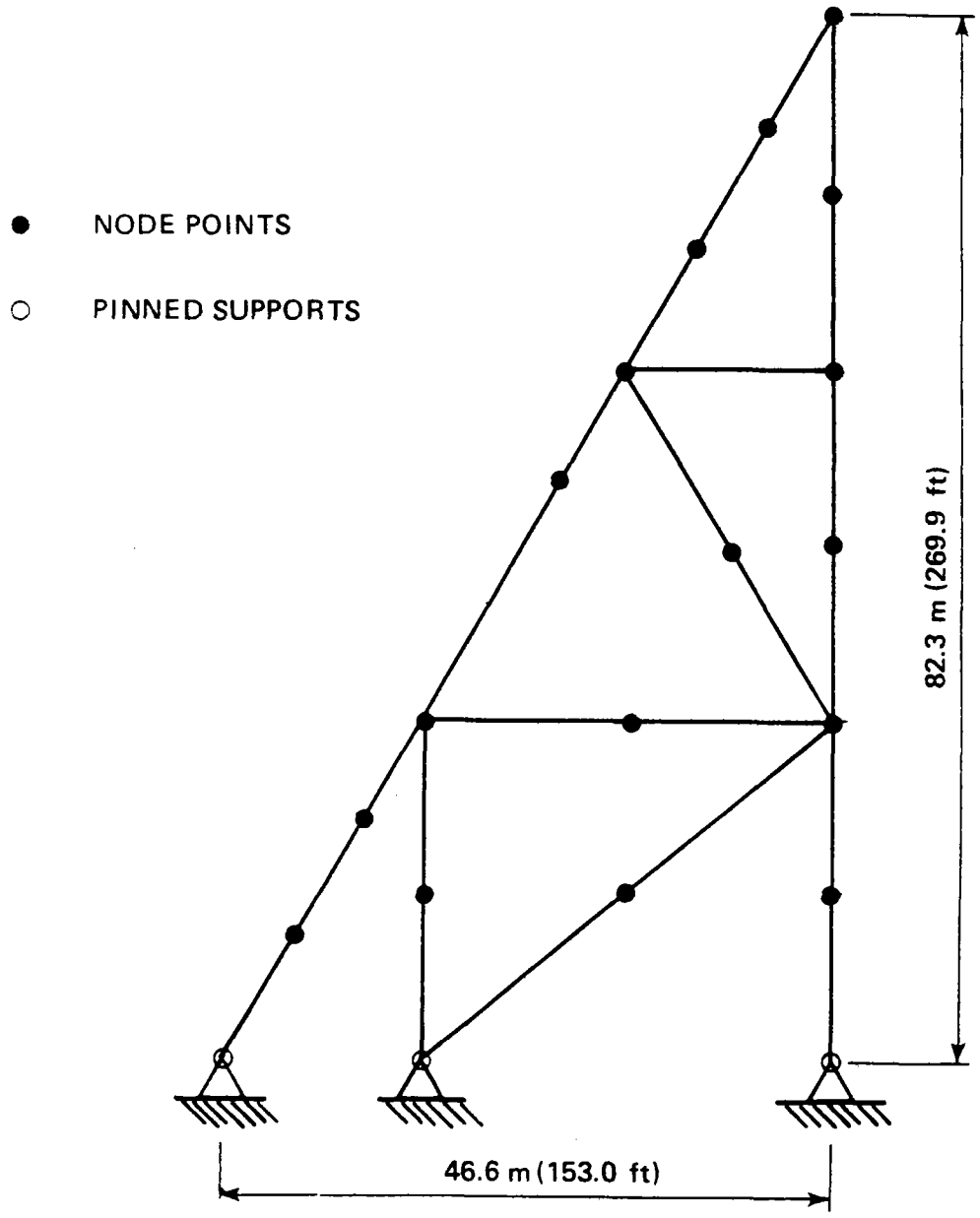

Figure 5-11. Idealized Model for the 10 MWt Array with 49 m^2 Heliostats.

steeper slope than the array using the 6 m^2 heliostats, more bracing members were used. Numerous node points were defined along the members in this model to obtain an accurate profile of the rotations of the slanting truss and to check the lateral deflections of the columns.

Computer results were given in terms of member stresses and rotations. Member stresses were checked against the allowable stresses but it was clear that these are generally low stress systems. The computer analysis could not check stability of members and so the array columns were manually checked against lateral buckling using the AISC interaction equation.

By checking the stresses of the 1 and 10 MWt arrays, for the 6 m^2 VIH heliostats, by this equation, it was found that buckling criteria had the most influence on the design of the structure rotations. Rotation of a heliostat at the top of the structure was 0.43 mrads for the 10 MWt array and 0.44 mrads for the 1 MWt array. This is well below the rotation limit of 1.5 mrads. This confirmed the efficiency of the design arrangement that was selected to reduce rotations.

Total steel quantities for the 1 and 10 MWt arrays and those estimated by extrapolation for the 25 MWt array are summarized in Table 5-7. By using structural optimization procedures, those quantities might be reduced. To account for bracing, access, walkways and ladders, an additional nominal twenty percent was added to the steel quantities. Since the stresses in the members for the VIH configurations are well within the allowable limits, and rotational criteria were easily met, optimization of these structures could reduce these quantities.

Table 5-7. Material Quantities for the 1:5 Aspect Ratio Arrays with 6 m^2 Heliostats.

Material	Units	Power Level (MWt)		
		1	10	25**
Steel*	ton	156	4380	14255
Concrete	cubic yard	102	2121	5754
Rebar	ton	3	47	156

* Includes 20% for bracing and acess
** Extrapolated quantities

It was determined from the analysis of the 10 MWt array having the 49 m^2 heliostats that stresses within the members were well within the allowable limits. Using the approximate method described earlier for finding the torsional properties of the supporting space frame, the maximum rotation of a heliostat at the top of the array was about 1.7 mrads. This exceeds the criteria limit of 1.5 mrads. However, by increasing some member sizes in this particular space truss, the maximum heliostat rotation could easily be reduced to 1.5 mrads or less. A summary of material quantities for this particular design is given in Table 5-8.

5.4.3 Costs Estimates of Modified Concepts

The results of the cost estimates for the more refined and detailed CRS structures are presented in Table 5-9 for four designs:

- A - 1 MWt array, 1:5 aspect ratio, 6 m^2 heliostat
- B - 10 MWt array, 1:5 aspect ratio, 6 m^2 heliostat

- C - 10 MWt array, 1:5 aspect ratio, 49 m^2 heliostat
- D - 25 MWt array, 1:5 aspect ratio, 6 m^2 heliostat

Table 5-8. Material Quantities for 10 MWt 1:5 Aspect Ratio Array with 49 m^2 Heliostats.

Materials	Quantities
Steel*	4036 tons
Concrete	516 cubic yards
Rebar	8.3 tons

* Includes 20% for bracing and access

The field costs presented here considered the same work items as were presented in the cost estimates for the preconceptual designs. However, the direct field costs were examined in much more detail than those given in the preconceptual designs and considered these additional work items:

- Heliostat installation
- Access, stairways
- Wiring

The indirect field costs were still taken as 60% of the direct field labor costs.

The total capital cost estimates are presented in Table 5-10. The total capital cost estimates include expenses for engineering services and an allowance for uncertainty in addition to the field costs.

Maintenance costs were also considered and include:

- o Heliostat mirror cleaning
- o Wiring system checking
- o Replacement of heliostat control wiring
- o Routine maintenance and miscellaneous items

Table 5-9. Conceptual Field Cost Estimates.

$ Thousands -- Second Quarter 1980

Configuration No.	A	B	C	D
Power Level	1 MWt	10 MWt	10 MWt	25 MWt
Aspect Ratio	1:5	1:5	1:5	1:5
Structure Height	72'	224'	270'	361'
Heliostat Size	6 m^2	6 m^2	49 m^2	6 m^2
No. of Heliostats	210	2046	252	5250
DIRECT FIELD COST*				
Heliostat Installation	100	940	150	2,420
Wiring	40	320	110	820
Access, Stairways	40	1,060	940	2,970
Foundation	40	690	150	1,890
Steel	290	7,690	6,650	23,900
DIRECT FIELD COST	510	10,700	8,000	32,000
INDIRECT FIELD COST**	160	2,780	1,760	8,100
FIELD COST	670	13,480	9,760	40,100
FIELD COST/MWt	670	1,348	976	1,604

*Second Quarter, 1980 Price & Wage Level **60% of Direct Labor Cost

Table 5-10. Capital Cost Estimate Summary

$ Thousands -- Second Quarter 1980

Configuration No.	A	B	C	D
Power Level	1 MWt	10 MWt	10 MWt	25 MWt
Aspect Ratio	1:5	1:5	1:5	1:5
Structure Height	72'	224'	270'	361'
Heliostat Size	6 m^2	6 m^2	49 m^2	6 m^2
No. of Heliostats	210	2046	252	5250
Field Cost	670	13,480	9,760	40,100
Engineering Services	130	1,320	990	3,900
Subtotal	800	14,800	10,750	44,000
Allowance for Uncertainity @ 15% of Subtotal	120	2,200	1,750	6,500
TOTAL CAPITAL COST	920	17,000	12,500	50,500
CAPITAL COST/MWt	920	1,700	1,250	2,020

Since the proposed site is in a desert environment, it was assumed that painting of the structure would not be required.

Bechtel's previous studies for ground mounted arrays have found annual maintenance costs of $0.90 per square meter of heliostat area. Due to the height of the UHA structures, labor rates for maintenance personnel must reflect hazard pay. Thus, a maintenance cost of $1.25 per square meter was estimated. Based on this estimate and a 30-year plant life, the life

cycle maintenance costs for these four designs, expressed in 1980 dollars, were estimated to be:

- o A - $ 60,000
- o B - $480,000
- o C - $480,000
- o D - $1,200,000

The net salvage values of these four arrays, based on a 30-year plant life and expressed in 1980 dollars, were determined to be:

- o A - $0
- o B - $140,000
- o C - $120,000
- o D - $435,000

The salvage values of these structures were considered and are dependent upon the need of the steel market during that particular period. Salvage values ranged from $0/ton to $50/ton of steel. Labor costs for design A, the smallest array, were so high that it was not cost-effective to salvage it.

5.5 OPTICAL PERFORMANCE

The detailed optical performance analysis was performed on Veda's Data General Eclipse C/350 digital computer. The Veda performance code is written in FORTRAN V and is both modular and operator interactive, thus permitting selection of both system description inputs and output functions.

The design specification established the number of rows and columns of heliostats to be used for structural design. The detailed optical performance modeling resulted in small increases to the number of columns of heliostats required in some designs. This was due to use of the 1976 Barstow

insolation data rather than the estimated data used during development of the design specification. A graph showing the annual average value and range of variation in the Barstow insolation as a function of time of day is shown in Figure 5-12.

Several intermediate outputs were developed in the performance analysis and recorded on magnetic tape for detailed post analysis. Among those developed were cosine, shading, and blocking factors for each heliostat, field cosine average, and cosine weighted averages for field shading and blocking factors.

Another intermediate output was an image at the aperture plane for each of 25 mirror segments on the Veda heliostat and for each of 64 segments on the repowering heliostat. The aperture plane was described in terms of a 45 x 45 array of square "bins" totaling 2,025 bins. The image at the aperture plane was evaluated for power delivered to each bin from each mirror segment. The area of one bin for the 1 MWt array was set at $0.01m^2$ and for the larger arrays at $0.1m^2$. The power accumulated in each bin over all the heliostats in the array was then added to determine the total collected power for each hour of each day investigated. The power distribution among the bins determines both radiant flux and accumulated power profiles. For visual analysis these power-per-bin levels were mapped on the aperture plane as alphabetic characters each representing a flux density increment of about 4%. A representative map is shown in Figure 5-13.

Inspection of these maps showed a steep dropoff in power density from a high intensity central image for arrays with the VIH. A typical flux density profile of the VIH heliostat is shown as Figure 5-14. Significantly,

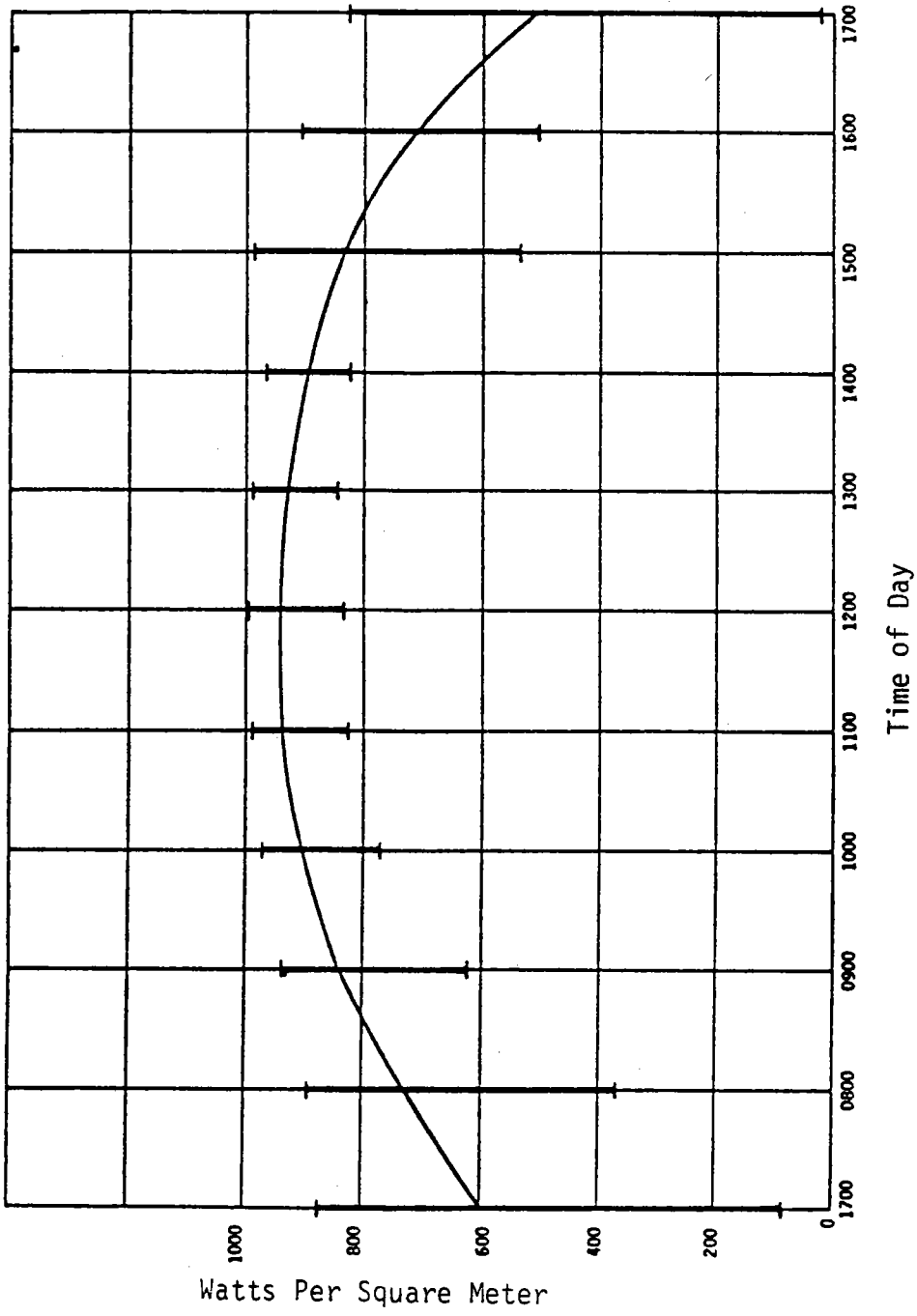

Figure 5-12. Barstow Annual Insolation 1976.

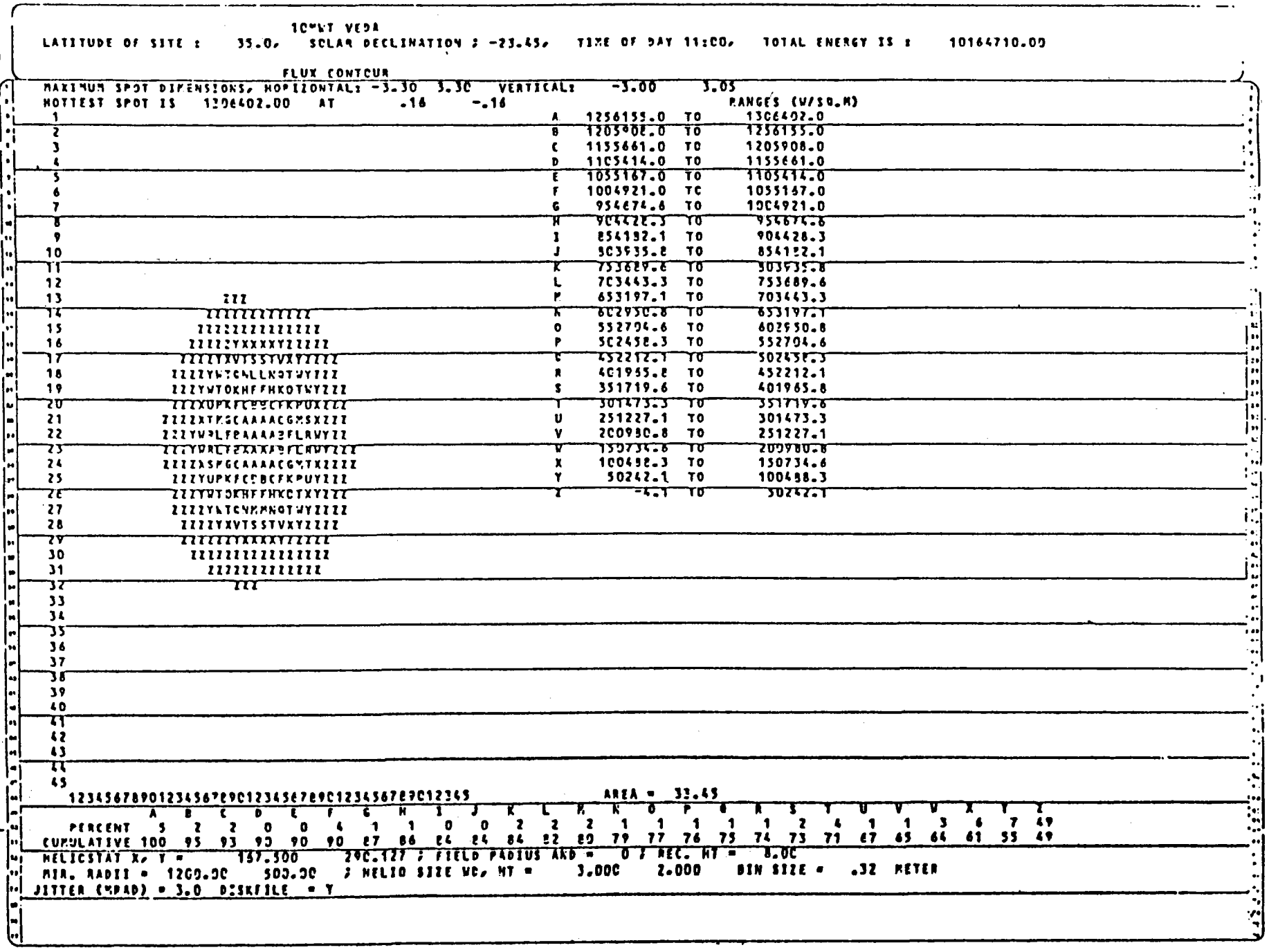

Figure 5-13. Example Map of Solar Image at Aperture Plane.

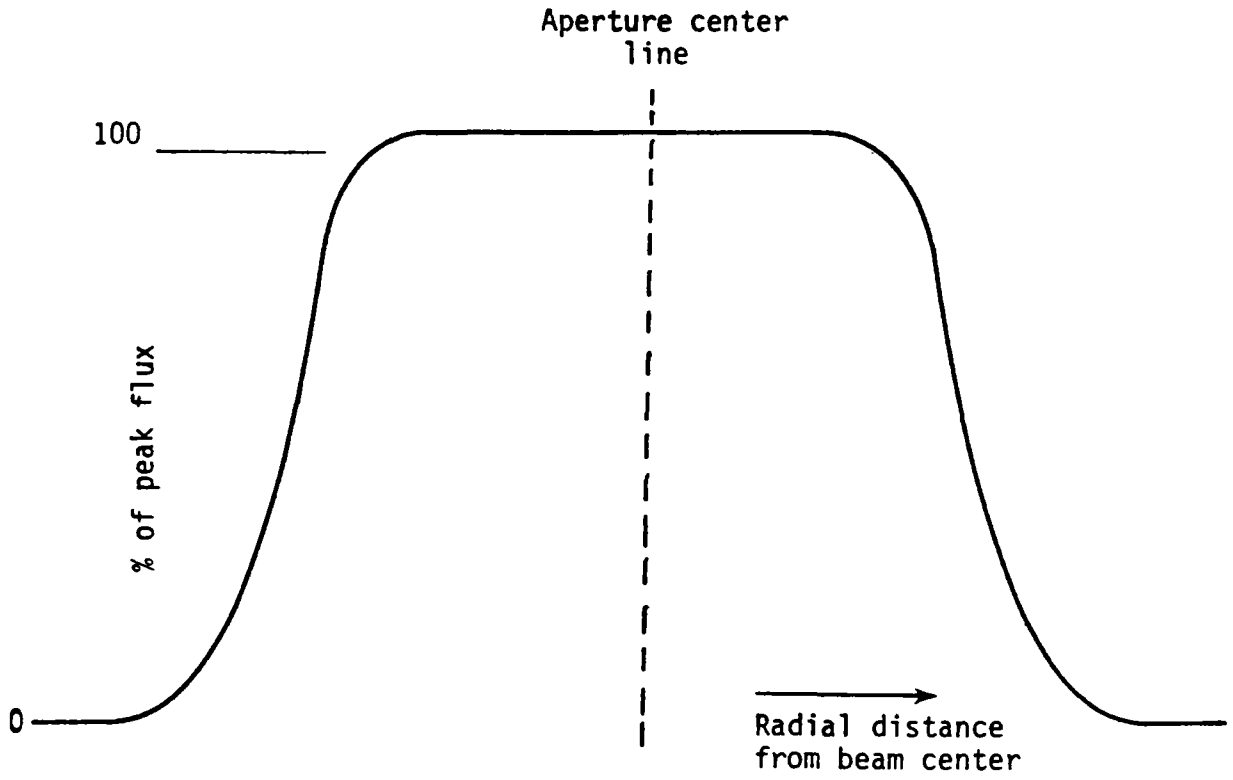

Figure 5-14. Typical Flux Distribution Profile for VIH.

the radius at which the dropoff occurs remains essentially constant throughout the day and throughout the year. By comparison, the repowering heliostat image is far more diffuse and variable throughout the year. Because of the strong radial dependence of flux density, both rectangular and circular apertures were chosen to meet design point power for each array. In each case the aperture dimensions were selected to provide the best compromise between annualized energy collected and total aperture size. The aperture sizes and resultant calculated annualized energy are shown in Table 5-11 for the four final designs. The "Percent of Total Power" is the percentage of the power delivered to the aperture plane that is actually collected by the aperture. These values were used in the calculations for cost of energy.

In sizing the apertures for the repowering heliostat to meet design point power, an effort was made to maintain an annual power level near that of the 10 MWt UHA using the VIH. This resulted in the UHA with the repowering heliostat having approximately 2% more net mirror area. However, due to the more diffuse image, the area of the aperture was still 14% to 21% larger than that required for the VIH. This resulted in a lower overall collection efficiency. As shown later, the diffuse image resulted in poorer high temperature capability for the repowering heliostat.

The two 10 MWt UHA configurations, studied under this contract, permitted a partial correlation of solar image characteristics, at the aperture plane, for the two different heliostats. Image size is related to heliostat size, focal length, slant range, and off-axis tracking angle. The repowering heliostat, due to the uniform radius of curvature usually employed, does not have the capability of minimizing the aberrations resulting from the variations

Table 5-11. UHA Apertures and Annualized Energy.

Design Point Power (MWt)	Annualized Energy (KWHT) Total Collected	Rectangular Aperture	Circular Aperture	Aperture Area (m^2)	Percent of Total Power
1 (VEDA)	2 467 082	2 379 283		2.1	96.44
			2 384 708	1.85	96.7
10 (VEDA)	24 209 839	23 741 744		18	98.1
			23 812 229	16.9	98.4
10 (Re-Powering)	24 814 556	23 400 598		20.97	94.3
			23 640 926	21.27	95.3
25 (VEDA)	60 198 778	59 517 621		42	98.9
			59 429 218	38.5	98.7

in off-axis tracking angles encountered throughout the day and throughout the year. The VIH, because of its dual radii of curvature and equatorial tracking mechanism, provides much better control of these abberations. Figures 5-15 through 5-20 provide side-by-side comparison of the images at the aperture plane for these two heliostats for early morning and noon at the winter solstice, equinox and summer solstice.

The range of flux density represented by each image description diagram extends from the peak flux density, to zero. This range is divided into 26 equal increments, the letter A representing flux densities between the peak flux and 25/26 of the peak flux, B the increment between 25/26 and 24/26, and

Repowering Heliostat

Peak Flux Density	0.593	$MWTm^{-2}$
Collected Power	6.488	MWT
Image Area	47.63	m^2

Veda Industrial Heliostat

Peak Flux Density	0.778	$MWTm^{-2}$
Collected Power	5.971	MWT
Image Area	33.95	m^2

Figure 5-15. Image Distribution at Aperture Plane.

Declination -23.44 Degrees
Time of Day 0800 Hours
Design Point Power 10 MWt
Scale: 1 Letter = 0.1m^2

Repowering Heliostat

Peak Flux Density	0.954	$MWTm^{-2}$
Collected Power	10.452	MWT
Image Area	35.65	m^2

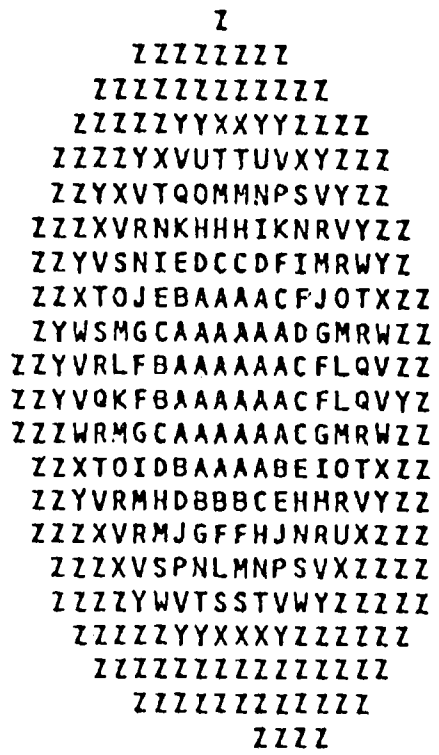

Veda Industrial Heliostat

Peak Flux Density	1.319	$MWTm^{-2}$
Collecter Power	10.266	MWT
Image Area	33.55	m^2

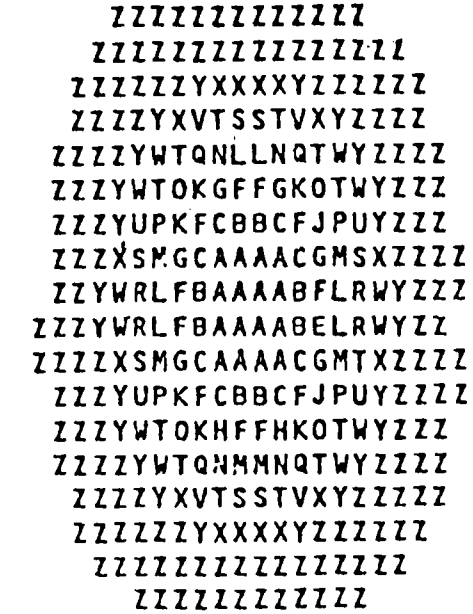

Figure 5-16. Image Distribution at Aperture Plane (Design Point)

Declination -23.44 Degrees
Time of Day 1200 Hours
Design Point Power 10 MWt_2
Scale: 1 Letter = 0.1 m^2

43905-80U/P0069

Repowering Heliostat

Peak Flux Density 0.311 $MWTm^{-2}$
Collected Power 3.427
Image Area 65.10 m^2

Veda Industrial Heliostat

Peak Flux Density 0.307 $MWTm^{-2}$
Collected Power 2.544 MWT
Image Area 33.65 m^2

Figure 5-17. Image Distribution at Aperture Plane.

Declination 0 Degrees
Time of Day 0700 Hours
Design Point Power 10 MWt
Scale: 1 Letter = 0.1m^2

Repowering Heliostat

Peak Flux Density	0.880	$MWTm^{-2}$
Collected Power	9.638	MWT
Image Area	43.04	m^2

Veda Industrial Heliostat

Peak Flux Density	1.216	$MWTm^{-2}$
Collected Power	9.465	MWT
Image Area	30.76	m^2

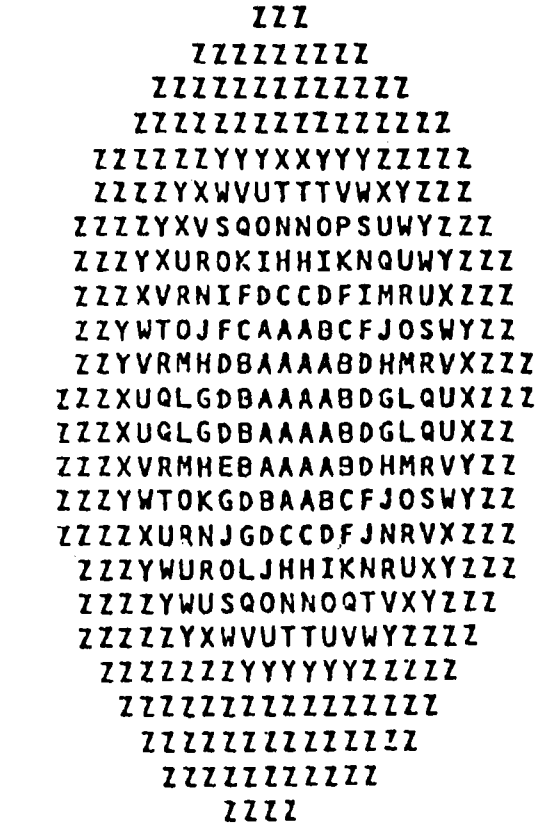

Figure 5-18. Image Distribution at Aperture Plane.

Declination 0 Degrees
Time of Day 1200 Hour
Design Point Power 10 MWt
Scale: 1 Letter = 0.1m^2

Repowering Heliostat

Peak Flux Density 0.159 $MWTm^{-2}$
Collected Power 2.148 MWT
Image Area 79. m^2

Declination 23.44 Degrees
Time of Day 0700 Hour
Design Point Power 10 MWt
Scale: 1 Letter = $0.1m^2$

Veda Industrial Heliostat

Peak Flux Density 0.409 $MWTm^{-2}$
Collected Power 3.312 MWT
Image Area 35.35 m^2

43905-80U/P0069

Figure 5-19. Image Distribution at Aperture Plane.

Peak Flux Density	0.766	$MWTm^{-2}$
Collected Power	8.466	MWT
Image Area	52.82	m^2

Peak Flux Density	1.068	$MWTm^{-2}$
Collected Power	8.307	MWT
Image Area	27.86	m^2

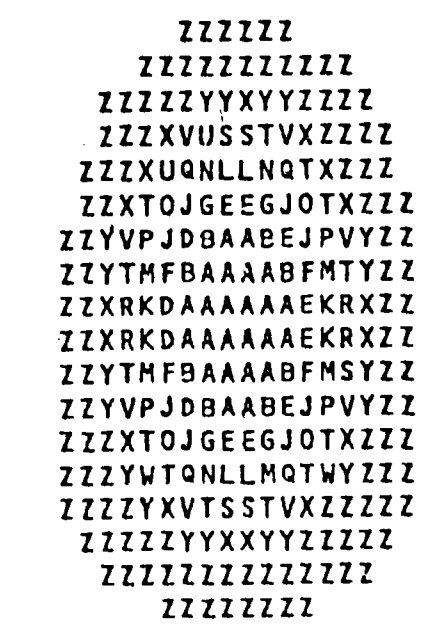

Figure 5-20. Image Distribution at Aperture Plane.

Declination 23.44 Degrees
Time of Day 1200 Hour
Design Point Power 10 MWt
Scale: 1 Letter = $0.1m^2$

so forth. Any bin containing zero flux is represented by a blank. Complete page prints for the computer output for these days are included within Appendix D. Additional data showing actual flux levels appears on these prints.

The radii of curvature were established to minimize image area for each heliostat type throughout the year. This curvature optimization was subject to the constraint that all heliostats in each UHA have the same mirror configuration. The optimization procedure is rather simple with the VIH design since the sagittal and tangential foci are controlled by orthogonal directions on the mirror surface. The equatorial mount maintains the proper orientation of the radii of curvature relative to the plane of the angle between the sun, mirror, and receiver.

The repowering heliostat optimization is a more difficult problem. Field experience has shown that minimizing image size throughout the year is best accomplished by adjusting the heliostat mirror facets such that the entire heliostat surface approximates a spherical surface. Since the curvature is spherical and remains essentially constant regardless of surface direction, controlling the sagittal and tangential foci can only be accomplished by changing this one radius of curvature. Variations in radius of curvature to correct for one deviation also affect the other, generally at a different time of year. Therefore, repeated cross checking must be done. Near the best radius of curvature, a variation of only a few tenths of 1% of the radius to improve one aberration seriously affects the other aberration at a different time of year. This is not a practical tolerance to impose on a production heliostat. The largest off-axis angles occur at 0700 on the summer solstice. The smallest off-axis angles occur at noon of the winter

solstice. The principle used to establish the radii of curvature is that the image should have the least area at each of these extremes consistent with retaining the image within the same linear dimensions throughout the year.

Referring to Figure 5-18, it can be seen that the image from the repowering heliostat at this time is very large. Attempts to reduce the image area for this particular day and hour resulted in an even more severe image expansion at other times during the year. Even with the optimized radius of curvature, the range of image area for the repowering heliostat was from 79.58 m^2 to 35.65 m^2. By comparison, the image from the Veda heliostat ranged in area from 35.35 m^2 to 27.86 m^2. The various radii of curvature used in this study are shown in Table 5-12.

Table 5-12. Radii of Curvature.

	1MWt VIH	10MWt VIH	10MWt RP	25 MWt VIH
Parallel to Declination Axis	180m	500m	-----	800m
Perpendicular to Declination Axis	275m	1200m	-----	1800m
Spherical	----	-----	850m	-----

Image quality is further illustrated by the flux contours shown in Figures 5-21 and 5-22. All the arrays produced a nearly circular image boundary at the 500 KWm^{-2} flux level. However, only the arrays with the VIH were capable of producing an image that exceeded 1 MWm^{-2} flux density. This illustrates that most of the energy delivered to the aperture plane by the arrays

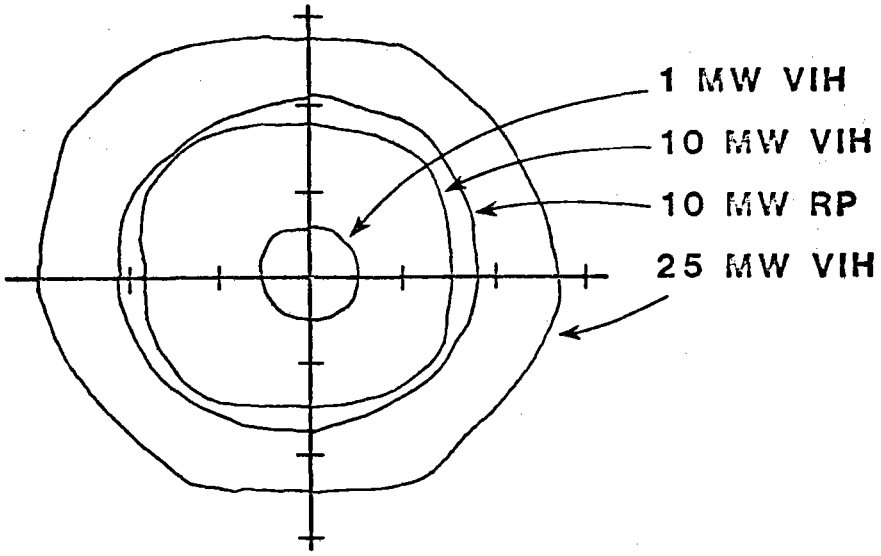

SCALE IN METERS

Figure 5-21. 500 KWm^{-2} Flux Contours at Design Point.

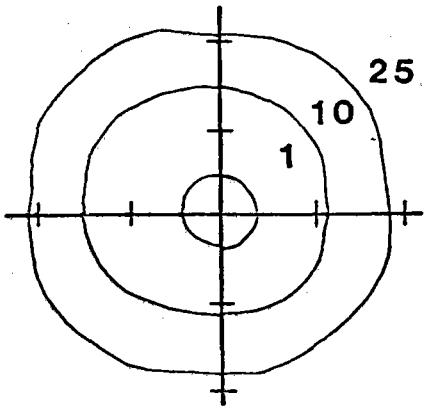

VIH 1, 10, 25 MWt
RP 10 MWt DID NOT
ACHIEVE 1 MW/m^2

SCALE IN METERS

Figure 5-22. 1 MWm^{-2} Flux Contours at Design Point.

with the VIH was concentrated in the central part of the image. In contrast, the diffuse image produced by the array with the repowering heliostat spread the energy over a much larger area. These plots show flux density at design point. Several salient features can be observed. The most important are: (1) the repowering heliostat never achieved a flux density of 1 MWm^{-2}; (2) the relatively diffuse quality of the repowering heliostat results in a larger aperture at the 500 KWm^{-2} boundary than is produced by the VIH; (3) the steep slope from 1 MWm^{-2} to 500 KWm^{-2} for the VIH plots, which is typical of the central region boundary of the VIH image throughout the day and year.

In applications which are oriented towards heating a working fluid for electrical power generation, the poorer imaging ability of the repowering heliostat may be acceptable. However, for applications which are oriented towards high temperatures or which depend on high flux densities, such as coal gasification, the imaging ability of the VIH provides a distinct advantage.

The image quality effects are most noticeable at aperture temperatures above 1200°K. The tables in Sections D-2 and D-3 of Appendix D illustrate this effect dramatically. The repowering heliostat, using the preferred round aperture, supplies usable power at 1500°K for between five and eight hours per day. The VIH consistently supplies more usable power for at least eight hours on each of the corresponding days.

Although it was not part of this contract, Veda investigated an azimuth-elevation mounted heliostat, with spherical curvature, having the same physical area as the VIH. The same effects were observed for this case as with the 49 m^2 heliostat. That is, the image exhibited the same

characteristics of diffuseness and variability of size. Even though it was slightly smaller than the image formed by the 49 m^2 heliostat the VIH produced image was still smaller throughout most of the year.

In order to develop the cost of usable energy, several apertures, smaller than the design point aperture, were selected for each array. Both rectangular and circular apertures were selected for analysis to determine which type of receiver geometry would be best suited to the beam characteristics. For each aperture selected, spillage was a variable which exceeded 50% in some cases. For each aperture/array combination, a range of working temperatures from 1000°K to 2000°K was used to calculate reradiation losses. The total remaining energy was then calculated for each combination as an annualized usable energy for a nominal 330 day operational year. These results were used in the cost of usable energy calculations.

5.6 COST OF ENERGY/COST OF USABLE ENERGY

5.6.1 Derivation of Costs

Use of the levelized charge methodology of Reference 4-2 develops a fixed price to be charged per unit of output energy. When collected as income over the system lifetime it will exactly provide for payment of all expenses.

Expenses include: capital expenditures for the construction phase, return on investment for the capital expended, recovery of capital at a constant rate, operation and maintenance during the system life, and General and Administrative expenses (G&A).

The major capital expenditures occur at various times throughout the construction phase. Prior to expenditure, capital earns at the cost of money. After expenditure, but prior to the first year of commercial operation, the return to investors on the expended capital must be obtained from the remaining capital. Once earnings begin, the year of first commercial operation, all current expenses are paid from income, and retained earnings begin to earn at the cost of money. At the end of system life, all expenses, including return on investment, have been paid. The capital on hand, including that recovered by salvage, is equal to the capital investment and is returned to the investors. Major milestones of the project lifetime are shown in Figure 5-23.

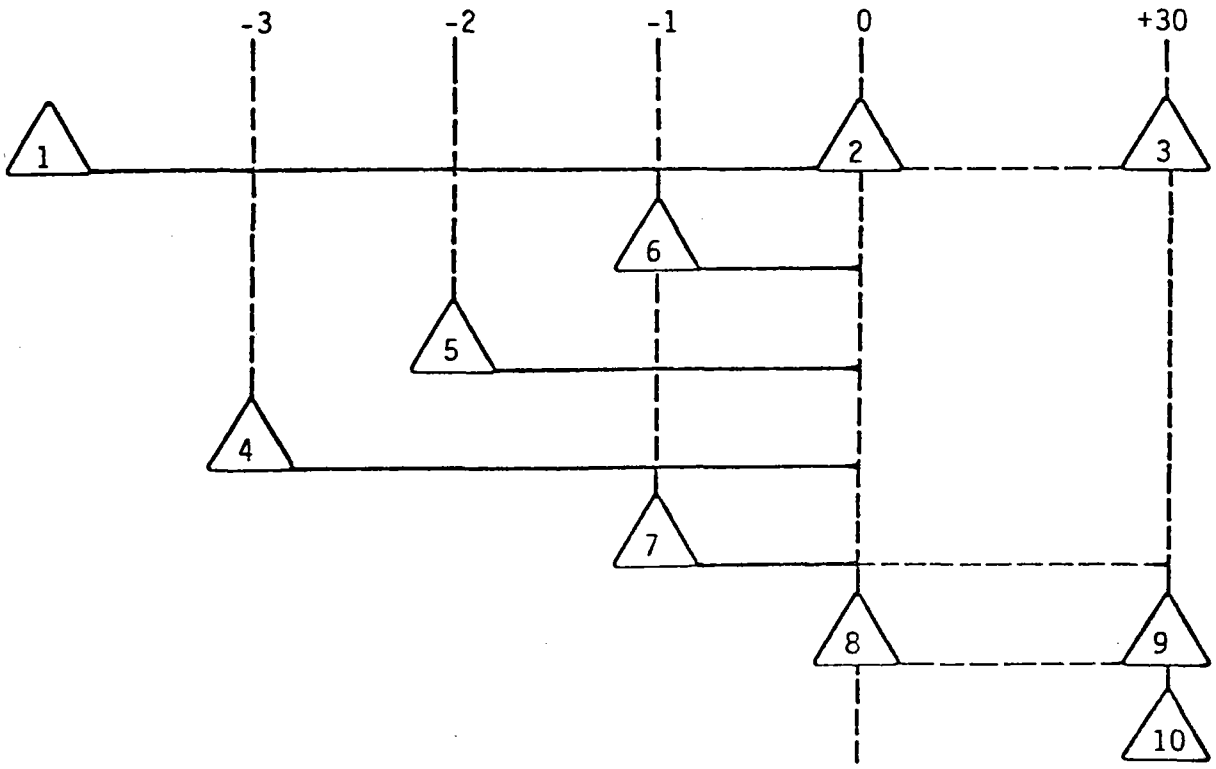

Figure 5-23. Milestones for Cost Analysis.

Milestones 1, 2, and 3 are the initial capital accumulation, first commercial operation and the end of the system life. Milestones 4, 5, and 6 are the major capital expenditures required during system construction. Milestone 7 is the start of operational expenses. Milestones 8 and 9 are the start and end of the levelized earnings. Milestone 10 is the capital payback at the end of the system life.

Bechtel National, Incorporated priced the construction effort for each of the four UHA designs based on the design specification, Reference 5-1. The detailed optical performance analysis showed a requirement for a small quantity of additional heliostats which could be added in such a manner as to linearly increase the cost of the arrays to which they were added. The modified heliostat count is included as the final table of Appendix C. The final field layout is shown in Figure 5-24. Veda linearly extrapolated Bechtel's price estimates of the structure to accommodate the added heliostats.

The total capital expenditures required for each UHA was composed of four elements. The cost for land, taken at $10,000 per acre, included the total rectangular area given as Area II in Figure 5-24. The second element was the cost of the structure as extrapolated by Veda from Bechtel's basic estimates. (It should be noted that these estimates include heliostat installation and wiring). The third cost element was the heliostats. The 6 m^2 VIH was estimated at $\$125/m^2$ and the 49 m^2 repowering heliostat at $\$230/m^2$. The last cost element was the heliostat central controller. Its cost of $39,200 was based on current prices for Eclipse S/140 computer systems and the interface drivers. These elements were subject to the cost of money rates assumed, but were not subject to the escalation rates.

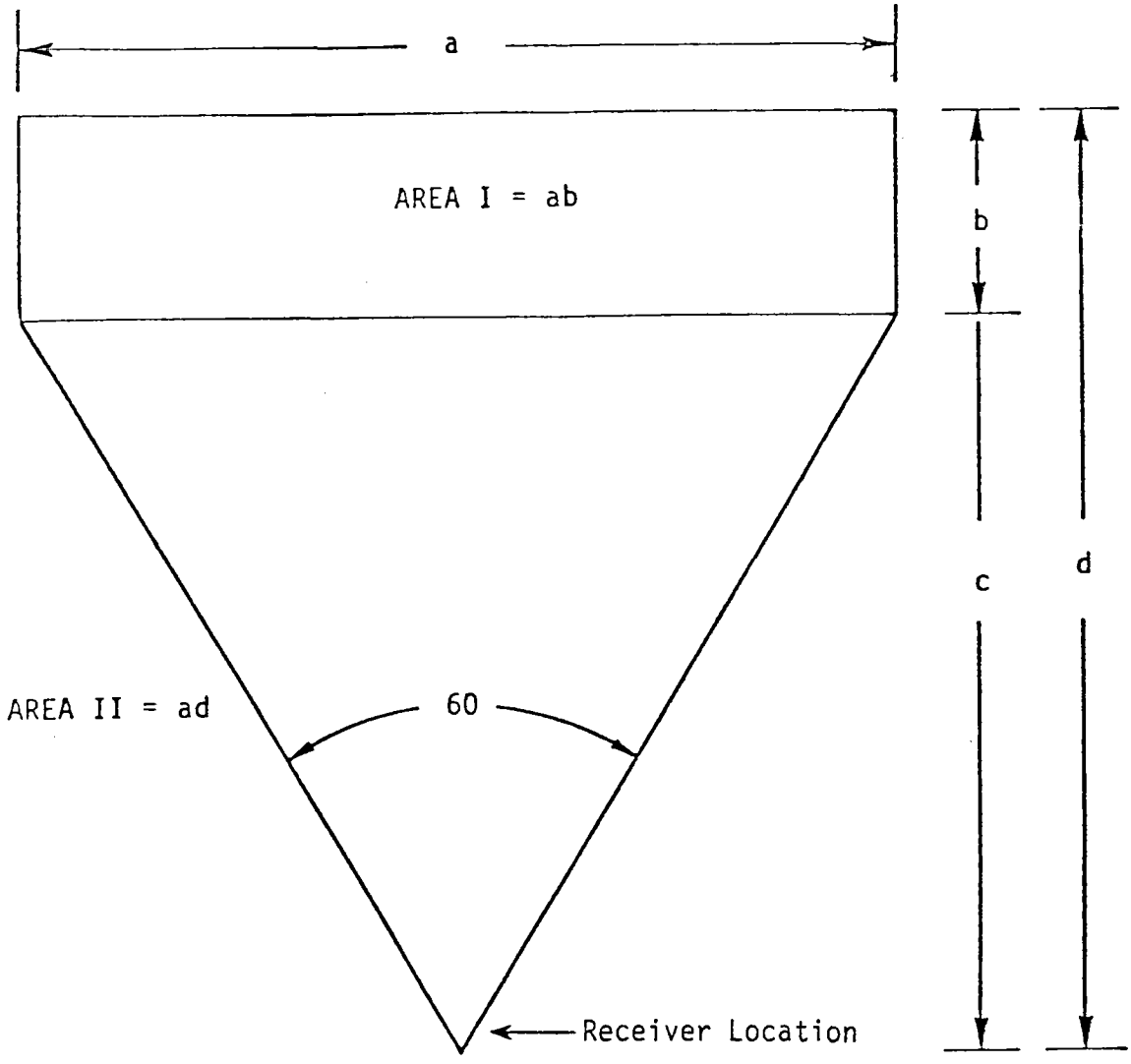

UHA Field Layout 1:5 Aspect Ratio

Power MWT)	Helio-stat	a	b	c	d	Area I	Area II
1V	VIH	105M	20M	90.93M	110.93M	0.52A	2.88A
10V	VIH	340M	62M	294.45M	356.45M	5.21A	29.95A
25V	VIH	530M	100M	458.99M	558.99M	13.10A	73.21A
10	Rep.	425.36M	46.62M	368.38M	415M	4.91A	43.62A

Figure 5-24. UHA Field Layout.

Escalatable costs for each UHA include: the cost of heliostat maintenance, electrical power for operation and structural lighting, direct labor for operation and maintenance, G&A expense, and an allowance for contingencies. The basis for estimation of direct labor includes, for the 1 MWt UHA, fourteen person days per week at a rate which would pay wages and employer paid taxes, insurance, and other fringe benefits. For the 10 MWt UHA it was assumed that the labor force would be double that required for the 1 MWt design, and for the 25 MWt UHA the requirement would be three times that required for the 1 MWt design. G&A was estimated at 50% of direct labor, and contingencies were estimated at 5% of heliostat maintenance cost.

The capital expenditures and the costs subject to escalation are shown in the top half of Tables 5-13 through 5-16 for each UHA configuration. The capital expenditure items are shown in the calendar year in which they occur. The cost items subject to escalation are shown only in the first year in which they occur.

This cost analysis assumed three costs of money, equal to the internal rate of return, of 8%, 10%, and 15%. This leads to three different capital investments for each UHA design to account for the accumulated interest for the three year construction period. This results in three different capital recovery factors and three different amounts for annual return on investment. Three escalation rates were assumed of 6%, 8%, and 10%. Thus, escalatable costs for system lifetime result in three different values of total O&M costs for each UHA. Since retained earnings earn at cost of money, each set of O&M costs associated with its escalation factors, results in three different requirements for annual earnings for each cost of money rate.

Table 5-13. Cost Analysis Summary: 1 MWt - VIH.

(All Values In 1000's of 1980 Dollars)

DIRECT CAPITAL EXPENDITURES				
Year of Expenditure	1981	1982	1983	1984
Land At $10,000 Per Acre	28.8			
Structure	130.0	600.0	190.0	
Heliostats At $125.50 m^{-2} net area = 1260 m^2		158.13		
Central Controller			39.2	
Total Capital Expenditures	158.8	758.13	229.2	
COSTS SUBJECT TO ESCALATION				
Heliostat Maintenance Cost At $1.25 m^{-2}			1.575	
Electrical Power Costs At $0.06/KWH				
0.1 KWH/Day/Heliostat			0.46	
3.0 KWH/Day Central Controller			0.066	
12.0 KWH/Day structural Lighting			0.263	
ELECTRICAL POWER SUBTOTAL			0.789	
Direct Labor At $100/Person/Day Size Multiplier = 1			73.0	
G&A At 50% Of Direct Labor			36.5	
Contingencies At 5% of Maintenance			0.08	
Total O&M Subject To Escalation			111.944	

Cost Of Money	Capital Investment Required Total / Per Ins KWt	Capital To Be Recovered Less Salvage Of -0-	Annual Capital Recovery Factor	Annual Interest On Capital Investment	Escalation Rate	31 Year O&M Costs	Levelized Annual Earnings For O&M	Total Annual Levelized Charge
8%	1233.20 / 1.23	1233.20	11.862	98.66	6%	9493.04	236.16	346.68
					8%	13807.83	308.26	418.78
					10%	20367.47	411.45	521.97
10%	1255.29 / 1.26	1255.29	8.446	125.53	6%	9493.04	223.00	356.90
					8%	13807.83	283.35	417.33
					10%	20367.47	368.124	502.10
15%	1311.06 / 1.31	1311.06	3.476	196.66	6%	9493.04	200.47	400.57
					8%	13807.83	240.12	440.26
					10%	20367.47	293.281	493.42

Table 5-14. Cost Analysis Summary: 10 MWt - VIH.

(All Values in 1000's of 1980 Dollars)

DIRECT CAPITAL EXPENDITURES				
Year of Expenditure	1981	1982	1983	1984
Land At $10,000 Per Acre	299.5			
Structure	1000.0	11127.46	5357.58	
Heliostats At $ 125.50 m^{-2} net area = 12648 m^2		1587.13		
Central Controller			39.2	
Total Capital Expenditures	1299.5	12714.59	5396.78	
COSTS SUBJECT TO ESCALATION				
Heliostat Maintenance Cost At $1.25 m^{-2}			15.810	
Electrical Power Costs At $0.06/KWH				
0.1 KWH/Day/Heliostat			4.481	
3.0 KWH/Day Central Controller			0.066	
36.0 KWH/Day structural Lighting			0.789	
ELECTRICAL POWER SUBTOTAL			5.336	
Direct Labor At $100/Person/Day Size Multiplier = 2			146.0	
G&A At 50% Of Direct Labor			73.0	
Contingencies At 5% of Maintenance			0.791	
Total O&M Subject To Escalation			240.937	

Cost Of Money	Capital Investment Required Total / Per Ins KWt	Capital To Be Recovered Less Salvage Of 140.0	Annual Capital Recovery Factor	Annual Interest On Capital Investment	Escalation Rate	31 Year O&M Costs	Levelized Annual Earnings For O&M	Total Annual Levelized Charge
8%	20644.27 / 2.06	20504.27	197.232	1651.54	6%	20431.86	508.28	2357.05
					8%	29718.58	663.46	2512.23
					10%	43836.9	885.50	2734.27
10%	20955.22 / 2.10	20815.22	140.046	2095.52	6%	20431.86	479.92	2715.49
					8%	29718.58	609.82	2845.39
					10%	43836.9	792.32	3027.89
15%	21737.15 / 2.17	21597.15	57.266	3260.57	6%	20431.86	431.42	3749.26
					8%	29718.58	516.80	3834.64
					10%	43836.9	621.23	3939.07

Table 5-15. Cost Analysis Summary: 10 MWt - Repowering.

(All Values In 1000's of 1980 Dollars)

DIRECT CAPITAL EXPENDITURES				
Year of Expenditure	1981	1982	1983	1984
Land At $10,000 Per Acre	436.2			
Structure	900.0	10139.29	2800	
Heliostats At $230.00 m^{-2} net area = 12884 m^2		2963.32		
Central Controller			39.2	
Total Capital Expenditures	1336.2	13102.61	2839.2	
COSTS SUBJECT TO ESCALATION				
Heliostat Maintenance Cost At $1.25 m^{-2}			16.105	
Electrical Power Costs At $0.06/KWH				
0.2 KWH/Day/Heliostat			1.222	
3.0 KWH/Day Central Controller			0.066	
36.0 KWH/Day structural Lighting			0.789	
ELECTRICAL POWER SUBTOTAL			2.077	
Direct Labor At $100/Person/Day Size Multiplier = 2			146.0	
G&A At 50% Of Direct Labor			73.0	
Contingencies At 5% of Maintenance			0.805	
Total O&M Subject To Escalation			237.985	

Cost Of Money	Capital Investment Required Total / Per Ins KWt	Capital To Be Recovered Less Salvage Of 120	Annual Capital Recovery Factor	Annual Interest On Capital Investment	Escalation Rate	31 Year O&M Costs	Levelized Annual Earnings For O&M	Total Annual Levelized Charge
8%	18548.56 / 1.85	18428.56	177.25	1483.88	6%	20181.53	502.03	2163.16
					8%	29354.47	655.33	2316.46
					10%	43299.81	874.63	2535.76
10%	18868.87 / 1.87	18748.87	126.14	1886.89	6%	20181.53	474.05	2487.08
					8%	29354.47	602.34	2547.36
					10%	43299.81	782.61	2701.54
15%	19674.33 / 1.97	19554.33	51.85	2951.15	6%	20181.53	426.11	3429.11
					8%	29354.47	510.47	3513.47
					10%	43299.81	623.50	3626.50

Table 5-16. Cost Analysis Summary: 25 MWt - VIH.

(All Values In 1000's of 1980 Dollars)

DIRECT CAPITAL EXPENDITURES				
Year of Expenditure	1981	1982	1983	1984
Land At $10,000 Per Acre	732.1			
Structure	3000.0	27981.0	10000.0	10000.0
Heliostats At $ 125.50 m^{-2} net area = 31800 m^2		3990.82		
Central Controller			78.4	
Total Capital Expenditures	3732.1	31971.9	10078.4	10000.0
COSTS SUBJECT TO ESCALATION				
Heliostat Maintenance Cost At $1.25 m^{-2}			39.75	
Electrical Power Costs At $0.06/KWH				
0.1 KWH/Day/Heliostat			11.607	
6.0 KWH/Day Central Controller			0.131	
50.0 KWH/Day structural Lighting			1.095	
ELECTRICAL POWER SUBTOTAL			12.833	
Direct Labor At $100/Person/Day Size Multiplier = 3			219.0	
G&A At 50% Of Direct Labor			109.5	
Contingencies At 5% of Maintenance			1.99	
Total O&M Subject To Escalation			383.075	

Cost Of Money	Capital Investment Required Total / Per Ins KWt	Capital To Be Recovered Less Salvage Of 435.0	Annual Capital Recovery Factor	Annual Interest On Capital Investment	Escalation Rate	31 Year O&M Costs	Levelized Annual Earnings For O&M	Total Annual Levelized Charge
8%	62878.07 / 2.52	62443.07	60.72	5030.25	6%	32485.40	808.12	6439.09
					8%	47250.72	1054.85	6685.82
					10%	69697.98	1407.86	7038.83
10%	64739.66 / 2.59	64304.66	448.55	6473.97	6%	32485.40	763.05	7685.57
					8%	47250.72	969.56	7892.08
					10%	69697.98	1259.73	8182.25
15%	69549.06 / 2.78	69114.06	183.24	10432.36	6%	32485.40	685.88	11301.48
					8%	47250.72	821.69	11437.29
					10%	69697.98	1003.62	11619.33

The annual levelized charge is the sum of three annual levelized quantities: (1) capital recovery factor; (2) return on investment; and (3) earnings to supply O&M expenses. The nine combinations of three escalation rates and three cost of money rates yield nine levelized charge values for each UHA. These values are shown as the final column in the bottom half of the cost analysis summary tables (5-13 through 5-16). It is these values which are divided by the total annual collected energy to give the levelized cost of energy required by the methodology.

The second column in the bottom part of the tables shows the capital investment required as a function of the cost of money. In addition to the total investment, the cost per installed kilowatt is also given. These values are plotted in Figure 5-25, as a function of the cost of money, for each UHA configuration. Because the scales are linear, the installed cost may be determined for any interest rate. This figure also further illustrates the effect of structure size on total cost due to increased structure height.

5.6.2 Cost of Energy

The levelized charge per unit of energy is derived by dividing the annual levelized charge by the annual energy produced. This resultant value is commonly referred to as the cost of energy. For purposes of this study, the energy produced is equated to the energy delivered through an aperture by the UHA. The basic cost of energy, as developed by this study, has no assumed temperature dependence. That is, at temperatures below 811°K (1000°F), it is assumed that reradiation losses from the receiver aperture are negligible. Evaluation of convection and conduction losses were outside of the scope of effort. To determine the delivered energy, two apertures for each UHA design

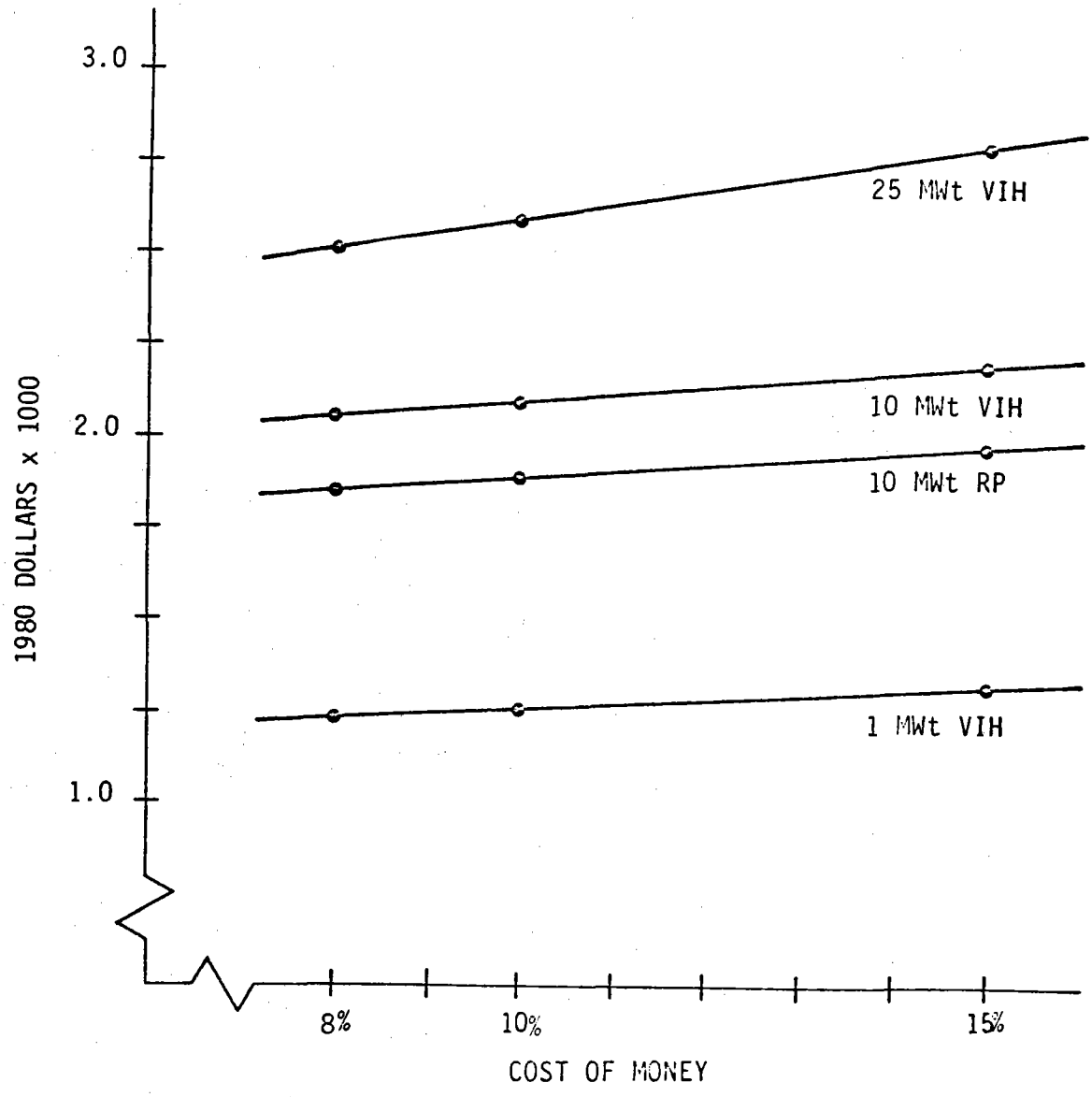

Figure 5-25. UHA Installed Cost Per KWt.

were chosen such that the spillage was approximately 2% of the annual energy delivered to the aperture plane. Each set of two contained a rectangular and a circular aperture to account for receiver geometrics currently under study by DOE. These four sets of apertures were called the design point apertures since, after spillage losses, the design point power rating for each UHA was achieved.

Because of the nine values of annual levelized charge for each array, the two apertures result in eighteen values of the cost of energy for each array. The tabular values of this cost are presented in Appendix E of this report. Tables E-1 through E-8 give the values in dollars per KWHt and Tables E-9 through E-16 express them in dollars per 10^6BTU. There is a negligible difference between the rectangular and circular apertures for the basic, temperature independent, cost. This basic cost is shown for the four arrays, as a function of cost of money, in Figure 5-26. To simplify the figure, the values corresponding to an escalation rate of 8% were plotted since this rate most accurately reflects current economic conditions.

This figure, in addition to providing a graphic of basic costs, illustrates the interaction of capital investment and O&M costs for projects of this type. The larger arrays show cost trends which rise relatively linearly with interest rate and maintain the same relative positions that were shown in the capital investment curves of Figure 5-25. However, the 1 MWt array demonstrates a relative insensitivity to interest rate, but has reversed its position from Figure 5-25. This is due to the dominance of O&M costs. The 1 MWt pays an O&M penalty primarily due to the lifetime cost of operational personnel. For example, it only produces one tenth of the output of the

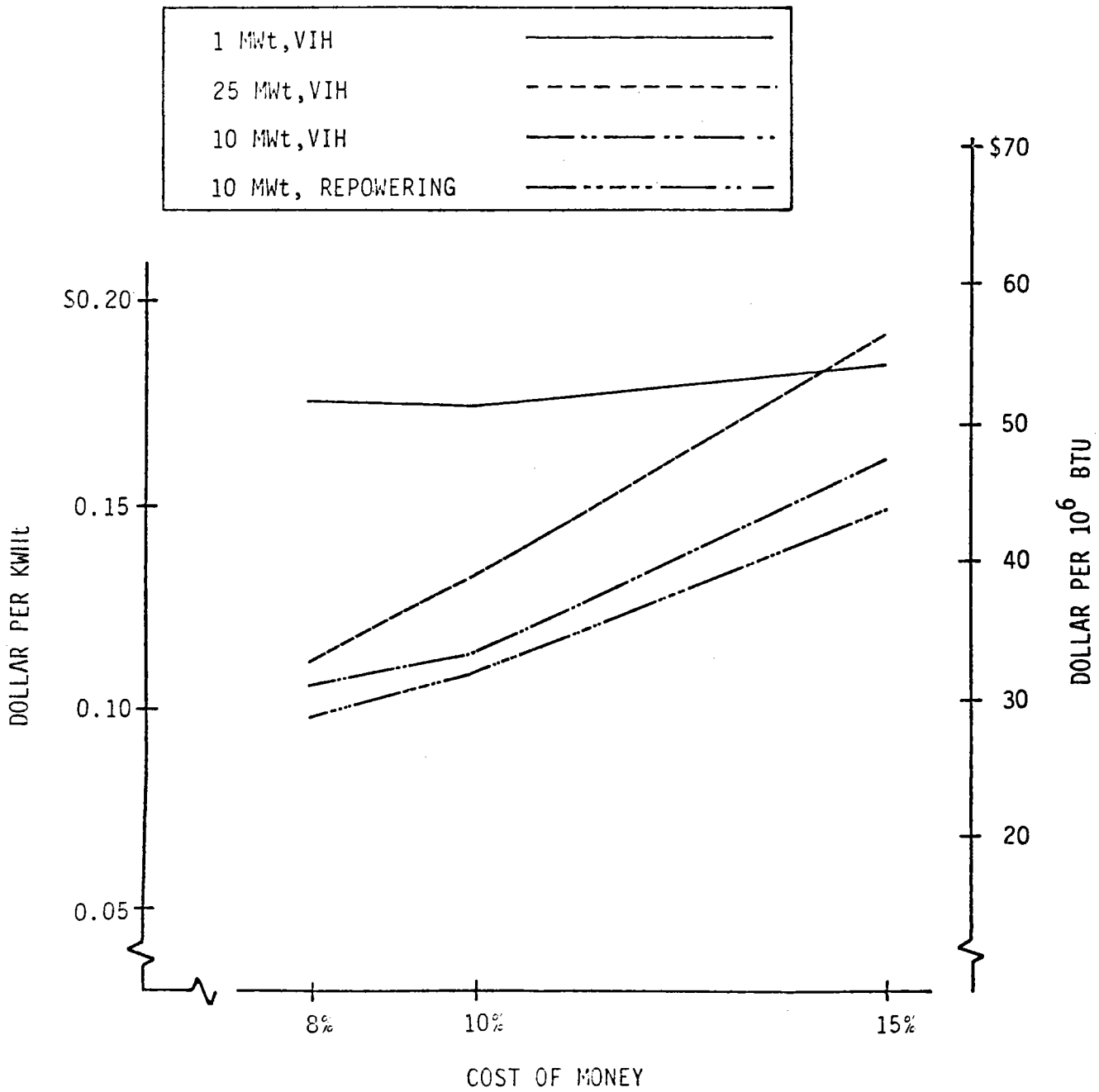

Figure 5-26. Cost of Energy for 8% Escalation.

10 MWt arrays but requires a staffing level that is one half that of the larger arrays. It is this difference in O&M cost per unit output, accumulated over 30 years of operation, that puts the smaller array at an economic disadvantage.

5.6.3 Cost of Usable Energy

Most published documents relating to central receiver systems do not express cost of energy as a function of temperature. Temperature is usually assumed, or stated, to be a constant operating temperature for the system and is usually below 811°K (1000°F). The UHA concept was specifically designed to provide industrial process heat at much higher operating temperatures, generally in the range of 1000°K to 2000°K. In this high temperature range, the cost of energy exhibits a strong temperature dependence.

In order to provide a meaningful comparison of costs for this temperature range, this study introduces the concept of the "cost of usable energy". At temperatures of 1000°K and above, reradiation losses become dominant, on the order of one to two orders of magnitude larger than all other losses in a well designed receiver. Therefore, for this study, reradiation losses were assumed to be the total losses at higher temperatures and "usable energy" was defined as the difference between the energy delivered through the aperture by the collector field and the energy lost through the aperture by reradiation. The cost of usable energy is then determined by dividing the annual usable energy collected by the annual levelized charge.

This study evaluated the cost of usable energy from 1000°K to 2000°K in steps of 250°K. Thus, for each aperture for each array, forty-

five values of the cost of usable energy were developed to reflect the nine combinations of interest and escalation rates for each of five temperatures. This data is presented in the tables in Appendix E.

Since reradiation losses are directly proportional to aperture area, it was felt that energy costs at the higher temperatures could be lowered by reducing reradiation losses at the expense of greater spillage. To this end, several aperture sizes, smaller than the design point apertures, were investigated for each array. In general, it was found that reducing the aperture size did lower the costs below those for the design point apertures at the higher temperatures. The resultant cost of energy values are given in Tables E-17 through E-30 in Appendix E.

Figures 5-27 through 5-30 show the operational efficiency for various aperture sizes as a function of temperature for each of the arrays. Operational efficiency is defined to be the ratio of usable energy collected by an aperture divided by the total energy directed to the aperture by the collector field. The figures plot this ratio as a percent. The shaded area is that region in which no temperature dependence was assumed. That is, the temperature scale has no meaning below 1000°K.

The figures illustrate that for all the arrays, the crossover point in allowing increased spillage to minimize reradiation losses occurs between 1250°K and 1500°K. Beyond 1500°K the negative slope of the design point aperture curves is so great that 1750°K operation is precluded. Thus, to operate beyond 1500°K, very small apertures are necessary. This again emphasizes the need to maintain a small, well controlled image. Referring to Figures 5-28 and 5-29, it can be seen that the superior image quality of

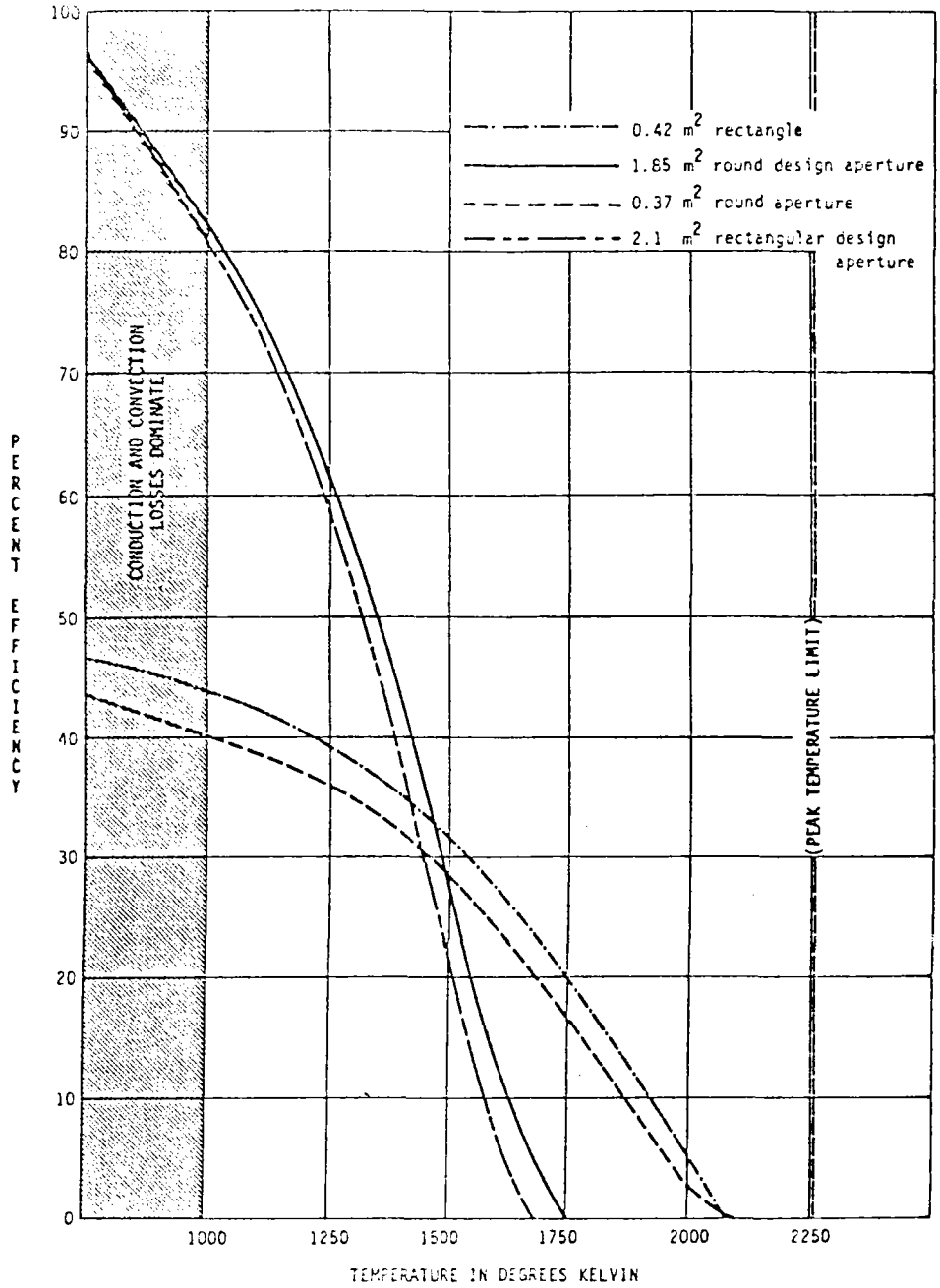

Figure 5-27. Aperture Efficiencies: 1 MWt - VIH.

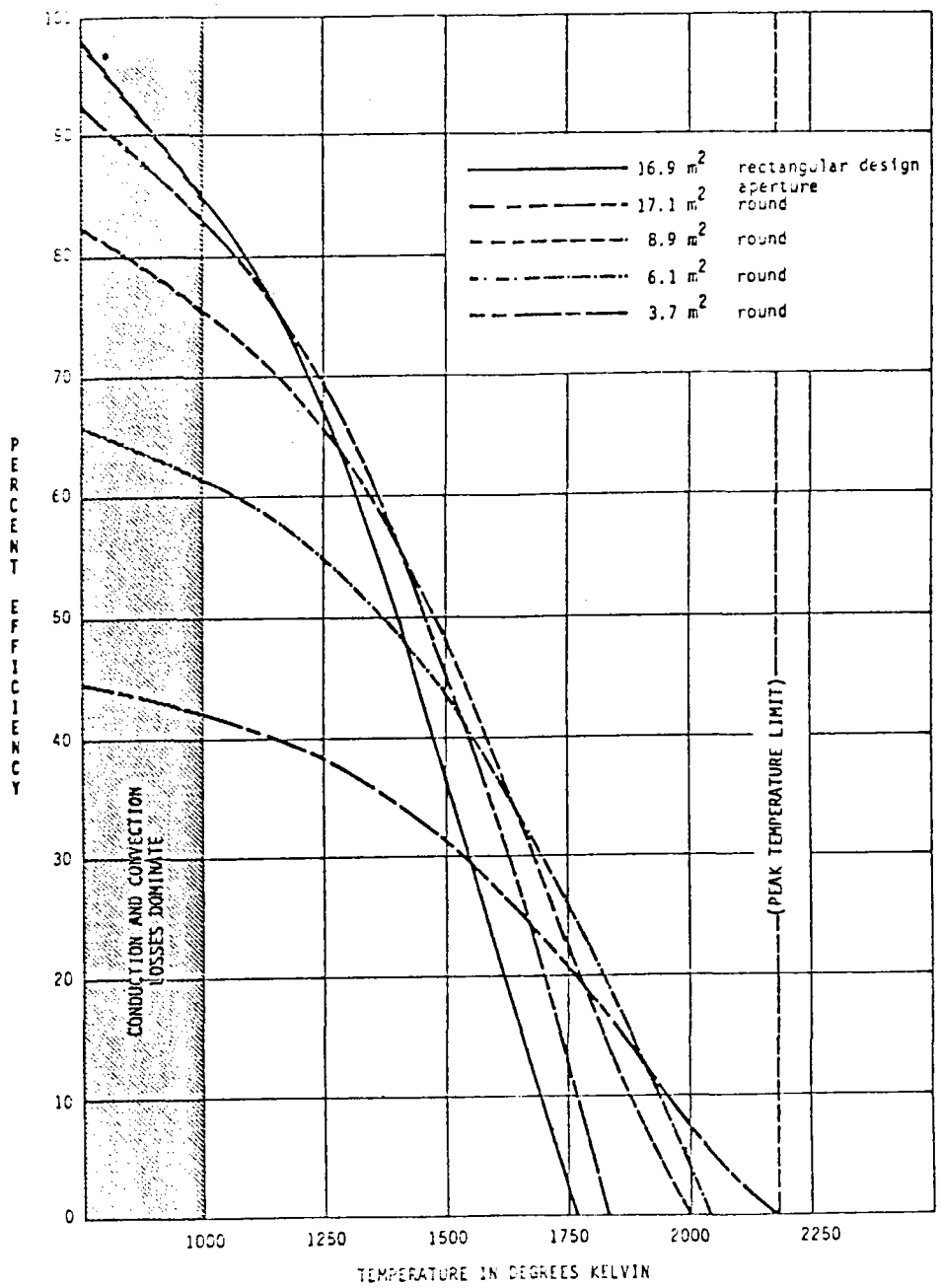

Figure 5-28. Aperture Efficiencies: 10 MWt VIH.

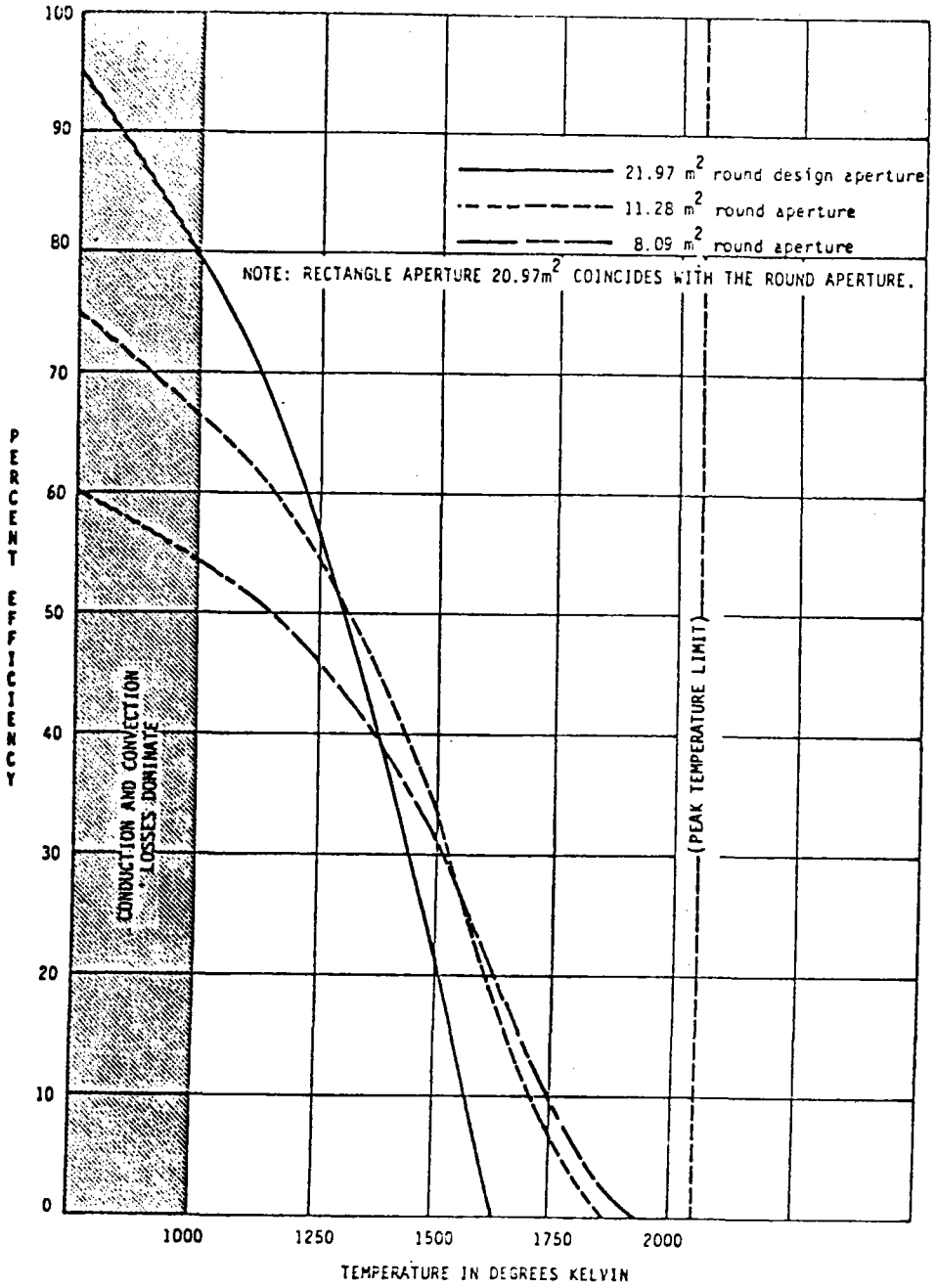

Figure 5-29. Aperture Efficiencies: 10 MWt - Repowering.

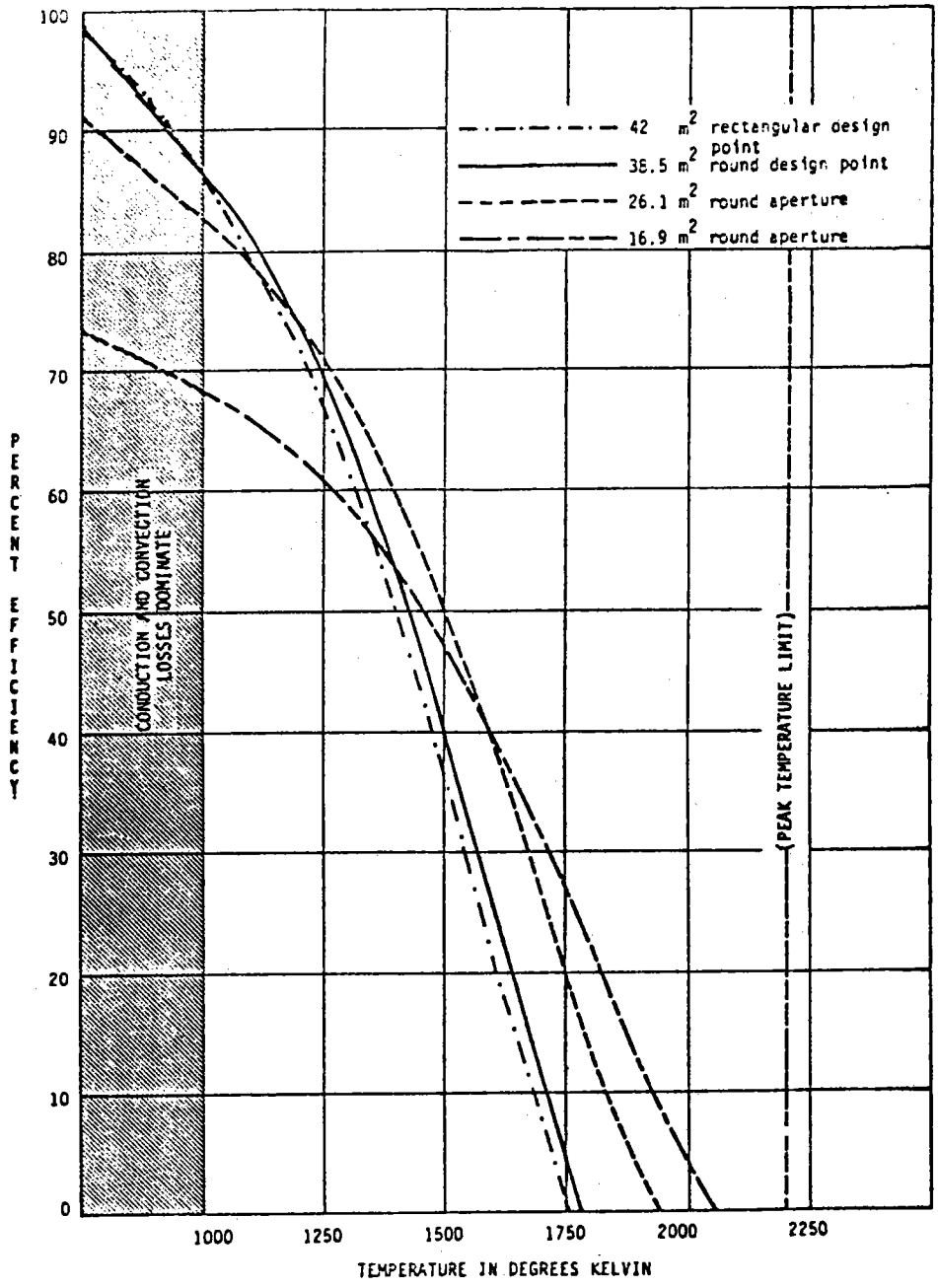

Figure 5-30. Aperture Efficiencies: 25 MWt - VIH.

the VIH results in an efficiency at 1750°K that is two and one half times better than the repowering heliostat efficiency.

Figure 5-31 plots the best efficiency, for the apertures investigated, as a function of temperature for each of the arrays. That is, as temperature increases, the size of the aperture is allowed to vary to obtain the maximum amount of usable energy. Since the aperture size is shrinking as temperature increases, the only way to increase efficiency is to reduce the size of the image. As discussed in Section 6.0, a spacing change in VIH placement resulted in an 80% increase in maximum flux density with a 25% decrease in image size. This indicates that an optimization of heliostat spacing on the UHA offers the potential of increasing the efficiency at 1750°K from 25% to over 60%. This would reduce the cost of usable energy at this temperature by more than a factor of two.

The tables in Appendix E give the cost of energy as a function of all the variables involved. Figure 5-32 presents the minimum costs, for a given temperature, as found in these tables. Cost of money and escalation rate are held constant at their minimum values and aperture size is allowed to shrink as temperature increases. Thus, Figure 5-32 shows the minimum costs associated with the operational efficiency curves shown in Figure 5-31.

This figure again illustrates the cost penalty, due to O&M, paid by the 1 MWt. However, it also shows the ultimate cost penalty paid by the repowering heliostat due to its poorer image quality. Up to 1200°K the costs for the three larger UHA configurations are comparable. At 1400°K the configuration with the repowering heliostat is about 20% more expensive than the VIH configurations. At 1600°K it becomes 100% more expensive

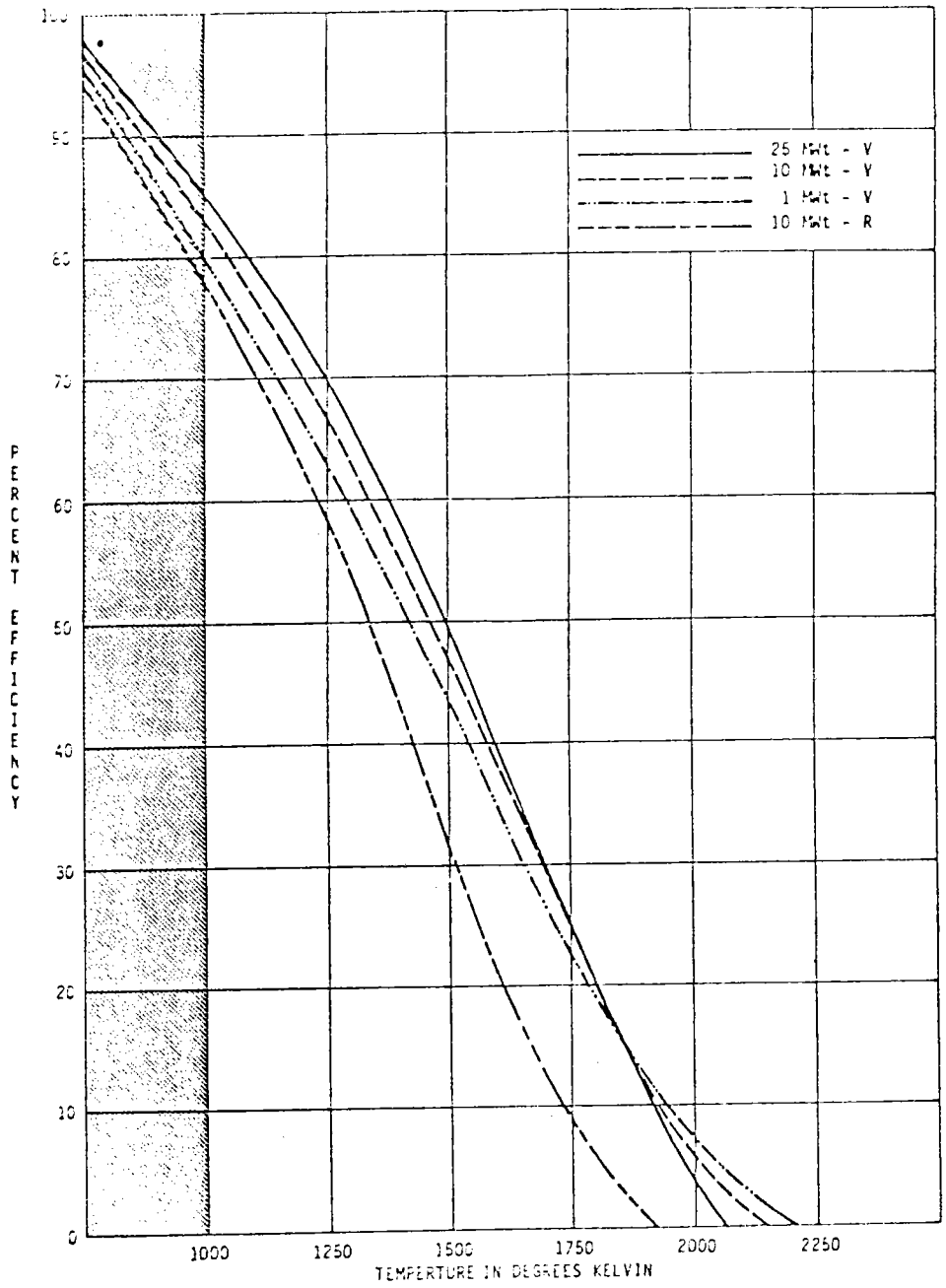

Figure 5-31. Efficiency for the Optimized Apertures.

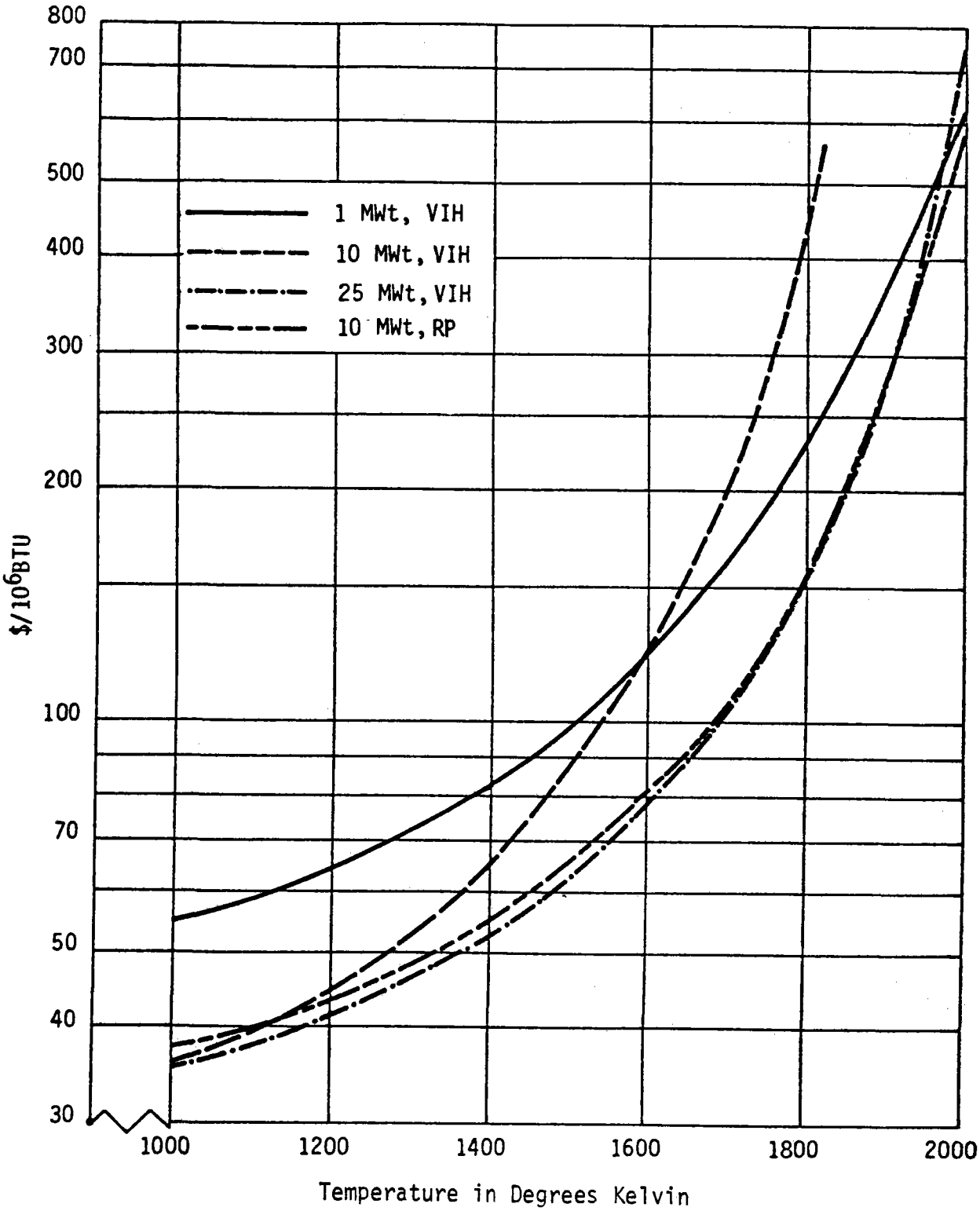

Figure 5-32. Cost of Usable Energy.

and at 1800°K it rises to 300% more expensive. An optimized placement of heliostats would not only significantly reduce the costs for the VIH configurations, but would also further exaggerate these cost differences.

In summary, the basic cost of energy produced by the UHA is approximately $\$10/10^6$BTU more expensive ($30 v.s. $20) than energy produced for other competing solar thermal systems (c.f. Reference 5-5). However, for high temperature processes, the UHA-VIH offers the capability of supplying the energy at a much lower price than competing solar thermal systems. The high potential for reducing the costs through heliostat placement optimization and further structural refinement may make the UHA-VIH system the only viable solar thermal approach for high temperature processes.

SECTION 6.0
DISCUSSION

6.1 SPECIFICATION

The specification was developed by combining information from several sources. Specification FSCM Number 14214 was the primary guideline from which applicable sections were used intact. Telephone conversations with J. C. Gibson, C. L. Mavis, and other Sandia Laboratory Livermore personnel served to clarify the intent and add necessary details for clearly specifying the repowering heliostat. Additional technical data was excerpted from SAND-78-8180. W. Mitchell of Reflective Modules, Incorporated (formerly Solaramics, Incorporated) provided a mechanical design, costs, and loads analysis for the Veda Industrial Heliostat design. Bechtel National, Incorporated assisted in verification that referenced standards were correct and current. Based on prior analysis of the Unified Heliostat Array characteristics, Veda established the preliminary heliostat field layout. Following internal review, the specification was issued for approval of the sponsor as Veda publication 43342-80U/P0069.

Only minor changes were made during the performance analysis to increase the total mirror area for some configurations. These changes are incorporated as the final design configuration table in Appendix A of this report.

It was expected that heliostat rotational tolerance, localized at the heliostat pedestal attachment, might be the cost driver for the UHA design. In the final analysis, survival wind loads and soil conditions became the cost drivers. Since the specification used soils conditions from one site and wind and insolation data from a second site, the resulting UHA designs were somewhat generic. To establish more accurate cost, the explicit conditions for a

particular site should be used. More favorable soil conditions and wind loads would lower costs while less favorable conditions could cause an increase.

6.2 STRUCTURAL DESIGN

The significant structural factors developed during this study were:

> An open structural design is controlled primarily by survival wind loads. The tolerance in heliostat foundation rotation is more than adequately satisfied when survival wind criteria are met.
>
> In such an open structure, the cost increase with height varies approximately as the square root of the height ratio. This significantly affects the design to favor a long low structure.
>
> The structural cost for the designs studied depends directly on the amount of steel used. Conditions which permit reduction in steel content will result in reduced costs.
>
> The amount of steel and concrete in a design solely to support heliostats is only a few percent of that required for a similarly sized structure intended for human occupancy.

It was determined that the modified structural concepts developed for the arrays having the preferred aspect ratio of 1:5 did indeed reduce steel tonnages. The amount of steel in the conceptual estimates considered other quantities such as bracing and access which were not considered in the preconceptual designs. However, in the more detailed analysis, the foundation quantities also increased significantly for the modified structural designs compared with those computed for the preconceptual designs due to a better definition of loadings.

By attaching the 6 m^2 heliostats directly to the main frames, the rotation criteria of $\pm$1.5 mrads did not have a significant influence on the structural design. The rotation criteria were more significant in the design of the array having the 49 m^2 heliostats placed on truss members spanning between the main frames. This was because the larger heliostats caused large torsional forces in their supports. The resultant calculated maximum rotation of $\pm$1.7 mrads would not have a significant effect on the optical performance due to the relative closeness of the heliostats to the receiver as compared to distances encountered in a horizontal field. However, the potential for reducing steel quantities in this design would be limited.

The capital cost of the 10 MWt array having the 6 m^2 heliostats was found to be about one third more than the array having the 49 m^2 heliostats. This was due to an increase in the foundation, steel, and heliostat installation costs. However, it is felt that the costs of both concepts could be made more comparable by reducing the steel tonnages and foundation quantities in the design for the 6 m^2 heliostats. This could be accomplished by further structural optimization, and more detailed soils criteria to determine actual foundation requirements. Because the rotational criteria of $\pm$ 1.5 mrads was easily met for this design, a further reduction in steel quantity appears more feasible than with 49 m^2 design which slightly exceeded this criteria.

This study confirmed that increased UHA height is accompanied by substantial increases in steel tonnages and unit costs. The tallest structures, the 25 MWt power arrays, are substantially heavier and have higher costs per MWt than the other arrays studied. The quantity of steel weight

per cubic foot was used to compare the UHA structures with the steel used in other large buildings. Normally steel weight per square foot of floor area is used for comparing tall buildings. Since the UHA structures are unoccupied they require no floor or roof systems as found in conventional tall buildings, hence the total steel tonnages for the arrays appear low. The weight per unit volume of the 25 MWt array is significantly lower than the weight per unit volume of either the World Trade Center in New York or the Sears Tower in Chicago.

Since the cost of a structure is directly related to the amount of materials and labor entering into it, the direct conclusion from these factors is that combining heliostat supports into a structure designed for human occupancy will add very little to the cost of such a structure. It would probably be more practical to combine housing human endeavors and heliostat support into a new stucture than to redesign and modify most existing structures to accommodate heliostats. However, there are several existing structures in the United States possessing the same generally terraced configuration required for the UHA. This architectural design is being incorporated in motels such as the Hyatt Regency in Knoxville, Tennessee and the Sheraton in Baja, California. There is a similar structure in the architectural plans being considered for the redevelopment area in central Los Angeles, California. The location of a UHA type structure in an urban or near urban area is apparently not esthetically undesirable. Since the floor space in such an area is required for a variety of endeavors, it is reasonable to consider the UHA as both an energy source and as a revenue source by using it as a commercial, industrial, and/or residential building.

An environmental impact analysis of the UHA was outside the scope of this contract. However, constructing a UHA in an urban environment would require such an analysis. While it is expected that any potential hazards would be no greater than those associated with the horizontal field, a receiver at ground level will require shielding to protect structures and activities in the near vicinity. Shielding installed for this purpose will not interfere with the collection of solar energy. As with wind and soil conditions, actual safety requirements would be very site specific and would have to be addressed as part of a particular applications study.

6.3 OPTICAL PERFORMANCE

This study showed that the UHA concept is capable of delivering solar thermal power to a low receiver. While it has been generally recognized that elevating the heliostats would make a lower receiver possible, serious doubts existed in the solar thermal community concerning the ability of this arrangement of heliostats to "see" the sun except for a few hours a day. This study showed that for the approximately 45° to 50° sloping structure, located at a latitude which includes most of the southwestern states, the heliostats could not only see the sun, but deliver substantial quantities of energy at any time the sun was above 30° above the horizon. For the summer months this translates into a useful operational day of 10 hours, from 0700 to 1700. Since insolation levels are generally too low to be of use before or after this time period, the performance period of the UHA concept is comparable to that of the surround field.

This aspect of the performance was the same for both heliostat types investigated. However, in measures related to quality of energy, the performance of the two heliostats was very different. The specific measures which affect the quality of energy are solar image size, fluctuation in image throughout the day and year, and the flux density distribution in the image.

The solar image formed by the repowering heliostat was considerably larger than that formed by the VIH. Since it is eight times larger than the VIH, this was not unexpected. Even though it is possible to adjust the radius of curvature to obtain a very small image for a specific instant in time, it was pointed out in Section 5 that the radius is a compromise to obtain good performance throughout the total range of off-axis tracking angles. In order to obtain optimum performance, two orthogonal radii should be used. In practice the repowering heliostat only uses one. Therefore, very large off-axis angles, such as those experienced in the early morning and late afternoon, cause the image from this heliostat to be very diffuse. However, if the repowering heliostat mirror facets were adjusted such that the mirror surface had the two required radii of curvature, the azimuth-elevation mounting system would have to be changed. As discussed in Section 2.0, the mirror surface must track such that the planes of the radii of curvature maintain their proper orientation relative to the plane of the angle formed by the sun-heliostat-receiver. This requires a tracking system capable of providing the type of motion produced by the equatorial mount employed on the VIH.

In general, the solar image from the repowering heliostat was diffuse with a nearly gaussian flux distribution. The size of the image was also variable due to the focusing problem. Because of the size of the image and

the flux distribution in the image, the repowering heliostat could not achieve a flux density of 1 MW m^{-2}, even at the design point. For lower temperature applications, below 811°K (1000°F) this has little effect on the utility of the system. However, in the higher temperature regions, above 1250°K, the repowering heliostat became very inefficient. This was due to the significant reradiation loss from the large apertures necessitated by the diffuse image.

In contrast, the image from the VIH was smaller, very constant in size throughout the day and year, and had a very even flux distribution. While direct comparisons between the two heliostats were only made at the 10 MWt power level, observations on the image quality for the VIH are equally valid for the 1 MWt and 25 MWt arrays.

The well focused image from the VIH is composed of a very high flux density central zone which rapidly decays to a low flux density surround area. In the central zone, flux densities in excess of 1 MW m^{-2} are achieved throughout most of the year. This is true even for the small 1 MWt array. This image quality allows for apertures, which are relatively small, to be completely filled with only a moderate amount of spillage. The graphs in Section 5, which plot efficiency versus temperature for several aperture sizes, illustrate the potential performance available from the UHA-VIH combination.

A very significant result is that high flux density, high temperature performance is achievable with small arrays. This offers the potential of using the UHA-VIH combination in the 5 MWt to 20 MWt range, for processes that would require a 50 MWt or even 100 MWt horizontal field configuration to obtain necessary flux density or operating temperature. Thus, for specific

applications, the UHA-VIH could prove to be considerably less expensive than the coventional approach to solar thermal energy central receiver systems.

This contract did not fund a heliostat spacing optimization study. The spacings chosen resulted from preliminary computer studies aimed at minimizing shading and blocking losses for a restricted range of structure sizes. In order to perform the required structural studies, these spacings were fixed in the design specification during the first month of the contract period. In-house studies were subsequently performed which addressed spacing factors, as part of an effort to refine Veda's optical analysis computer program. As a result of this effort, it appears that there is good probability that minor variations in the spacing pattern could result in significant performance improvements.

In looking at the 10 MWt UHA-VIH configuration, one set of spacing changes along the East-West axis resulted in a 20% reduction in the structure width, 30% reduction in total land area required and approximately a 25% reduction in aperture size. The peak flux was achieved with this configuration 1.973 MW m^{-2} at design point. At summer solstice the peak flux was above 0.5 MW m^{-2} at 0700 and increased to 1.12 MW m^{-2} by 0800. These are rather dramatic changes and point to an area where further study would not only improve performance but, also would have a very favorable cost impact.

6.4 COST

Funding for this contract did not provide for a systems study; only an evaluation of the cost of energy delivered to a low receiver of undefined design except for aperture size. A system study is necessary to relate the cost advantages and disadvantages of Veda's approach to other methods of

collecting and utilizing solar thermal energy for industrial process heat applications which involve high temperatures and are not concerned with the production of electricity as the primary output. While it is tempting to interpret the costs of energy developed in this study as equivalent fuel charges and use those costs as the sole basis of comparison with other alternatives, that interpretation could be very misleading. The cost benefits of using less land, having a low fixed receiver, attaining high flux densities with relatively small collector fields and operating at high temperatures are highly application dependent. These advantages may combine such that the UHA-VIH is the only available solar alternative capable of displacing fossil fuels in a particular process or application. Given a specific process and product, a meaningful cost comparison could be made based on the cost of producing the product using the UHA-VIH versus other approaches.

In addition to the lack of a well defined system or application, other elements in the study approach contributed to the costs being maximized rather than optimized. In particular, three factors directly impacted the cost results. They were: (1) non-optimum heliostat spacing on the array; (2) attributing the entire function, design and cost of the UHA structure solely to heliostat support; and (3) the use of the cost methodology specified in Reference 4-2. Of these, the latter two were intentionally incorporated in the approach to provide both a worst case cost and a common methodology for comparison with other solar thermal approaches. The dramatic effect of heliostat spacing was not discovered until the optical performance analysis for this study had been completed and an in-house effort was being conducted to improve the versatility of the analysis program.

As discussed earlier, one of the spacing changes resulted in a 20% reduction in structure width and a 30% reduction in total land area required. For the 10 MWt array with the VIH, this change would reduce the required capital investment by 3.6 million dollars and reduce the basic cost of energy approximately $\$3/10^6$BTU. These figures assume a linear reduction in structure width only, and do not address further reductions in the cost of energy made possible by using a receiver aperture that would be 25% smaller.

Throughout the report it has been pointed out that the structures designed during this study were for heliostat support only. This means that the cost of energy carries the entire burden of the structural cost. In an actual installation, the structure could be designed to house part of the plant or process, or may just be rented out to tenant activities. To whatever alternate use the structure were put, its cost may be partially, or even entirely, offset by income from that use. Therefore, the cost of energy values developed in this study represent a worst case to the extent that they must offset the entire structural cost.

The cost methodology used in this study develops a levelized charge per unit of energy produced such that, over the system lifetime, this charge will recover the capital investment, pay all system operation and maintenance costs and provide a return to investors. By comparison, an industrial energy user pays an annual fee for energy at the rate applicable to that year. In general, this energy cost escalates at or above the general inflation rate. Since it is a cost of doing business, it is passed on to his customer in the form of periodic price increases and deducted as an expense in his tax returns.

If the industrial user could predict his actual energy costs, he could develop a levelized charge for his planned business life, and thus keep this component of his pricing structure at a constant value. A realistic approach to developing a levelized charge for his product would require that he treat labor, rent, utilities, taxes, etc. in the same manner. Whether or not he could treat his income, when using this approach, in such a manner as to make it tax free, while it was held as retained earnings, is questionable. It could become a tax liability. He would also be faced with a loss of customers if he should reach the end of his levelized charge period and be forced to raise his prices by a factor of 10 to 30 times in order to remain solvent at his previous average profit level. Because of these problems he would probably not use the cost of energy methodology employed in this study.

Although the cost methodology employed in this study allows comparison with utility costs of energy, it is probably not the appropriate methodology to employ. Since the UHA was originally conceived to provide energy for industrial applications, a separate analysis of the costs, more in line with the industrial users approach, should be conducted. This is particularly true for very high temperature processes where large quantities of fossile fuel are burned at the process site to maintain the necessary operating temperatures.

SECTION 7.0

CONCLUSIONS AND RECOMMENDATIONS

7.1 GENERAL COMMENTS

In all efforts to bring solar thermal energy to the current marketplace, two fundamental issues must be addressed - applicability and cost. This study addressed a concept, the Unified Heliostat Array, which offers the potential extension of solar thermal technology to currently neglected applications. The results were expressed in terms of cost; cost determined by a methodology that, while not necessarily appropriate for the envisioned applications, provides a basis for comparison with other systems currently under development.

Veda has long maintained that the range of applications for central receiver technology could be significantly extended by simply doing one thing: bringing the energy to the work place. To accomplish this, several problems must be solved. The two most important are land usage and receiver location. For industrial processes which require both high temperatures and large energy inputs (several megawatts or more), these problems become magnified.

The point focus tracker is capable of providing the necessary temperatures and, as a single collector-receiver set, does not require large parcels of land. However, the mechanical constraints of the system limit both the energy input and the potential applications. Input is limited by the size that material constraints place on the dish. Application restrictions arise from the fact that the receiver moves with the dish and is, therefore, subject to a large variation in gravitational orientation. For high temperatures,

piping, joints, and other material limitations make it too costly or impossible to bring the energy to a fixed process.

A tower mounted central receiver, at the focal zone of a horizontal field of heliostats, eliminates the problems of variable process orientation and small input. However, a horizontal field is land intensive and requires the receiver to be located at a substantial height above the heliostats. The amount of land required for the surround field could preclude its use in urban and near urban areas where a large percentage of our nation's current industrial capacity is installed. Evidence of this problem surfaced during the repowering program when many candidate sites had to be dropped due to lack of land. Further applications at other sites had to be limited due to the geometry of the available land.

For applications where the process requires the heating of a fluid or a gas, the receiver height does not present an insurmountable obstacle. However, for industrial applications that require the processing of large quantities of solid material, such as coal or oil shale, transporting the material to the top of the tower and bringing the process products and waste back down may be neither feasible nor cost-effective. Also, the energy expended in the material transport reduces the overall energy efficiency of such systems.

The Unified Heliostat Array (UHA) and the Veda Industrial Heliostat (VIH) combine to fill a gap in the power/temperature regime between the horizontal field and the point focus tracker for applications considered candidates for solar thermal technology. Land usage is considerably less than the horizontal field and the energy may be directed to a fixed receiver

located at a position convenient to the process. These characteristics, coupled with the superior imaging ability of the VIH, offer the potential expansion of this technology to processes hitherto not considered as viable applications for solar energy.

7.2 CONCLUSIONS

The environmental constraints imposed by the specification are a cost driver for the UHA. In particular, survival winds, seismic magnitudes, and soil conditions are generalized factors which would be modified for an actual site. In some cases the costs would be higher, in some lower. However, in order to optimize the UHA for an application, these factors must be considered and appropriate design factors included.

The solar image at the aperture plane determines, to a large extent, whether any specific application can utilize concentrated solar energy as either a total or supplementary fuel source. The collector field should produce an image that is best adapted to the application. A collector field that can produce a very small image at high intensity offers the best chance of being able to fit a large variety of applications. Such a collector field can be defocused if necessary to meet receiver constraints, but a collector field that cannot provide a high quality solar image will be either useless or low in efficiency for any process requiring high temperature or high flux input. The UHA-VIH produces a very small, very uniform image for the total power delivered. It thus lends itself to the widest variety of industrial processes.

The solar image varies throughout the year with the excursions of the tangential and sagittal foci. One part of the image linear size can

be attributed to the distance between heliostat and receiver multiplied by the sun's angular diameter. The remainder can be attributed to the combined effect of off-axis angle and heliostat dimensions. The azimuth-elevation mounting used in the repowering heliostat precludes minimizing the area of the solar image by separately adjustable sagittal and tangential foci excursions, and the large mirror size imposes a still further restraint in attempting to minimize the aperture of the receiver. For the specific applications for which this type of heliostat was designed, it may be the most cost-effective approach. Its applicability to higher temperatures is limited by its poor solar image quality on both a daily and an annual basis. The image is diffuse and varies widely in size and shape throughout the day and throughout the year.

In order to provide usable power at temperatures above about 1200°K for a large part of the solar day throughout the year, and without frequent refocusing of heliostat facets, the conventional horizontal field with current heliostat designs must be sized on the order of several tens to a few hundreds of megawatts thermal. The UHA-VIH combination provides high efficiency power even with a very small heliostat field.

Prior solar thermal market analyses have been concerned with total quantity of energy required and final temperature achieved. This approach ill defines the potential for application of solar energy to the process. Most industrial processes require a heat rate and temperature combination which varies throughout the process. In a continuous process, the variations are controlled by moving the process through variable power/temperature zones with an appropriate dwell time in each. Batch processing generally leaves the

process resident in one location and varies the power/temperature profile by environmental control methods. The UHA-VIH collector system is adaptable to both of these methods.

Thus, it is important to look closely at the power/temperature/time relationship in industrial processes. By developing profiles of these requirements, it will be possible to determine a best fit of the solar power/temperature/time profile. It may be found that processes currently using high quality fossil or synthetic fuels adapt readily to the solar profile with very little modification. If such an adaptation still requires a hybrid fuel technology, solar power may be able to contribute significantly to fuels conservation. Veda has previously formally proposed such a study to DOE, and again recommends that such a study be initiated.

7.3 RECOMMENDATIONS

Based on the results of this contract, the following specific recommendations are made for further study efforts.

a. Perform a heliostat spacing optimization study to determine the improvements in optical performance and assess potential cost reduction due to reduced land requirements and decrease in structure size.

b. Conduct a structural study to determine expected cost deltas for upgrading structures, which are primarily designed for other purposes, to include supports for heliostats.

c. Perform a study of several candidate processes that could benefit from central receiver technology and the type of high quality energy provided by the UHA-VIH system. The study would develop power/temperature/time profiles for the processes to assess the applicability of solar thermal power and potential fuel savings.

d. Perform a detailed feasibility study to determine specific cost tradeoffs between various solar collection technologies for one of the industrial processes identified in the process profile study.

e. Develop and field test a prototype of the Veda Industrial Heliostat to verify optical performance and production techniques.

REFERENCES

2-1 E.A. Igel and R.L. Hughes, Optical Analysis of Solar Facility Heliostats. SAND 77-0582, Sandia National Laboratories, Albuquerque, N.M. (May 1977)

4-1 Methodology for Optical Performance Analysis, Veda Report 44112-80U/Q0401-3, Veda Incorporated, Camarillo, California (November 1980)

4-2 The Cost of Energy from Utility-Owned Solar Electric Systems, ERDA/JPL-1012-76/3. Jet Propulsion Laboratory, California Institute of Technology, Pasadena, California (June 1976)

5-1 Specification for the Unified Heliostat Array, Veda Report 43342-80U/P0069, Veda Incorporated, Camarillo, California (April 1980)

5-2 C. Mavis and C. Lundbom, Collector Subsystem Requirements FSCM Number 14214, Issue C. Sandia National Laboratories, Livermore, California (October 1979)

5-3 R. Shogren and J. Phillips, 10 MW(e) Solar Thermal Central Receiver Pilot Plant: Heliostat Foundation and Interface Structure Investigation, SAND-78-8180. System Development Corporation, Santa Monica, California (August 1978)

5-4 T. Tanaka, Solar Thermal Electric Power Systems in Japan. Solar Energy 25, 97. Pergamon Press, Elmsford, New York (1980)

5-5 Fuels and Chemicals made from Solar Energy: Options for the 1900's and beyond, DOE/CS/21051-01, OAO Corporation, Washington, D.C. (August 1980)

APPENDIX A

VEDA REPORT 43342-80U/P0069

SPECIFICATION FOR THE UNIFIED HELIOSTAT ARRAY

Prepared by:

VEDA INCORPORATED
400 N. Mobil, Bldg. D
Camarillo, CA 93010

7 April 1980

Under Contract Number
DE-AC03-80SF10802

Prepared for:

Department of Energy
1333 Broadway
Oakland, CA 94612

Revision A
31 October 1980

TABLE OF CONTENTS

SPECIFICATION FOR THE UNIFIED HELIOSTAT ARRAY

1.0 GENERAL

1.1 SCOPE

This specification establishes the performance and design, requirements for Unified Heliostat Array (UHA).

2.0 DOCUMENTS

The equipment, material, and design of the UHA shall comply with standards, regulation, and codes, which are currently applicable for siting in Barstow, California. These shall include, but are not to be limited to, the documents itemized below. The following documents in effect on the date of contract award form a part of this specification to the extent specified herein.

2.1 STANDARDS

MIL-STD-454	Standard General Requirements for Electronic Equipment
MIL-STD-1472	Human Engineering Design Criteria
ANSI CI-1975	American National Standards Institute
ANSI A58.1-1972	Building Code Requirements for Minimum Design Loads in Buildings and other Structures

National Electrical Manufacturer's Association (NEMA) Standards.

Manual of Steel Construction, 7th Edition, 1969, American Institute of Steel Construction.

Uniform Building Code - (UBC) 1979 Edition, applicable portions.

American Iron and Steel Institute (AISI) "Cold-Formed Steel Design Manual,"1977 Edition.

American Concrete Institute (ACI) "Building Code Requirements for reinforced Concrete" - (ACI-318-77).

American Welding Society (AWS) "Structural Welding Code" - (AWS D 1.1 - 80)

National Electrical Code, NFPA 70-1975

2.2 OTHER PUBLICATIONS

"Wind Forces on Structures", ASCE Paper No. 3269, Transactions, American Society of Civil Engineers, Vol 126, Part II, 1961

Environmental Conditions (see Appendix A)

3.0 REQUIREMENTS

3.1 UHA DEFINITION

The UHA is an array of heliostats supported on a common foundation which is a terraced structure. The terraces extend in an easterly-westerly direction (see Figure 1). The upward slope of the terraces is away from the equator (i.e., to the North in the northern hemisphere.) The heliostat array reflects solar radiation onto the receiver system in a manner which satisfies receiver incident heat flux requirements. The receiver may be located at any elevation such that there is a clear line of sight between the heliostats and the receiver. An optimum receiver height is latitude and user sensitive. The height of the center of the focal zone for this analysis will be eight meters above the low edge of the lower heliostat when its mirror element is in a vertical plane at the installed location of the heliostat.

The structural elements of the UHA are:

a. Foundation
b. Framework and support for the heliostats at the mounting interface
c. Access and safety structures.

Illustrations of the two heliostat configurations of concern are contained in Appendix B. The Heliostat components are:

a. Mirror modules
b. Mirror support
c. Drive units
d. Control sensors
e. Pedestal and mounting interface
f. Heliostat cabling

3.2 SPECIFICATIONS

3.2.1 Performance

In order to attain overall plant field performance such that 95% of the redirected energy will impinge on the receiver, the following requirements have been established for designing and evaluating individual heliostats:

a. Maximum beam pointing error (tracking accuracy) shall be limited to 1.5 mrad standard deviation for each gimbal axis under the following conditions:

- Wind - none
- Temperature - 0° to 50°C (32° to 122°F)
- Gravity Effects - at all elevation and azimuth angles that could occur in a heliostat field.
- Azimuth Angles - at all angles except during gimbal lock.
- Sun Location - above the horizon, but not earlier than 0700 nor later than 1700 any time of year
- Heliostat Location - any position in the field.

Pointing error is defined as the difference between the aim point and measured beam centroid for all of the above conditions for any tracking aim point (on target or at standby).

b. Overall structural support shall limit reflective surface static deflections to an effective 1.7 mrad standard deviation for a field of heliostats in a 12 m/s (27 mph) wind. Wind deflections of the foundation, pedestal, drive mechanism, torque tube, and mirror support members shall be included, but not the slope errors due to gravity and temperature effects. Wind deflection limits apply to the mirror normal (not reflected beam) for each axis fixed in the reflector plane. Both beam quality and beam pointing are affected. To assure that the net slope errors of a field of heliostats is less than 1.7 mrad, the rms value of the slope errors taken over the entire reflective surface of an individual heliostat, computed under the worst conditions of wind and heliostat orientation (but excluding foundation deflection), shall be limited to 3.6 mrad for a single heliostat. This limit represents a 3-sigma value for the field derived by subtracting foundation deflection from the total surface slope error (1.7 -.5 = 1.2 mrad standard deviation x 3 = 3.6 mrad). The conditions under which this requirement applies are:

- Wind, including gusts - 12 m/s (27 mph) at 10 m (33 ft) elevation

- Temperature 0° to 50°C (32° to 122°F)
- Heliostat Location - any position in the field at any time of the year.
- Gravity Effects - not included
- Mirror Module Waviness - none
- Facet Alignment Error - none

c. The allowable tilt and/or torsional rotation of a heliostat foundation shall not exceed ±1.5 mrads total angular deflection per axis, when the heliostat is subjected to a 12 m/s (27 mph) operational wind load. This total deflection shall, in addition to elastic response, include the amount of plastic or permanent deflection, including any distortion of the UHA structure resulting from a prior 22 m/s (50 mph) wind experience. The allowable plastic or permanent deflection of the foundation resulting from a 22 m/s (50 mph) wind load shall not exceed ±0.45 mrads.

Both deflection allowances are 3-sigma limits expressed for a single heliostat/foundation field position, and are computed under the worst condition of wind and heliostat orientation. For a full field of heliostat foundations, the effective limits will result in a standard deviation or 1/3 of the deflection allowances specified for a single foundation.

The deflections specified are applicable at the foundation-to-heliostat interface located on a plane parallel to and approximately 50.8 mm (2 inches) above the UHA mounting surface, which is represented by the contact face of the heliostat pedestal mounting flange. Standard deviation as used in these requirements shall be determined from a sample of at least 20 data points from each individual heliostat tested.

3.2.2 Environmental Design Conditions

"Environmental Conditions" (Appendix A) describes representative site conditions to be encountered and survived by the UHA. The UHA must maintain structural integrity in any applicable combination of the environments. Appendix 2 contains design and load calculations provided by Solarmics Inc. for an equatorically mounted six square meter heliostat and for the McDonnald-Douglas 49 square meter heliostat selected by DOESAN.

3.2.2.1 Wind Loading

The natural wind environment specified produces a vibratory response both from the oscillatory nature of the gusts and from periodic vortex shedding.

The UHA shall be designed to withstand, and/or operate when subjected to, the loads produced by this vibration. The actual loads must be computed taking into account structural configuration and dynamic characteristics and the velocities of the winds. In computing the angle between the wind direction and the plane of the heliostat reflective surface, the wind shall be assumed to deviate by $\pm 10°$ from the horizontal.

3.2.2.2 Operational Limits

The Collector Subsystem must meet performance requirements for the following conditions unless the component is located in a controlled environment (building):

Environment	Level
Wind, including gusts	12 m/s maximum (27 mph)
Temperature	0 to 50°C (32 to 122° F)
Gravity	All elevation angles

To achieve morning operational position or evening stow position, the heliostat will be required to function with ambient temperatures down to -9°C (16°F) and component temperatures that are colder or hotter than ambient temperatures due to thermal lag and/ or absorption of direct insolation.

3.2.2.3 Stowage Initiation

The heliostats will continue to track the target with wind speeds up to 16 m/s (35 mph), but with degraded performance allowed, above which stowage action will be initiated as a result of an externally provided signal. The heliostat must maintain structural integrity in a non-operational state in a 22 m/s (50 mph) wind in any orientation.

3.2.3 Transportability UHA components or assemblies shall be designed for transportability by highway handling equipment within applicable Federal and State regulation.

3.3 DESIGN AND CONSTRUCTION

Commercial design and construction standards shall be employed. Where applicable, the Uniform Building Code (1979 edition) and the American Institute of Steel Constructions Manual of Steel Construction (8th edition) shall be used. ANSI A58.1 1972 and ASCE paper No. 3269, Wind Forces on Structures (ASCE Transactions, Vol 126, Part II, 1961) shall be used during design when determining loading due to winds. For electrical components, the National Electrical Code (ANSI C1), the National Electrical Manufacturer's

Association (NEMA) and MIL-STD-454 standards for electronic equipment shall be used.

Preliminary initial design point data for both the 6 square meter and 49 square meter heliostats are contained in Appendix C.

Design and material selection is to be based on a 30-year plant life.

3.3.1 Materials, Processes, and Parts

To the maximum extent possible, standard materials and processes, and off-the-shelf components shall be used. Wherever possible, commercial specifications shall be employed. All non-commercially available parts shall be defined and documented in deliverable documents.

3.3.2 Flammability

In a high temperature, low humidity environment of a typical desert, the heliostat field shall not be vulnerable to extensive fire damage. Given that a fire exists in any part of the heliostat field, the fire should not damage any heliostats, that are not directly adjacent to the fire, due to burning of a heliostat or any heliostat wiring. If a heliostat or any part of a heliostat burns, for any reason, the heliostat fire should not spread to other parts of the field due to blowing winds, component explosions, or any other means.

3.3.3 Safety

The UHA shall be designed to minimize safety hazards to operating and service personnel, the public, and equipment. Electrical components shall be insulated and grounded. All components with elevated temperatures shall be insulated against contact with or exposure to personnel. Any moving elements shall be shielded to avoid entanglements, and safety override controls/interlocks shall be provided for servicing.

3.3.4 Human Engineering

The UHA shall be designed to facilitate manual operation, adjustment, and maintenance as needed and provide the optimum allocation of functions between personnel and automatic control. The UHA design shall provide electrical and electronic packaging which ensures rapid repair and replacement, placarding of hazardous work areas, and equipment for item removal and handling. MIL-STD-1472, Human Engineering Design Criteria, shall be used as guide in Designing equipment.

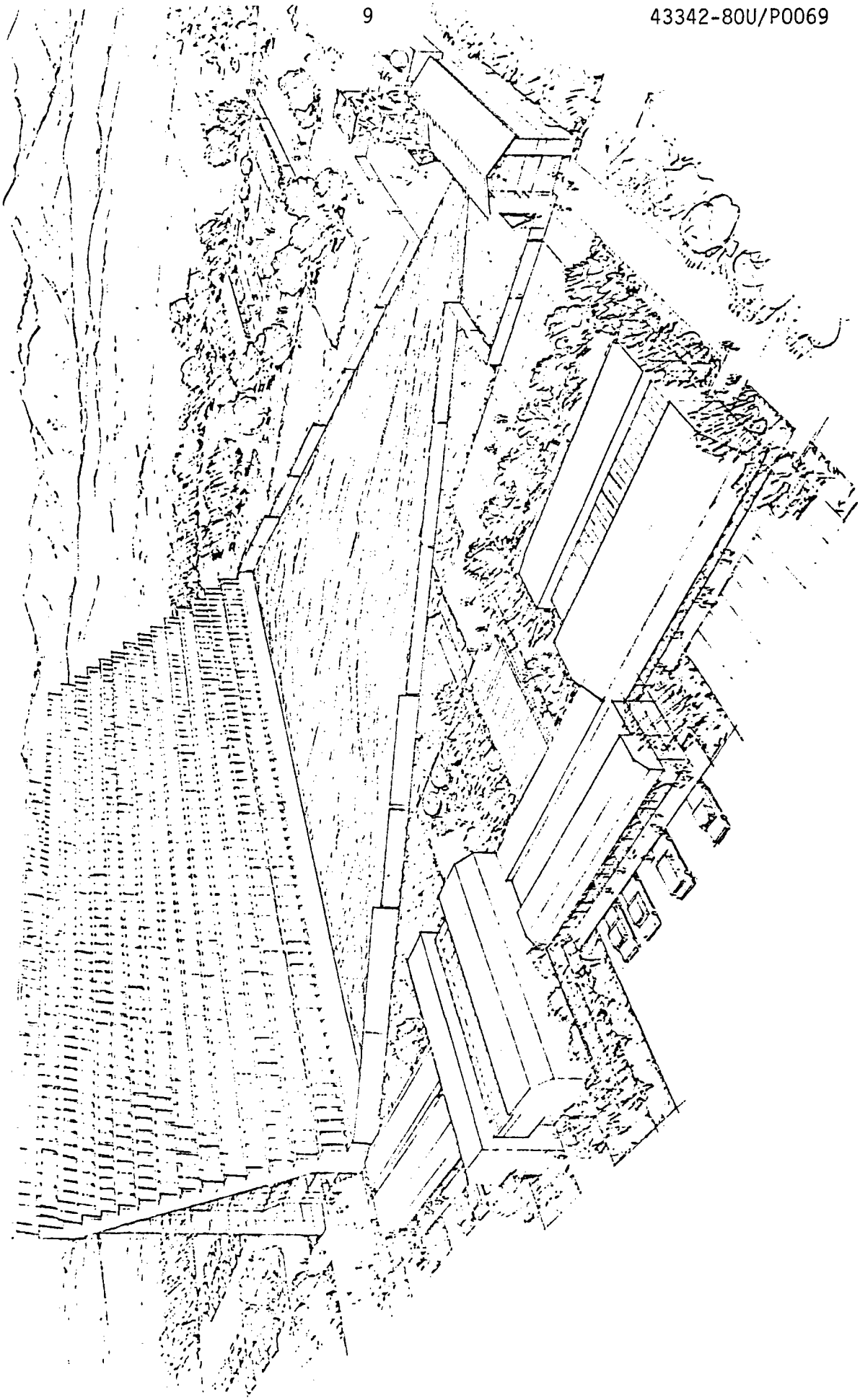

Figure 1. Unified Heliostat Array.

APPENDIX A

ENVIRONMENTAL CONDITIONS

1.0 GENERAL

1.1 SCOPE

This document lists representative environmental conditions for a Solar Central Receiver Plant.

2.0 DOCUMENTS

The following documents for a part of this specification to the extend stated herein.

MIL-STD-810B Environmental Test Methods

Uniform Building Code - 1979 Edition, Volume 1 by International Conference of Building Officials

3.0 ENVIRONMENTS

Environmental conditions include winds and gusts, temperature extremes, rain, sleet, hail, snow, earthquake and soil conditions as follows:

3.1 WIND

The wind speed specifications during daylight hours at a reference height of 10m (30 ft.) shall be:

3.1.1 Speed Frequency

Speed, m/s (mph)		Frequency, Percent
0-2	(0-4.5)	29
2-4	(4.9-9.0)	21
4-6	(9.0-13.5)	19
6-8	(13.5-18-0)	14
8-10	(18.0-22.5)	8
10-12	(22.5-27.0)	5
12-14	(27.0-31.5)	3
14-	(31.5-)	Less than 1

For the calculation of wind speed at other elevations, assume the following Model:

$$V_H = V_1(H/H_1)^C$$

Where: V_H = wind velocity at height H
V_1 = reference wind velocity
H_1 = reference height (assume 10 m (30 ft.)
C = 0.15

An operational wind speed of 12 m/s (27 mph) at 10 m (33 feet) elevation will be considered applicable for this design study.

3.2.1 Wind Rise Rate

Under normal conditions, the maximum wind rise rate is 0.01 m/s (0.02 mph/s). A maximum wind of 22 m/s (50 mph) from any direction may occur resulting from unusual rapid wind rise rates, such as severe thunderstorm gust fronts.

3.1.3 Survival Wind

A maximum wind speed, including gusts, of 40 m/s (90 mph).

3.1.4 Dust Devils

Dust devils with wind speeds up to 17 m/s (38 mph).

3.1.5 Sandstorm Environment

Sandstorm limits within tests per MIL-STD-810B, Method 510.

3.2 TEMPERATURE

Ambient air temperatures range from -30 to +50°C (-22 to +122°F).

3.3 PRECIPITATION

3.3.1 Rain

Average annual: 750 mm (30 in) maximum 24-hour rate: 75 mm (3 in).

3.3.2 Ice

Freezing rain and ice deposits in a layer up to 12.7 mm (0.5 in) thick.

3.3.3 Hail

Diameter	25 mm (1 in.)
Specific Gravity	0.9
Terminal Velocity	23 m/s (75 ft/s)
Temperature	-6.7°C (20°F)

3.3.4 Snow

Maximum 14-hour rate: 0.3m (1 ft.); maximum loading: 250 Pa (5 lbs/ft);

3.4 INSOLATION

3.4.1 Maximum Flux

Direct normal nominal insolation of 1100 watts/square meter maximum at the plant site.

3.4.2 Rate of Change

The maximum rate of change of incident flux shall be assumed as that which would result from the passage of an opaque cloud across an otherwise clear sky where the sharp leading or trailing edges of the shadow move across the plant site site at a velocity of 20 m/s (45 mph).

3.5 EARTHQUAKE

Seismic zone 3 will be used for the criteria applicable to this study. The structure shall be designed to resist minimum total lateral seismic forces in accordance with formula 12-1 of the UBC.

3.6 SOIL PROPERTIES

The soil properties to be used for heliostat foundation design are extractions from the soil analyses report of the Albuquerque Solar Facility (Soil and Foundation Investigation Report, 5MW STTF, Sandia Labs) and are as follows:

3.6.1 Description

. Rolling terrain sloping gently toward the west.

. No free ground water was encountered and soil moisture is very low. As indicated by the exploratory borings, the subsoils and rock underlying the site can be generalized onto a 3-strata profile as follows:

a. Stratum No. 1

This stratum consists predominantly of silty sands with varying amounts of gravel interbedded with lesser amounts of sandy silts and relatively clean sands which extend to depths of about 30 feet below existing grade. These soils are generally low in plasticity to nonplastic. This deposit is stratified and contains layers which are weakly to moderately cemented, the amount of cementation generally increasing with depth. The soils are generally moderately firm to firm near the surface becoming very firm to hard with depth. However, erratically distributed softer or looser zones were noted at several of the borings to depths of up to approximately 8 feet.

b. Stratum No. 2

Silty sands and gravels were encountered underlying the surface stratum and extended to depths of about 45 feet below existing grade. These soils were generally moderately to strongly cemented and very firm to hard throughout their extent. Auger drilling into this deposit was very difficult. The hollow stem auger refused within this stratum in some instances.

c. Stratum No. 3

Conglomerate was encountered at depths of about 45 feet and extended to the full depth of the borings. This rock consists of very strongly cemented sand and gravel with occasional cobbles and is generally moderately hard to hard. However, occasional thin softer layers containing considerable clay are present. Auger drilling to any extent into this formation was not possible and tricone rollercone bits and NX diamond coring equipment were used to penetrate this deposit. Although thin layers are present which are soft geologically, the entire unit is very hard and an excellent foundation material from an engineering standpoint.

The change between Stratum No. 2 and 3 appears to be a transitional zone without a well defined contact.

In the transitional zone, the materials generally become more cemented with increased depth. However, the materials are highly stratified throughout with softer zones or lenses present in all intervals.

3.6.2 Seismic Refraction Survey Data

Seismic refraction surveys consisting of approximately 3600 lineal feet oriented along two orthogonal surface traverses were conducted on the site. The surveys were performed using a partakle analog refraction seismograph consisting of SIE RS-44, 12 channel, dry recording system, and low frequency (4.5 Hz) MARK L-1 vertical and horizontal geophones. The values of compression wave velocity (V_p), poisson's ratio, and elastic modulus (E) determined from the seismic surveys are summarized in Table 1.

Table A-1. Seismic Refraction Survey Data.

Depth Intervals, m (ft)		V_p		Poisson's Ratio	E	
From	To	m sec	(ft) sec		kg/cm^2	psi
0	0.5 -0.9 (1.5-3)	274-366	900-1200	0.33	935 1,603	13,300 22,800
0.5-0.9 (1.5-3)	2.4-3.7 (8-12)	488-610	1600-2000	0.33	3,129	44,500
2.4-3.7 (8-12)	7.6-10.7 (25-35)	793-914	2600-3000	0.20- 0.30	10,968- 12,093	156,000 172,000
7.6-10.7 (25-35)	18.29 (60)	-	-	0.42	12,937 38,810	184,000 552,000
18.29 (60)	- -	-	-	0.42	72,417 137,803	1,030,000 1,960,000

The values of E are based on shear strains of about 10^{-4} percent

3.6.3 Penetration and Moisture Content Data The data in Table A-2 are average values as determined from boring logs B5, B6, B8, B9, B18, and B19.

Table A-2. Penetration and Moisture Content.

Depth m (ft)	Blows per Foot (140 pounds 30 inches free fall drop hammer)	Moisture Content % of dry weight	Unified Soil Classifications
0-1.5 (0-5)	30	5.6	SM and ML
1-5.3 (5-10)	21	4.3	SM and ML
3-4.5 (10-15)	24	3.3	SM
4.5-6.1 (15-20)	66	4.5	SM
6.1-7.6 (20-25)	75	2.6	SM and SP
7.6-9.1 (25-30)	62	4.0	SM and SP
9.1-10.7 (30-35)	50	4.0	SM
10.7-12.2 (35-40)	50	4.0	SM

* A detailed description of testing, test equipment, and boring logs is available upon request from Sandia Laboratories. (Reference: Soil and Foundation Investigation Report, 5MW STTF, Sandia Laboratories)

** See "The Unified Soil Classification System" Corp of Engineers, US Army Technical memorandum No. 3-357 (Revised April 1960) or ASTM Designation D2487-66T

3.6.4 Summary of Direct Shear Tests

Boring No. B11 at 5.94 m (19.5 Ft)
C = 0
0 = 36.5°

Test No.	Normal Stress, kg/m^2	(lb/ft^2)	Shearing Stress kg/m^2	(lb/ft^2)
1	4880	(1000)	3220	(660)
2	9765	(2000)	6440	(1320)
3	14650	(3000)	11720	(2400)

Boring No. B8 at 0.76 m (2.5 ft)
C = 684 kg/m^2 (140 lb/ft^2)
Ø = 39°

Test No.	Normal Stress, kg/m^2	(lb/ft^2)	Shearing Stress, kg/m^2	(lb/ft^2)
1	2200	(450)	2440	(500)
2	7810	(1600)	6350	(1300)
3	12450	(2550)	10990	(2250)

APPENDIX B

HELIOSTAT DESIGN LOAD CALCULATIONS

1.0 INTRODUCTION

Design load calculations were provided by Solaramics for an equatorially mounted 2 meter by 3 meter heliostat. This heliostat is selected for the basic design of the UHA as required for Tasks 3, 4, 5, and 6. Heliostat weight = 434 pounds.

Data for the "49m^2" heliostat selected by DOESAN for the comparative UHA design of Tasks 4, 5, and 6, is extracted from SAND 78-8180, "10 MWE Solar Thermal Central Receiver Pilot Plant: Heliostat Foundation and Interface Structure Investigation."

2.0 DESIGN CRITERIA

		Wind Speed
Operational	-	To 30 mph (13 m/s)
Survival, Any position	-	To 50 mph (22 m/s)
Survival - Stowed	-	90 mph (40 m/s) From -10° Elevation

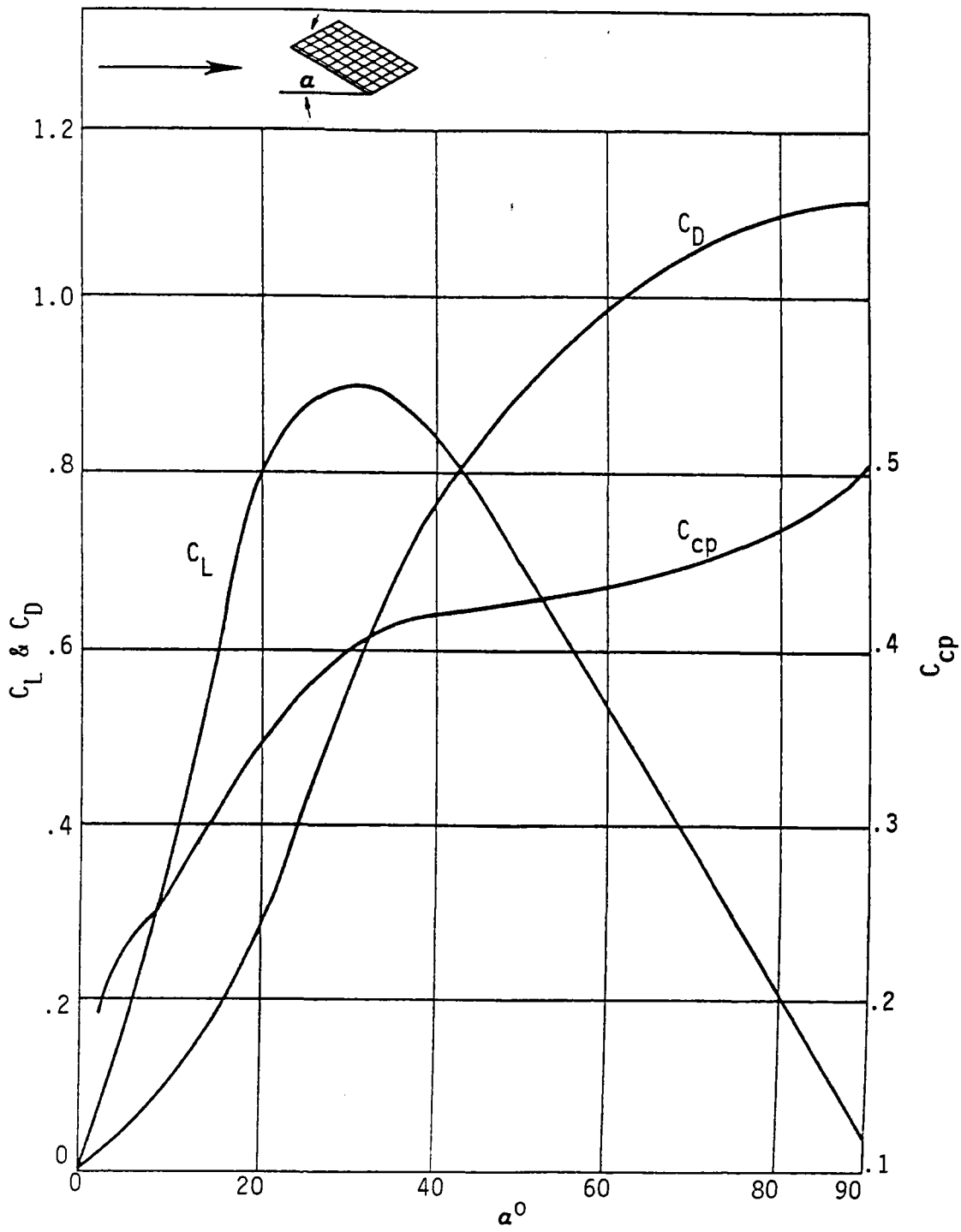

Figure B-1. Aerodynamics Coefficients
(Ref: ASCE Paper #3269
Wind Forces on Structures)

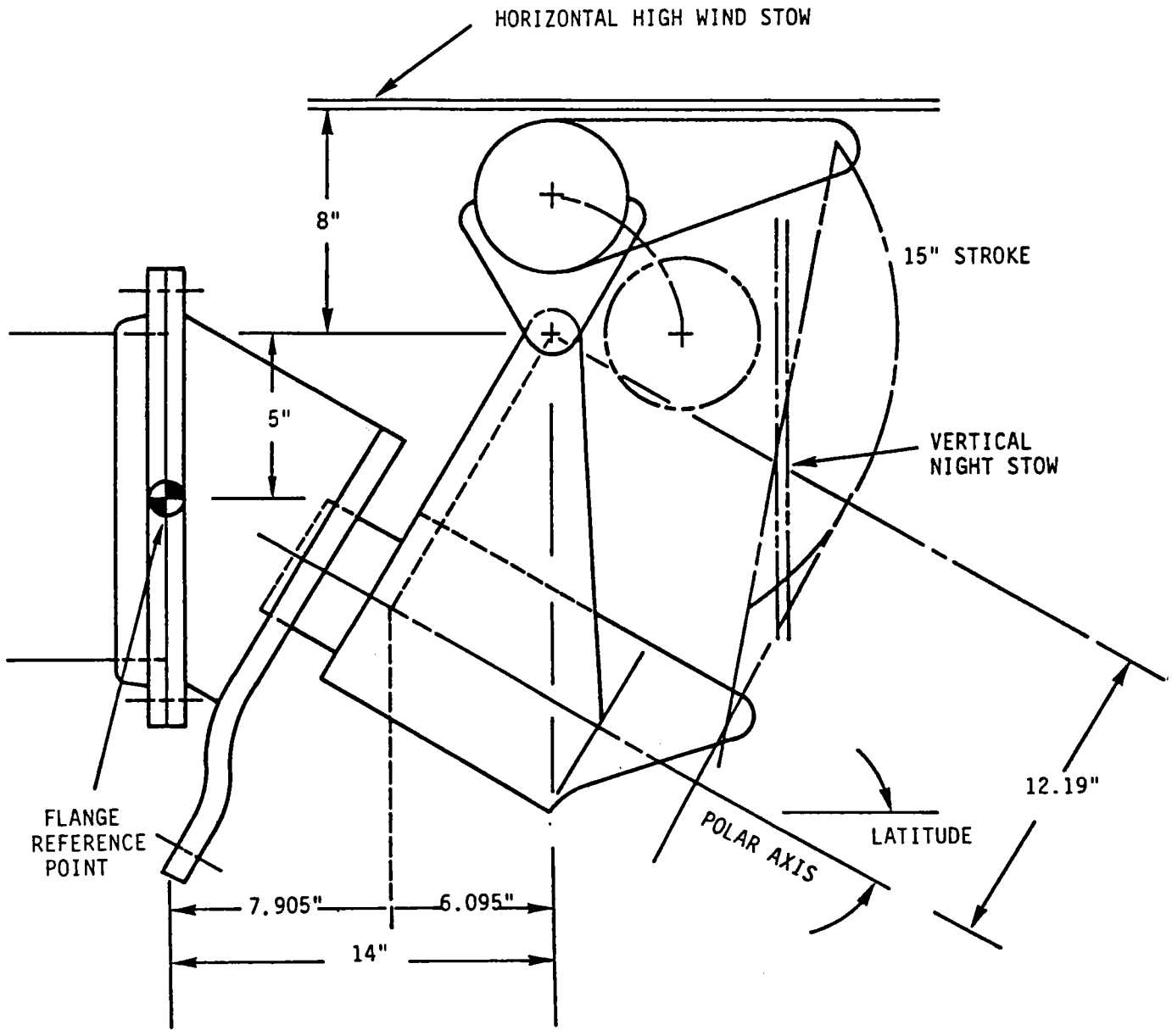

Figure B-2. Polar and Declination Mechanism for 2 x 3 Meter Heliostat.

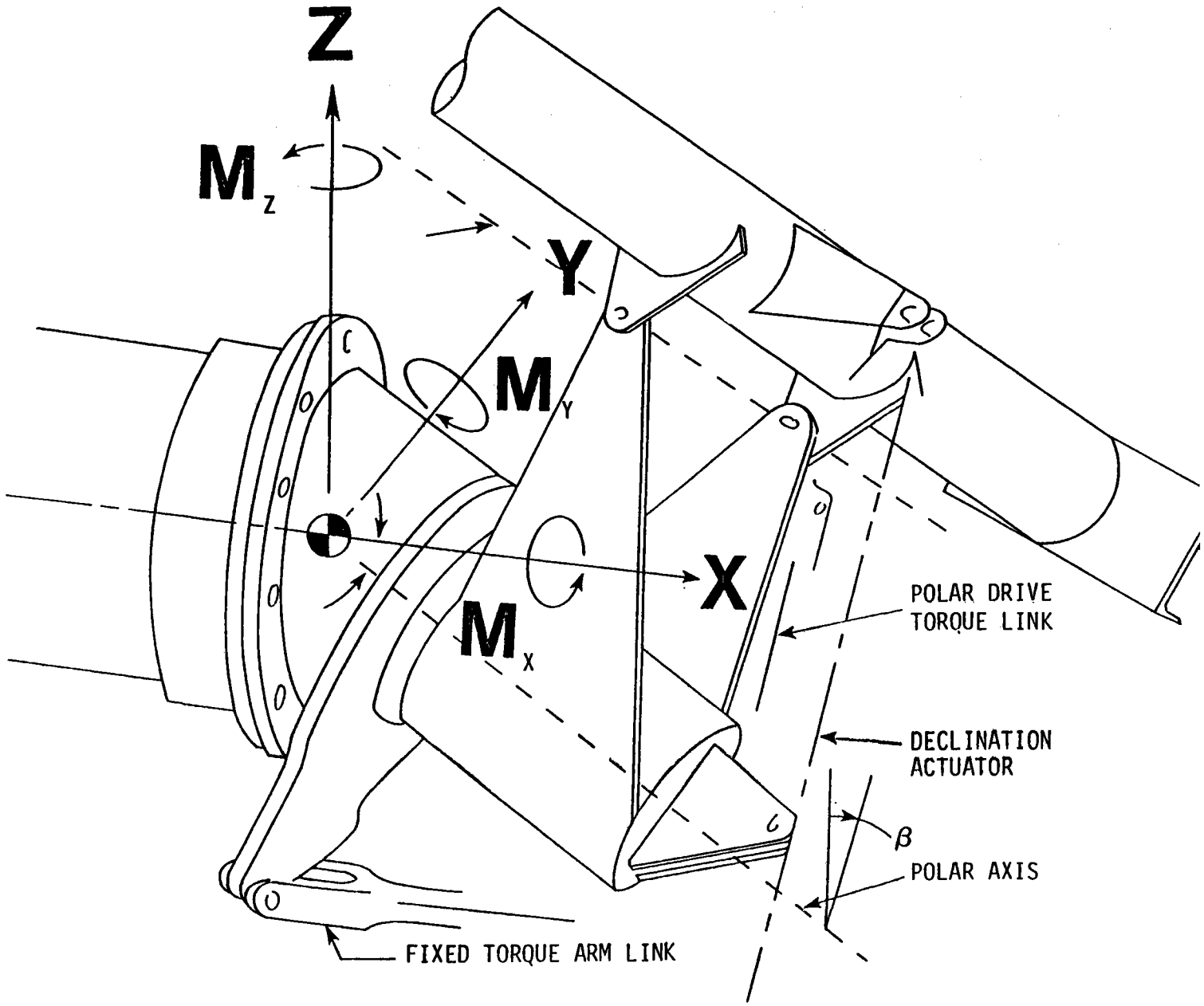

Figure B-3. Load Sign Convention for 2 x 3 Meter Heliostat.

Table B-1. Base Loads on 2 x 3 Meter Heliostat.

Wind Conditions: 50 mph from front or rear (south or north)
Heliostat Position: α ° = horizontal mirror plane
α positive = mirror tilted up toward vertical about the declination axis
β ° = 0, roll angle about polar axis
Lift, L, and Drag, D, are positive for rear wind. Lift is negative for frontal wind.

						Rear Wind	Frontal Wind
α	C_{cp}	C_L	C_D	L Z	D X	M_y	M_y
0	-	-	-	-	-	-	-
10	.26	.36	.106	148	43.7	1221	4569
15	.30	.60	.18	247	74.3	1107	7010
20	.34	.80	.28	330	115.5	440	8371
25	.375	.88	.42	363	173	-57	7973
30	.4	.9	.58	371	239	-117	7058
35	.413	.89	.67	367	276	-210	6460
40	.42	.85	.75	350	309	-16	5893
50	.428	.70	.88	289	363	860	4389
60	.438	.54	.98	223	405	1632	2873
70	.45	.38	1.06	157	437	2275	1390
80	.465	.22	1.1	91	454	2641	-91
90	.5	-	1.2	-	495	2970	-2970

Note: Moments are positive clockwise, negative counterclockwise.
Moments are graphed in Figure B-5.

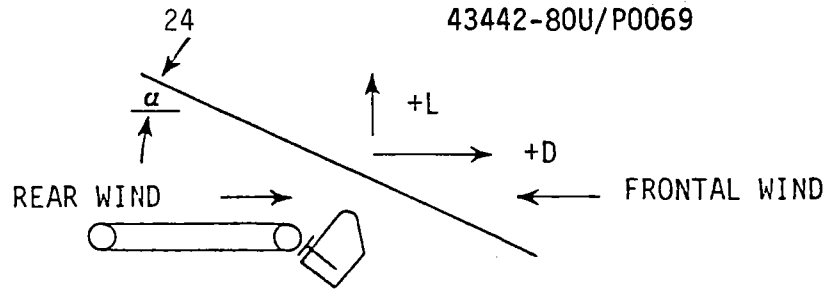

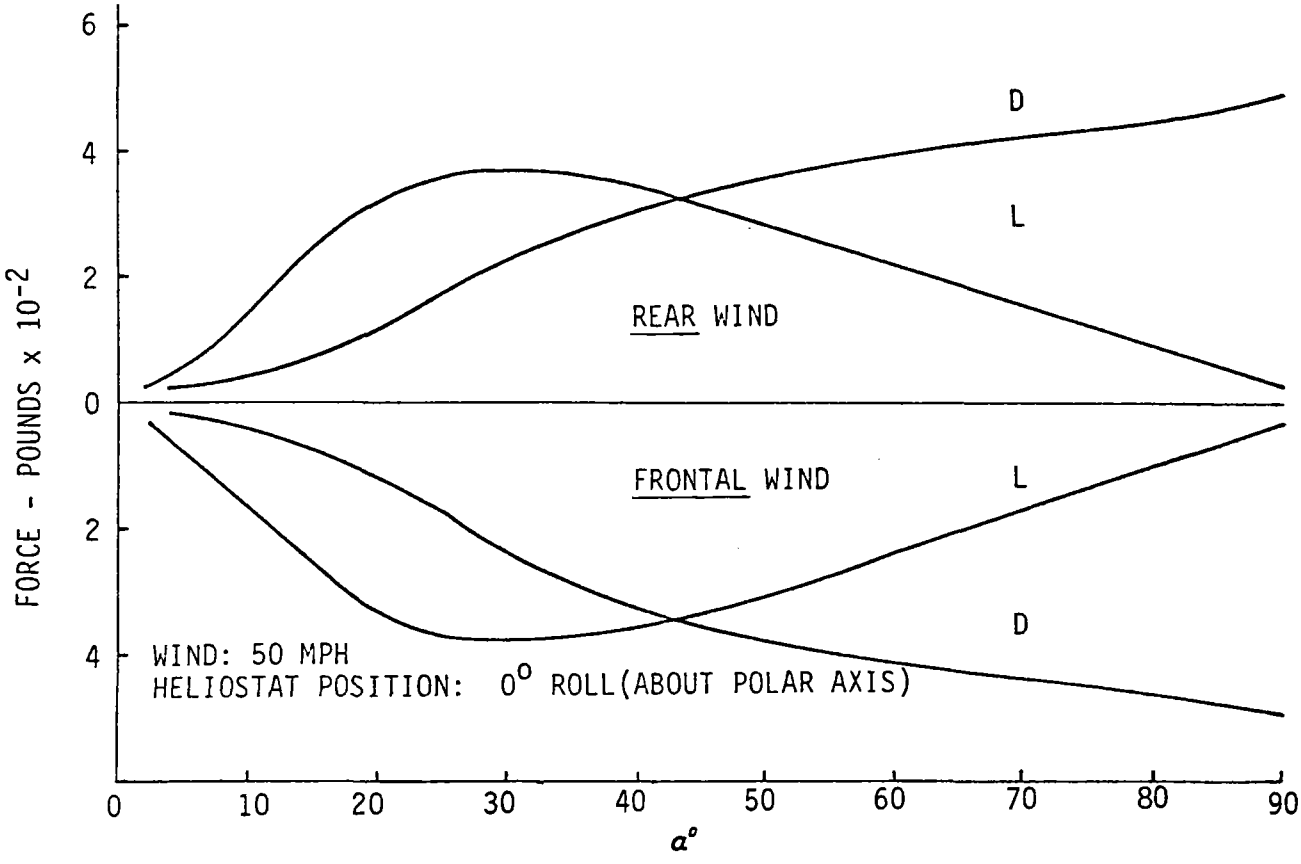

Figure B-4. Lift and Drag on 2 x 3 Meter Heliostat.

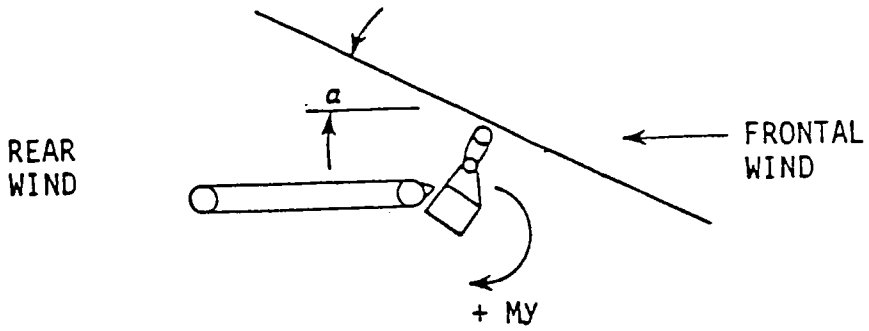

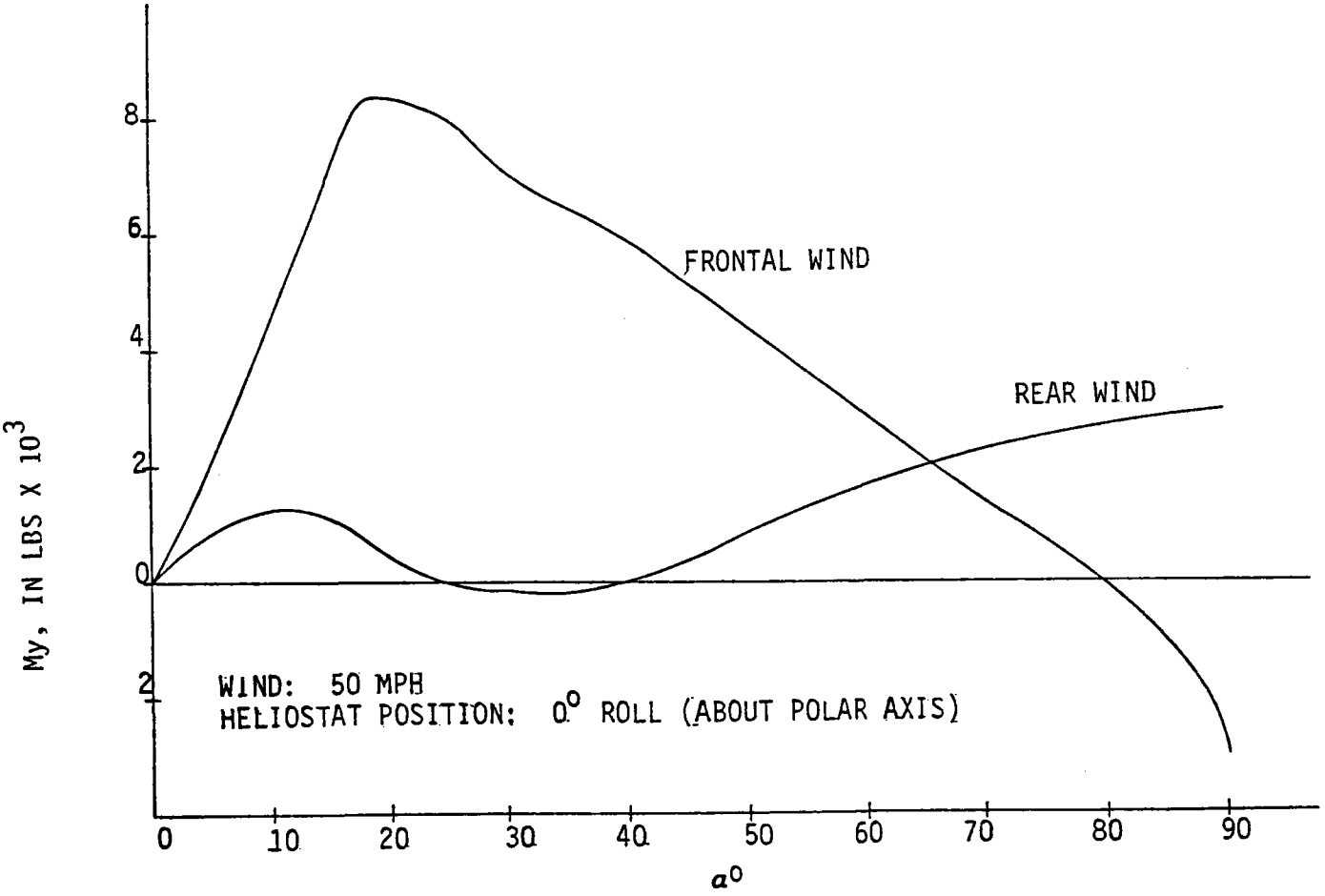

Figure B-5. Base Moments on 2 X 3 Meter Heliostat.

Table B-2. Base Loads on 2X3 Meter Equatorial Heliostat for 50 MPH Side Wind.

WEIGHT = 435 POUNDS

WIDE ANGLE	LIFT (LBS)	DRAG (LBS)	Aero. Coeff.	Polar Rotation	Mirror Centroid Position (inches from Ref. Point)			Center of Pressure Position (Inches from Ref. point)			Moments at Ref. Point (Inch-Pounds)		
β°	L_z	D_y	C_{cp}	β°	X_m	Y_m	Z_m	X_{cp}	Y_{cp}	Z_{cp}	M_x	M_y	M_z
10	-148	- 43.7	.26	8.682	13.93	3.229	13.75	13.93	31.12	8.83	-4219	2062	-608.7
15	-247	- 74.3	.3	13.064	13.84	4.826	13.45	13.84	27.62	7.34	-6277	3419	-1028
20	-330	-115.5	.34	17.495	13.72	6.40	13.02	13.72	24.14	6.56	-7208	4527	-1584
25	-363	-173	.375	21.99	13.55	7.945	12.47	13.55	21.31	6.24	-6657	4921	-2345
30	-373	-239	.4	26.56	13.35	9.451	11.81	13.35	19.67	5.91	-5925	4982	-3192
35	-367	-276	.413	31.23	13.11	10.909	11.01	13.11	19.32	5.13	-5675	4813	-3620
40	-350	-309	.42	36.00	12.83	12.31	10.10	12.83	19.54	4.04	-5592	4492	-3966
50	-289	-363	.428	45.90	12.15	14.88	7.92	12.15	20.34	1.42	-5365	3510	-4409
60	-223	-404	.438	56.31	11.28	17.07	5.29	11.28	20.73	-1.044	-5045	2517	-4571
70	-157	-437	.45	67.20	10.27	18.75	2.26	10.27	20.77	-3.282	-4695	1612	-4486
80	- 91	-450	.465	78.49	9.12	19.82	-1.068	9.12	20.54	-5.135	-4180	830	-4104
90	0	-495	.5	90	7.90	20.19	-4.564	7.90	20.19	-4.564	-2259	0	-3913
-10	148	- 43.7	.26	- 8.682	13.93	- 3.229	13.75	13.93	24.66	18.67	4465	-2062	-608.7
-15	247	- 74.3	.30	-13.084	13.84	- 4.826	13.45	13.84	17.97	19.55	5891	-3419	-1028
-20	330	-115.5	.34	-17.495	13.72	- 6.40	13.02	13.72	11.34	19.48	5992	-4527	-1584
-25	363	-173	.375	-21.99	13.55	- 7.945	12.47	13.55	5.42	18.71	5205	-4921	-2345
-30	373	-239	.4	-26.56	13.35	- 9.451	11.81	13.35	.767	17.71	4518	-4982	-3192
-35	367	-276	.413	-31.23	13.11	-10.91	11.01	13.11	- 2.50	16.90	3748	-4813	-3620
-40	350	-309	.42	-36.00	12.83	-12.31	10.10	12.83	- 5.08	16.17	3220	-4492	-3966
-50	289	-363	.428	-45.90	12.15	-14.88	7.93	12.15	- 9.42	14.43	2516	-3510	-4409
-60	223	-405	.438	-56.31	11.28	-17.07	5.29	11.28	-13.41	11.63	1718	-2517	-4571
-70	157	-437	.45	-67.20	10.27	-18.75	2.26	10.27	-16.74	7.81	784	-1612	-4486
-80	91	-450	.465	-78.49	9.12	-19.82	-1.068	9.12	-19.11	3.00	- 389	- 830	-4104
-90	0	-495	.5	-90	7.90	-20.19	-4.564	7.90	-20.19	-4.564	-2259	0	-3913

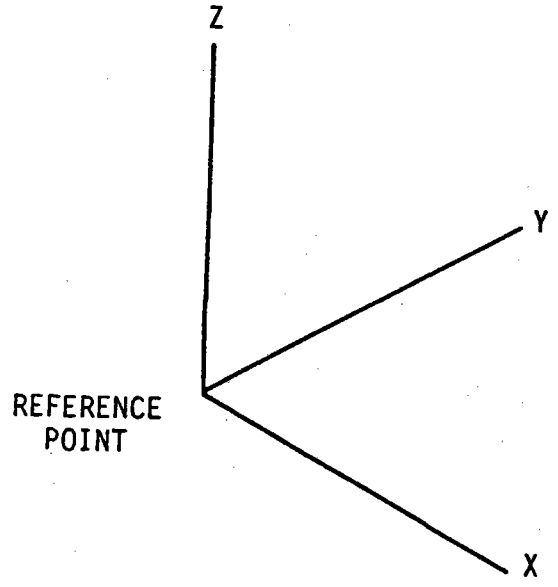

Figure B-6. Notes for Table B-2.

$-X_1$ is horizontal north through the heliostat reference point
β' is the rotation around the polar axis
α is the rotation about the declination axis

When $\beta' = \alpha = 0^\circ$ the declination axis is horizontal, and the mirror position is in a horizontal plane. At that position, a north south line in the mirror face is paralled to the X axis. As β' varies, the value of α is varied to maintain this direction on the mirror face parallel to the X axis.

β is the angle between the mirror plane and the horizontal wind blowing from the +y (east) direction.

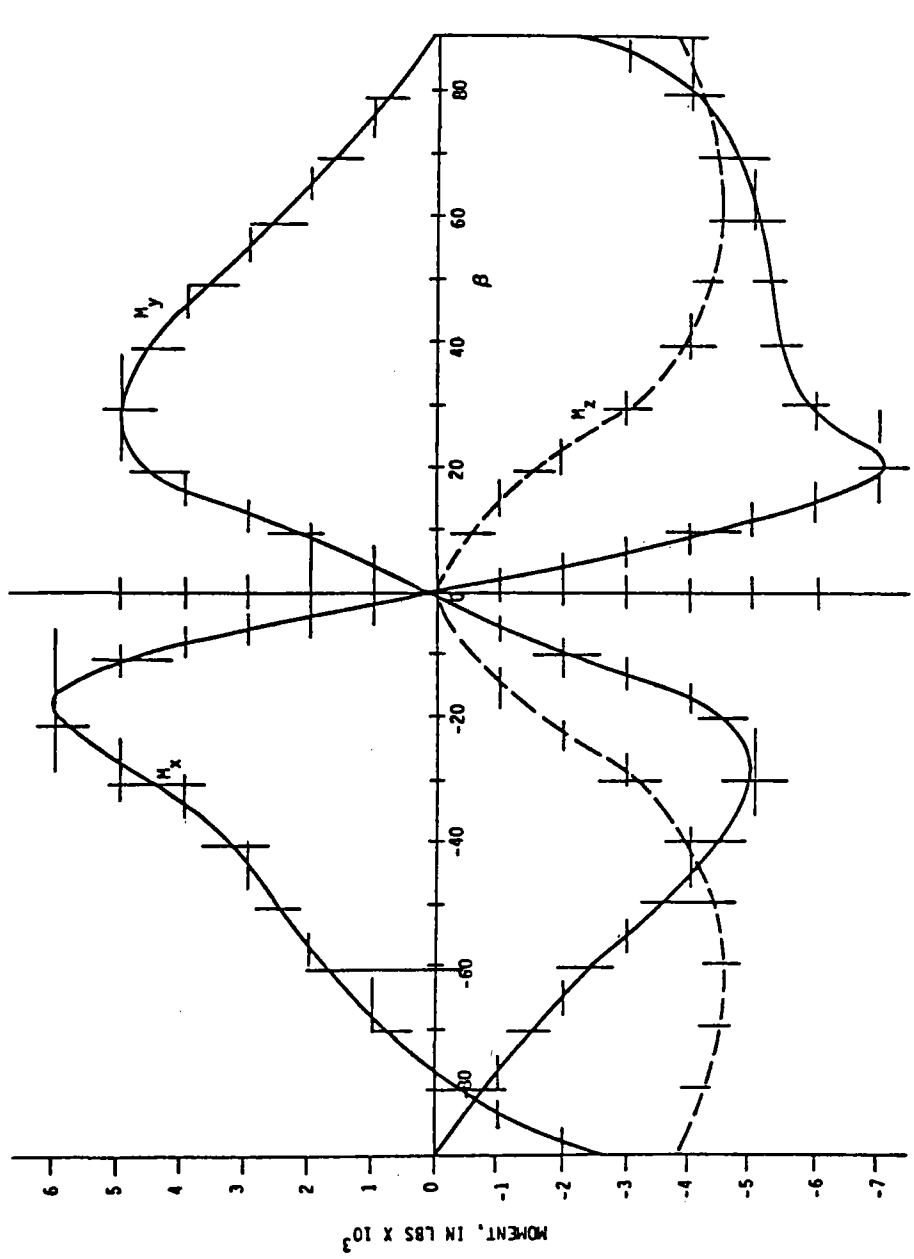

Figure B-7. Base Moments on 2X3M Equatorial Heliostat for 50 MPH Side Wind.

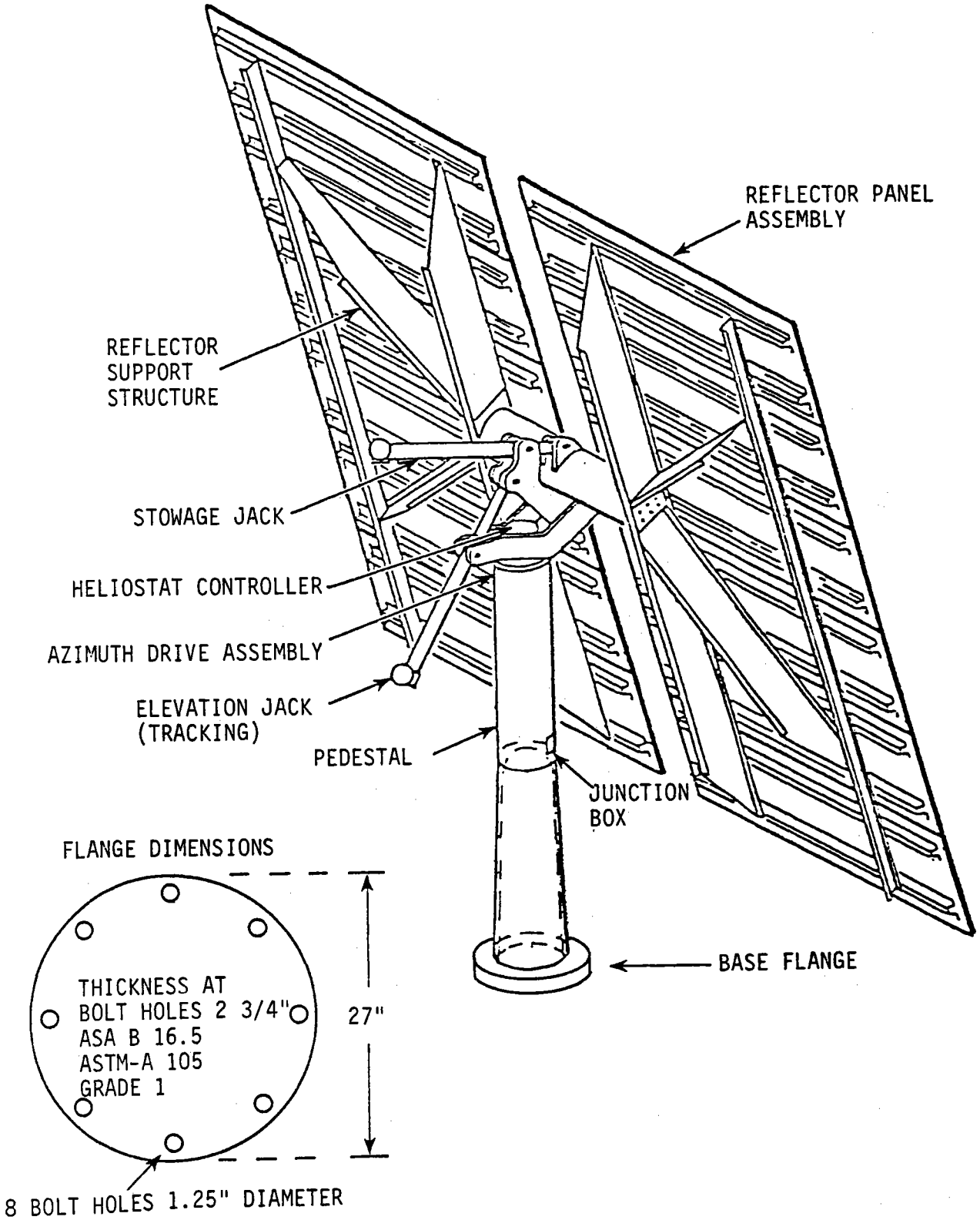

Figure B-8. 49m^2 Heliostat.

Table B-3. Characteristics of the UHA Heliostat to be Used for the "49m^2" Heliostat.

Total Size: 528 square feet, 4132 pounds
No. of Panels: 12
Size of Each Panel: 4 x 11 feet
Elevation of Axis: 13.4 feet
Configuration: Approximately square
Minimum Spacing between heliostat Centers: 34.44 feet
Reflectivity: 0.90
Beam Quality (Reflected Beam): Plus/minus 2 milliradians (1 sigma)
Pointing Accuracy (Reflected Beam): PLus/minus 1.5 milliradians (1 sigma)
Cost: $79/M sq. Nth plant
$230/M sq. first plant
(1980 dollars)
This is installed cost including all wiring and collector computer. Does not include land cost.

Collector Electrical Interface and Characteristics

Communication with heliostat field will be via a bidirectional data line (shielded twisted pair)
Standard RS-232 11 bit serial interface
5 volt signal level
9600 Baud or 19.2 kilobaud

Table B-4. Design Loads For Mounting the "49m^2" Heliostat. Extracted from SAND 78-8180

MIRROR TILT $\alpha°$	WIND AZIMUTH $\beta°$	WIND SPEED MPH	BASE MOMENT INCH-LBS. M_{y-y}	BASE MOMENT INCH-LBS. M_{x-x}	HINGE MOMENT INCH-LBS. M_{y-y}	HINGE MOMENT INCH-LBS. M_{x-x}	HORIZONTAL FORCE LBS. F_x	HORIZONTAL FORCE LBS. F_y	TORQUE INCH-LBS. M_{z-z}
30	180	27	102640	-1760	38453	334	507	-16	724
60	135	27	93816	32555	16461	11849	613	164	19705
60	180	27	130639	-1188	22434	1183	856	-18	52
30	180	35	172475	-2957	64616	561	852	-27	1217
60	135	35	157647	54705	27661	19911	1030	276	33112
60	180	35	219524	-1996	37698	1988	1438	-30	87
30	180	50	351989	-6036	131869	1145	1739	-55	2483
60	135	50	321728	111643	56451	40634	2102	562	67575
60	180	50	448008	-4074	76934	4057	2936	-62	178
-10	0	90	-411219	-7681	-233510	-36091	-1402	228	6794
-10	45	90	-274993	322562	138107	118744	-1078	1606	-8891

Note: Calculated from coefficients obtained from wind tunnel tests.

APPENDIX C

PRELIMINARY DESIGN POINT CALCULATIONS

1.0 INTRODUCTION

The calculations for this contract are to be based on Barstow, CA as site. Design point is noon of the winter solstice. Insolation for these calculations is assumed as 950 WM^{-2}. A height of 8 meters above the lower edge of the lowest heliostat is the arbitrary choice of center of the aperture. for a "low" central receiver location. A heliostat reflectance of 0.9 is used. Atmospheric transmission factor was selected as 0.99. The aperture angle in the East-West direction was chosen as 60°.

A sensitivity analysis for cost reduction for changes of aperture angle and height above reference line is not part of the intitial contract.

The preliminary design point calculations included as Tables C-1 and C-2 will be used to establish conceptual structural designs.

Table C-1. Preliminary Design Configuration for UHA Using $6m^2$ Heliostat

DESIGN POINT POWER	UHA ASPECT RATIO H:L	UHA COSINE FACTOR	NO. OF ROWS	NO. OF COLUMNS	TOTAL NO. OF HELIOSTATS	TOTAL HELIOSTAT AREA	UHA HEIGHT M	UHA LENGTH M	POWER AT APERTURE MWT
1 MWT	1:5	0.95713	10	21	210	1260	22	105	1.021
	1:3	0.94984	13	16	208	1248	28.6	80	1.003
	1:1	0.91866	22	10	220	1320	48.4	50	1.026
10 MWT	1:5	0.95713	31	66	2046	12276	68.2	330	9.946
	1:3	0.94984	41	51	2091	12546	90.2	255	10.087
	1:1	0.91866	69	31	2139	12834	151.8	155	9.980
25MWT	1:5	0.95713	50	105	5250	31500	110	525	25.520
	1:3	0.94984	65	80	5200	31200	143	400	25.085
	1:1	0.91866	110	50	5500	33000	242	250	25.661

Note: Aperture 60° E-W
Receiver at 8m above reference plane
Atmospheric transmission coefficient assumed 0.99

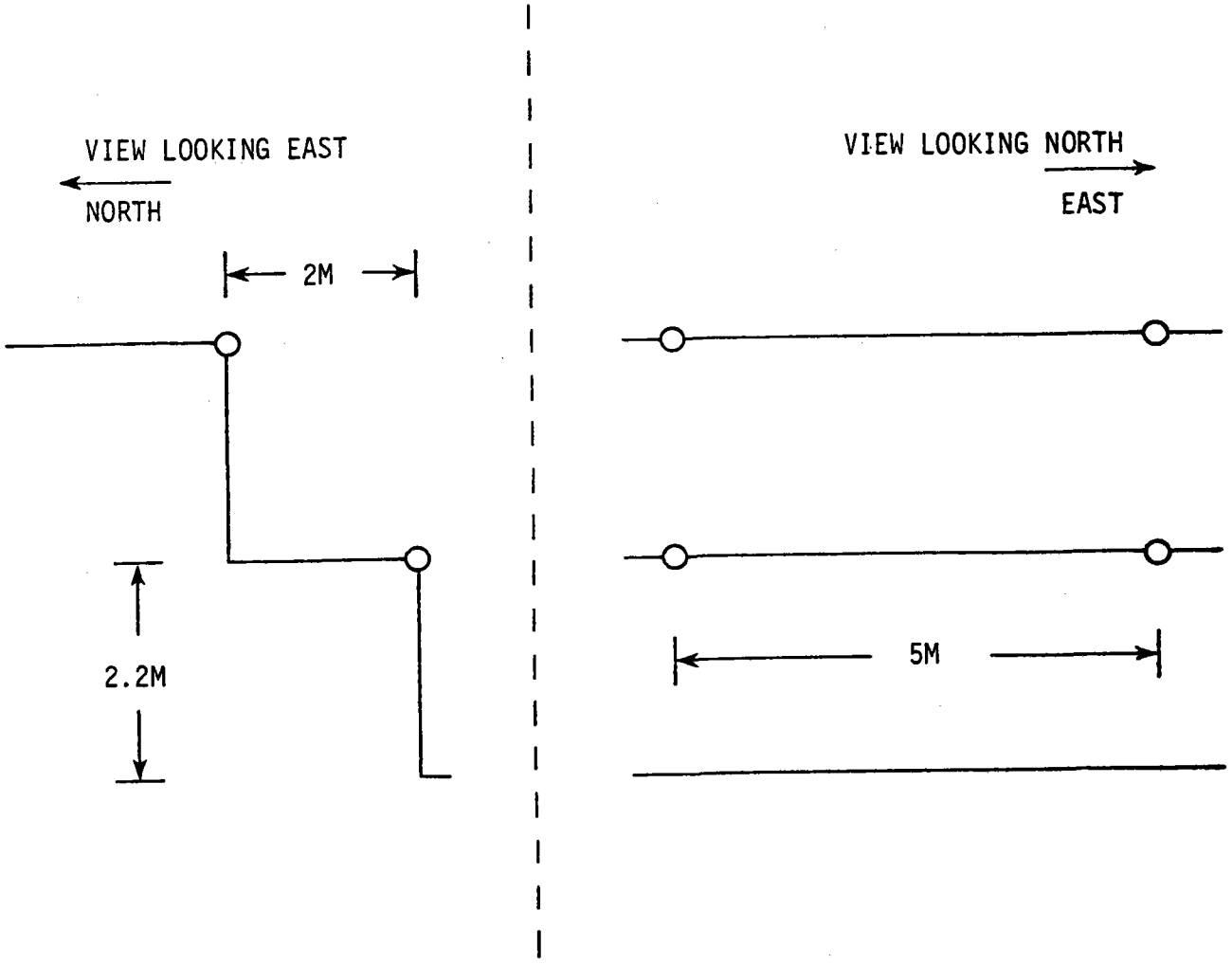

Figure C-1. Flange Reference Point Locations for the 2 x 3 Meter Heliostat on the UHA.

43342-80U/P0069

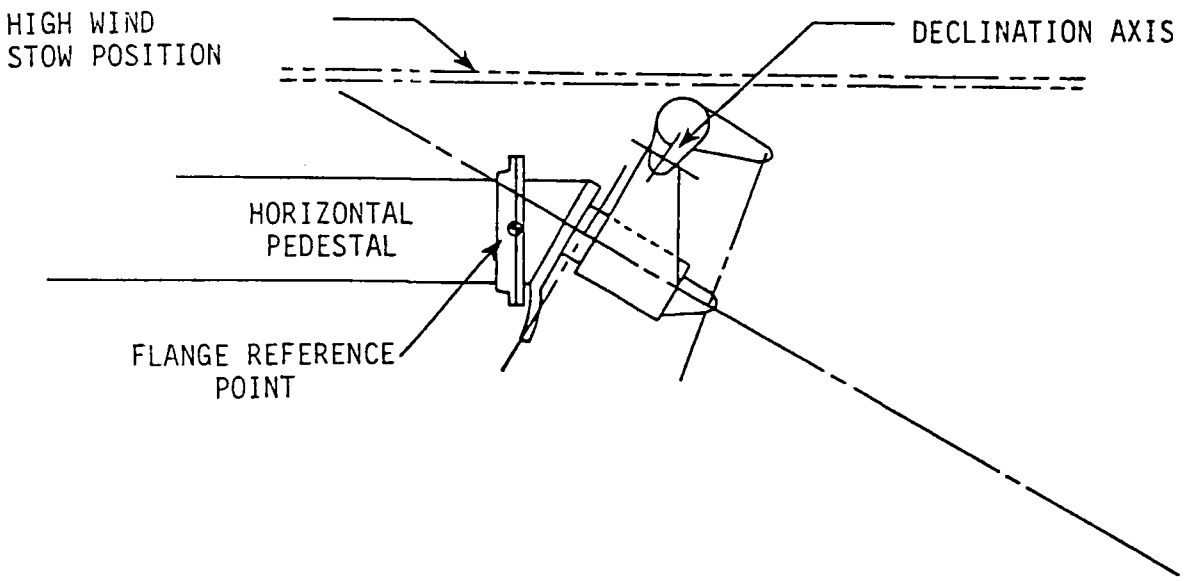

Figure C-2. High Wind Stow Position For 2X3 Meter Heliostat: $\alpha = 0^0$, $\beta = 0^0$

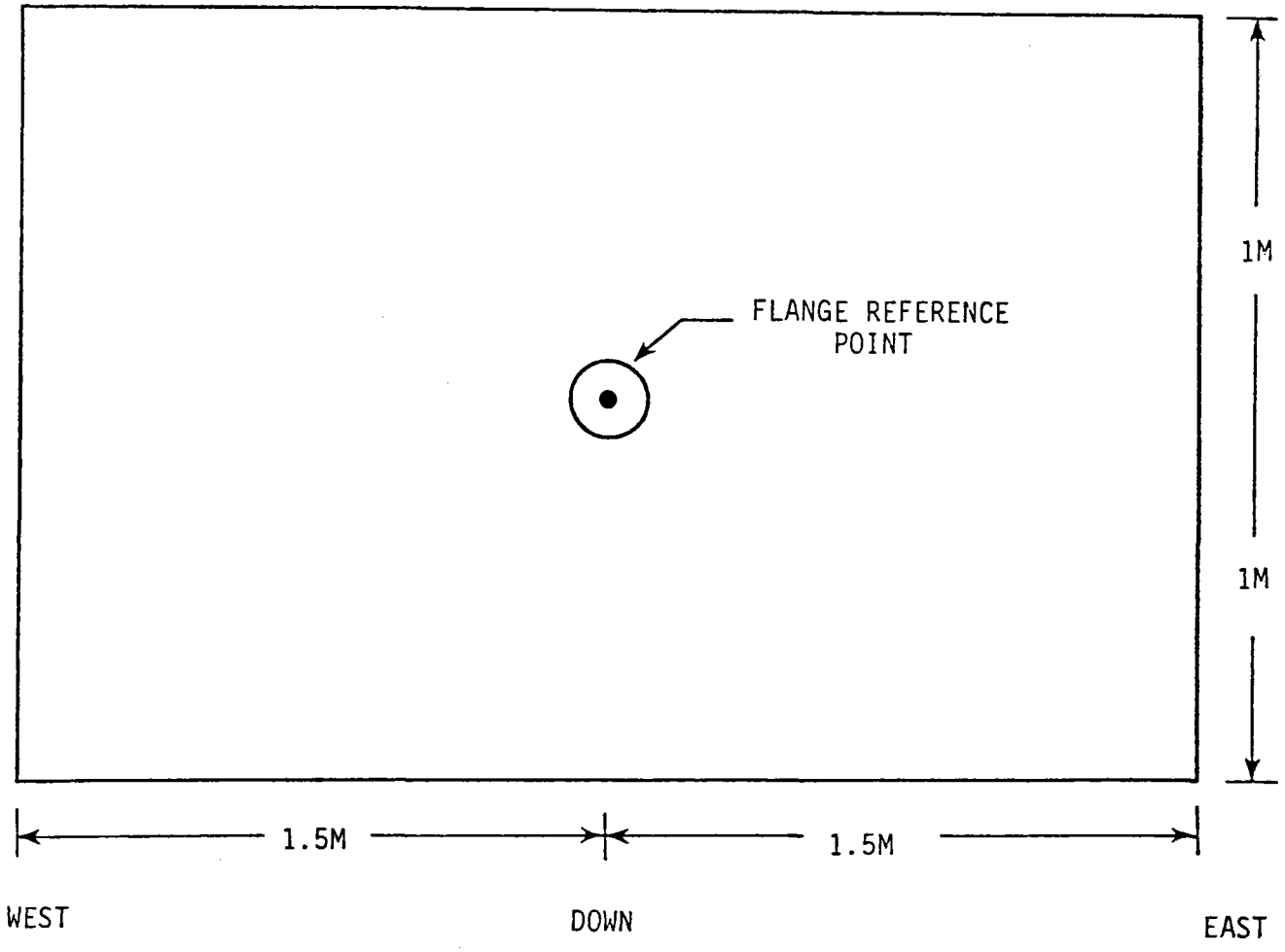

Figure C-3. 2X3 Meter Heliostat: $\alpha = 90^{o}$, $\beta = 0^{o}$ (View looking north, mirror element vertical, declination axis horizontal).

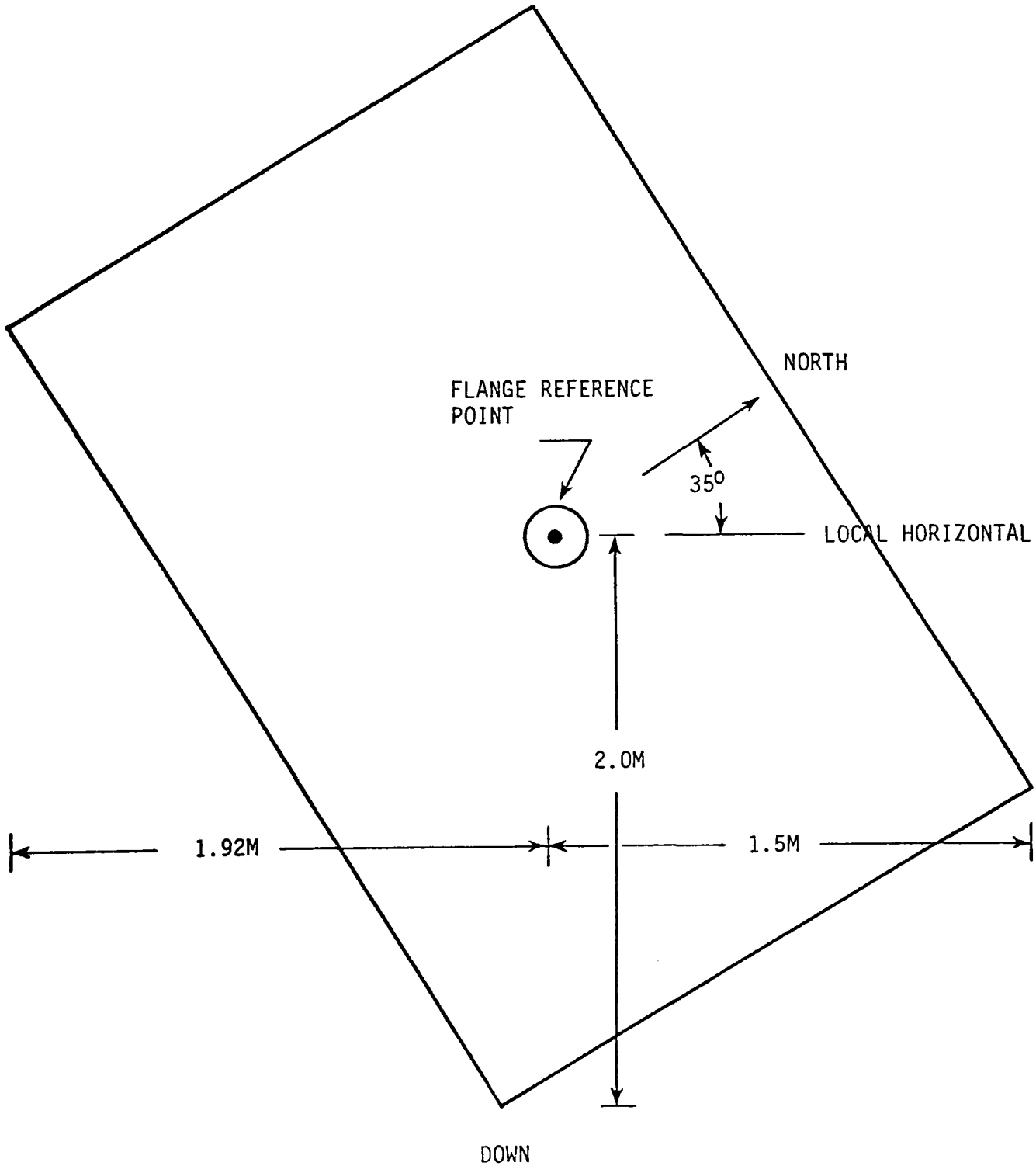

Figure C-4. 2X3 Meter Heliostat: $\alpha = 0^{o}$, $\beta = 90^{o}$

VIEW LOOKING WEST

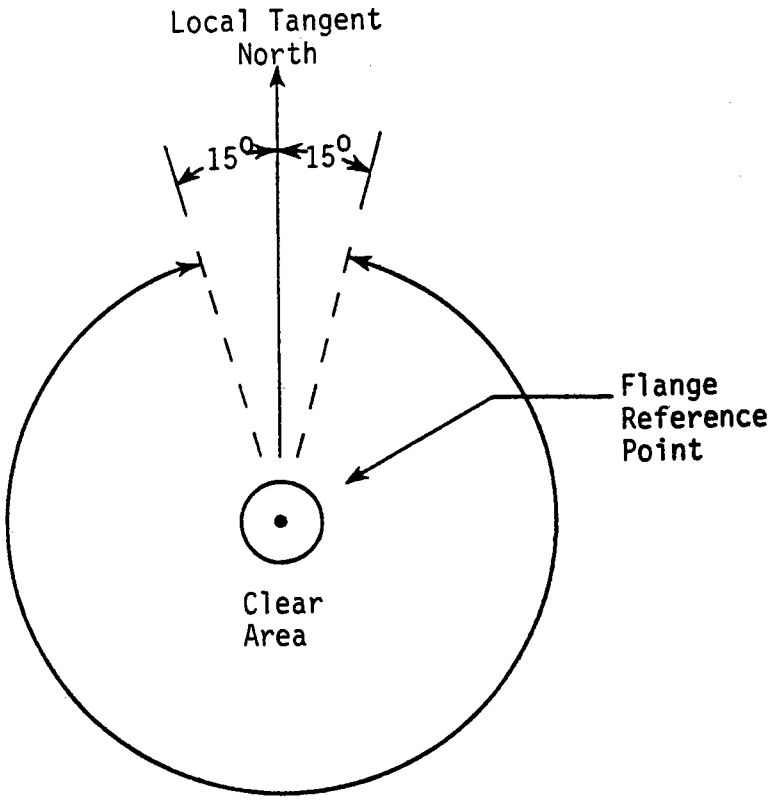

Figure C-5. View of Horizontal Plan Clearance Circle For 2 X 3 Meter Heliostat.

Table C-2. Preliminary Design Configuration for Using 49m^2 Heliostat.

DESIGN POINT POWER	UHA ASPECT RATIO H:L	UHA COSINE FACTOR	NO. OF ROWS	NO. OF COLUMNS	TOTAL NO. OF HELIOSTATS	TOTAL HELIOSTAT AREA	UHA HEIGHT M	UHA LENGTH M	POWER AT APERTURE MWT
1 MWT	1:5	0.95713	3	9	27	1323	28	123.5	1.072
	1:3	0.94984	4	7	28	1372	37	96	1.103
	1:1	0.91866	6	5	30	1470	55	68.6	1.143
10 MWT	1:5	0.95713	9	28	252	12348	82.3	384.2	10.004
	1:3	0.94984	11	23	253	12397	100.5	315.6	9.967
	1:1	0.91866	20	13	260	12740	182.8	178.6	9.906
25 MWT	1:5	0.95713	14	45	630	30870	128	618.3	25.010
	1:3	0.94984	18	35	630	30870	164.5	480.9	24.819
	1:1	0.91866	31	21	651	31899	283.4	288.54	24.805

Note: Aperture 60° E-W
Receiver at 8m above reference plane
Atmospheric transmission coefficient assumed 0.99

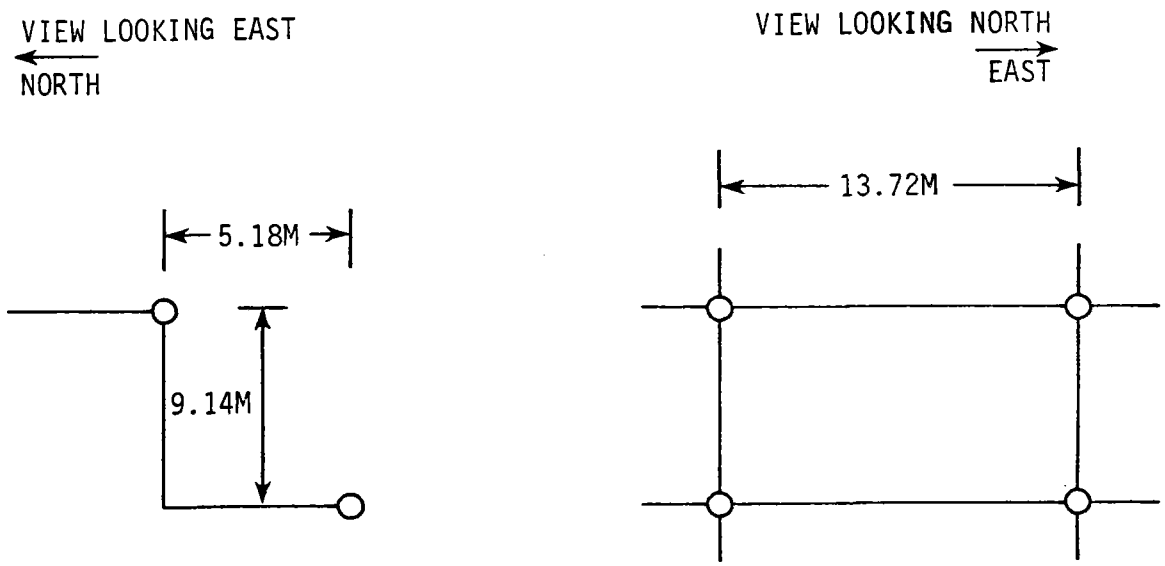

Figure C-6. $49M^2$ Heliostat Pivot Point Locations When Used on the UHA.

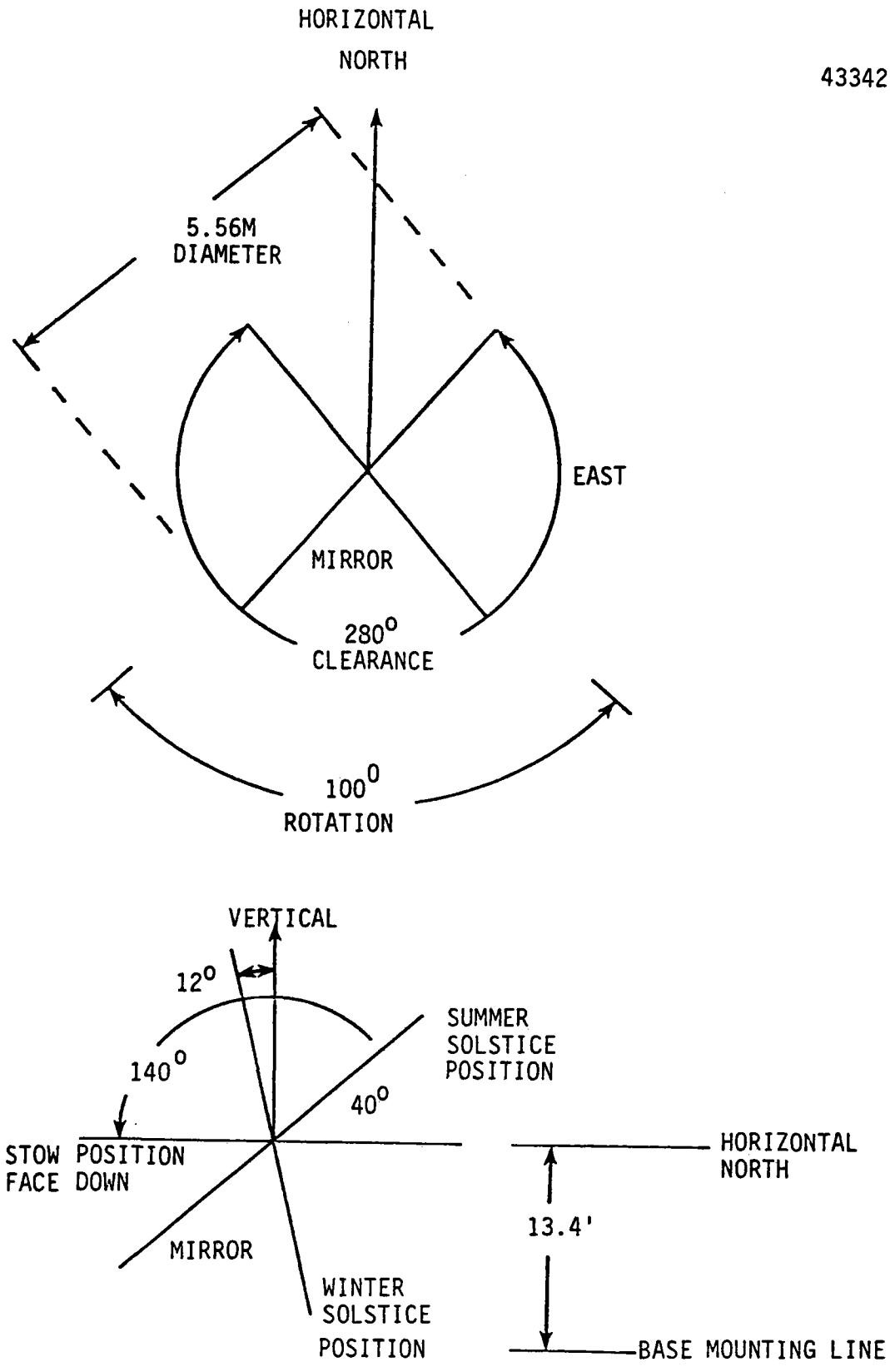

Figure C-7. Extreme Positions for $49M^2$
Heliostat On A UHA Having An East-West Aperture = 60^o

Table C-3. Final Design Configuration.

FINAL DESIGN CONFIGURATIONS FOR THE UHA								
Design Point Power		Aperture Size (M^2)	Heliostat Type	Number of		Total Heliostat Area (M^2)	UHA	Size (M)
Nominal	Analytic			Rows	Columns		Height	Length
1 MWT	1.011 MWT	Round 1.85	V-6M^2	10	20	1260	22	105
	1.007 MWT	Rectangle 2.1						
10 MWT	10.031 MWT	Round 16.9	V-6M^2	31	68	12648	6.82	340
	10.013 MWT	Rectangle 18						
10 MWT	10.26 MWT	Round 21.27	49M^2	9	31	12884	82.3	425.36
	10.18 MWT	Rectangle 2.1						
25 MWT	25.11 MWT	Round 385	V-6M^2	50	106	31800	110	530
	25.15	Rectangle 42						

APPENDIX B

FINAL REPORT

DEVELOPMENT OF STRUCTURAL CONCEPTS FOR THE UNIFIED HELIOSTAT ARRAY

Prepared for VEDA Incorporated
Under Subcontract No. 13222-80U-Q0069
Bechtel Job No. 13870

Bechtel National, Inc.
Research and Engineering Operation
P.O. Box 3965
San Francisco, CA 94119

November 1980

ABSTRACT

Bechtel National, Inc. conducted a study for the conceptual structural development of the patented Unified Heliostat Array (UHA) proposal by Veda, Inc., Camarillo, California. Concepts were developed for the UHA support structures and foundations for heliostat sizes, configurations, and power levels designated by Veda. Essential structural design criteria were also established. Nine preconceptual candidate designs were developed along with capital costs. Based on these capital cost estimates, Veda selected the preferred aspect ratio for three power levels for further development by Bechtel. Consequently, Bechtel analyzed, upgraded, and determined costs for three selected conceptual arrays in more detail than those given in the preconceptual designs. Bechtel also determined the effect of substituting the 49 m^2 (MDAC) heliostat in place of the 6 m^2 Veda/Reflective Modules heliostat for the selected 10 MWt array.

CONTENTS

CONTENTS (cont'd)

ILLUSTRATIONS

ILLUSTRATIONS (cont'd)

TABLES

Section 1

INTRODUCTION

The work described in this report was performed by Bechtel to support the conceptual development of the patented Unified Heliostat Array (UHA) proposed by Veda, Inc.. This concept is designed to provide industrial process heat or utility power from solar energy. In the UHA system, the solar receiver is placed near ground level, close to the industrial process or power plant, and a large, sloping support structure is provided to raise the heliostats into positions to suitably reflect solar energy.

The Bechtel work was directed to developing concepts for the UHA support structure and foundations to carry heliostat sizes and configurations designated by Veda Inc. to suit their process parameter studies. The Bechtel work was planned for Tasks 1, 2, 4 and 6 while Veda performed the work in Tasks 3 and 5. The Bechtel tasks encompassed the following:

- Task 1 - Design Review
- Task 2 - Array Parametric Analysis
- Task 4 - Heliostat Parametric Analysis
- Task 6 - Economic Analysis

The work began in Task 1, Design Review, by establishing the essential criteria to be used in the conceptual designs of the array structures. This work is described in Section 2. For Task 2, Array Parametric Analysis, a literature review was performed to identify existing structural forms and concepts that may be used in the development of candidate

designs. This work is described in Section 3. Nine conceptual structural designs covering particular power capacities of 1, 10, and 25 MWt using a beam-girder framing system were developed in Task 2 along with capital cost estimates for each. It was intended that these nine preconceptual designs would give only comparative cost estimates and would be within the realm of low cost structures for this application. Section 4 describes this development work as well as the cost estimating covered by Task 6. Based on the capital cost estimates presented in Task 2, Veda Inc. performed Task 3 in order to select the preferred aspect ratio (ratio of the structure's height to its length) of 1:5 for all the power levels for further development by Bechtel Task 4.

To begin work in Task 4, Heliostat Parametric Analysis, it was determined that a large percentage of the steel tonnages of the preconceptual designs developed in Task 2 came from the heliostat support system. Therefore, based on engineering judgment and experience, a modified heliostat support concept was developed for Task 4 in an attempt to further reduce the amount of steel and reduce the costs of the structures having the preferred aspect ratio. Veda performed the work in Task 5 to study the energy performance of the different size heliostats for the selected UHA. Using the modified support concept for the heliostats, selected conceptual arrays were analyzed in more detail than the preconceptual designs developed in Task 2. These more detailed analyses used the STRUDL computer program for determining stresses and rotations. This work led to improved cost estimates, performed under Task 6, for Veda to establish the cost of energy from the arrays.

In Task 4 Bechtel also considered the effect of substituting the 49 m^2 McDonnell-Douglas (MDAC) heliostat in place of the 6 m^2 Veda/Reflective Modules heliostat for selected conceptual array. A modified support concept was again used for the heliostats and an analysis performed in the same level of detail as was done for the array with the 6 m^2 heliostats. The Task 4 work is described in Section 5 of this report.

Section 2

DESIGN CRITERIA

During Task 1, the general structural design criteria were developed for the conceptual designs and parametric study of the Unified Heliostat Arrays (UHA). The design of a structure always requires the initial definition of design criteria. Two basic aspects of this step are the specification of the acceptance criteria for the materials and members involved in the structures and the specification of loads and load combinations. Accordingly, this section began by considering the criteria to be used for structural evaluation of the design concepts. These criteria were taken from existing building codes and handbooks, and DOE criteria, since no specific code is directly applicable to the UHA structure.

2.1 ACCEPTANCE CRITERIA

2.1.1 Deflection Criteria

The specific document governing the deflection criteria is Reference 2-1. In order to obtain specified overall field performance for the UHA, some limit on the deflections of the heliostat array must be imposed. Six degrees of freedom are possible for a member of a structure - three translations and three rotations.

Translations of the heliostats will have a small effect on the intensity of total radiation delivered at the receiver. However, to minimize tracking errors, the rotations at the base of the heliostat pedestals

must be limited. Specifically, the rotations about two axes in a vertical plane parallel to the length of the array are limited to $\pm$ 1.5 mrads in an operational wind of 12 m/s (27 mph). The rotation about the axis normal to the vertical plane parallel to the length of the UHA has no significant effect on the tracking error of the heliostats.

2.1.2 Steel Design Criteria

Codes and standards used in the steel design are as follows:

- Manual of Steel Construction, 7th Edition, 1969, American Institute of Steel Construction (AISC)
- American Iron and Steel Institute (AISI) "Cold-Formed Steel Design Manual," 1977 Edition
- American Welding Society (AWS) "Structural Welding Code" (AWS D 1.1-80)

For the development of the structural concepts, a commonly used steel, ASTM A-36, was assumed. The working stress method was used for design following the AISC Manual in which the allowable stresses in members are limited to about 60% of yield stress.

It was found that stability criteria for buckling governed the design of many members in the UHA structure. For example, in a column allowable stresses are a function of the length and details of its end conditions supports. Shown in Figure 2-1 is a plot of the allowable stresses in a column as a function if its slenderness ratio L/R (ratio of the length of a column to its radius of gyration). Using A-36 steel and following the AISC specifications and the American Association of State Highway Officials (AASHO) specifications, 1969 (Reference 2-2),

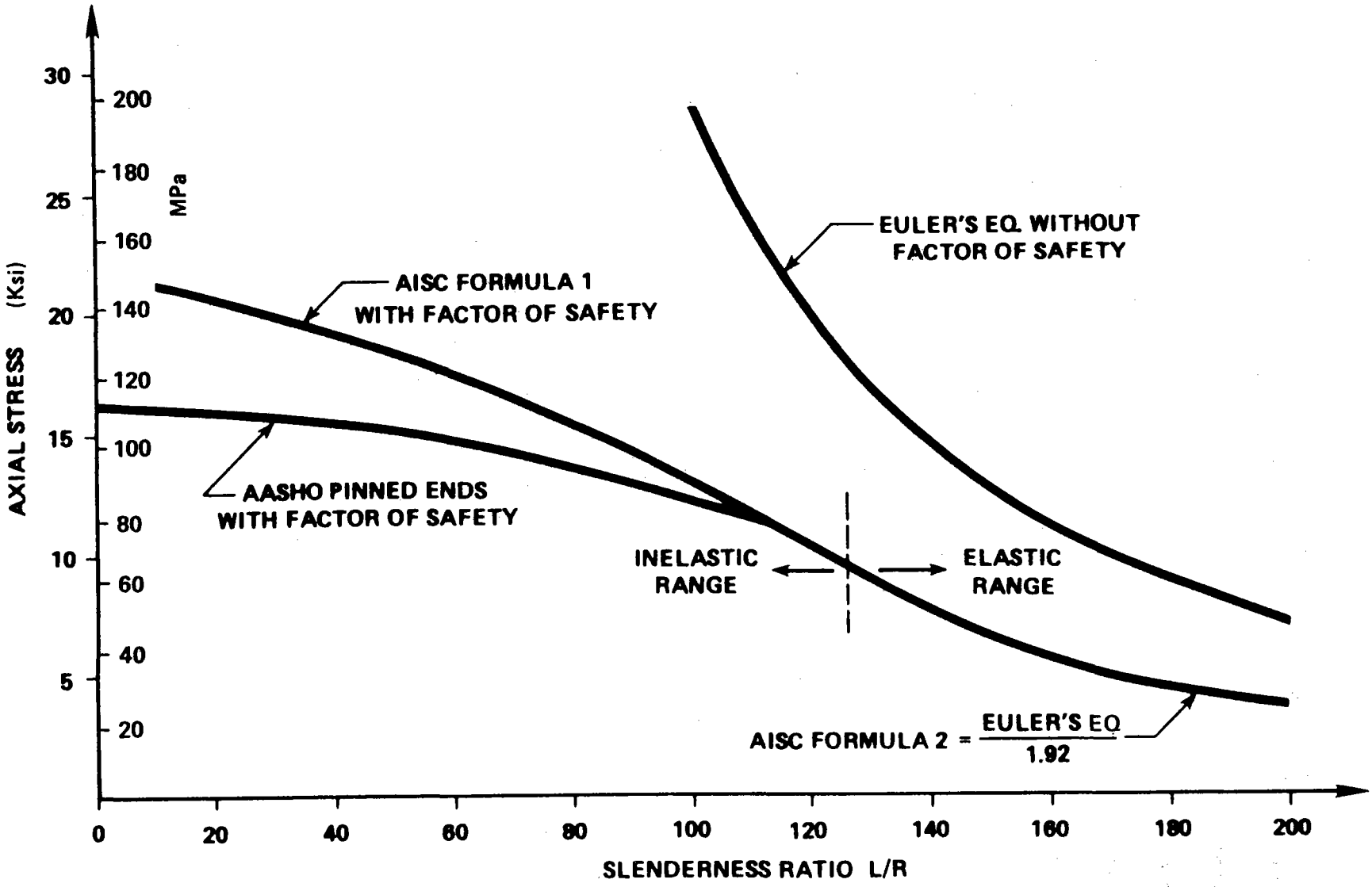

NOTE: CURVES ARE FOR 1969 SPECS. AND A 36 STEEL

Figure 2–1 Allowable Stresses for Columns

both specifications indicate varying factors of safety with regard to the theoretical buckling load given by Euler's equation.

2.1.3 Concrete Design Criteria

The standard used in the design of concrete components and structures in the building industry is the American Concrete Institute Code ACI 318 "Building Code Requirements for Reinforced Concrete." This standard is generally incorporated verbatim into local building codes and is used nationwide. In this work, the latest (1977) edition was used.

The design strength of the concrete was assumed to be 3000 psi. The reasons for this choice are:

- It is a widely used, readily available concrete and many contractors are familiar with working with this mix.
- Higher strengths are not warranted by the imposed loads.
- Higher strength concretes are relatively more expensive

2.1.4 Foundation Design Criteria

The design standard used in the design of the foundations is the Uniform Building Code (UBC), 1979 edition. In particular, the foundations were designed using the allowable stresses specified in Chapter 29 of the UBC. Design for uplift, overturning and sliding was in accordance with Sections 2311 (c), 2311 (i) and 2907 (f) respectively.

2.1.5 Soil Properties for Foundation Design

Soil properties used for the UHA foundation design are specified in the soil analyses report of the Albuquerque Solar Facility (Reference 2-3) as follows:

- o 0'-0" to 2'-0" Silty Sand, 98 pcf, N=10, $1500 < q < 1800$ psf
- o 2'-0" to 6'-0" Silty Sand, 103 pcf, N=22, $1800 < q < 3000$ psf
- o 6'-0" to 10'-0" Silty Sand, Gravelly Sand 106 pcf, N=31, $3000 < q < 4200$ psf
- o 10'-0" to 20'-0" Silty Sand, Gravelly Sand 106 pcf, N=50, $4200 < q < 4500$ psf

where N = blow counts
q = bearing pressure, psf

2.2 LOADING CRITERIA

In order to develop realistic comparative costs for different designs, a detailed and definitive loading specification is needed. The loadings considered for the UHA structures are listed below:

- o Dead Load (D)
- o Wind Load (W)
- o Earthquake Forces (E)

The above list of loadings is not totally inclusive of all forces that may be experienced by the UHA structure. Snow, ice, hail, and temperature variations will produce additional loadings on the structure. However, these loadings are so small in comparison to the dead and wind loads that they were not considered for conceptual design purposes.

The magnitude of many of these loads may not always be accurately determined. That is, the maximum possible load to be expected is not always known. Therefore, for design purposes, upper bound values are usually specified by the governing Codes such as the UBC. The

determination of these values is based on:

- o Historical records
- o Likely hazard to human life created by structure failure
- o Risks of economic loss due to failure
- o Expected economic life for the structure.

Characteristics of each load are discussed below and preliminary recommendations for design values are made.

2.2.1 Dead Load

This load is easily determined and consists of the weight of the heliostats, mounted equipment, platforms, and the supporting structure. Design values are those calculated using material unit weights and equipment weights furnished from handbooks or from suppliers. The dead load was taken to be 435 lbs for a 6 m^2 heliostat and 4132 lbs. for the 49 m^2 heliostat since these values were specified by Veda, Inc.

2.2.2 Wind Load

This load has the most influence on the design of the UHA structure. The load is essentially random and is normally specified by designing to an upper bound. The upper bound of wind velocities specified for the design of the UHA structures is:

$$V_H = V_1 (H/H_1)^C$$

Where

V_H = wind velocity at height H

V_1 = reference wind velocity at 30 ft. (10 m)

H_1 = reference height 30 ft. (10 m)

C = 0.15

This is commonly referred to as the 1/7-power law for determining wind velocities.

Using Bernoulli's theorem, wind pressure may be derived from the velocity as:

$$q = 1/2\ pV^2$$

Where at height H:

q = wind pressure

p = density of air

V = wind velocity

This equation is modified by lift and drag coefficients suitable for the heliostat structures. These coefficients were suggested by Veda, Inc. and gave total wind forces as the structure. No gust factors are applied in this work.

Information regarding the derivations of the power law and pressure may be found elsewhere (References 2-4 and 2-5).

The UHA performance requirements are specified for the heliostats operating in a wind velocity of 12 m/s (27 mph) at a reference height of 10 m (30 ft.). Shown in Figure 2-2 is a plot of the operational wind profile used in the preconceptual UHA design.

To simplify the computer input used in the more detailed conceptual design, the wind pressure profile described above was approximated as

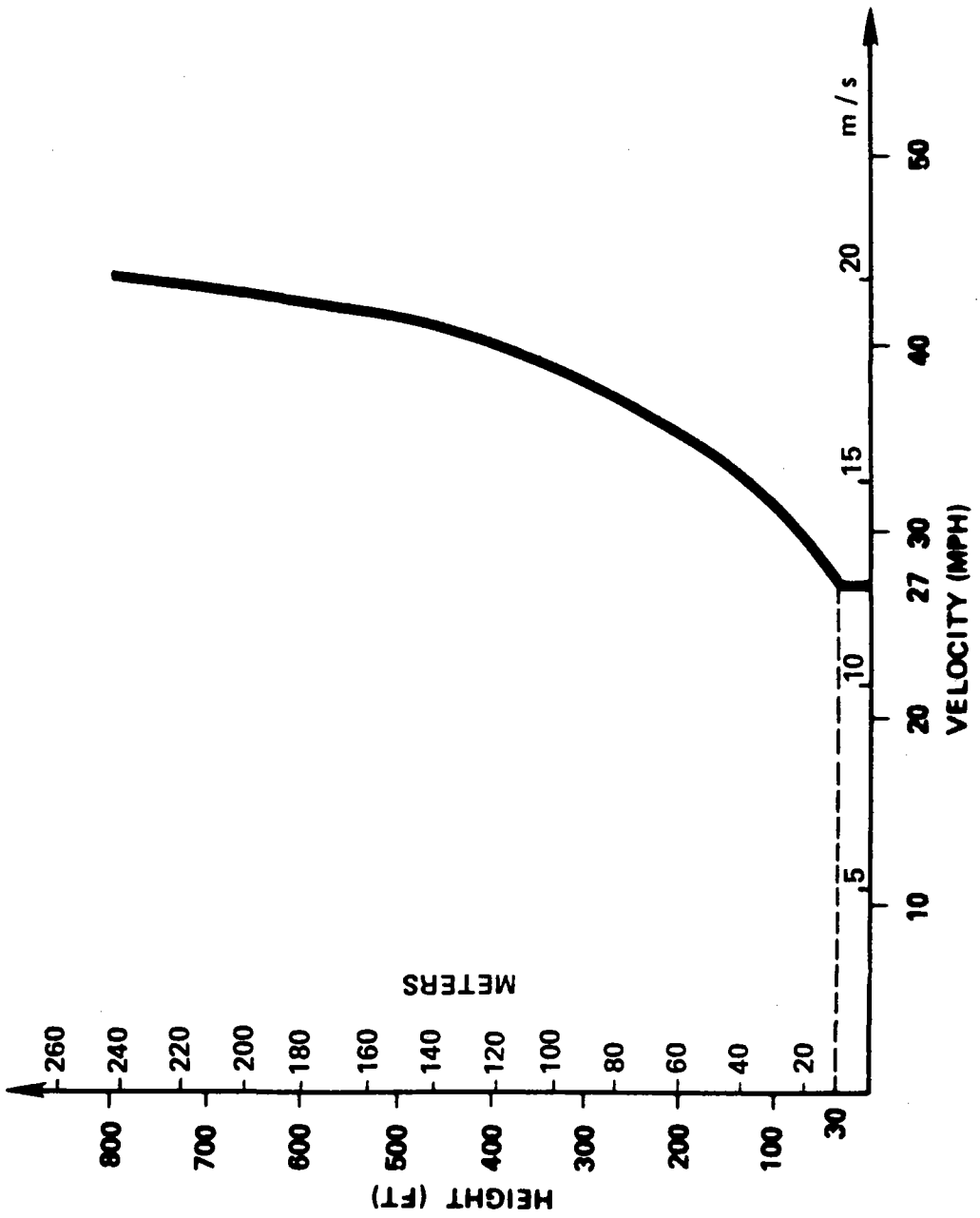

Figure 2–2 Operational Wind Profile for the UHA

a linear variation with height.

The heliostats are specified to maintain structural integrity in a non-operational state (while stowed) in a 22 m/s (50 mph) wind in any orientation. The structure and heliostats must also be able to survive a maximum wind speed, including gusts, of 40 m/s (90 mph) while heliostats are stowed (mirrors horizontal).

For the UHA design, three different wind loadings were used. These include:

- o W_{27}, operational wind velocity of 12 m/s (27 mph)
- o W_{50}, stowing wind velocity of 22 m/s (50 mph)
- o W_{90}, survival wind velocity of 40 m/s (90 mph)

2.2.3 Earthquake Forces

These forces come from the combination of structural mass and the accelerations of the ground supports due to the seismic event. Consequently, a lightweight structure will experience relatively small forces on its supports for a given peak acceleration. A heavier structure will experience higher loads. The location and magnitudes of earthquakes are predicted on a probability basis.

Critical structures and systems are designed for seismic forces by using advanced dynamic analysis, but simpler structures, such as those used in the UHA concept, may be analyzed using a static equivalent force method. This method is described in the Uniform Building Code (Reference 2-6).

The design equation (UBC eq 12-1) for base shear V is:

$$V = ZIKCSW$$

The following values are assigned to the above variables:

Z = 3/4 for Zone 3

I = 1.00 for occupancy importance

K = 1.00 for structural type

CS = 0.14 for resonance type

W = weight of the structure

Using these values in the equation for base shear leads to a value of:

$$V = 0.11W$$

for lateral forces. These values are derived for a location near Barstow, California. The Barstow site is in a UBC seismic zone 4 but, for design purposes, a seismic zone 3 was chosen to represent a typical earthquake seismicity found in the west and southwestern states. The UBC seismic zone map of the United States is shown in Figure 2-3.

However, because seismic loads for these light structures are not critical compared to the wind forces, they are not included in the following load combinations.

2.3 LOADING COMBINATIONS

The specified loads are assumed to act on the structure in various combinations. These combinations are arranged to reflect the fact that there is a reduced probability that all of the loads will act simultaneously on the structure.

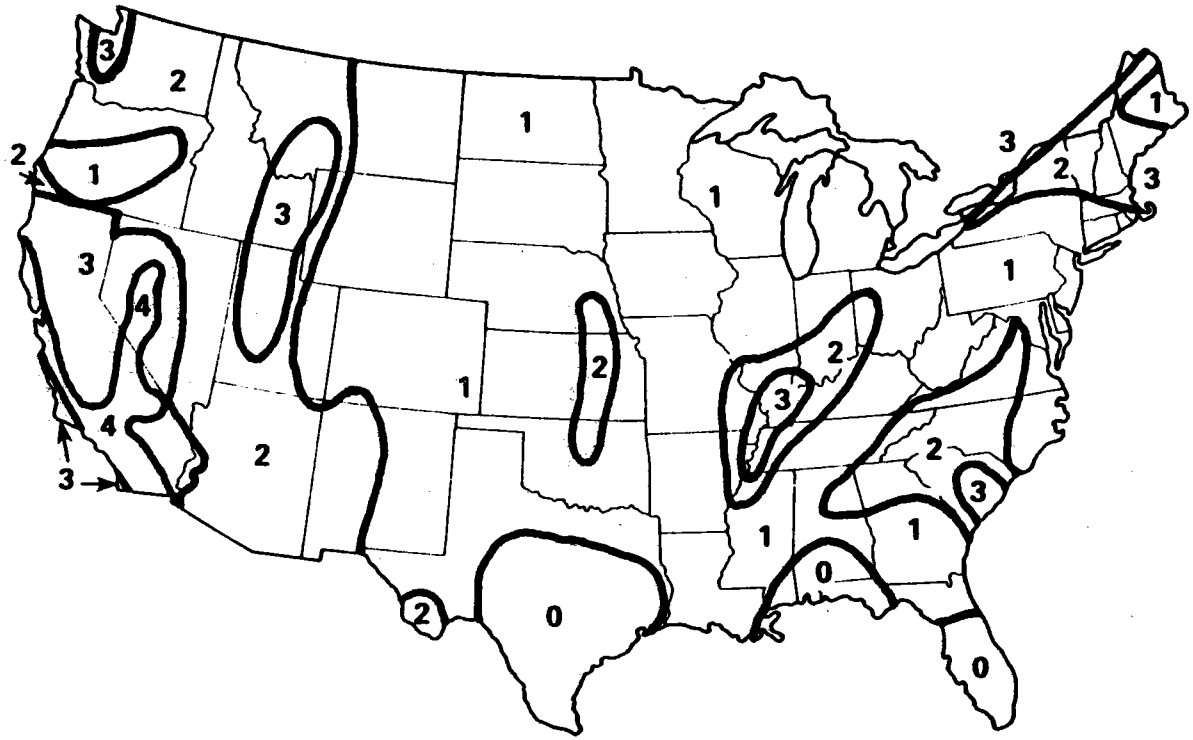

Taken from Reference 2–6

Figure 2–3 Seismic Zone Map of the United States

For preliminary design, the following load combinations were considered for the UHA structure design:

(1) W_{27}

(2) $D + W_{50}$

(3) $D + W_{90}$

Where

D= Dead Load

The wind loads include any uplift that may occur either on the structure or on the heliostats. The W_{27} load was considered in order to determine if the rotations of the heliostats were within the tolerances specified in the deflection criteria.

Section 3

REVIEW OF CANDIDATE STRUCTURAL CONCEPTS

3.1 INTRODUCTION

The overall sizes and dimensions were developed in Task 1 for the conceptual designs of the 1, 10, and 25 MWt arrays using the 6 m^2 heliostats. The optical dimensions and heliostat spacings for the arrays indicated that the supporting structure must have a slanting, terraced frame similar to a stadium. The structure serves the following functions for the heliostat arrays:

- Provides support for the heliostats against environmental forces
- Provides proper orientation of the heliostats to maximize solar power requirements

Consequently, a literature search was performed to find existing designs or structural configurations that serve functions similar to the UHA concept.

3.2 ARRAY SIZES AND DIMENSIONS

Shown in Figures 3-1 to 3-3 are the plan views of each array for various power levels and aspect ratios including major dimensions. For comparison, the length of the largest structure (25 MWt array with an aspect ratio of 1:5) is almost as long as 5 football fields.

Shown in Figures 3-4 to 3-6 are the elevations of each array for various power levels and aspect ratios. The heights of a one and ten story building are also plotted to demonstrate comparisons with the 1 and 10

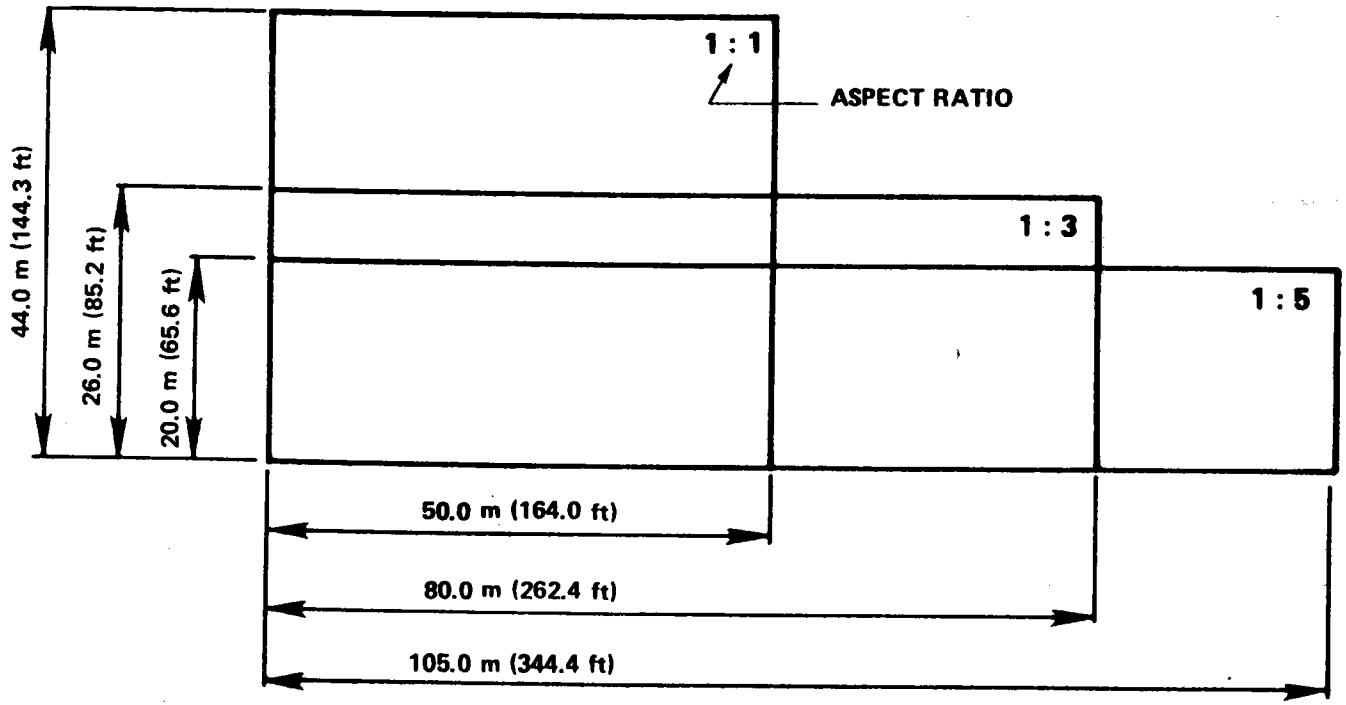

Figure 3–1 Plan View of 1 MWt Arrays with Various Aspect Ratios

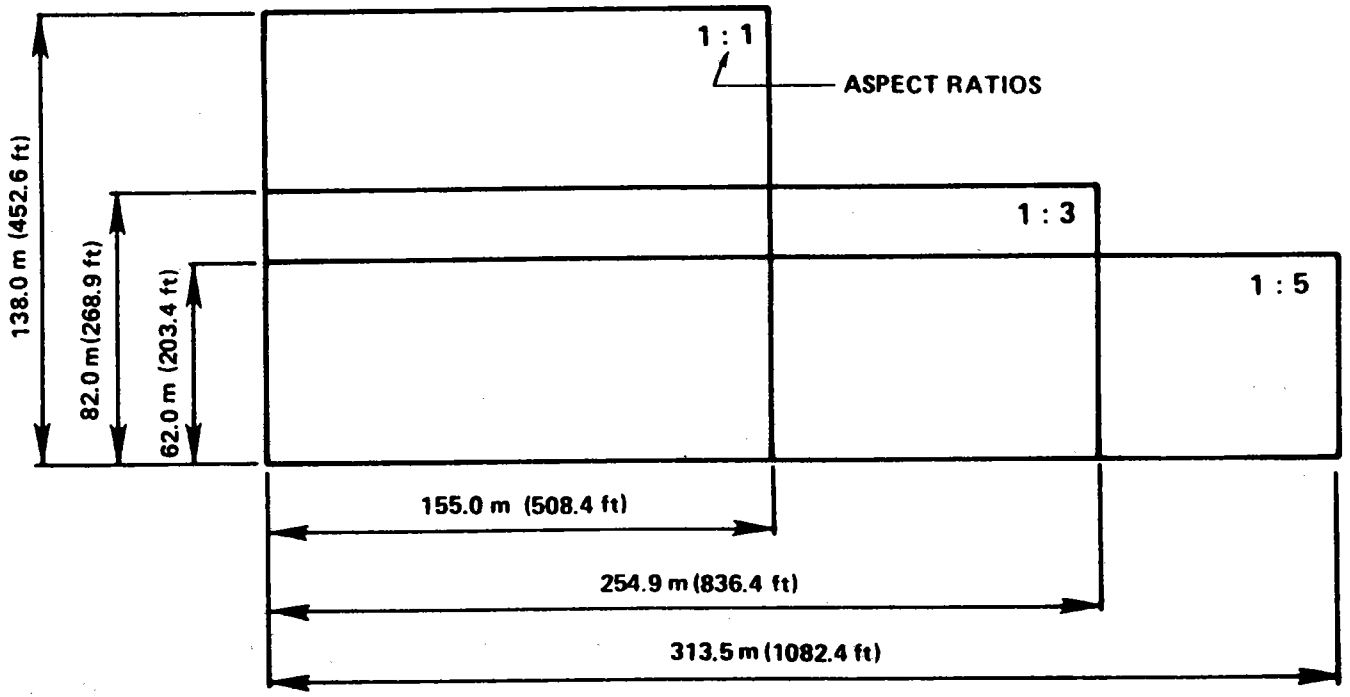

Figure 3–2 Plan View of 10 MWt Arrays with Various Aspect Ratios

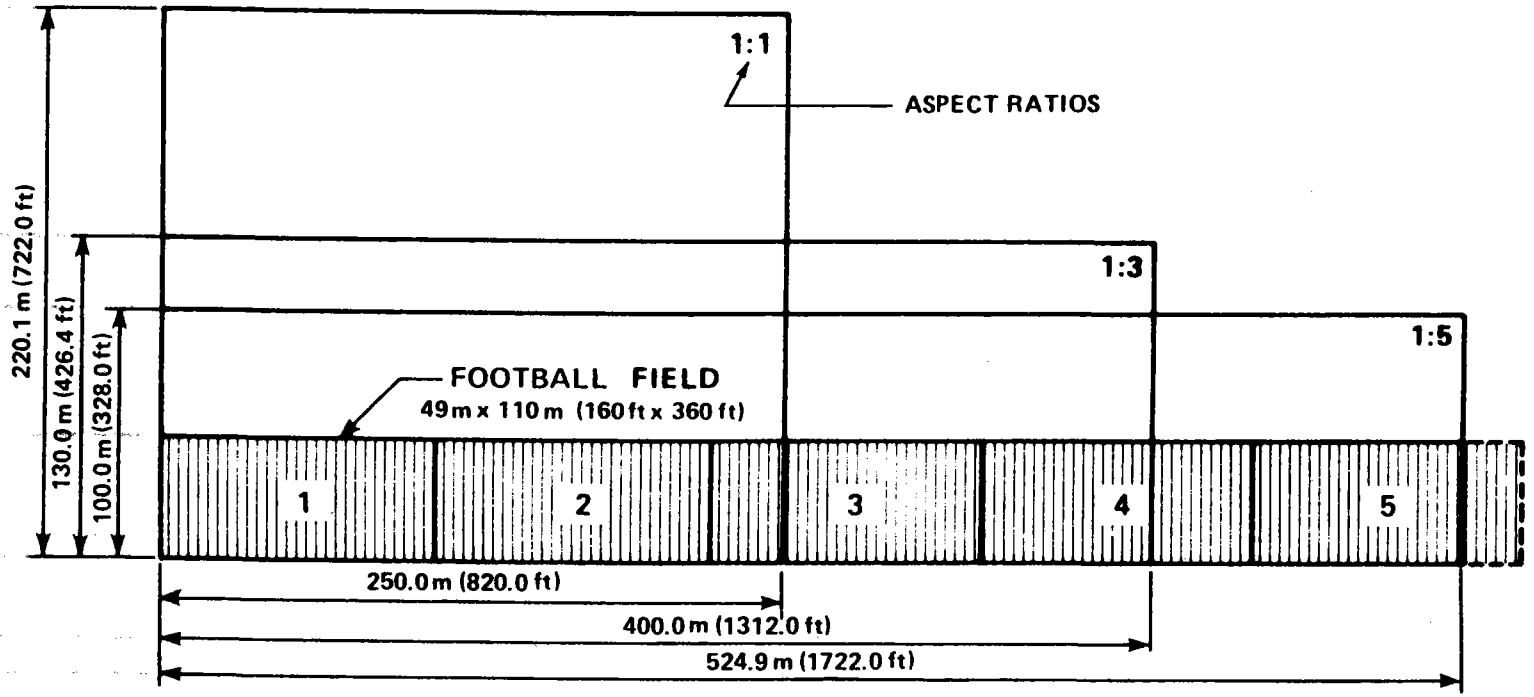

Figure 3–3 Plan View of 25 MWt Arrays with Various Aspect Ratios

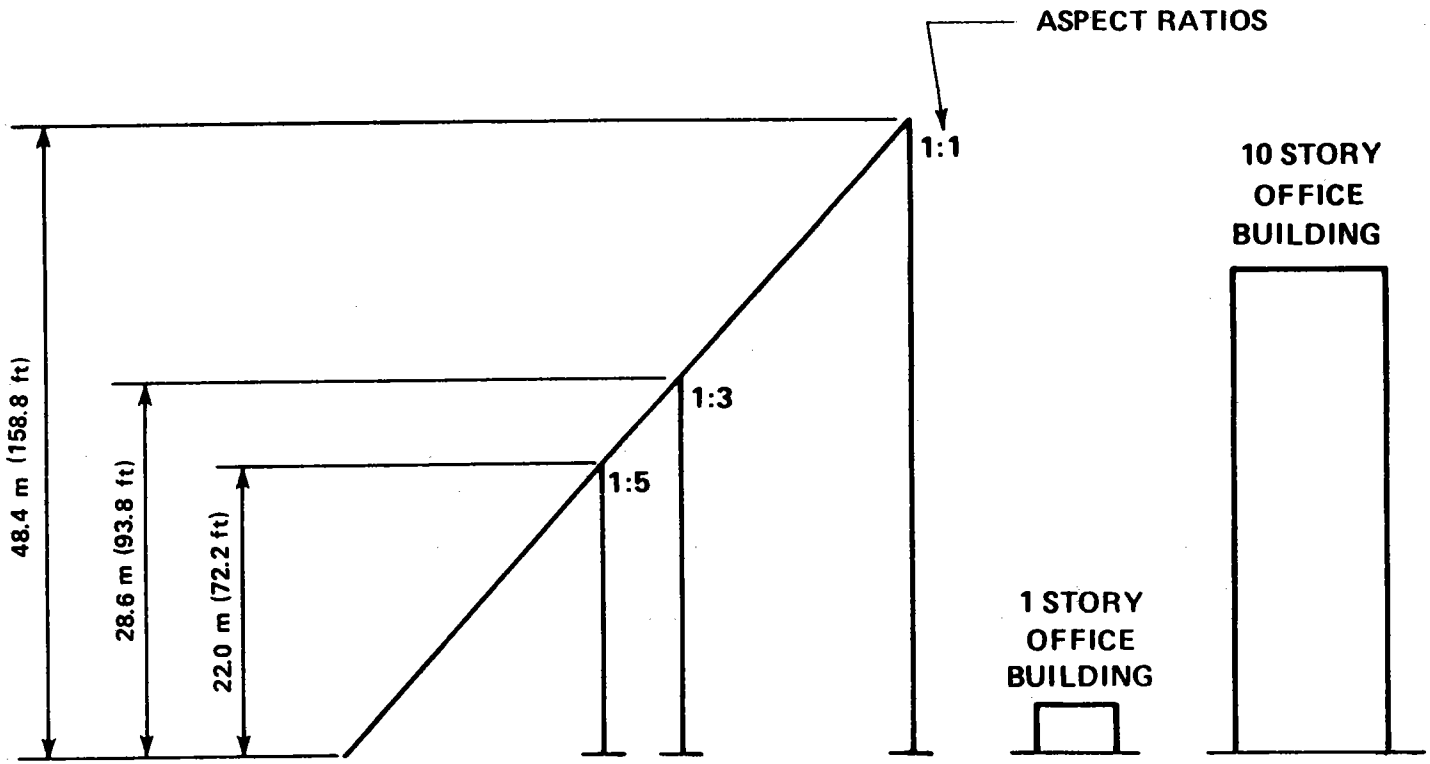

Figure 3–4 Elevation of 1 MWt Arrays with Various Aspect Ratios

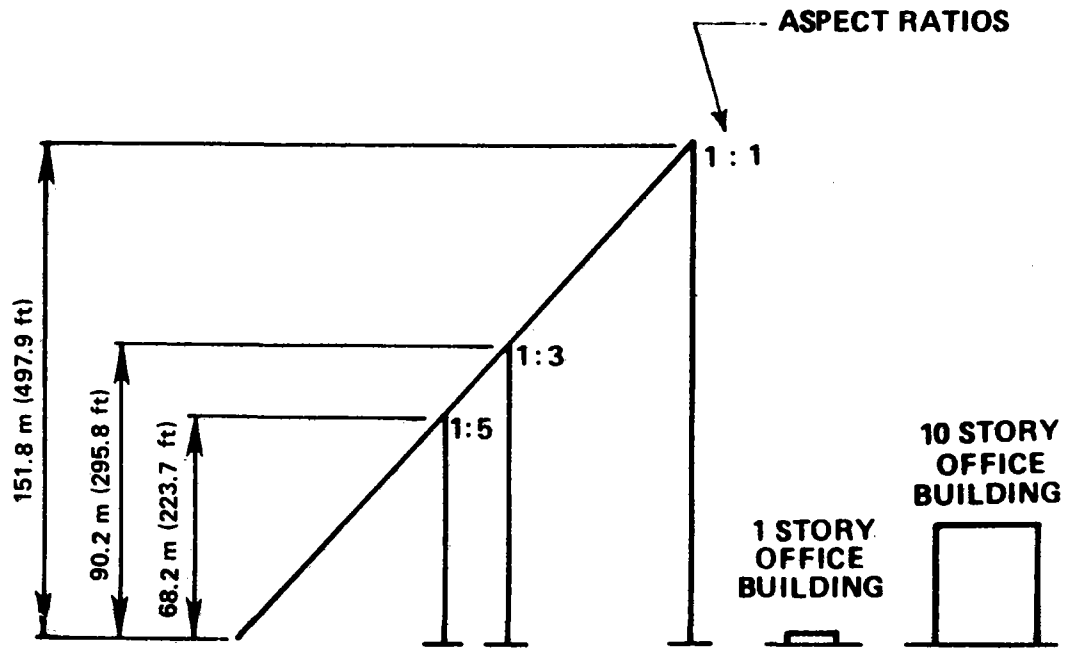

Figure 3–5 Elevation of 10 MWt Arrays with Various Aspect Ratios

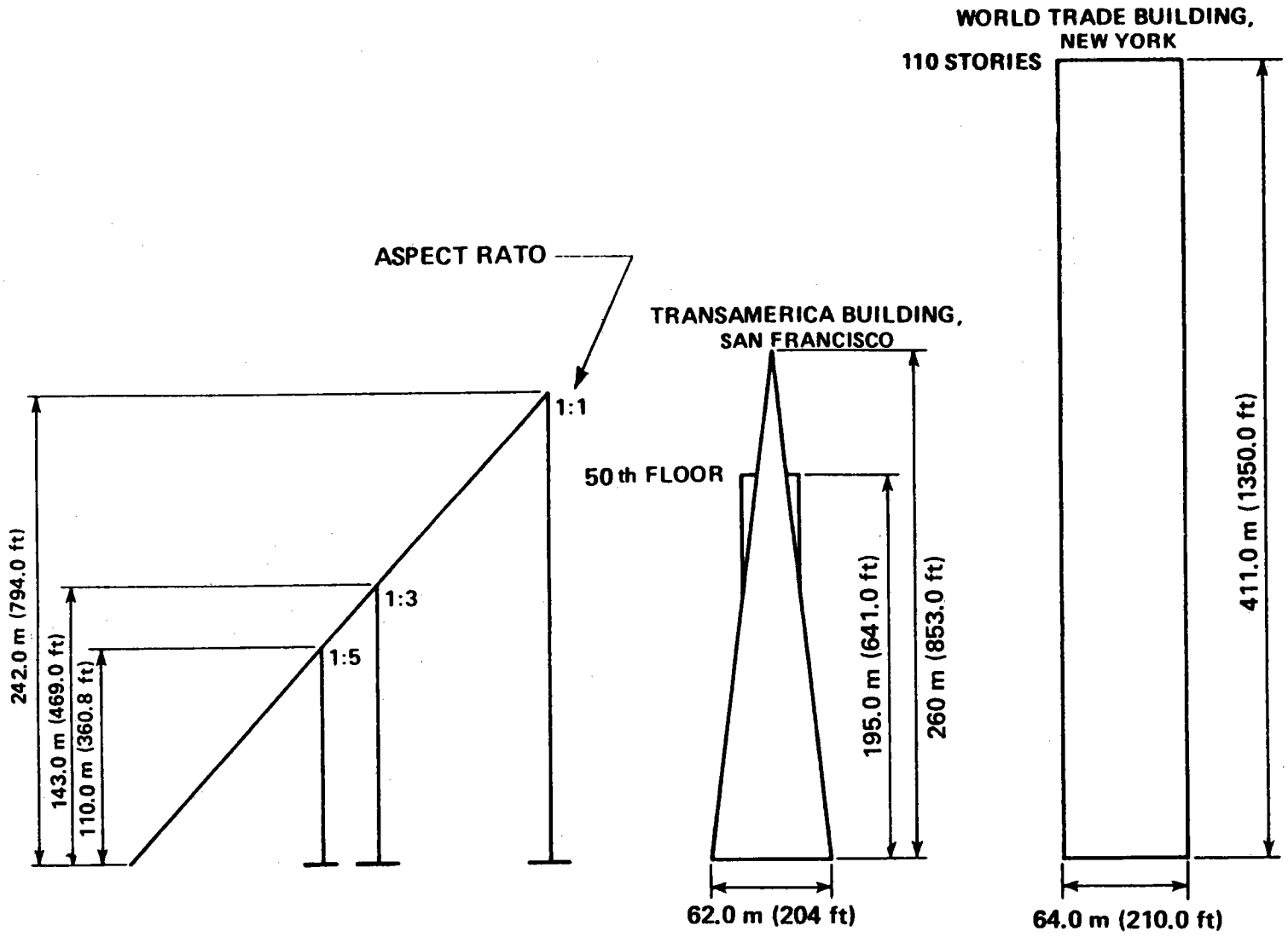

Figure 3–6 Elevation of 25 MWt Arrays with Various Aspect Ratios

MWt array heights. The height of the highest structure (25 MWt, aspect ratio 1:1) is almost that of the Transamerica Building in San Francisco or about 60% of that of the World Trade Building in New York. Hence the larger power systems are seen to be major structures for design, fabrication, and construction.

3.3 LITERATURE SURVEY

The literature search encompassed general technical and trade literature. General technical literature consists of proceedings papers, technical papers, reports, and various government publications. The trade literature consists of commercial publications directly concerned with structural support systems and engineered construction, and includes magazines such as the Engineering News Record and Civil Engineering.

Computer searches were performed on two engineering data bases which are described below. To access them, key words were selected from a standard thesaurus to describe the topics of interest.

o COMPENDEX (COMPuter ENgineering InDEX)

Source documents:	1500 U.S./Foreign journals, monographs, conference proceedings
Dates:	1970 to date (monthly updates)
Supplier:	Engineering Index Inc.
Description:	Access to technical sources in the published literature dealing with: Civil/petroleum/mechanical/electrical/ chemical/water/marine/railroad/control/ engineering

o NATIONAL TECHNICAL INFORMATION SERVICE (NTIS)

Source documents:	Reports from NASA, Department of Commerce, DOT, HEW, ERDA, DDC, and 200 other Federal Agencies
Dates:	1964 to date (bi-weekly updates)
Supplier:	NTIS, U. S. Commerce Department
Description:	Consists of government-sponsored research & development. Corresponds to Weekly Government Reports Announcements (monthly).

Even though the computer search did not reveal any references directly applicable to the UHA concept, it did provide concepts of different framing systems which were considered for the preliminary design.

Since the computer data bases for specialty journals usually extend back only to 1970, a random survey was also made to expand the results of the computer search. This was to done to spot articles which might be pertinent but not fall in the categories of the descriptors used in the computer search.

The literature search revealed one array structure similar to the UHA concept and found several other structural configurations that serve similar functions as the UHA structure. More details of these structures are given in the next section.

3.4 SIMILAR STRUCTURAL CONFIGURATIONS

The dimensions and heliostat spacings for the UHA concept indicate the structure must have a slanting, terraced supporting face. A similar terraced structure is currently under construction in Japan by the Electric Power Development Co. Ltd. (EPDC) and Hitachi Ltd (Reference 3-1). Designed as a 1 MWe solar thermal pilot plant, it has a plane-parabolic

collector system utilizing a one-axis tracking mechanism which delivers approximately 5.8 MWt of solar energy to the focal line.

Other terraced structures were considered that serve similar functions as the UHA concept. Stadiums are terraced structures which provide seating arrangements on a sloping surface. Instead of directing reflected solar radiation to a receiver, stadiums direct the lines of sight of an audience to a particular location, the playing field or court. For example, New York's Shea Stadium, shown in cross section in Figure 3-7, is a sloping, terraced structure whose height is comparable to the 1 MWt UHA, aspect ratio of 1:1 (Reference 3-2). Another example of a tiered or terraced structure would be the Hartford Jai-Alai Fronton. This structure, whose partial cross section is given in Figure 3-8, consists of mostly W10 to W12 riser beams and W14 columns attached to cast-in-place concrete piles (Reference 3-3).

The tiered roof of Gund Hall, Harvard University's Graduate School of Design at Cambridge, Massachussetts, is just another example of a terraced structure. The roof, shown in Figure 3-9, is supported by pipe trusses 11 feet deep by 134 feet long and spaced 24 feet on centers. Each roof truss weighs 13 tons and has top and bottom chords of 12 inch diameter pipes with wall thickness ranging from 0.344 inches to 0.625 inches. Web members are 6 inch diameter pipe sections with wall thickness ranging from 0.156 to 0.344 inches (Reference 3-4).

3.5 CONCLUSIONS

The literature search found limited details of one solar power generating array system in Japan with similarities to the UHA concept. It revealed

several other structures such as stadiums and roof support frames that provide somewhat similar services as the UHA structure but with quite different loadings. No structures were found that directly compared with the UHA concepts and so structural configurations for this study had to be evolved from basic principles.

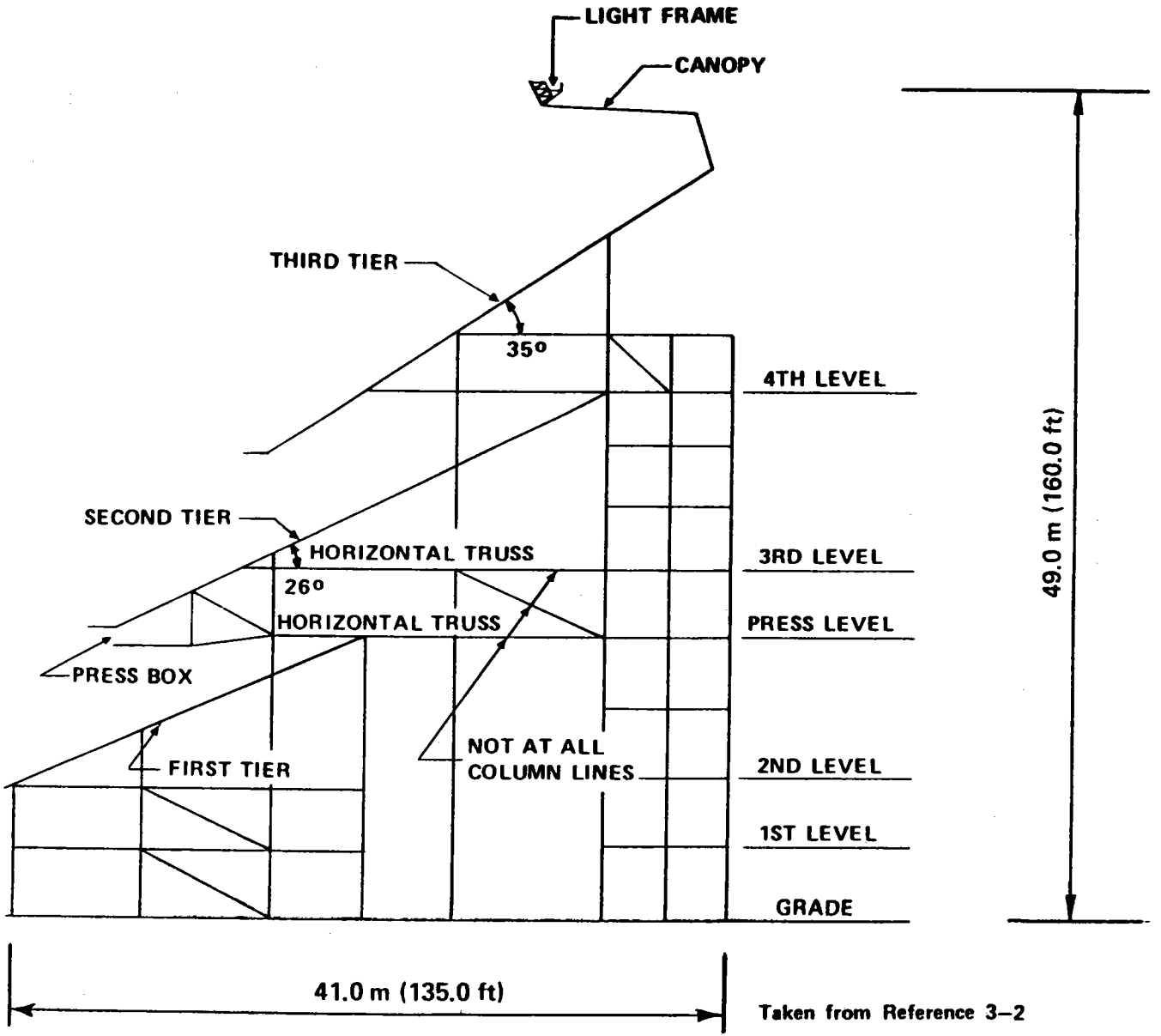

Figure 3–7 Cross Section of Shea Stadium

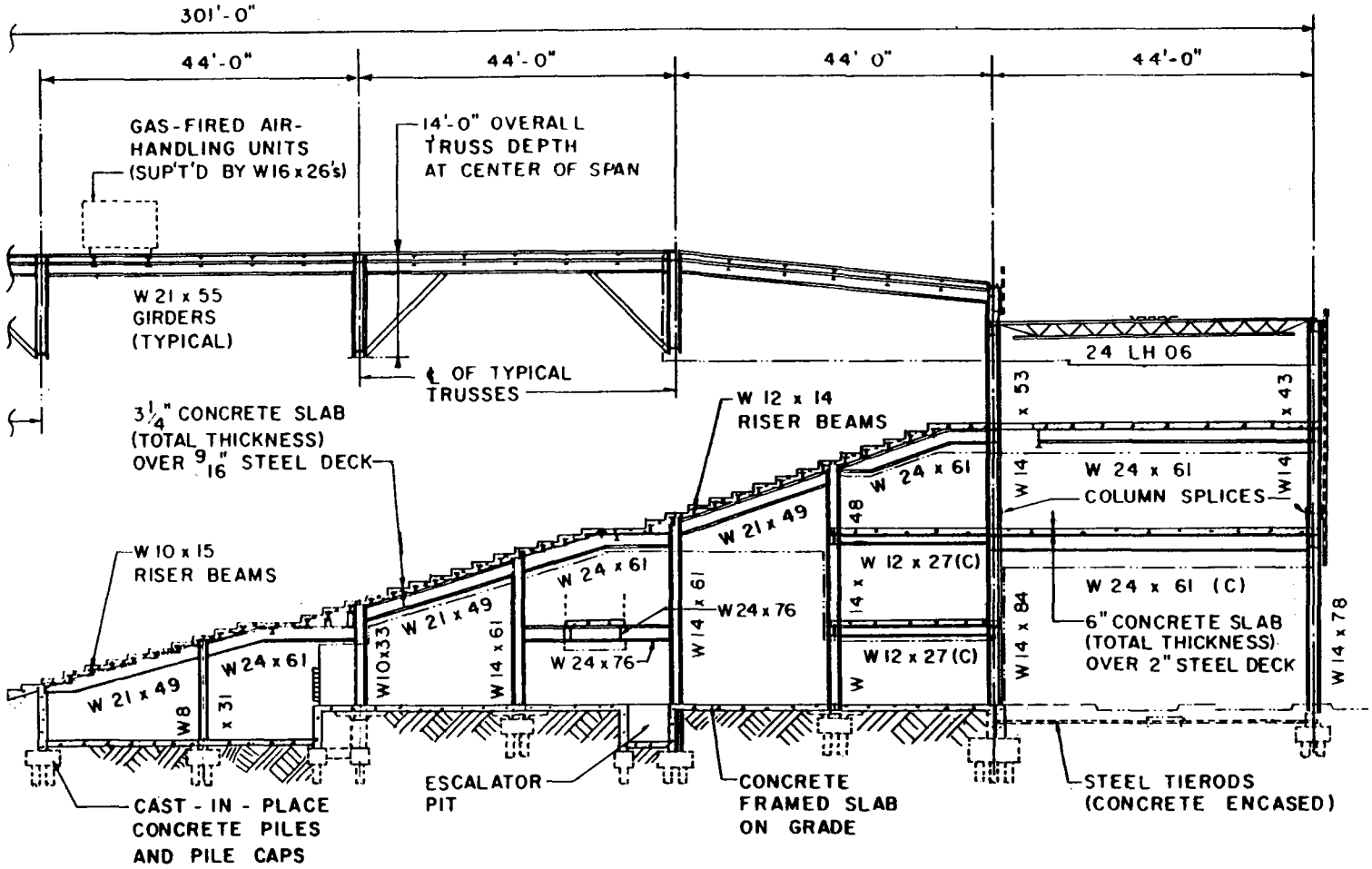

Taken from Reference 3–3

Figure 3–8 Partial Cross Section of the Hartford Jai– Alai Fronton

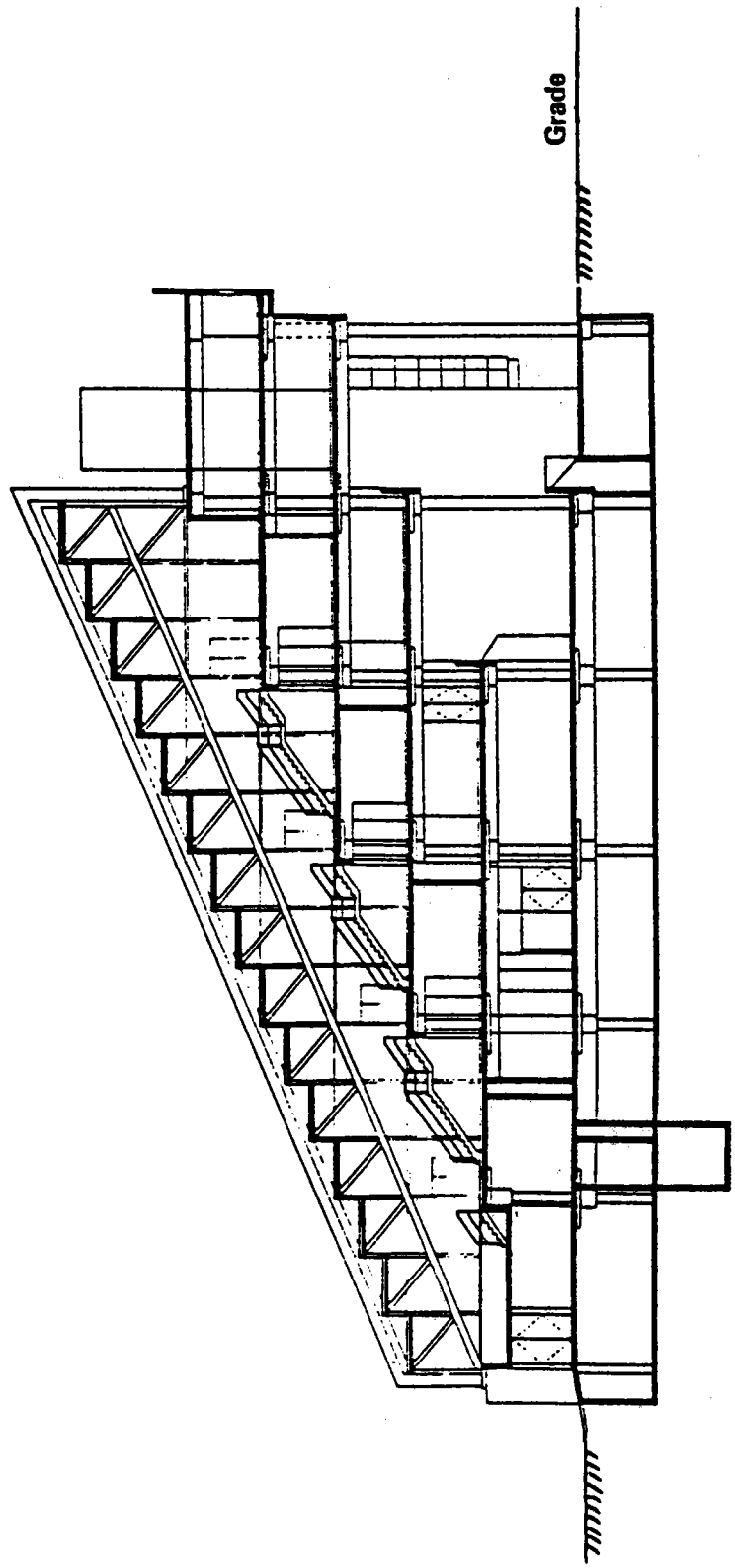

Taken from Reference 3–4

Figure 3–9 Cross Section of Gund Hall, Harvard University

Section 4

DEVELOPMENT OF PRECONCEPTUAL DESIGNS

4.1 INTRODUCTION

During Task 2, structural preconceptual designs were developed for three aspect ratios of 1:5, 1:3, and 1:1 for each power level of 1, 10, and 25 MWt. The aspect ratio is the ratio of height to length of the structure and normally affects two factors:

- o The solar performance
- o The structural requirements

For an aspect ratio of 1:5 where the structure is low but long, the heliostats located at the end of the array are farther away from the receiver than those at the center. For an array with an aspect ratio of 1:1 where the structure is high, the heliostats located at the top are also farther away from the receiver than those at the bottom. Ideally the solar performance of an array is increased whenever the distance from a heliostat to the receiver is decreased. However, the structural requirements of a support system are relaxed whenever the structure is low.

Once the basic structural configuration had been determined, a logical approach was used to develop a design concept for the UHA structure. The approach used in this study included:

- o Selection of structural materials
- o Study of the design considerations and parameters
- o Development of preconceptual designs

- o Structural analysis
- o Cost analysis

4.2 STRUCTURAL MATERIALS

Candidate materials considered in this study for the construction of the UHA structure included:

- o Timber
- o Concrete
- o Steel

Each of these materials is discussed separately with considerations of physical properties, current usage in building construction, availability, and workability.

4.2.1 Timber

The most abundant structural material available in the United States is wood. It exceeds steel and concrete both in tonnage and volume of annual production. Due to its natural origins and the many different species available, the physical properties of wood vary considerably. The allowable stresses of wood are also below those used for steel.

The primary wood species used for structural work are douglas fir, pine, and redwood, and these materials are readily available in all city locations and most other regions of the country. Wood is very attractive because of its ready workability, availability, and involves no difficult procedures or specialized machinery.

Several decades of research have significantly improved the grading of wood sections to be used for fabrications. The industry standard governing wood construction is given in Reference 4-1.

A structural advantage of timber is its ability to tolerate large overstresses for short time periods under varying loads. Wood also has the characteristic of strongly damping an applied dynamic loading. Disadvantages may include:

- o Low strength
- o Low stiffness
- o Maintenance requirements for untreated members
- o Size limitations of the lengths and shapes of standard members

Due to the required heights of the UHA structures, the large cross section areas necessary to meet the stiffness and hence the rotation criteria, and the member sizes required to resist the loadings, timber was deleted as a candidate structural material.

4.2.2 Concrete

Concrete is commonly used in all forms of building construction. It is not generally used for structures needing only very light framing because of connection detailing and dimensional limitations. Concrete may be precast, where complete members are shipped to a site, or it may be mixed and placed in forms to construct the building in situ. Concrete is generally competitive with timber in specialized applications. For example, railroad ties and power poles are now often made of precast concrete.

Concrete is readily available almost anywhere in the continental United States. Certain manufactured (precast) shapes may be proprietary and may have to be shipped some distance to the site or made under license by a local firm. As with any material which has very competitive alternatives, the economic advantage of concrete depends on the project, the location and the capability of the construction company doing the work.

Since concrete by itself is weak in tension and strong in compression, its fabrication into structural members requires the inclusion of tensile reinforcement. In large scale structures, this reinforcement is typically provided by steel rods but for small, light components it may also be provided by including chopped glass or metal fibers in the concrete mix. The industry standard that governs the use of concrete in ordinary buildings is ACI 318 (1977 version, Reference 4-2), and various ASTM Specifications govern the quality of the material.

The compressive strength of concrete varies widely depending on the mix design. Concrete for backfill applications may have strengths of 1500 to 2000 psi, while typical structural concrete will vary in strength from 3000 to 5000 psi.

High strength concrete for prestressed concrete beams may be designed to reach a strength of 9000 psi. Not only may the strength of the concrete be modified by suitable mix design, but other attributes, such as workability, speed of hardening, frost resistance and permeability may be altered by using special admixtures during the mixing process.

Concrete sometimes is used in a structure to provide weight such as in machinery foundations, gravity dams, and in footings subjected to uplift forces. This feature of concrete is detrimental here since the required heights of the UHA structures would dictate extremely large dead loads and massive columns. With such dead loads, the UHA structures made of concrete would need to be more resistant to earthquake forces than those structures made of much lighter materials such as steel.

Therefore, to minimize the dead loads and the required earthquake resistance, concrete was deleted in lieu of steel as a candidate structural material for the UHA structures.

4.2.3 Steel

Structural steel is one of the most widely used building materials. It is used in the building industry either as cold rolled and formed products or as hot rolled structural shapes. The quality of the material is governed by ASTM Standards which are referenced in the steel industry standard specifications, References 4-3 and 4-4.

Due to its wide range of applications, steel is readily available from mills and warehouses in a large variety of shapes or forms. There is a large production base available for supply in the United States even though long lead-times for ordering large quantities of special shapes or alloys are typical.

Steels have wide use because of their workability and strength. Welding of the normal construction steels is straightforward, and many different fastening systems exist which allow for fast assembly operations.

In steel design, consideration must be given to the provision of appropriate corrosion resistance. This may be done by using a corrosion resistant steel or by coating the steel. Typical surface treatments are hot dip galvanizing or painting, and both processes are used for steel structures in exposed environments. Another approach is to increase the thickness needed for strength of the steel members by the amount estimated to be lost due to corrosion over the life of the facility.

The design of steel structures is often based on the working stress method where the allowable stress is normally limited to about 60% of the yield stress. Depending upon the material specifications, the nominal yield stresses of readily available structural steel are 36,000 psi and greater. However, for long slender steel members, buckling requirements may lower the allowable stress to a value much lower than 60% of the yield strength.

Steel has many advantages over concrete as a structural material. These advantages may include:

- Ease of erection
- Standardization and prefabrication of many structural elements
- Variety of strengths available
- Easier-to-make connections
- Easier shipment
- Less structural weight
- Flexibility for field changes
- Lower quality assurance costs

The advantages listed above, were judged to impact forwardly the UHA application in question and result in the lowest structural system cost. As a result, steel was chosen as the primary structural material for the UHA structures.

4.3 DESIGN CONSIDERATIONS AND PARAMETERS

4.3.1 Superstructures

From the specified array sizes and dimensions and the review of candidate structural concepts, a steel beam-girder framing system was chosen for the preconceptual design of the UHA structures. This type of framing system has the advantage of using standardized structural elements such as rolled wide flange (WF) or pipe sections. Standardization of elements makes connections easier, reduces erection times, provides more flexibility for field changes, and lowers construction costs.

Shown in Figure 4-1 is a typical UHA structure using a beam-girder framing system. This system has a series of braced frames each of which are composed of the following:

- Heliostat support beams
- East-West (E-W) beams
- North-South (N-S) beams
- Sloping girders
- Columns
- X-cable bracing
- Foundations

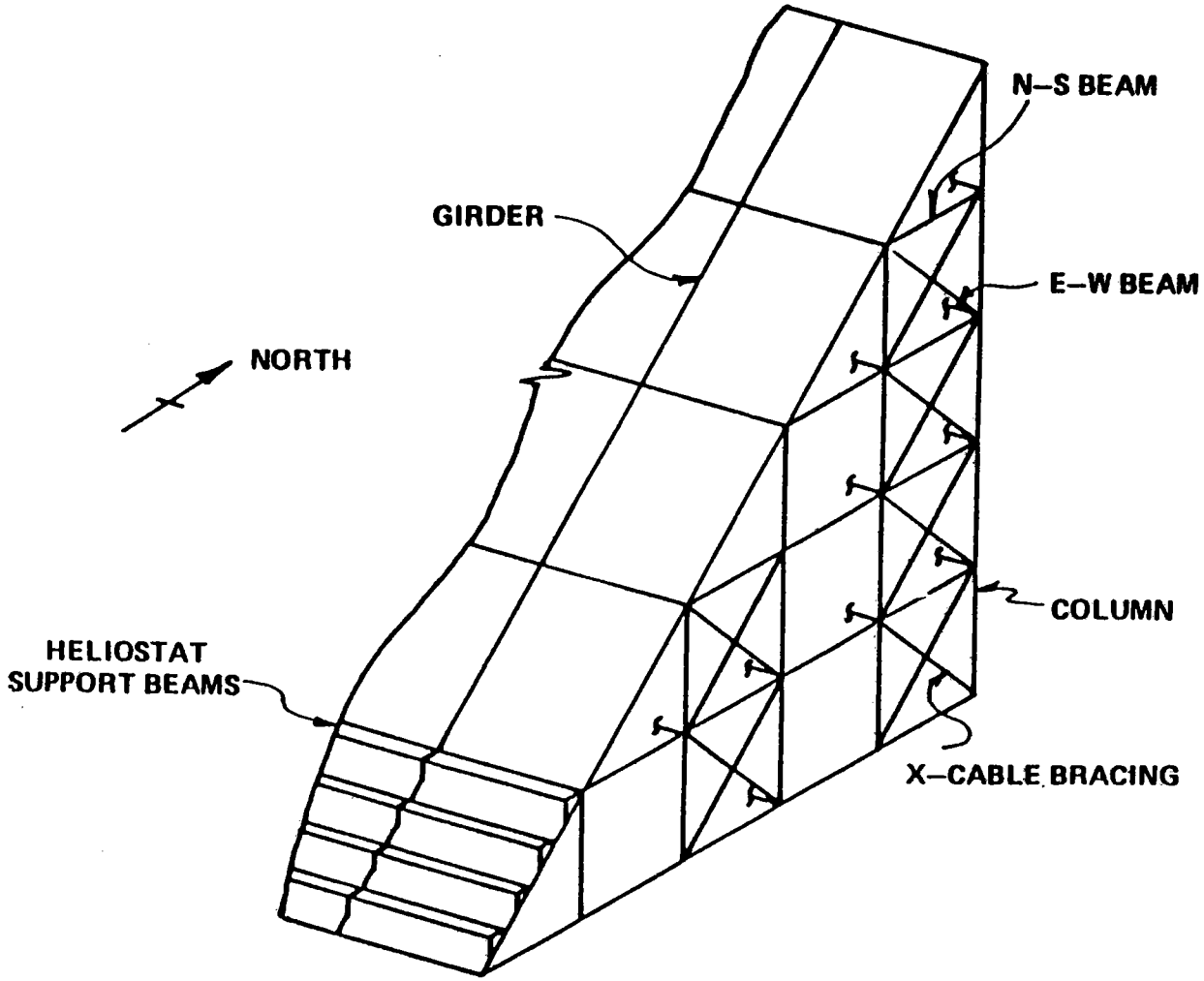

Figure 4–1 A Typical Unified Heliostat Array Structure

Each frame has a sloping main girder supported by equally spaced columns and is braced against sidesway in the longitudinal direction by the E-W beams and the heliostat support beams. The heliostat support beams provide rotational stiffness to the heliostat pedestals and provide access for attachments and maintenance of the heliostats. More details of the support beams are given later.

Lateral torsional buckling was the governing factor in the design of the support beams and the girders. Stability contraints had the largest influence in the design of the main beams, columns, the E-W beams, and the N-S beams.

For all the preliminary conceptual designs, standard WF sections were used throughout for the main members of the arrays. Main members were limited to lengths of 90 feet to permit conventional transportation.

To provide lower costs, minimization of weight for the arrays is a function of several variables, some of which are:

- o Array dimensions
- o Girder spacing
- o Column spacing
- o Dead loads
- o Governing wind loads

The above variables, which influence weight minimization, do not comprise a complete list, nor are they totally independent of each other. For example, one may design an array with a long girder spacing which would increase the total load to each frame and thereby increase the column

loads. Greater column loads would therefore dictate either larger columns or many more smaller ones per frame.

All wind load cases were calculated to determine which one produced the largest stresses in the UHA members. For all power arrays, the W_{90} wind load case was found to govern the design.

4.3.2 Structural Details

To ensure that the beam-girder framing system was viable for the UHA structure, certain connection details were given detailed consideration Figure 4-2 is a preconceptual design showing the connection of the slanting main girder, the N-S beam, and the support beams with the main column. The main girder is shown field spliced with the columns and the beams being attached using AISC standard framed beam connections.

In section 2, Design Criteria, the maximum permissible rotations of the heliostats at the base of their support pedestals were specified to be $\pm$ 1.5 mrads under an operational wind of 12 m/s (27 mph). Single WF support beams for the heliostats were found not to have adequate torsional stiffness to meet the rotation criteria. Therefore, for the $6m^2$ heliostat, double WF beams, side-by-side as shown in Figure 4-3, were used to obtain the needed torsional stiffness. The horizontal pedestal, as well as the removable handrail, clamps to the top flanges of the beams by U bolts. The metal grating attached to the lower beam flanges provides bracing to the torsional system and provides a walkway for access and maintenance. Shown in Figure 4-4 is a partial elevation of the 25 MWt array using the 6 m^2 heliostats with an aspect ratio of 1:1 that demonstrates how this torsion-resisting system is attached to

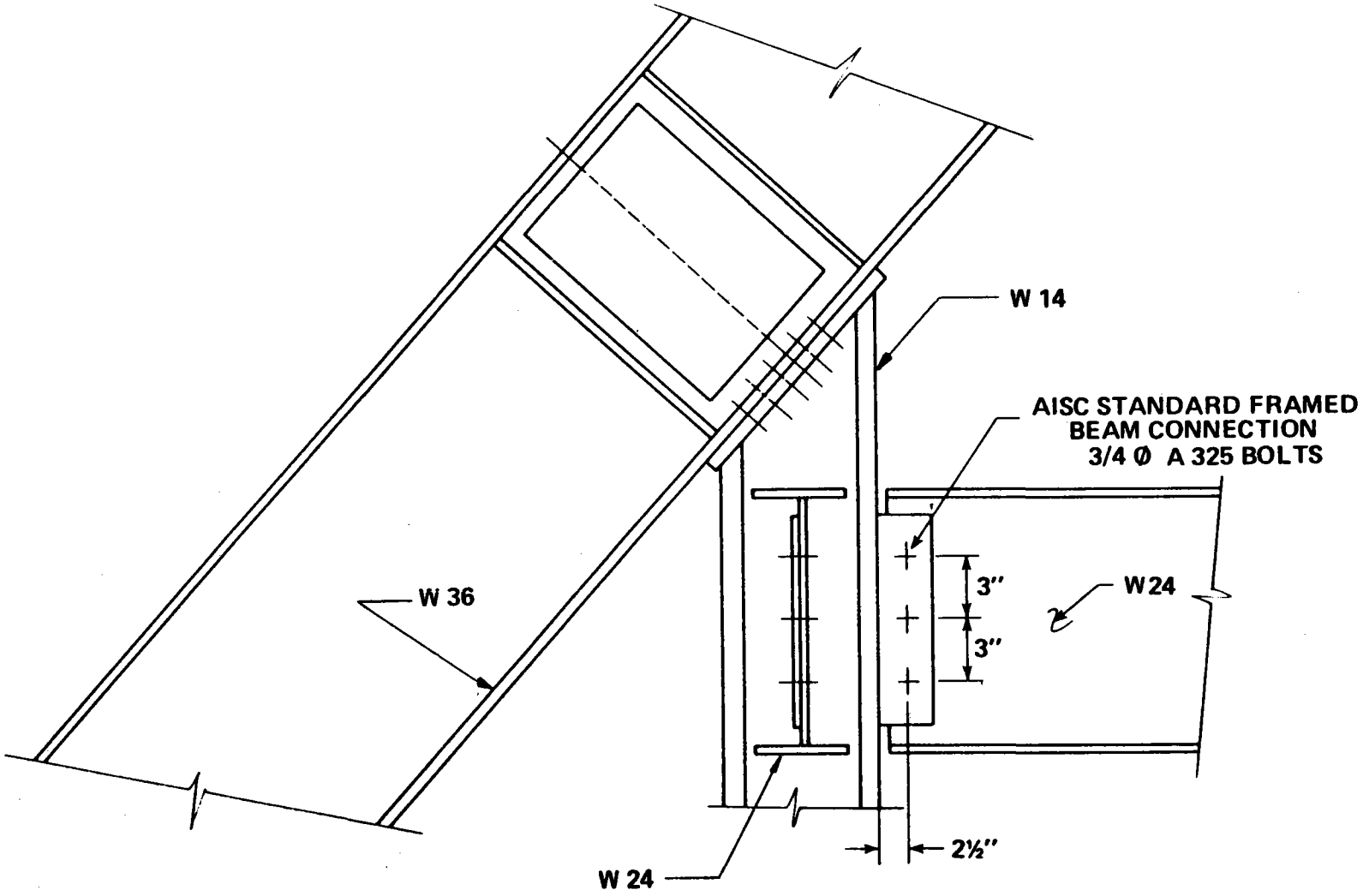

Figure 4–2 Connection Scheme

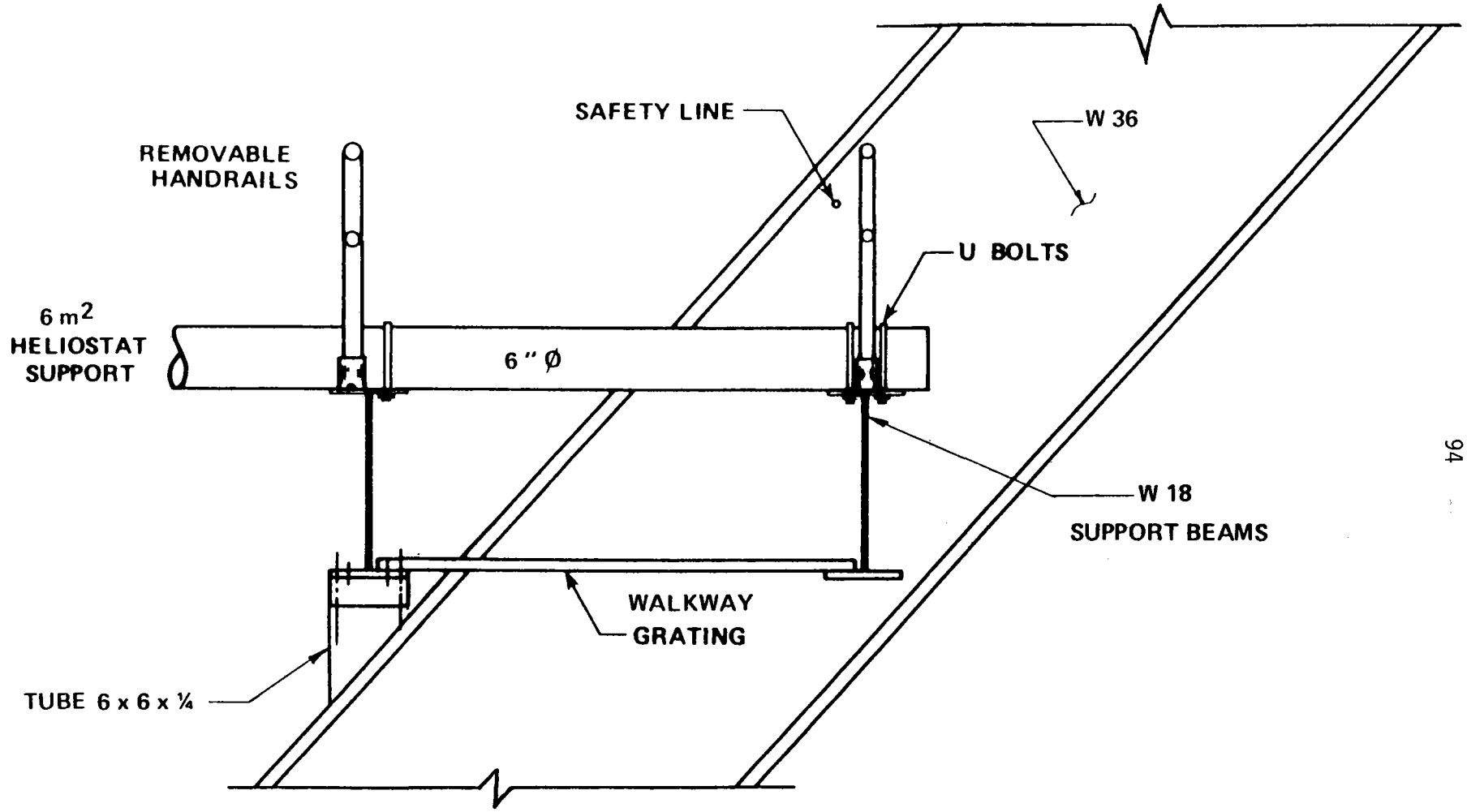

Figure 4–3 6 m ^{2} Heliostat Attachment Scheme

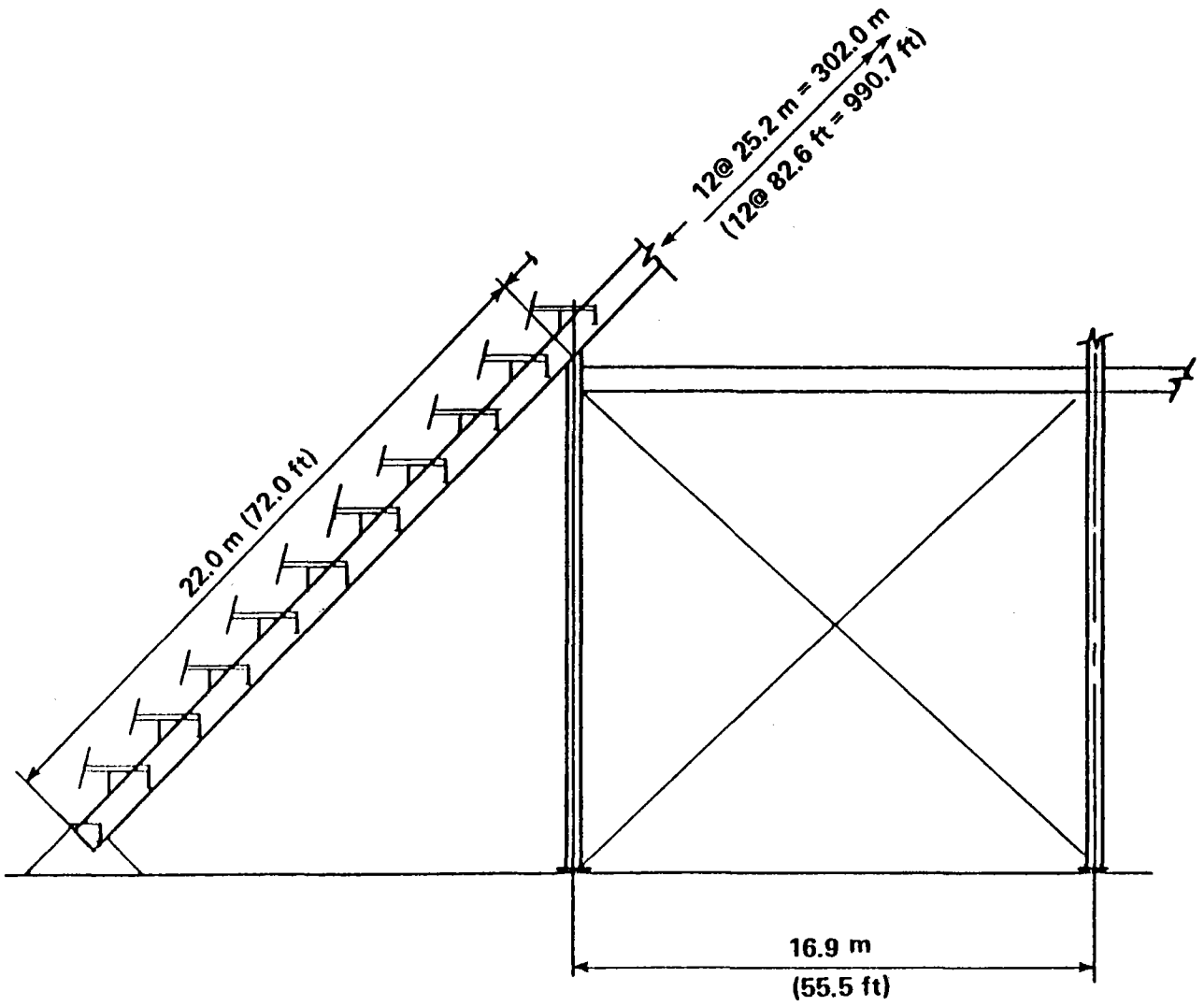

Figure 4–4 Partial Elevation of 25 MWt Array, 1:1 Aspect Ratio, 6 m ^{2} Heliostat

the main girders.

Task 4 specifies that the vertically supported 49 m^2 heliostat will be substituted for the horizontally mounted 6 m^2 heliostat. Therefore, a torsional system similar to the one used for the 6 m^2 heliostat was conceptually designed for the 49 m^2 heliostat. For this system, shown in Figure 4-5, the metal grating is attached to the top flanges of the beams with the base of the vertical heliostat being bolted to the transverse diaphragms.

4.3.3 Foundations

For the preconceptual designs, two types of foundations, caissons and spread footings, were examined. The caisson design shown in Figure 4-6 was chosen for the following reasons:

- Needs no forming hence gives lower costs
- Provides sufficient weight to resist uplift forces and sliding
- Is installed easily and rapidly in good soil conditions

The spread footing design shown in Figure 4-7 was also chosen for the following reasons:

- Design is relatively insensitive to soil conditions
- Footing dimensions may be easily increased to provide sufficient weight against uplift if needed.
- Separate footings may be economically linked up into a continuous strip footing

The actual foundation design will depend on site conditions, locally available equipment and contractor preferences. For this stage of the

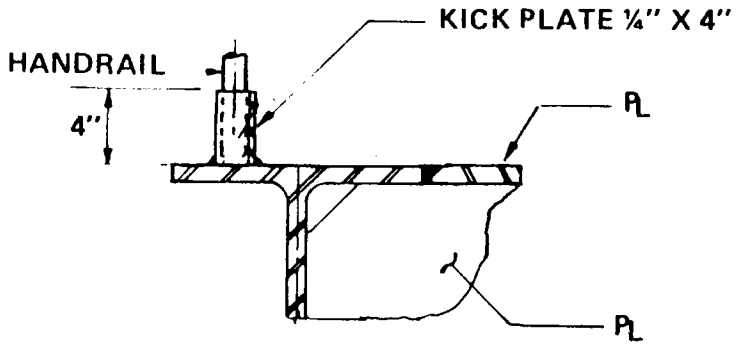

DETAIL 1

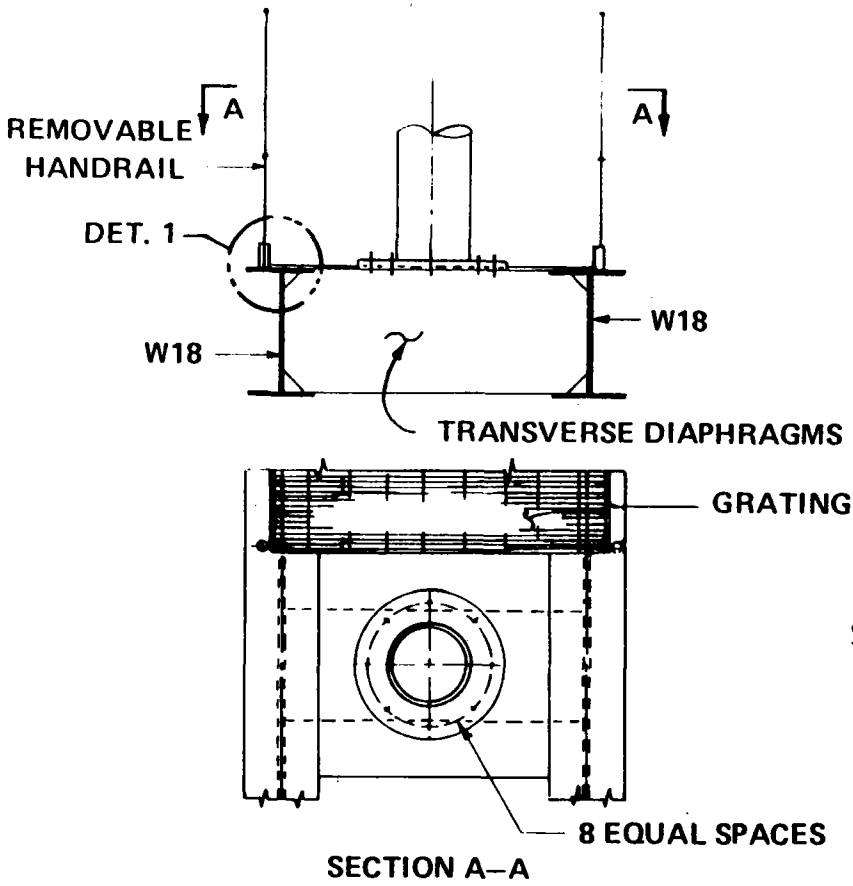

SECTION A–A

Figure 4–5 49 m^2 Heliostat Support Details

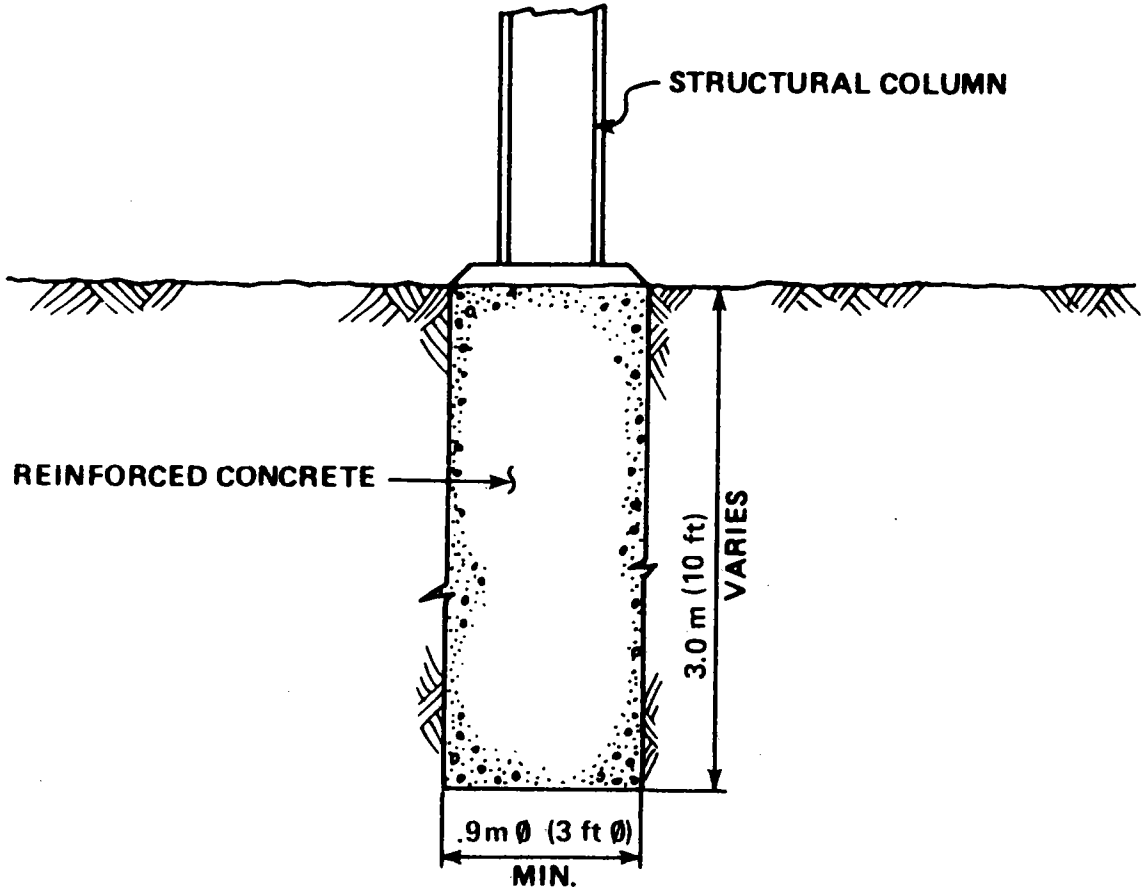

Figure 4–6 Typical Caisson Foundation

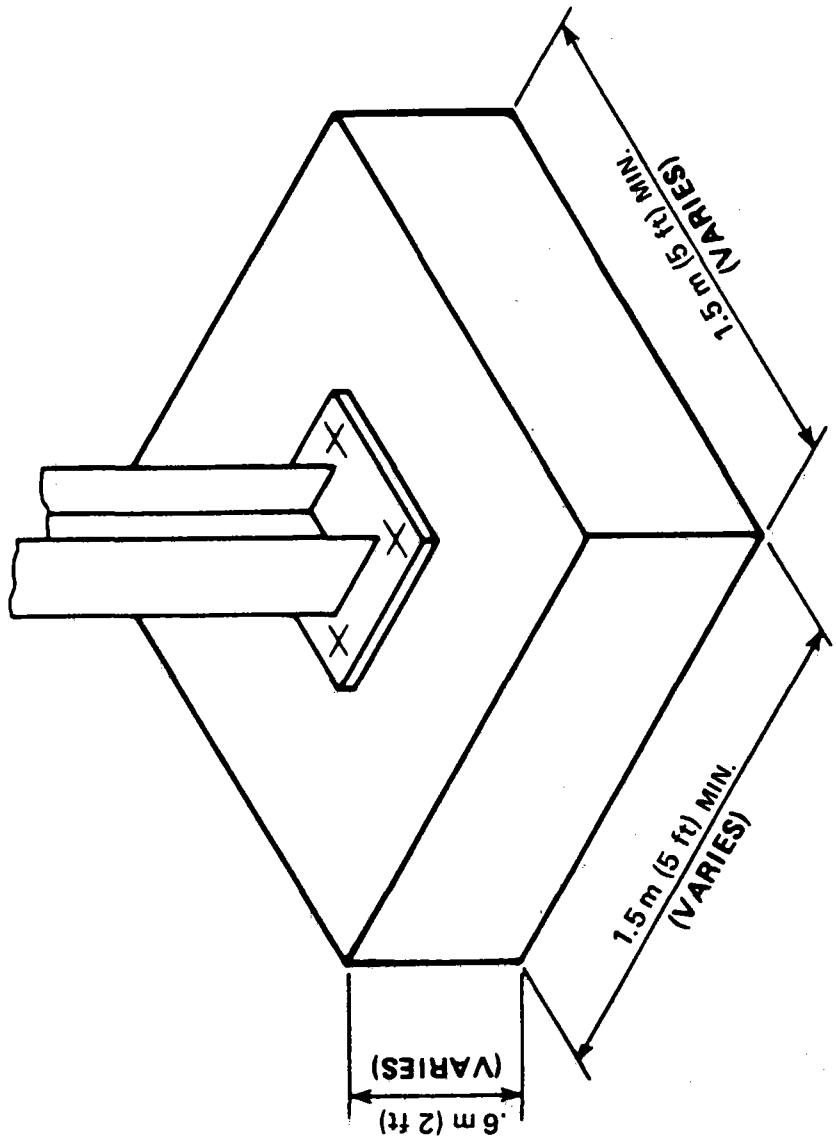

Figure 4–7 Typical Spread Footing Foundation

design effort the foundations were sized according to the dead load and preliminary calculations of the overturning moment due to wind.

4.4 ANALYSIS PROCEDURE

Only the dead loads and the governing wind load were considered in the preliminary conceptual design of the UHA structure. The W_{90} load was found to be the governing factor in the wind analysis.

To obtain reaction forces, an approximate analysis was used in which the centroid of the triangular shaped structure was found to distribute the vertical dead loads and the forces created by the wind overturning moments were distributed linearly to the foundations. The total horizontal shear load of the wind was distributed uniformly to all foundations. These foundation loads were then used to determine the column loads.

For the UHA structure, the double WF beam torsional system was designed under the W_{27} wind load to limit the local rotation to 1.5 mrads of a heliostat located at the top of the structure. Here the local rotation is defined by the rotation of only the WF beams with their ends torsionally restrained. The rotation of the structure itself was not considered in this preliminary work.

4.5 STRUCTURAL CONCEPTS

In this section the structural concepts are given for the 1, 10, and 25 MWt arrays. For any given power level, many similarities exist in the design of the structures for the three aspect ratios. For all the preconceptual designs, W14 size columns are used throughout.

4.5.1 1 MWt Arrays

Shown in Figures 4-8 to 4-10 are the preconceptual designs of the 1 MWt array for the different aspect ratios. For each structure, two W12x19 beams were used in each terrace with a W24x76 section being used for the main sloping girder. A summary of the total quantities are given in Table 4-1.

4.5.2 10 MWt Arrays

Shown in Figures 4-11 to 4-13 are the preconceptual designs of the 10 MWt array for the different aspect ratios. For each structure, two W18x60 beams were used in each terrace with a W36 section being used for the main sloping girder. A summary of the total quantities are given in Table 4-2.

4.5.3 25 MWt Arrays

The preconceptual designs for the largest power array, 25 MWt, are shown in Figures 4-14 to 4-16 for the three aspect ratios. Two W18x60 beams were used in the terrace of each structure, and a W36 section was selected for the main girder. Total quantities of the 25 MWt array for the different aspect ratios are summarized in Table 4-3.

4.6 PRECONCEPTUAL COST ESTIMATES

The results of the preconceptual cost estimate, its basis, qualifications and exclusions are presented in this section. This estimate is an order-of-magnitude evaluation of the constructed cost. A summary and detailed presentation of this estimate is exhibited in Table 4-4. The purpose of this estimate was to provide relative comparisons on UHA

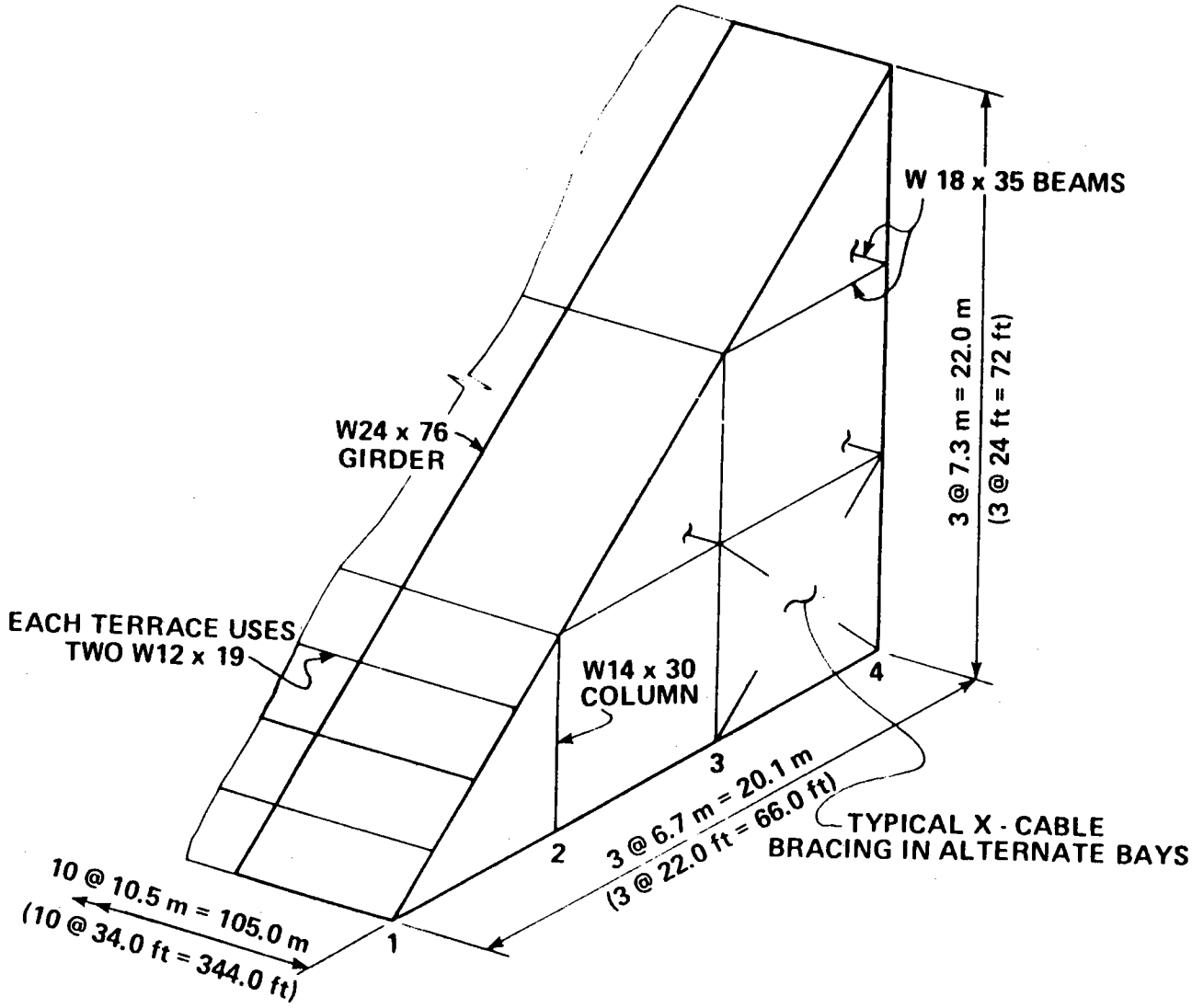

Figure 4–8 1 MWt UHA Structure, Aspect Ratio 1:5

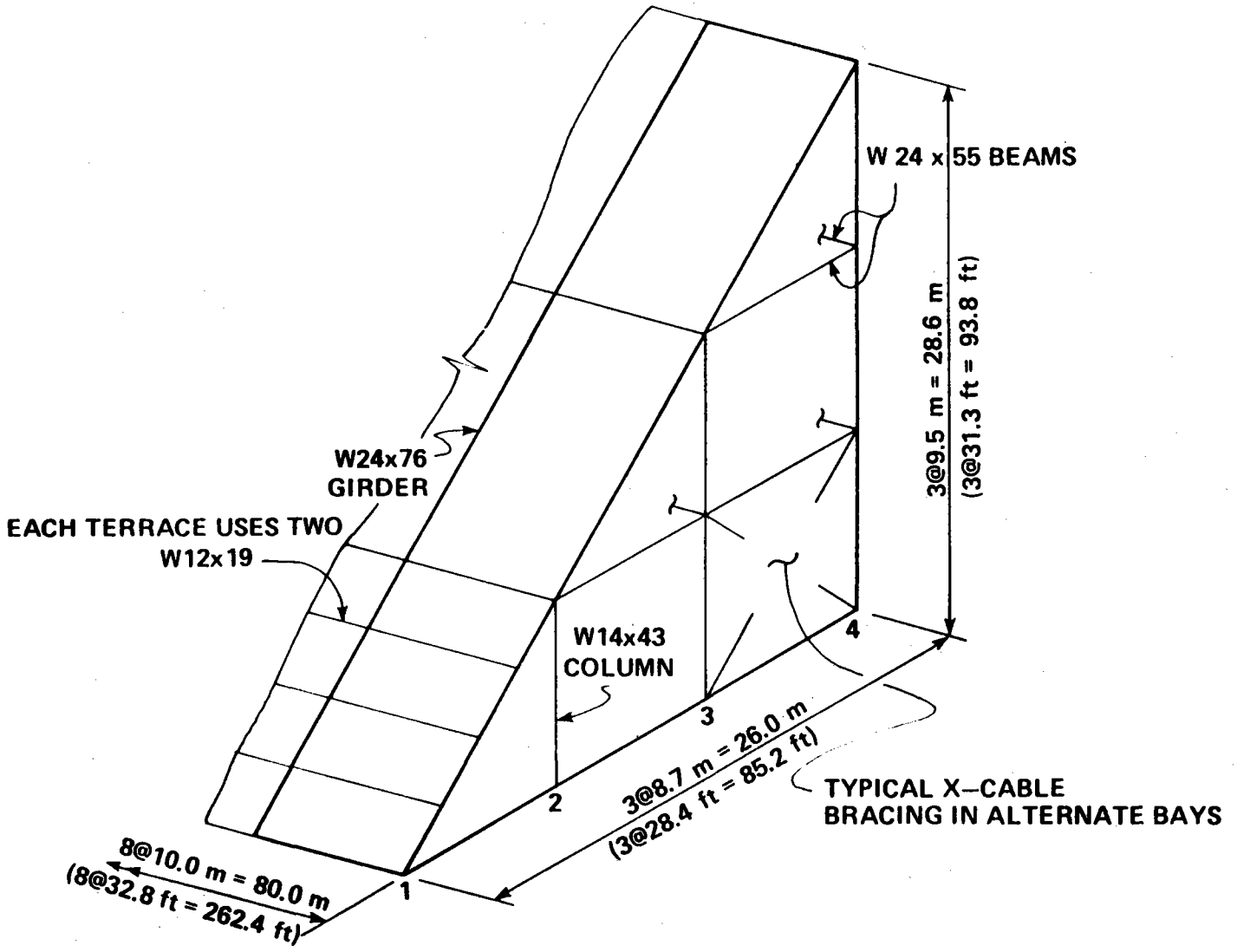

Figure 4–9 1 MWt UHA Structure, Aspect Ratio 1:3

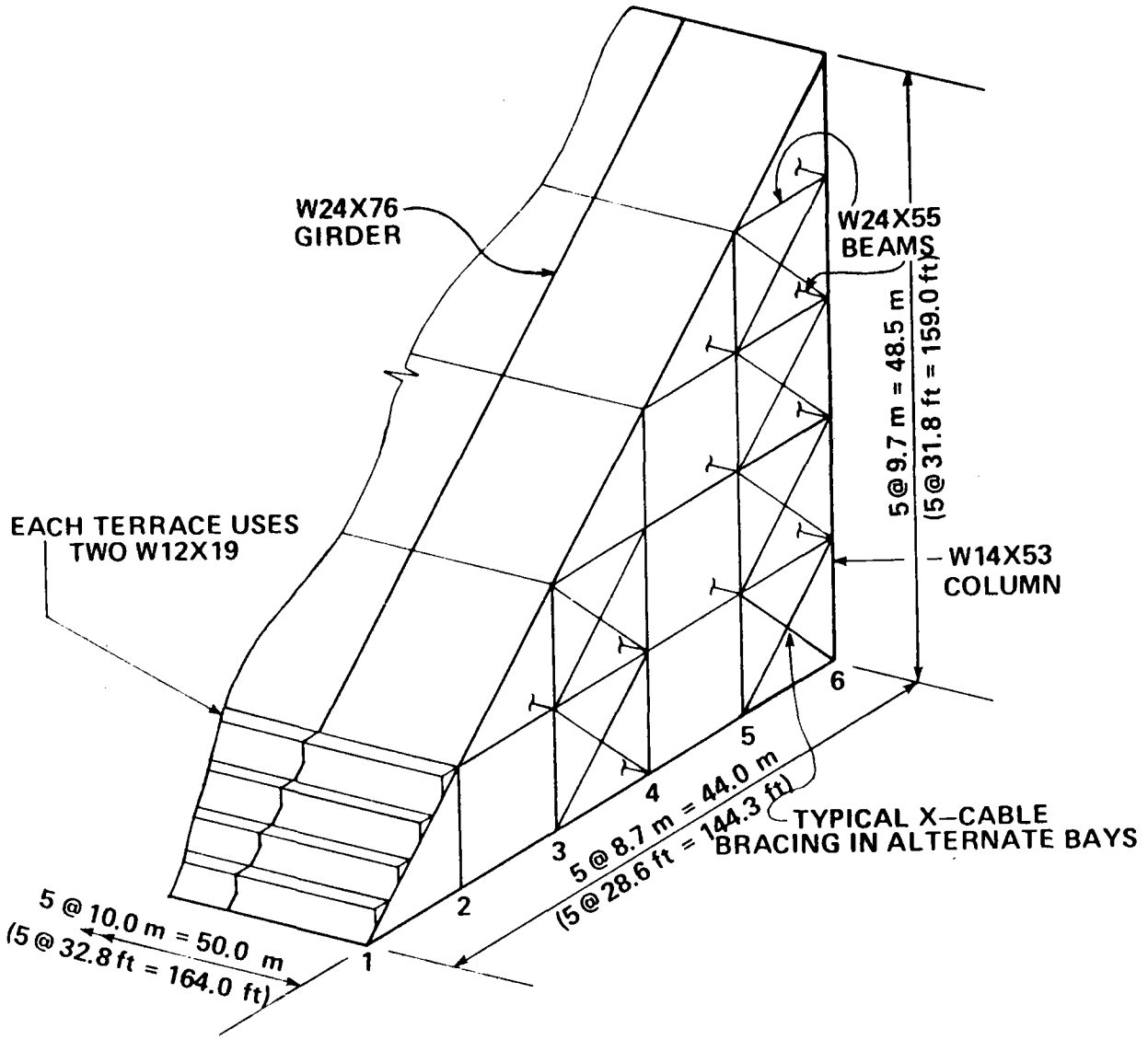

Figure 4–10 1 MWt UHA Structure, Aspect Ratio 1:1

TABLE 4-1 MATERIAL QUANTITIES FOR 1 MWt ARRAY

Materials	Units	Aspect Ratio		
		1:5	1:3	1:1
Steel	ton	161	236	290
Concrete	cubic yard	122	117	120
Rebar	ton	2.4	2.4	2.4

TABLE 4-2 MATERIAL QUANTITIES FOR 10 MWt ARRAY

Materials	Units	Aspect Ratio		
		1:5	1:3	1:1
Steel	ton	4493	5343	7827
Concrete	cubic yard	724	745	912
Rebar	ton	14	15	18

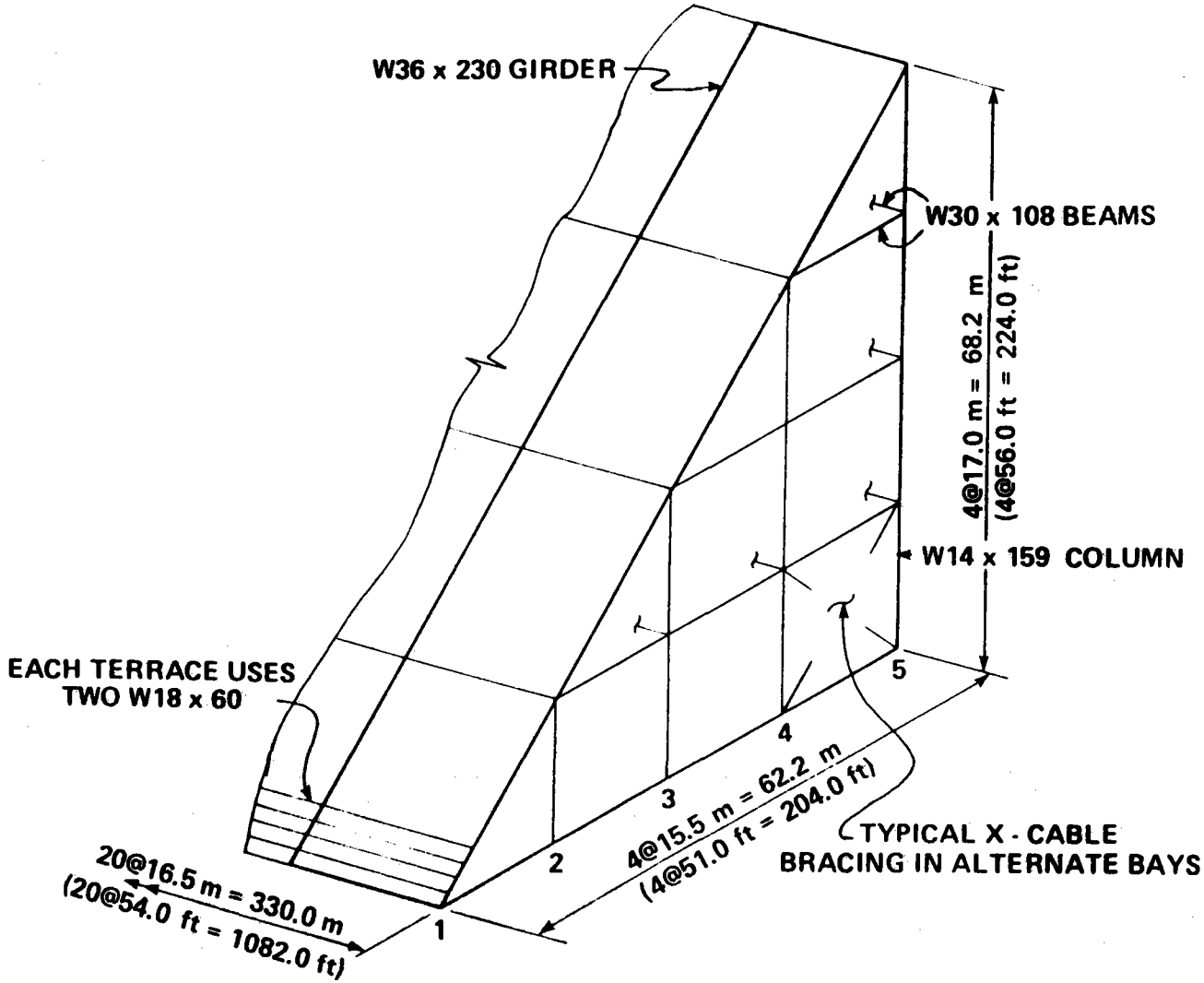

Figure 4–11 10 MWt UHA Structure , Aspect ratio 1:5

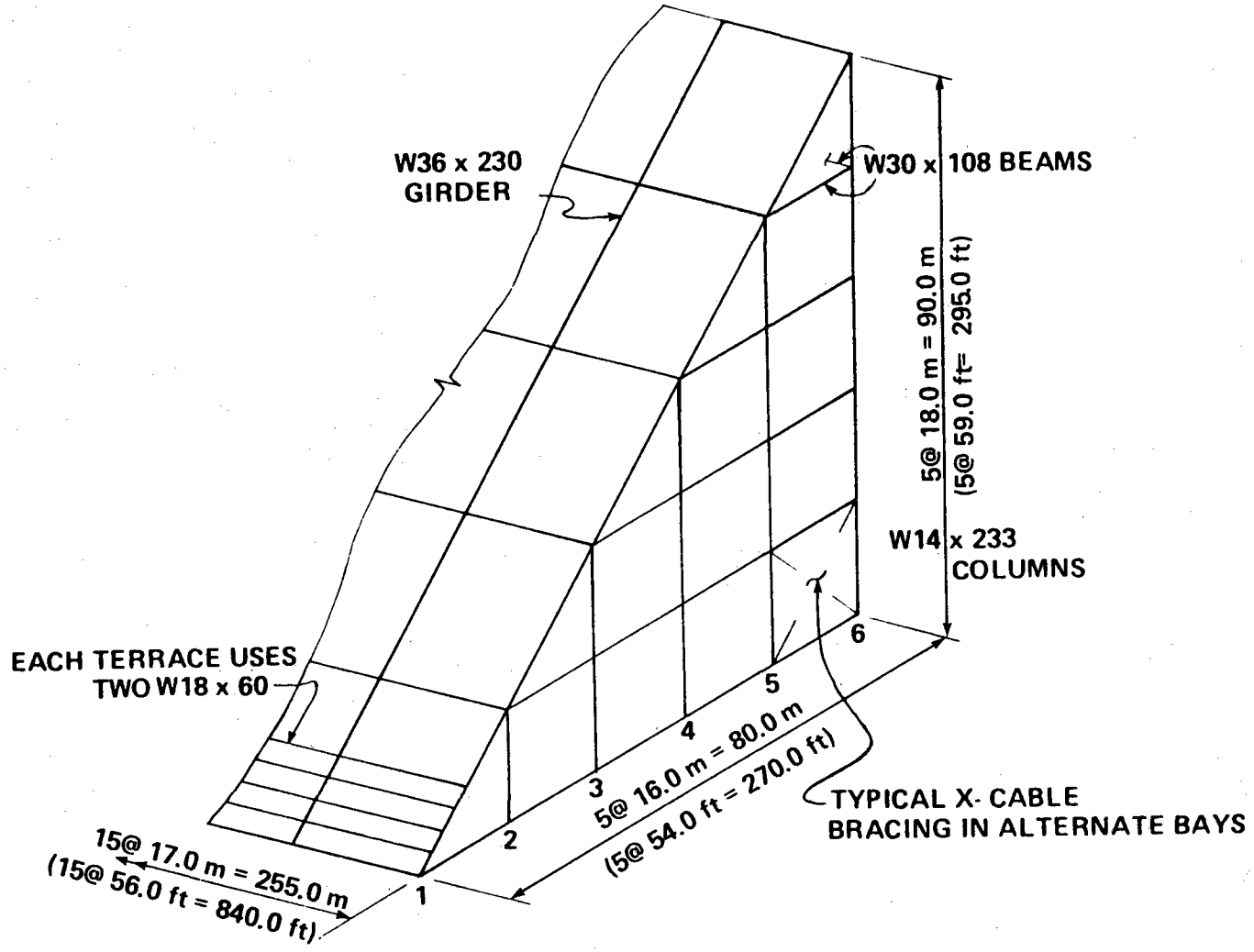

Figure 4–12 10 MWt UHA Structure, Aspect Ratio 1:3

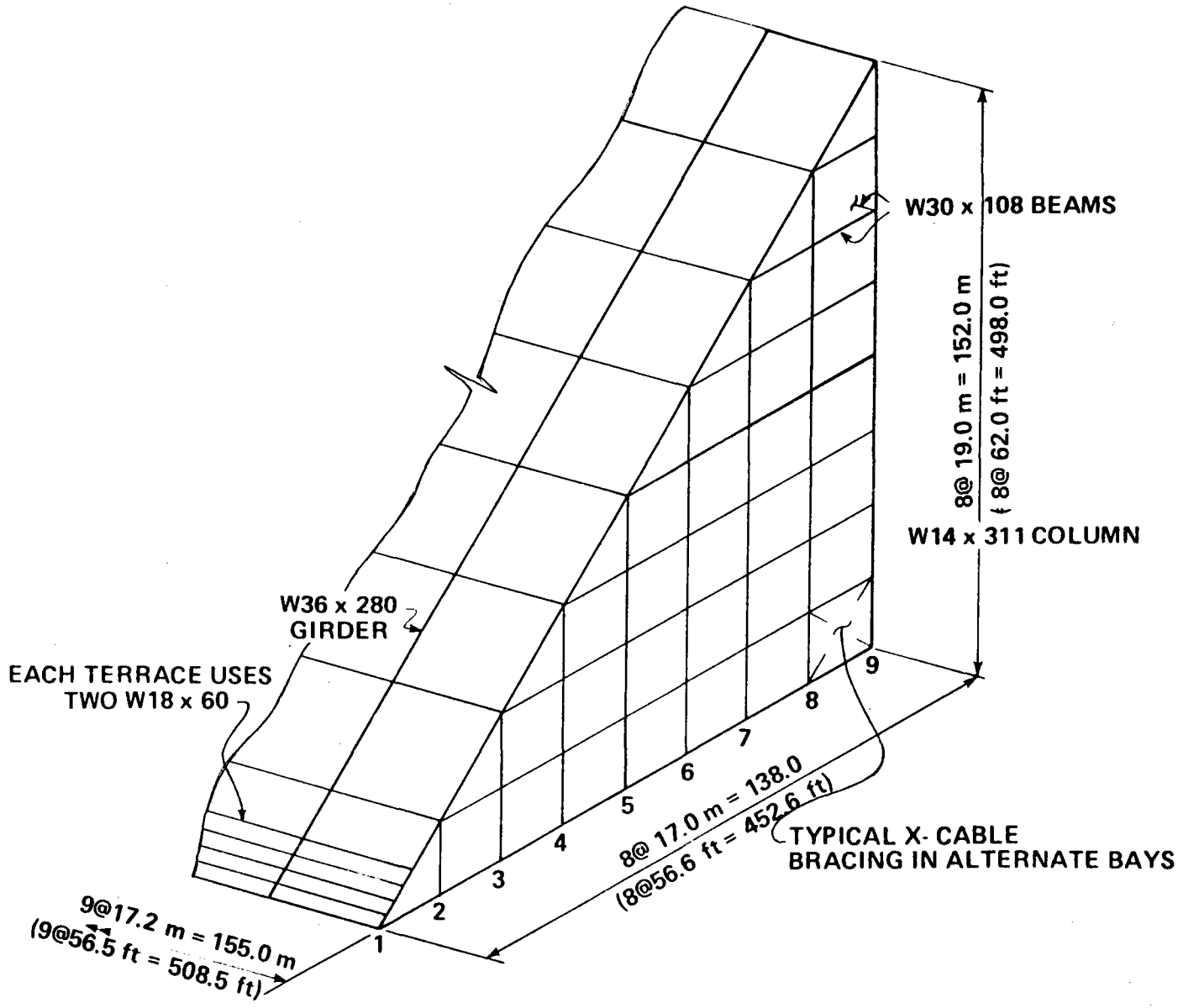

Figure 4–13 10 MWt UHA Structure , Aspect Ratio 1:1

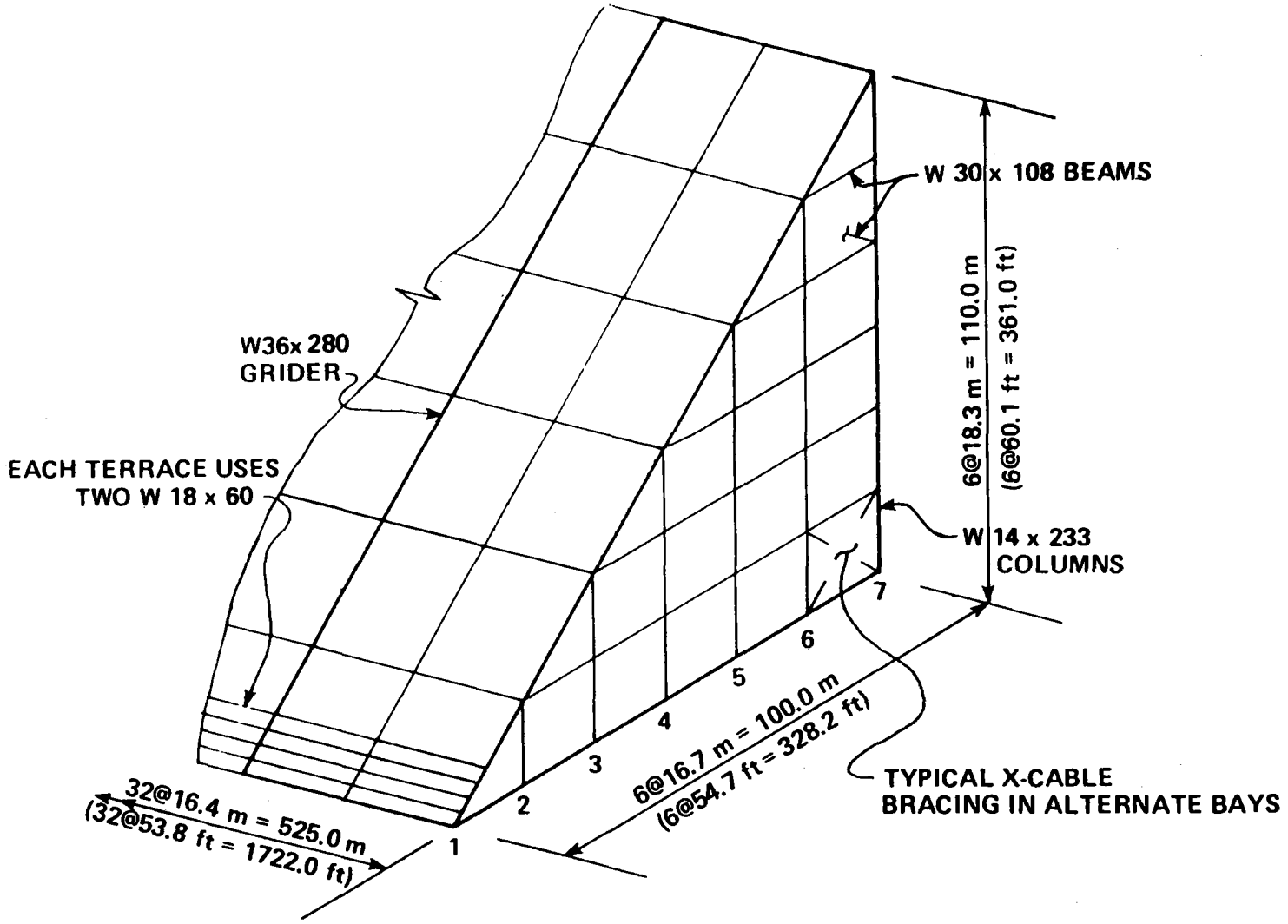

Figure 4–14 25 MWt UHA Structure, Aspect Ratio 1:5

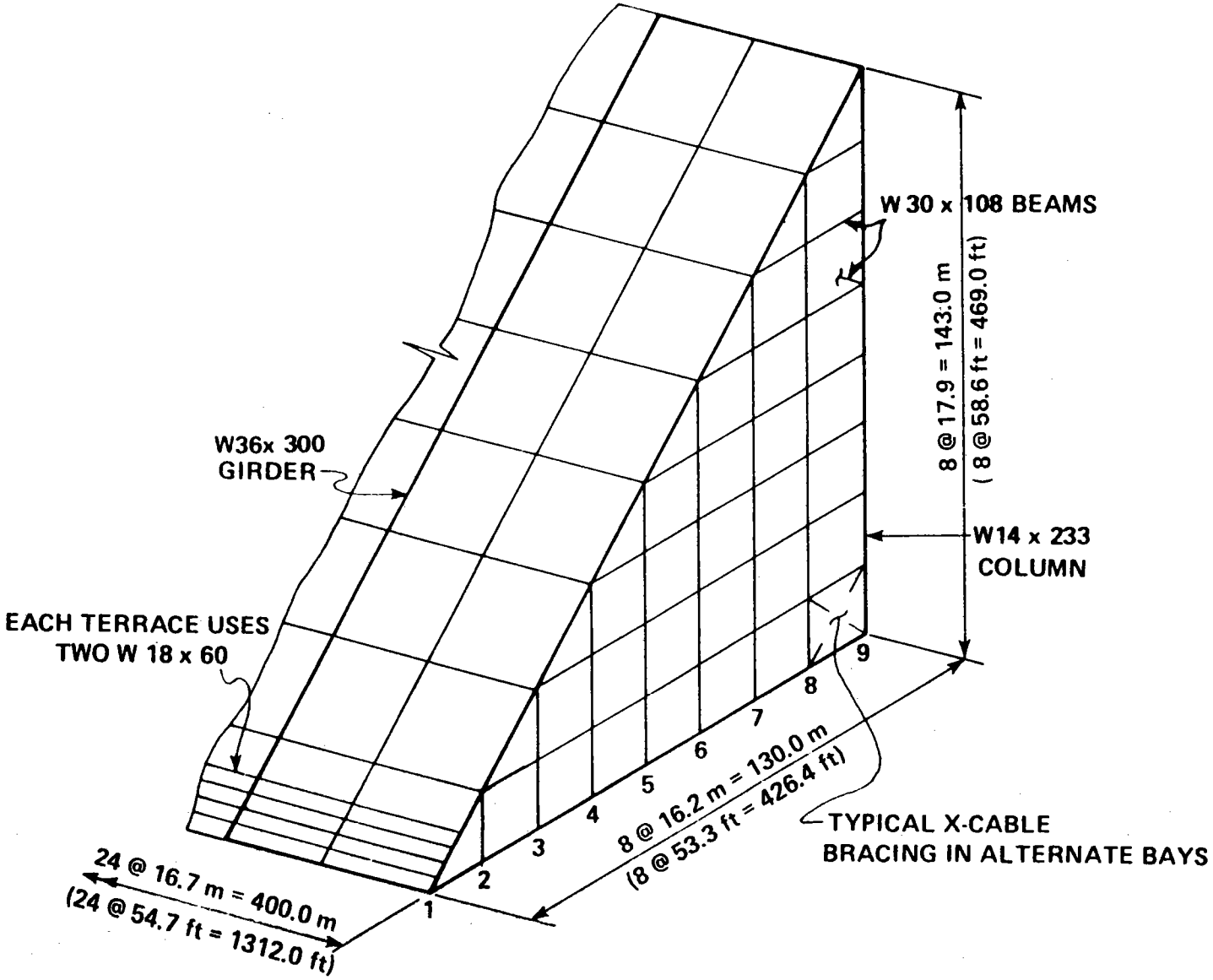

Figure 4–15 25 MWt UHA Structure, Aspect Ratio 1:3

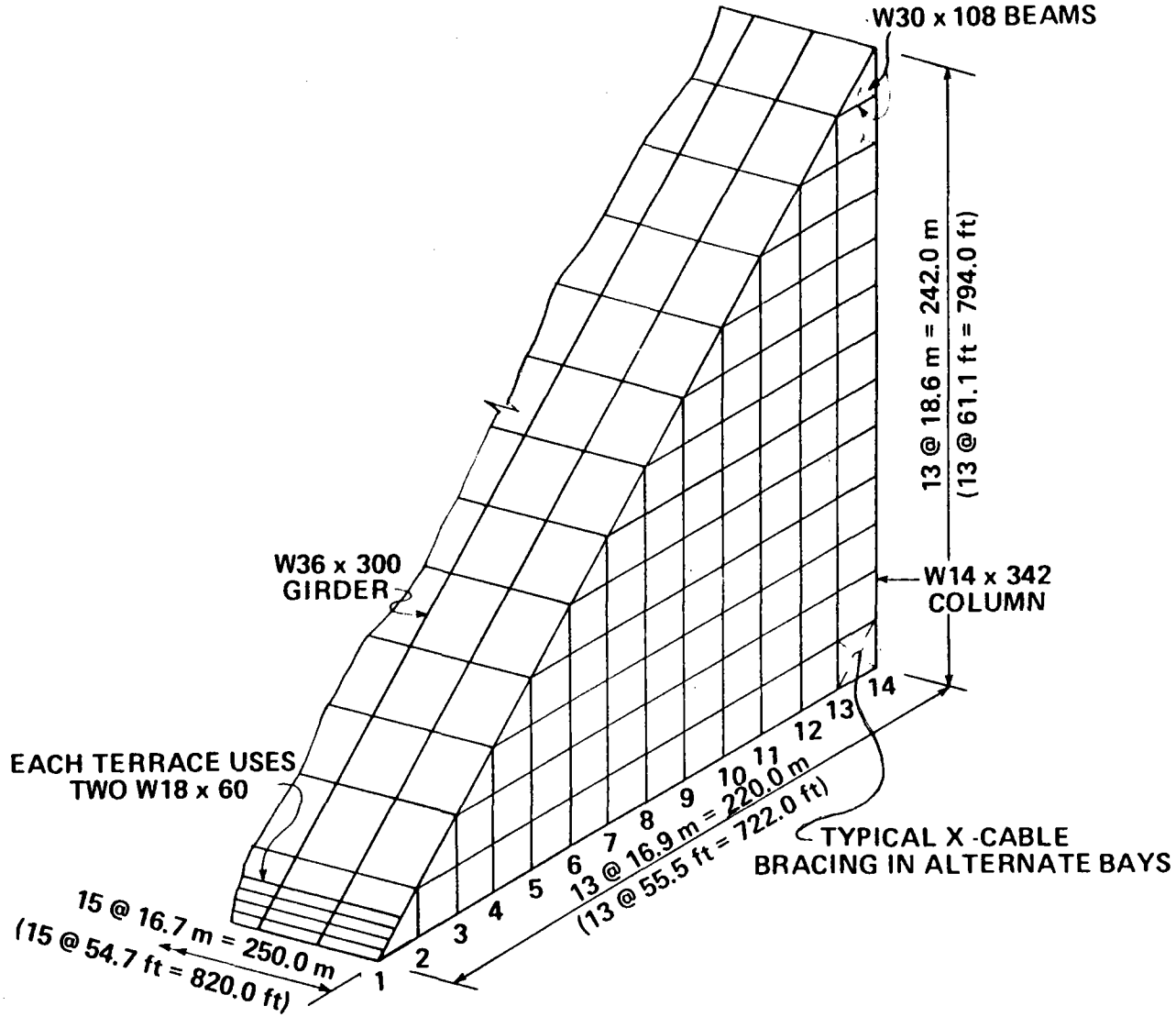

Figure 4–16 25 MWt UHA Structure, Aspect Ratio 1:1

TABLE 4-3 MATERIAL QUANTITIES FOR 25 MWt ARRAY

Materials	Units	Aspect Ratio		
		1:5	1:3	1:1
Steel	ton	14668	16875	27984
Concrete	cubic yard	1826	1970	3165
Rebar	ton	36	39	63

TABLE 4-4

PRECONCEPTUAL FIELD COST ESTIMATES

$ THOUSANDS -- SECOND QUARTER 1980

Configuration No.	1	2	3	4	5	6	7	8	9
Power Level	25 MWt	25 MWt	25 MWt	10 MWt	10 MWt	10 MWt	1 MWt	1 MWt	1 MWt
Aspect Ratio	1:1	1:3	1:5	1:1	1:3	1:5	1:1	1:3	1:5
Structure Height	794'	469'	361'	498'	296'	224'	159'	94'	72'
DIRECT FIELD COST									
Excavation	20	10	10	5	5	5	1	1	1
Concrete	250	150	140	70	60	60	10	10	10
Rebar	170	100	100	50	40	40	6	6	6
Formwork	510	320	300	150	120	120	20	20	20
Steel	64,500	38,900	33,800	18,100	12,300	10,350	670	540	370
DIRECT FIELD COST	64,450	39,480	34,350	18,375	12,525	10,575	707	577	407
INDIRECT FIELD COST *	13,550	8,520	7,650	3,925	2,675	2,225	153	123	93
FIELD COST	79,000	48,000	42,000	22,300	15,200	12,800	860	700	500
FIELD COST/MWt	3,160	1,920	1,680	2,230	1,520	1,280	860	700	500

*60% of Direct Labor Cost

configurations in order to permit Veda, Inc. to select 3 configurations for more detailed costing. The pricing data was that of the 1980 second quarter.

4.6.1 Basis and Scope Definition

The estimate is based on the preconceptual designs described in Section 4.5. This cost estimate includes only the array support facility - a steel structure on which the heliostats are mounted.

Three nominal power levels of 1, 10, and 25 MWt were used for the basis of this cost estimate study. In each power level, three structural aspect ratios (ratio of height to length) of 1:1, 1:3, and 1:5 as defined by Veda, were analyzed.

The following paragraphs briefly address each of the major cost categories describing the project scope and the method employed to develop the estimate.

4.6.2 Direct Field Costs

The direct field costs include:

- o Material
- o Fabrication
- o Labor

These preconceptual installed costs for the civil/structural work are estimated for each configuration including the structural steel framework and concrete foundation, but excluding wiring and any auxiliaries. Five main field construction work items are selected to cover the areas of

the scope. They are:

- o Excavation
- o Concrete
- o Steel
- o Rebar
- o Formwork

Material unit cost data and the unit manhour data are based on Bechtel's experience. A composite wage rate was calculated based on Bechtel current project information.

Because of the extreme height of some steel structures the "high time" of the operating engineers and steel workers was carefully discussed and reviewed with Bechtel's Labor Relations department in terms of added costs.

4.6.3 Indirect Field Costs

The indirect field costs include:

- o Temporary construction facilities
- o Construction equipment and service
- o Field office cost

These costs were developed from Bechtel experience on previous domestic projects of a similar nature and adjusted for the particular characteristics of this project. A charge of 60% of the direct field labor cost was chosen as the suitable burden for this project.

Engineering services and allowance for uncertainty were not considered here as they do not affect the relative costs of the configurations.

They are considered in the Task 6 analysis effort.

4.6.4 Qualifications

Basic assumptions used for the cost estimate were:

- The estimate was prepared assuming that Bechtel's scope of services will be that of a prime contractor responsible to the owner for engineering, procurement, and construction.
- Material and equipment will be procured from U.S. sources, and lead times will be able to support the project schedule without cost penalties.
- A skilled labor force will be available to support a straight time, single shift work week for duration of construction period.
- Civil/Structural work only is considered, including excavation, concrete, steel, rebar, and formwork.
- Field costs only are included.

4.6.5 Exclusions

The following items are excluded from the estimate:

- Wiring and any auxiliary equipment
- Cost and installation of heliostats
- Ecological and environmental considerations other than incorporated in the present conceptual design.
- Owner's costs, such as land acquisition, cost of financing, owner's licensing, royalties, and the like.
- State and local taxes
- Assistance to the owner in obtaining EPA clearances, permits and authorization from the Department of Energy or other governmental agencies.
- Future escalation
- All the facilities beyond the hypothetical site boundary.

4.7 COMPARISON OF PRECONCEPTUAL DESIGNS

For the UHA structures, both a weight and cost basis were used to compare the preliminary conceptual designs. Based on these comparisons, as directed Task 3 of the Work Scope, the preferred aspect ratios for the 10 MWt power level was selected.

For a weight basis, the steel tonnage per MWt of energy delivered at the focal point was used for comparisons. Shown in Figure 4-17 are plots of the steel tonnage of each array excluding rebar for the three aspect ratios. These plots are normalized with respect to the 1 MWt array with an aspect ratio of 1:5. The graphs clearly indicate that the tallest arrays have more steel weight per MWt of energy than do the shorter arrays

Since the UHA structures are unoccupied and require no floor or roof systems as found in conventional tall buildings, the total steel tonnages for the arrays might appear low. For example, as shown in Figure 4-18, the weights of the 25 MWt arrays compare significantly lower than the weights found for the World Trade Center in New York and the Sears Tower in Chicago. The quantity of steel weight per cubic foot was used to compare the structures since the arrays do not require floor systems. Normally steel weight per square foot of floor area is used for comparing tall buildings.

The steel tonnage for the preconceptual designs may not be a minimum since the steel weight for the UHA structure is a function of several dependent variables. For example, for the 10 MWt array with an aspect

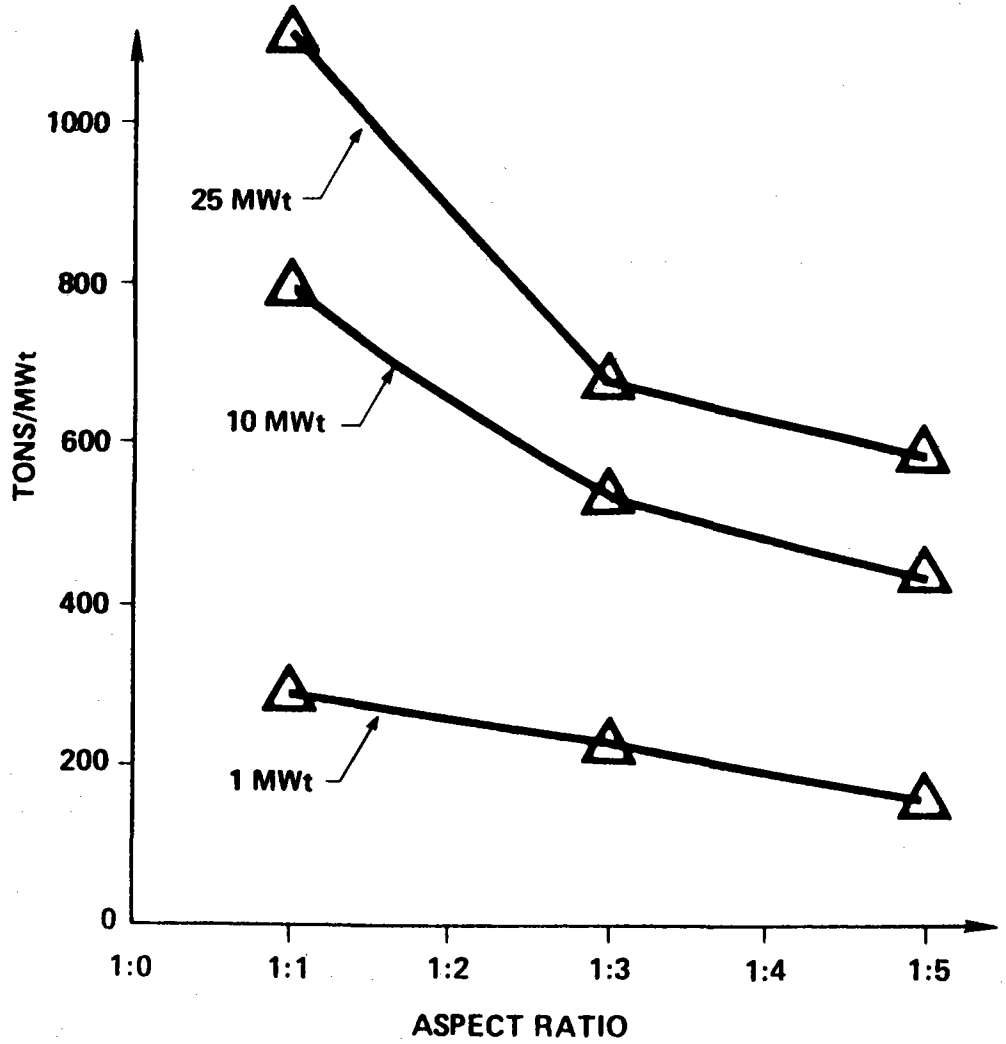

Figure 4–17 Steel Tonnages for the UHA Structures

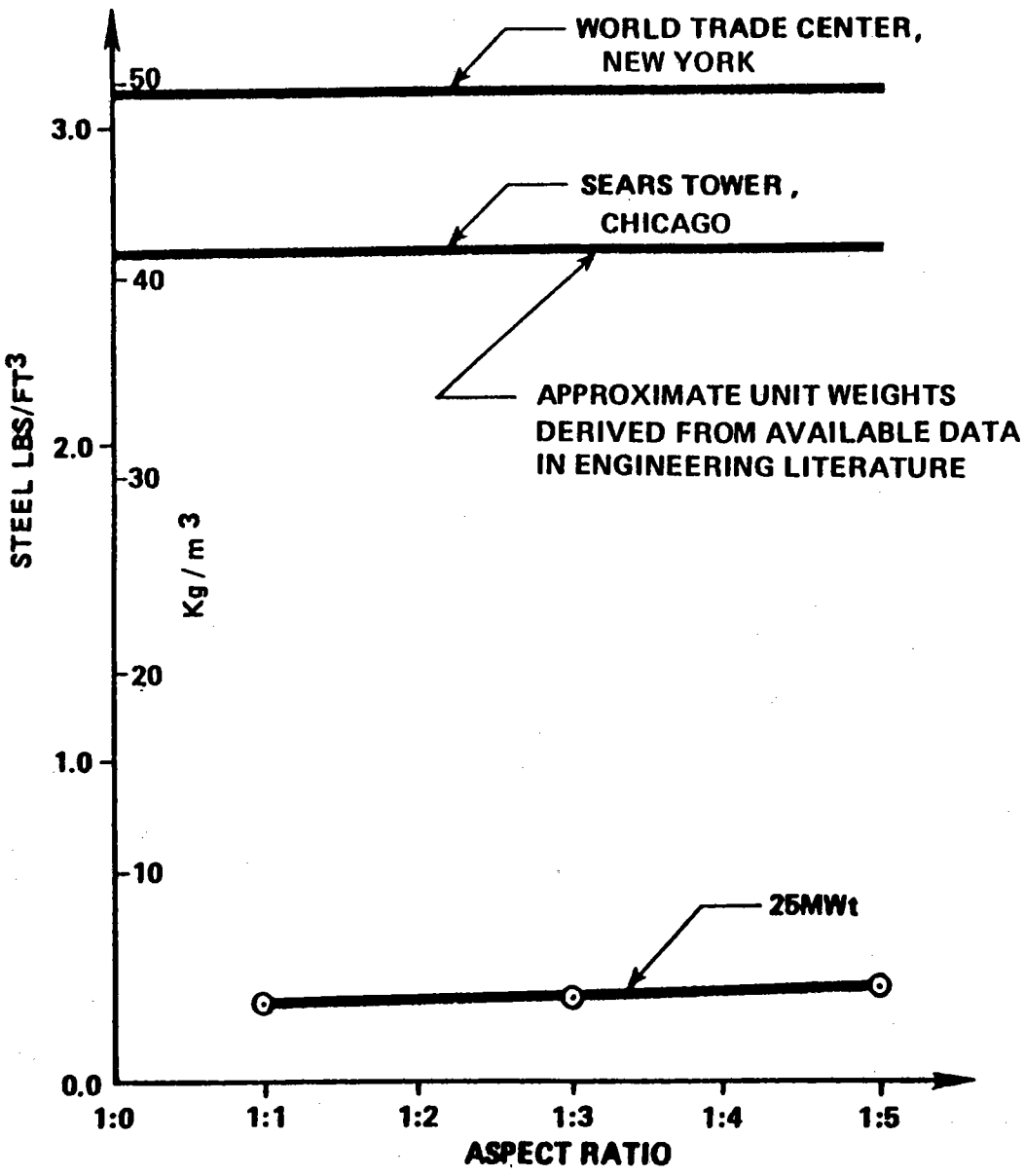

Figure 4—18 Steel Weight Comparisons

ratio of 1:1, the girder spacing was changed from 56.5 feet to 33.9 feet to investigate any changes that could occur in the total steel tonnage. These spacings correspond to having three heliostats per bay reduced down to two spanning between the main frames. As shown in Table 4-5, the total steel weight excluding rebar was apparently reduced 35% by decreasing the girder spacing.

No conclusions should be obtained from Table 4-5 other than demonstrating the fact that many variables are involved in the determination of steel weights. The total steel weights derived in the preconceptual designs for the various arrays represent good relative comparisons. However, in a more detailed analysis, these total weights could vary significantly.

Directly related to total steel weights are the total field costs estimated to construct the UHA structures. Shown in Table 4-6 and given graphically by Figure 4-19 is the total field cost ratio of each array normalized with respect to the 1 MWt array with an aspect ratio of 1:5. These numbers indicate the taller arrays cost more per MWt of energy than the shorter arrays.

4.8 EVALUATION OF PRECONCEPTUAL DESIGNS

Based on the information presented in Sections 4.7 and 4.8, the 1:5 aspect ratio was selected by Veda, Inc. in Task 3 as the preferred one for each power level. In Task 4 the 1:5 arrays were designed in more detail than those given in the preconceptual designs.

It was noted in Section 4.7 that the steel tonnages estimated for the preconceptual designs of the arrays were comparative weights and were

TABLE 4-5

GIRDER SPACING EFFECT ON STEEL TONNAGE, 10 MWt, 1:1 GEOMETRY

	Girder Spacing		
	Old 56.5 ft.	New 33.9 ft.	% Change in Steel Tonnage
Columns	3198	2403	-25
Girders	900	481	-47
Support Beams	2106	667	-68
N-S Beams	855	1141	+33
W-S Beams	769	392	-49
Total Tons	7828	5084	-35
Metric Tonnes	(7954)	(5166)	

TABLE 4-6

NORMALIZED FIELD COST PER MWt

POWER LEVEL MWt	ASPECT RATIO		
	1:1	1:3	1:5
25	6.32	3.84	3.36
10	4.46	3.04	2.56
1	1.72	1.40	1.00

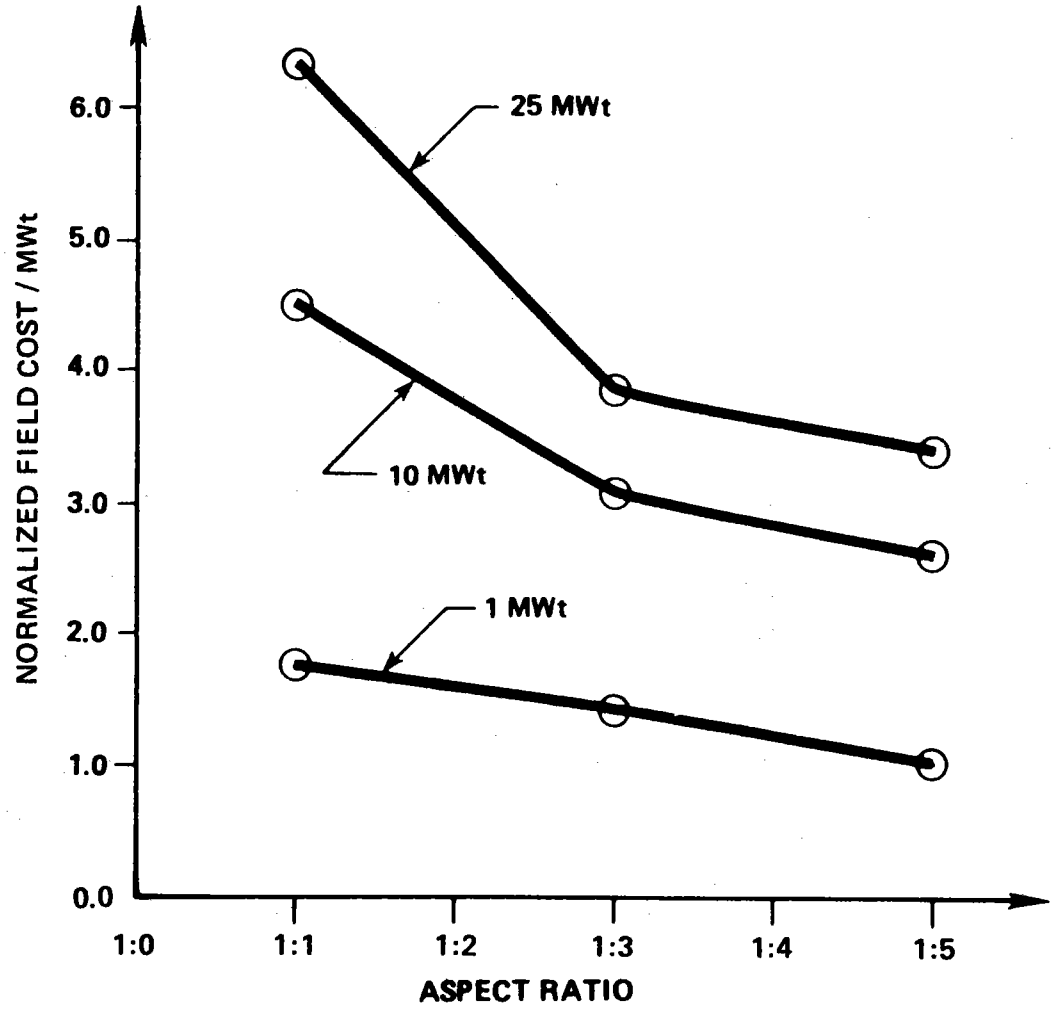

Results Normalized to Lowest Unit Cost Ratio

Figure 4–19 Normalized Field Cost Ratio Per MWt

not necessarily optimum. Therefore weight minimization was the primary factor considered to lower the total costs in the conceptual design of the arrays with the preferred aspect ratio.

Table 4-7 gives the breakdown of the steel tonnages for the different structural components with the preferred aspect ratio of 1:5. This list of tonnages clearly indicated that largest percentage of the total weight of the structure came from the support beams for the heliostats.

At this point, two different options were open to possibly reduce steel weights in the more detailed conceptual designs:

- Modify by more detailed computer analyses the existing preconceptual designs to determine if they meet the design criteria and then optimize the structure by varying the design parameters such as column and girder spacings
- Reduce the large percentage of steel in the support beams by using an alternate, more efficient supporting system for the heliostats and analyze the new system to check against the design criteria

After careful consideration the latter option was selected as a means of possibly reducing the total steel in the UHA structures. More details of the modified concept are given in the next section.

TABLE 4-7

STRUCTURAL STEEL TONNAGE AND PERCENTAGE COMPARISON
UHA ASPECT RATIO 1:5

STRUCTURAL COMPONENT	THERMAL POWER LEVEL					
	1 MWt		10 MWt		25 MWt	
	TONS	%	TONS	%	TONS	%
Girders	40.8	25	809	18	2,066	14
E-W Beams	18.1	11	351	8	1,394	10
N-S Beams	12.7	8	346	8	1,462	10
Columns	23.8	15	974	21	4,580	31
Support Beams	5.5	41	2,013	45	5,165	35
Total Weight	161	100	4,493	100	14,667	100
Metric Tonnes	(164)		(4,565)		(14,902)	

Section 5

MODIFIED CONCEPTUAL DESIGNS

5.1 INTRODUCTION

It is mentioned in Section 4.8 that modifying the UHA design concept would possibly reduce the total steel tonnages in the structure and lower the field costs. Therefore, a modified structure was developed for the selected arrays using the 6 m^2 heliostats.

This section gives a complete description of the design concept as well as describes the computer analysis used for the modified UHA structures. The results of the analyzes are given along with the cost of the new concepts.

5.2 DESCRIPTION OF MODIFIED STRUCTURAL CONCEPTS

The modified structural concept developed for the arrays consists of a series of frames, each of which are composed of a long sloping truss system supported by large diameter pipe columns. To meet the stringent rotation criteria of $\pm$ 1.5 mrads, the heliostats are attached directly to each frame instead of on beams spanning between them. Thus, in all cases considered, the spacings of the sloping members for the different arrays are identical to the heliostat spacings.

5.2.1 Support Structure for the 6 m^2 Heliostats

Shown in Figure 5-1 are structural details of a typical interior frame of the arrays using the 6 m^2 heliostats. The truss system of this array has two W12x53 beams acting as the main chords with 5 inch (12.7 cm) square

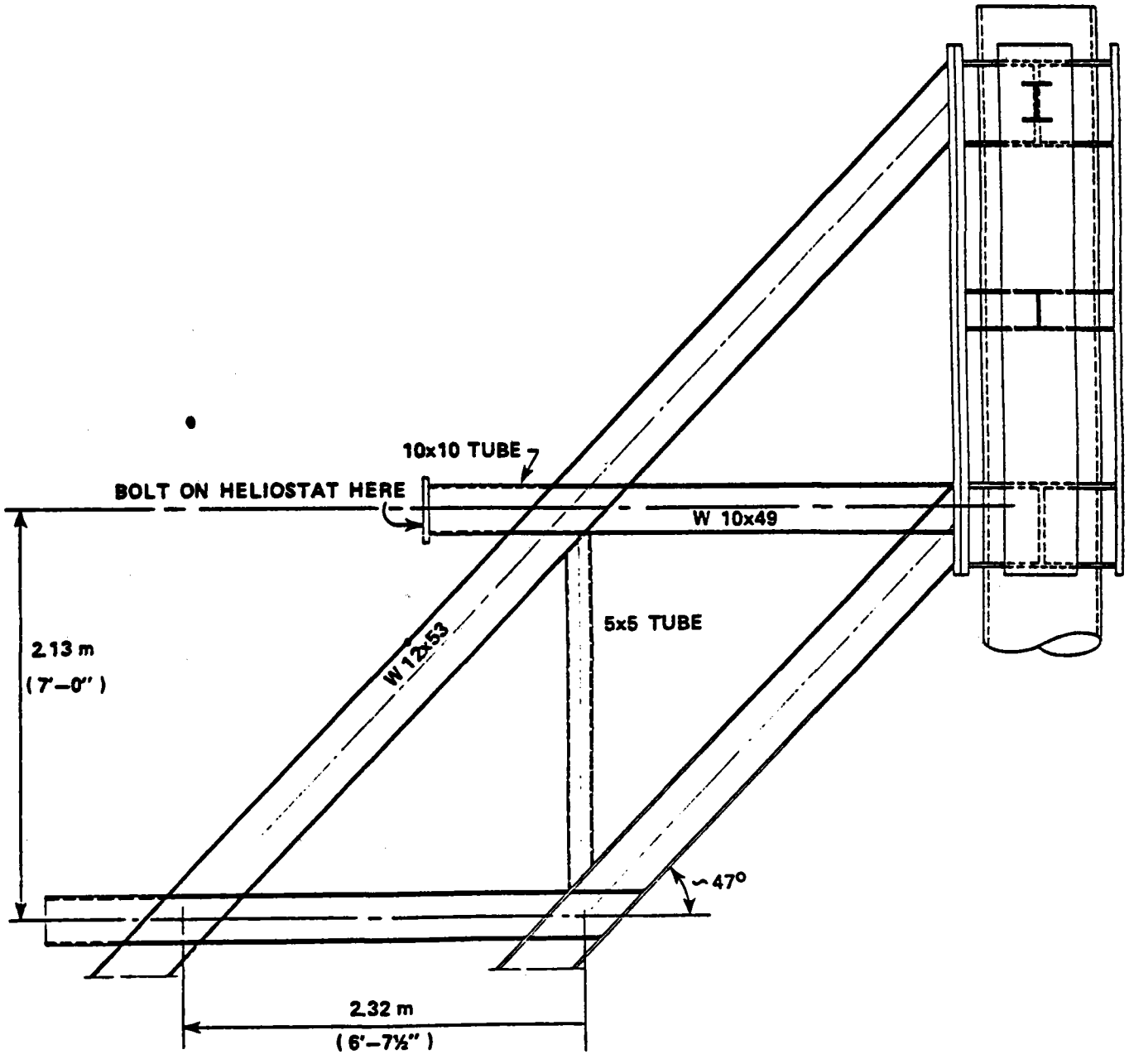

Figure 5–1 Detail For The 10 MWt Arrays With 6 m^2 Heliostats

tubes used for vertical web members. W10X49 sections were selected for the horizontal web members of the truss and are located at the same elevations as the heliostats.

The pedestal of the heliostat is a 10 inch (25.4 cm) square tube shop-welded to the exterior main chord of the truss. Gusset plates were used to transfer forces into the main frame from the pedestal and the horizontal web members. The heliostat units can be field bolted to the pedestals using this approach.

Twenty-four inch diameter pipe sections, 1/2 inch thick, were selected for the columns. Shown in Figure 5-2 is a Vierendeel truss used to tie the main frames together longitudinally. The top of the rear column is stiffened with plates to which the slanting truss and longitudinal tie trusses are bolted.

For the structure 1 MWt array using the 6 m^2 heliostats, it was found that only one column per frame was needed to meet the design criteria. Two W12x22 beams were used as the main chords of the truss system with 5 inch (12.7 cm) square tubes being used for the vertical web members and W10x22 sections being selected for the horizontal web members.

Fourteen inch diameter pipe sections, 3/8 inches thick, were chosen for the columns. The remaining structural details of the 1 MWt array are similar to the 10 MWt array.

The steel tonnages and foundation quantities of the 25 MWt structure were extrapolated from data of the nine preconceptual designs of the structures and the two modified detailed designs of the 1 and 10 MWt arrays.

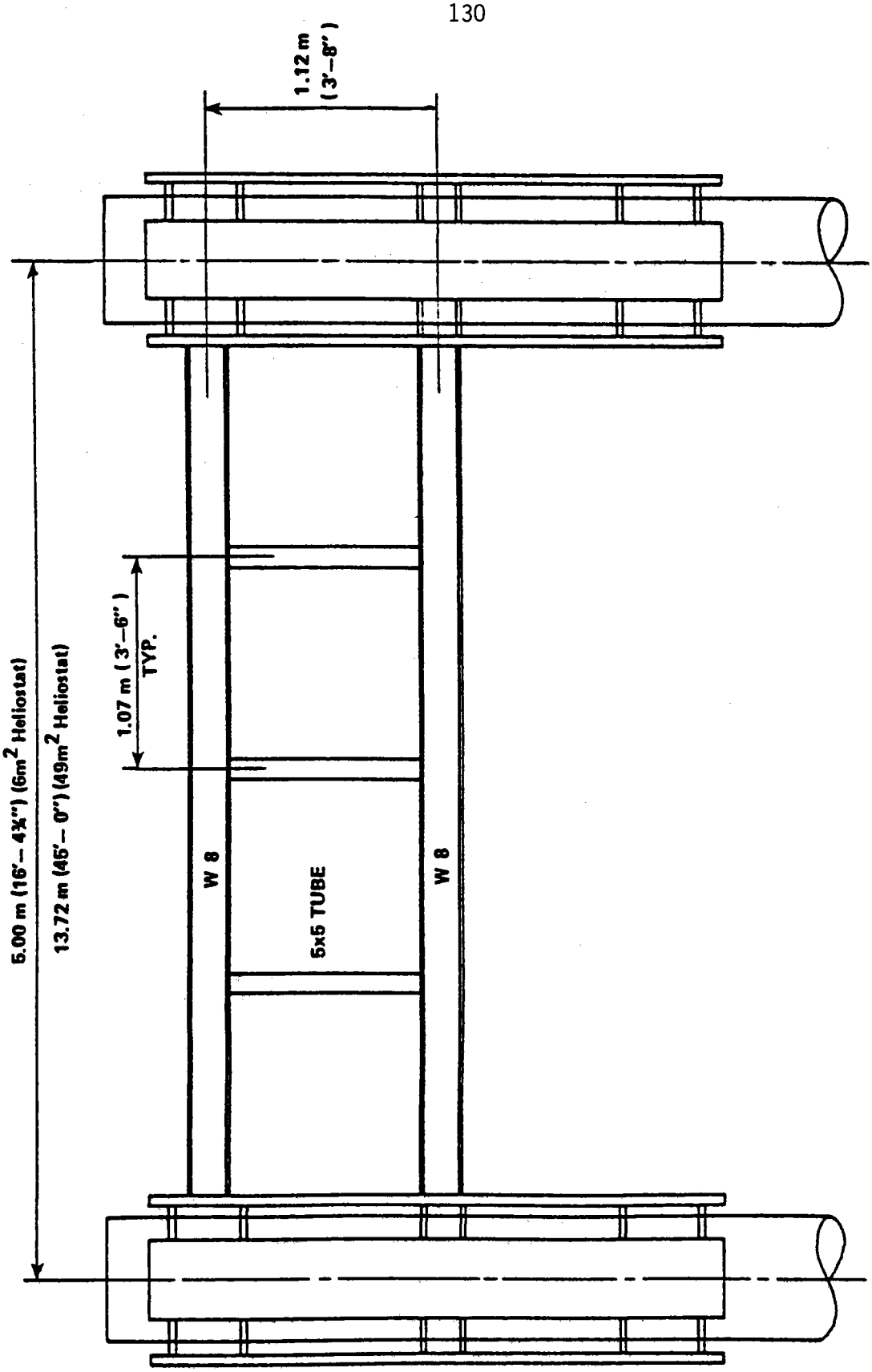

Figure 5–2 Vierendeel Tie – Truss Between Main Frames, Typical All Arrays

For tall structures like the UHA, lateral forces due to wind might cause the structure to rock or rotate about its base and cause uplift on the foundations. However, the weight of the structure was sufficiently large to prevent overturning. Due to the large lateral wind forces on the sloping member of each frame, the foundation designs for all three power levels had to provide sufficient mass to resist pullout on the front foundations. This fact, coupled with a need to provide resistance to sliding, and given the close spacing of columns, led to the decision to use a continuous strip footing with a caisson under each column. Primarily because of the better definition of pullout forces on the foundations, the amount of concrete and rebar increased over that given in the preliminary conceptual development.

5.2.2 Support Structure for the 49 m^2 Heliostats

Shown in Figure 5-3 are structural details of a typical interior frame of the 10 MWt array using the 49 m^2 heliostats. Two W12x87 beams were selected as the main chords of the main sloping truss with 5 inch (12.7 cm) square tubes as web members. The columns and horizontal struts in the main frame consist of 18, 20, and 24 inch diameter pipe sections with varying thicknesses ranging from 3/8 to 1/2 inch.

For this structure, however, the heliostat mirrors had problems in clearing the slanting truss system which would have required extensive structural detailing to solve. For this reason, the heliostats were spaced between the main frames instead of attaching directly to the sloping truss.

To meet the rotation criteria of 1.5 mrads for the array using the larger 49 m^2 heliostat, a triangular shaped space frame, as shown in Figures 5-4 and Figures 5-5, was specially designed to span between the main

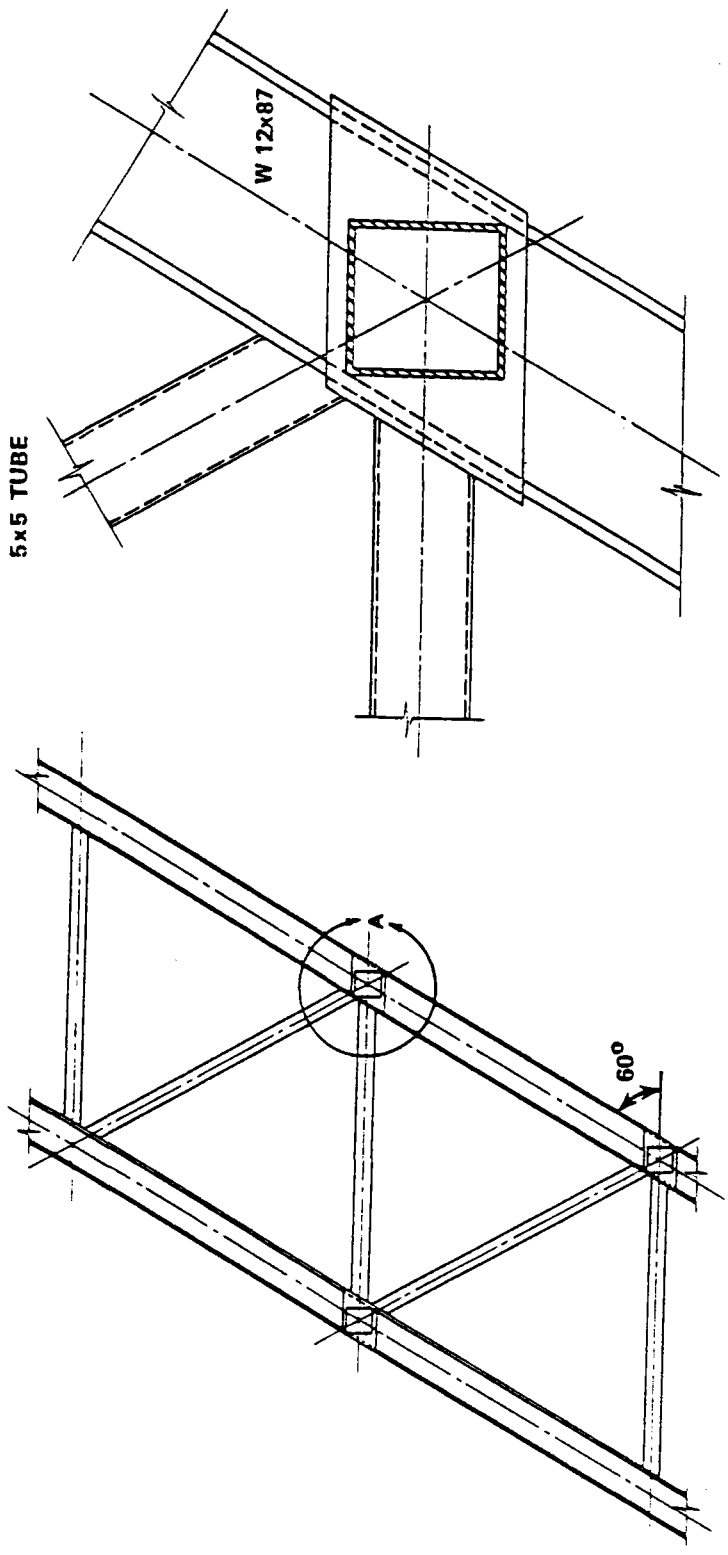

Figure 5–3 Detail For The 10 MWt Array With 49 m^2 Heliostats

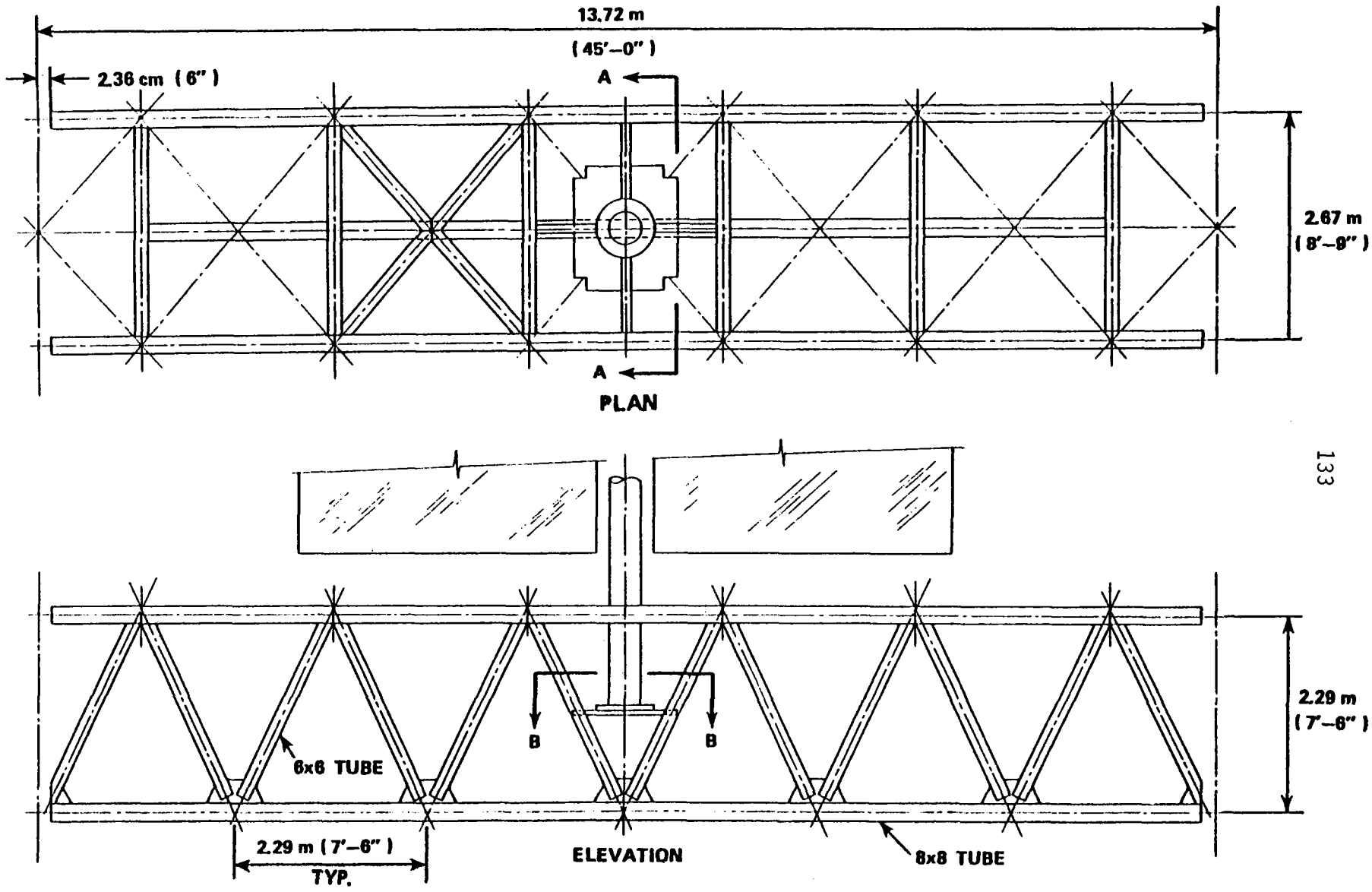

Figure 5–4 Triangular Space Frame Supporting 49 m^2 Heliostats

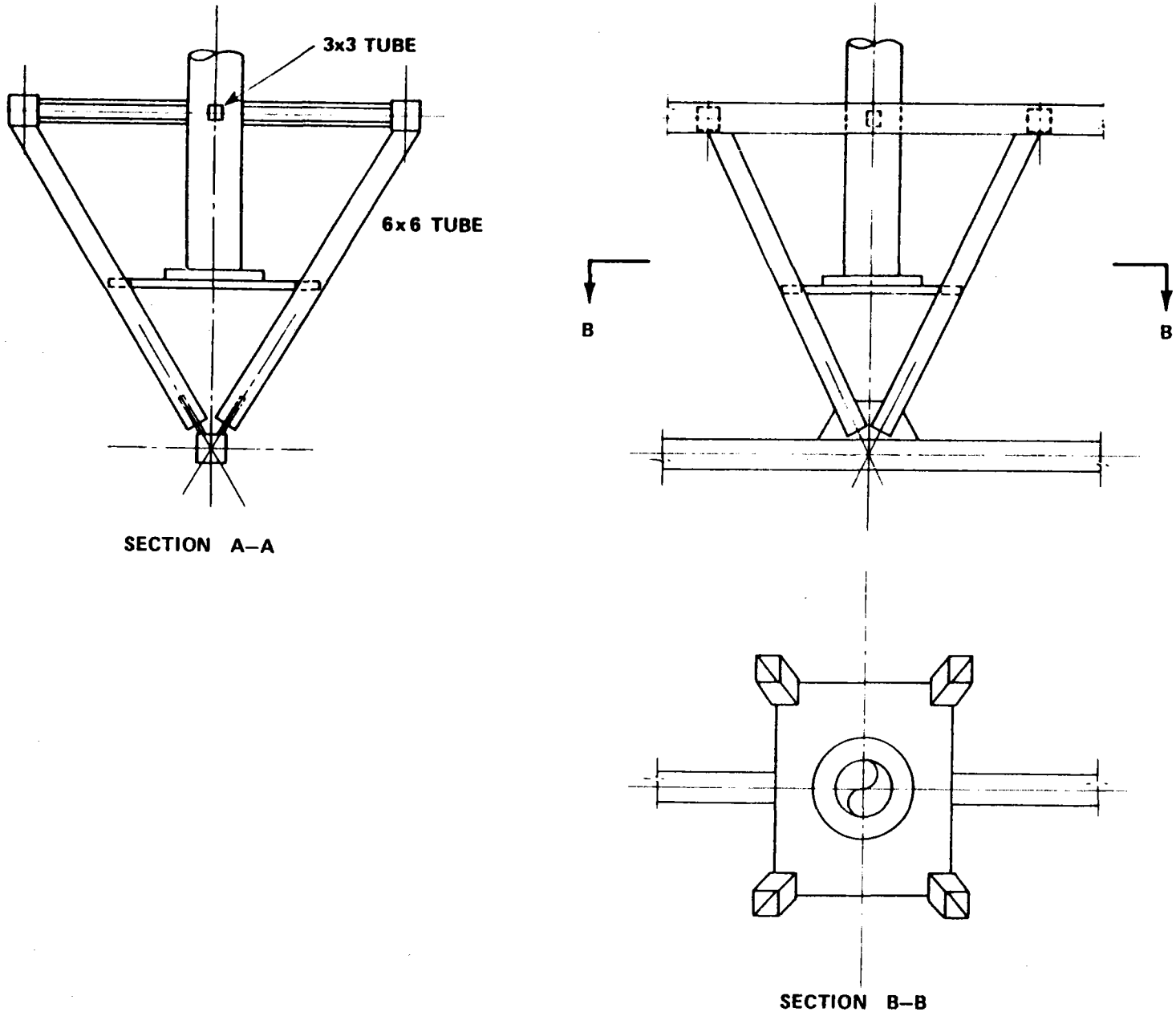

SECTION A–A

SECTION B–B

Figure 5–5 Details Of Space Frame Supporting 49 m^2 Heliostats

frames. The space frame has three 8 inch (20.3 cm) square tubes which form the chords of the main longitudinal triangular shape. Each space frame has segments comprised of four 6 inch (15.2 cm) square tubes shop welded to the lower longitudinal member to form the vertex of an inverted tetrahedron. A rectangular flat plate is welded to the side members of the inverted tetrahedron to which the base of the vertical heliostat is attached.

A specific problem in analyzing the space frame was to obtain its equivalent torsional properties for an accurate analysis of rotational deflections. The torsional properties of solid or open sections which are prismatic and homogeneous along their length can be computed exactly or approximately by many methods. However, the space frame is not homogenous longitudinally due to its transverse members and stiffeners, and its torsional properties cannot be directly approximated. Hence a modified method was adopted which finds the torsional stiffness of built-up frame members (Reference 5-1).

The foundation design for this structural concept followed the same approach as was performed for the arrays with the $6m^2$ heliostats. This structure is taller and steeper than the $6m^2$ arrays and, consequently is exposed to higher wind loads. However, the dead load available because of the size of the structure more than offsets overturning due to the lateral wind loads. The end result is that this concept is not subject to uplift forces for the loading cases considered. Because of the increased distance between the main sloping truss members, it was decided to use individual augered caissons. The distance separating

the main members and columns was also a reason the caissons were not connected together.

5.3 COMPUTER ANALYSIS PROCEDURE

As directed by the Task 4 Work Scope, the preliminary conceptual designs of the arrays with the preferred aspect ratio were to be developed in greater detail. The effect of substituting the 49 m^2 heliostats in place of the 6 m^2 heliostats for the 10 MWt array was also examined.

The modified structural concepts of the arrays were analyzed by using the STRUDL computer program (Reference 5-2), thus giving more detail than the preconceptual designs. STRUDL is an acronym for the Structural Design Language Program and consists of a series of computer programs for solving structural engineering problems. STRUDL was first developed at the Civil Engineering Systems Laboratory at the Massachusetts Institute of Technology.

STRUDL can analyze continuous mechanics problems and framed structures--which is the case of the UHA concepts. Framed structures are defined as two or three-dimensional structures composed of slender, linear members, which can be represented by their structural properties along a centroidal axis. Such a structure is composed of many members connected together at joints or nodes.

Input data for a particular analysis consists of:

- Geometry of the structure
- Topology of connectivity of the structure
- Member properties
- Boundary conditions

- Loading conditions

Geometry is specified by providing the coordinates of joints, and the topology by specifying the joint connections for each member or element. Properties of members may be provided in a number of ways, however, for this work the section properties of prismatic members were specified. Elastic constants for members and elements are also specified, so that different materials can be recognized. Force and displacement boundary conditions at support joints as well as end conditions for members must also be considered and specified for the structure being modeled. Any number of loading conditions may be considered, each consisting of any number and type of loads. Loads may act on members, elements, and joints and may have arbitrary orientation. Loading conditions may also be defined as consisting of linear combinations with prescribed factors of other loading conditions.

Output from STRUDL consists of member end forces and distortions, reactions and joint displacements, and member stresses and strains. Forces and stresses may be calculated at specified sections and may be compared among a number of loading conditions to produce force and stress envelopes.

All the structures analyzed by STRUDL for this study were run on the Bechtel in-house UNIVAC 1180 computer system.

For the STRUDL computer analyses, a typical interior frame of the UHA concept was modeled as a moment-resisting rigid frame. The large sloping truss which supports the heliostats was modeled as a beam with an equivalent bending stiffness. The columns and the struts were also modeled as

line elements. Since the foundations are expected to be rather flexible, pinned supports were assumed. A stiff, fixed foundation would require an expensive design treatment and so was not considered further.

Shown in Figure 5-6 and 5-7 are idealized computer models of the 1 MWt and 10 MWt arrays using the 6 m^2 heliostats. The slanting truss member of the arrays were modeled as a series of beams to obtain an accurate profile of the rotations along its length. The long columns and the horizontal struts of the arrays were also modeled as beams.

Shown in Figure 5-8 is an idealized computer model of the 10 MWt array using the 49 m^2 heliostats. Since this structure is higher and has a steeper slope than the array using the 6 m^2 heliostats, more bracing members were used. Numerous node points were defined along the members in this model to obtain an accurate profile of the rotations of the slanting truss and to check the lateral deflections of the columns.

Loadings for the analysis consisted of dead load weights of the heliostats, pedestals, and structural members as well as wind loads on the frame and the heliostats. Full wind intensities were applied on the heliostats and the slanting truss system. However, due to the probable shielding effect the heliostats would have on the structure, wind intensities on the columns were assumed to be somewhat reduced. For the wind blowing in a northerly direction, wind intensities applied to the columns were assumed to be two thirds of that on the truss. For the wind blowing in a southerly direction, full wind intensities were assumed to act on the columns.

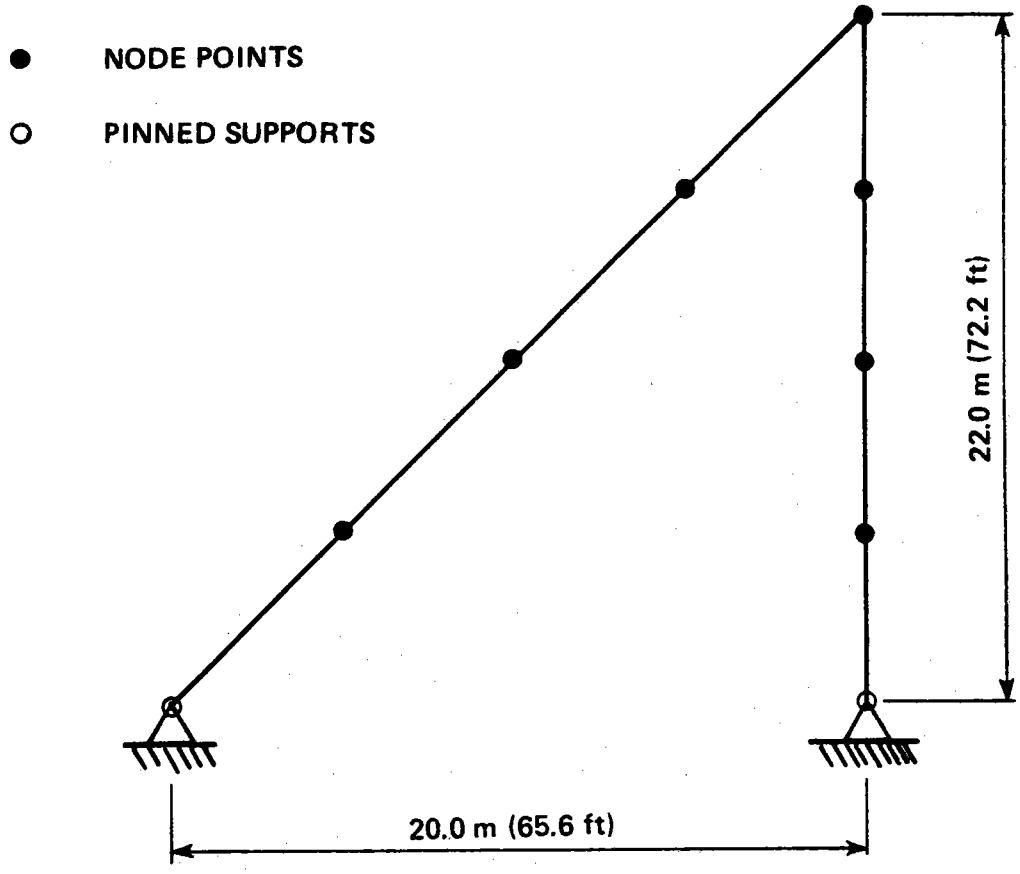

Figure 5– 6 Idealized Model for the 1 MWt Array with 6 m^2 Heliostat

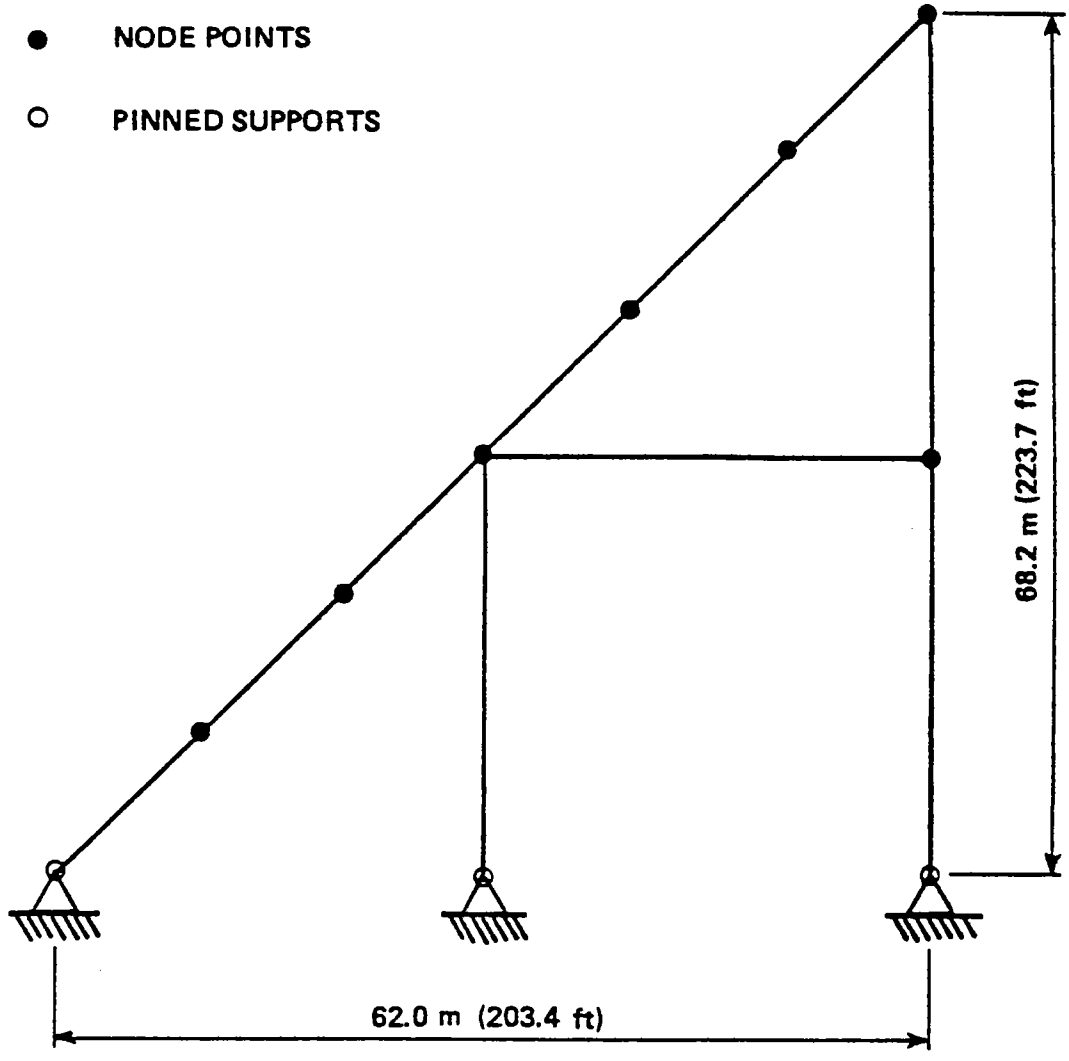

Figure 5–7 Idealized Model for the 10 MWt Array with 6 m^2 Heliostats

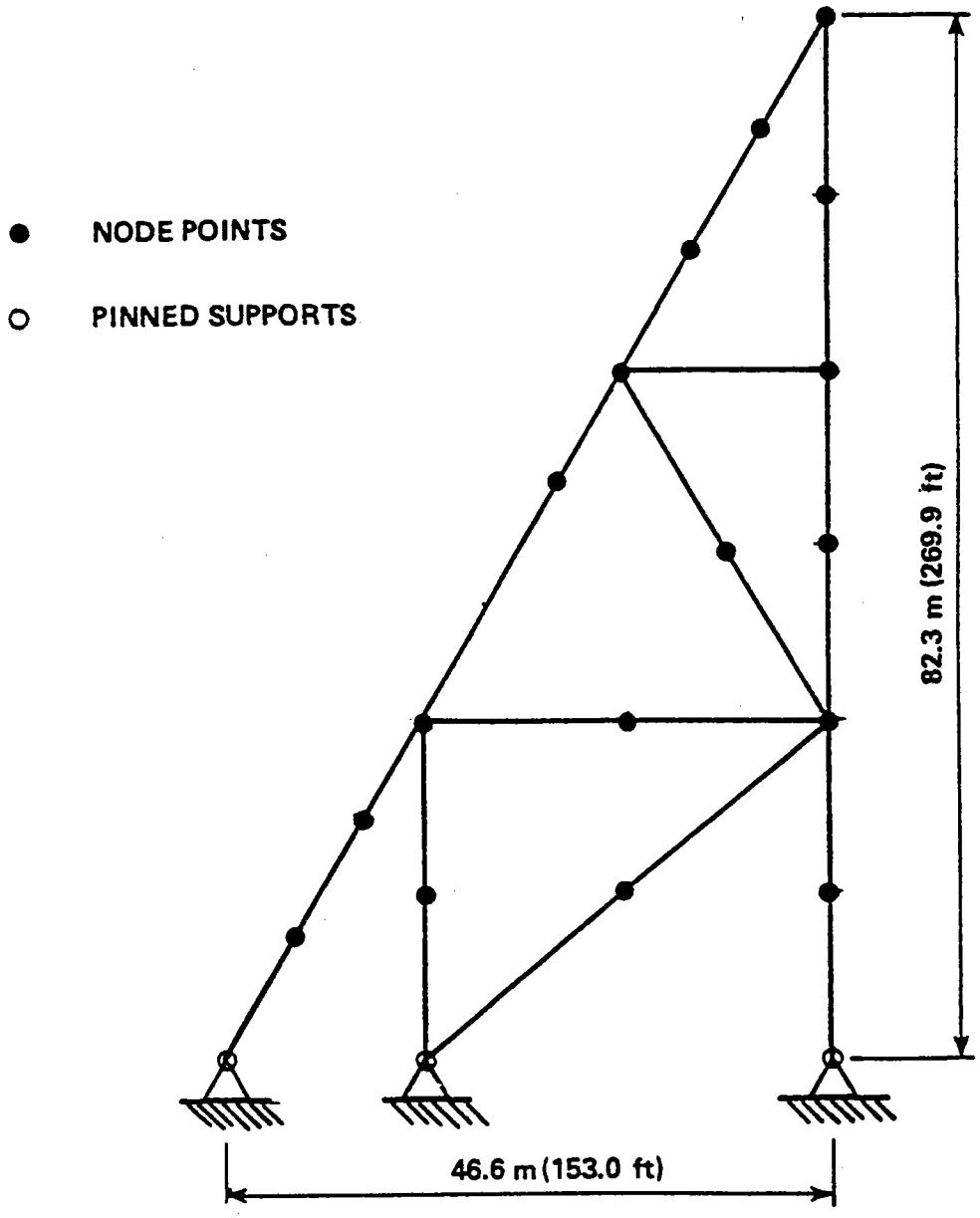

Figure 5–8 Idealized Model for the 10 MWt Array with 49 m^2 Heliostats

As explained in Section 2, to simplify the computer input wind forces were approximated as varying linearly with height of the structure. Shown in Figure 5-9 is a diagram of how the 25 MWt structure might appear. However, this array was not analyzed by STRUDL.

5.4 RESULTS OF ANALYSES

Computer results were given in terms of member stresses and rotations. Member stresses were checked against the allowable stresses but it was clear that these are generally low stress systems. The computer analysis could not check stability of members and so the array columns were manually checked against lateral buckling using the AISC interaction equation (Reference 5-3). This is applied where combined bending and axial forces occur using column loads from the analyses. For example, using A-36 steel, the buckling criteria for a column can reduce the allowable stress from 152 MPa (22 ksi) to as low as 27.5 MPa (4 ksi).

5.4.1 Arrays With $6m^2$ Heliostats

By checking the stresses from the analyses of the 1 and 10 MWt arrays by the AISC interaction equation, it was found that buckling criteria had the most influence on the design of the structures. The largest rotation, which is the sum of the local and structure rotations, of a heliostat at the top of the structure was 0.43 mrads for the 10 MWt array and 0.44 mrads for the 1 MWt array. This is well below the rotation limit of 1.5 mrads. This confirmed the efficiency of the design arrangement that was selected to reduce rotations .

Total steel quantities for the 1 and 10 MWt arrays and those estimated by extrapolation for the 25 MWt array are summarized in Table 5-1. By

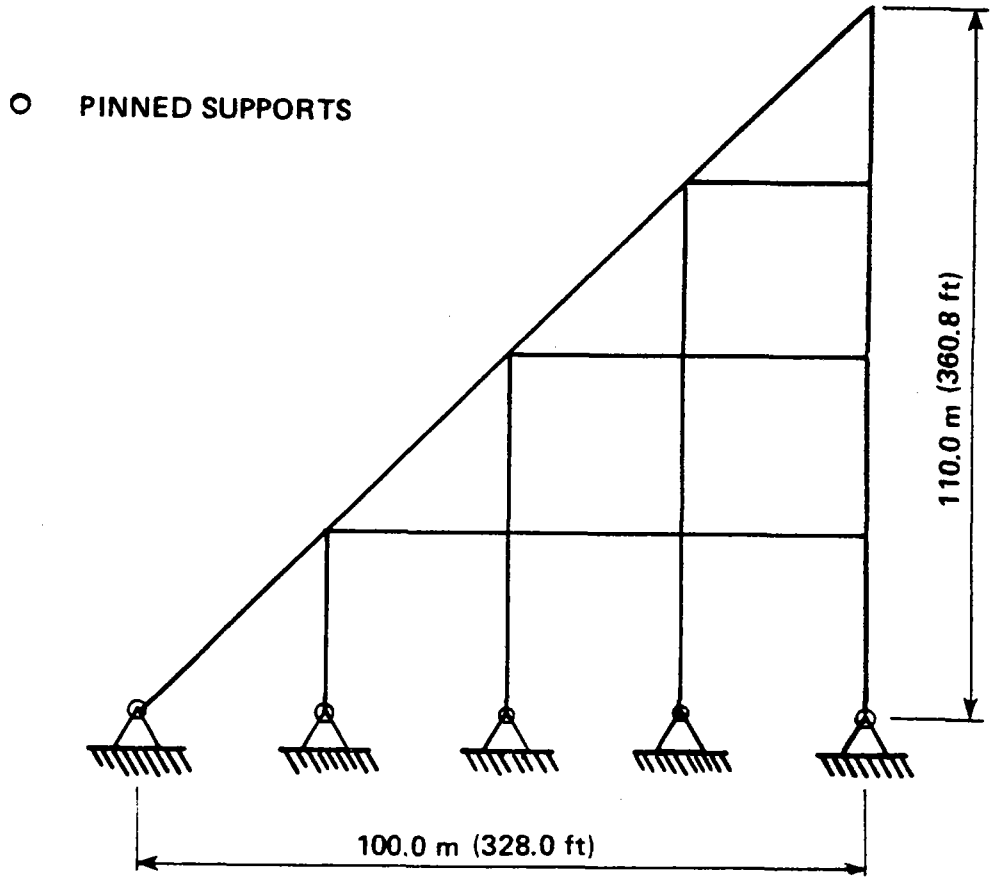

Figure 5–9 Diagram of the 25 MWt Array with 6 m^2 Heliostats

using structural optimization procedures, those quantities might be reduced. To account for bracing, access, walkways and ladders, an additional nominal twenty percent was added to the steel quantities.

5.4.2 Arrays With 49m^2 Heliostats

It was determined from the analysis of the 10 MWt array having the 49 m^2 heliostats that stresses within the members were well within the allowable. Using the approximate method described earlier for finding the torsional properties of the supporting space frame, the maximum rotation of a heliostat at the top of the array was about 1.7 mrads. This exceeds the criteria limit of 1.5 mrads. However, by increasing some member sizes in this particular space truss, the maximum heliostat rotation could easily be reduced to 1.5 mrads or less.

A summary of material quantities for this particular design are summarized in Table 5-2. Since the stresses in the members are well within the allowable, optimization of this structure could reduce these quantities.

5.5 COSTS ESTIMATES OF MODIFIED CONCEPTS

The results of the cost estimates for the more refined and detailed UHA structures are presented in this section. These estimates are shown in detail in Table 5-3 for four designs:

- A - 1 MWt array, 1:5 aspect ratio, 6 m^2 heliostat
- B - 10 MWt array, 1:5 aspect ratio, 6 m^2 heliostat
- C - 10 MWt array, 1:5 aspect ratio, 49 m^2 heliostat
- D - 25 MWt array, 1:5 aspect ratio, 6 m^2 heliostat

TABLE 5-1

MATERIAL QUANTITIES FOR ARRAYS
WITH 6 m^2 HELIOSTATS

Materials	Units	Power Level (MWt)		
		1	10	25**
Steel*	ton	156	4380	14255
Concrete	cubic yard	102	2121	5754
Rebar	ton	3	47	156

* Includes 20% for bracing and access
** Extrapolated quantities

TABLE 5-2

MATERIAL QUANTITIES FOR 10 MWt ARRAY
WITH 49 m^2 HELIOSTATS

Materials	Quantities
Steel*	4036 tons
Concrete	516 cubic yards
Rebar	8.3 tons

*Includes 20% for bracing and access

TABLE 5-3

CONCEPTUAL FIELD COST ESTIMATES

$ THOUSANDS -- SECOND QUARTER 1980

Configuration No.	A	B	C	D
Power Level	1 MWt	10 MWt	10 MWt	25 MWt
Aspect Ratio	1:5	1:5	1:5	1:5
Structure Height	72'	224'	270'	361'
Heliostat Size	6 m^2	6 m^2	49 m^2	6 m^2
No. of Heliostats	210	2046	252	5250
DIRECT FIELD COST*				
Heliostat Installation	100	940	150	2,420
Wiring	40	320	110	820
Access, Stairways	40	1,060	940	2,970
Foundation	40	690	150	1,890
Steel	290	7,690	6,650	23,900
DIRECT FIELD COST	510	10,700	8,000	32,000
INDIRECT FIELD COST **	160	2,780	1,760	8,100
FIELD COST	670	13,480	9,760	40,100
FIELD COST/MWt	670	1,348	976	1,604

*Second Quarter, 1980
Price & Wage Level

**60% of Direct Labor Cost

The field costs presented here considered the same work items as were presented in the cost estimates for the preconceptual designs. However, the direct field costs were examined in much more detail than those given in the preconceptual designs and considered these additional work items:

- o Heliostat installation
- o Access, stairways
- o Wiring

The indirect field costs were still taken as 60% of the direct field costs. The total capital cost estimates are presented in Table 5-4.

Maintenance costs were also considered and include:

- o Heliostat mirror cleaning
- o Wiring system checking
- o Replacement of heliostat control wiring
- o Routine maintenance and miscellaneous items

Since the proposed site is in a desert environment, it was assumed that painting of the structure would not be required.

Bechtel's previous studies for ground mounted arrays has found annual maintenance costs of $0.90 per square meter of heliostat area. Due to the height requirements of the UHA structures, a maintenance cost of $1.25 per square meter was assumed.

Based on this data and a 30-year plant life, the life cycle maintenance costs of these four designs were estimated to be:

- o A - $60,000

TABLE 5-4

CAPITAL COST ESTIMATE SUMMARY

$ THOUSANDS -- SECOND QUARTER 1980

Configuration No.	A	B	C	D
Power Level	1 MWt	10 MWt	10 MWt	25 MWt
Aspect Ratio	1:5	1:5	1:5	1:5
Structure Height	72'	224'	224'	270'
Heliostat Size	6 m^2	6 m^2	49 m^2	6 m^2
No. of Heliostats	210	2046	252	5250
Field Cost	670	13,480	9,760	40,100
Engineering Services	130	1,320	990	3,900
Subtotal	800	14,800	10,750	44,000
Allowance for Uncertainity @ 15% of Subtotal	120	2,200	1,750	6,500
TOTAL CAPITAL COST	920	17,000	12,500	50,500
CAPITAL COST/MWt	920	1,700	1,250	2,020

- B - $480,000
- C - $480,000
- D - $1,200,000

The salvage values of these four arrays based on a 30-year plant life were determined to be:

- A - $0
- B - $140,000
- C - $120,000
- D - $435,000

The salvage values of these structures were considered and are dependent upon the need of the steel market during that particular period. Salvage values ranged from $0/ton to $50/ton of steel.

Labor costs for design A, the smallest array, were so high that it was not cost effective to salvage it. This cost data was transmitted to Veda Inc. for their use in assessing the cost of delivered energy from the Unified Heliostat Array concept.

Section 6

CONCLUSIONS AND RECOMMENDATIONS

The capital costs of the 10 MWt arrays having the 6 m^2 heliostats were found to be about one third more than the arrays having the 49 m^2 heliostats. This was due to an increase in the foundation, steel, and heliostat installation costs. However, it is felt that the costs of both concepts could be made more comparable by reducing the steel tonnages and foundation quantities, by means of structural optimization and more detailed soils criteria.

It was determined that the modified structural concepts developed in Task 4 did indeed reduce steel tonnages for the arrays having the preferred aspect ratio. The amount of steel in the conceptual estimates considered other quantities such as bracing and access which were not considered in the preconceptual designs. However, in the more detailed analyses, the foundation quantities also increased significantly for the modified structural designs compared with those computed for the preconceptual designs due to a better definition of loadings.

By attaching the 6 m^2 heliostats directly to the main frames, the rotation criteria of 1.5 mrads did not have a significant influence in their design. However, other low-cost arrangements may require the use of more flexible heliostat support arrangements which can lead to higher rotations than the chosen design.

The rotation criteria was more significant in the designs of the arrays

having the 49 m^2 heliostats placed on truss members spanning between the main frames. This was because the larger heliostats caused large torsional forces in their supports.

This study confirmed that increased UHA height is accompanied by substantial increases in steel tonnages and unit costs. The tallest structures, the 25 MWt power arrays, are substantially heavier and have higher costs per MWt those systems of lower power generation and hence with lower heights. The lowest cost per MWt and lightest UHA structures are associated with the least-height arrangement for a given power level.

Some designers may seek further reductions in steel tonnage by increasing the allowable stresses. However this study confirmed that most members, already lighweight and slender, are governed by stability conditions rather than by allowable stresses. Thus a further reduction in steel tonnage could only be achieved by reducing the safety margins to buckling failure of the structural members. The increased risk associated with this would require careful design consideration and economic evaluation.

The following recommendations for further work were identified from this study:

- Perform more extensive structural optimization. Even though these structures are lightweight and within the realm of low cost, optimization by means of changing geometrically and quantitatively the members and foundations might still lower the costs.

- Perform a site wind investigation for a prototype to provide better wind design criteria. Since wind had the most influence on these designs, this might provide significant reductions in the design forces on the structures.

- Perform site soils investigation for a prototype in order to develop better design criteria for the foundations. Foundations may be varied across the plan of the UHA to achieve a least cost system.

Section 7

REFERENCES

2-1 Specification for the Unified Heliostat Array, by Veda Incorporated, Veda Report 43342-80U/P0069, March 19, 1980.

2-2 Standard Specification for Highway Bridges, American Association of State Highway Officials, Eleventh Edition, 1973.

2-3 Soil and Foundation Investigation Report, 5MW STTF, Sandia Labs.

2-4 "Wind Forces on Structures", ASCE Paper No. 3269, Transactions, American Society of Civil Engineers, Vol. 126, Part II, 1961.

2-5 Building Code Requirements for Minimum Design Loads in Buildings and Other Structures, A58.1-1972, American National Standards Institute, Inc.

2-6 Uniform Building Code, The International Conference of Building Officials, 1979.

3-1 "Solar Thermal Power Generation System in Japan", by the Sunshine Project Operation Bureau, Electric Power Development Co., Ltd., July 1979.

3-2 "Welded Construction Makes Shea Stadium Convertible Sports Center", Modern Welded Structures, Selections from Volume I and II, James F. Lincoln Arc Welding Foundation, 1965.

3-3 "Giant Trusses Span Jai-Alai Fronton", Modern Steel Construction, American Institute of Steel Construction, Volume XVII/Number 1 & 2, First & Second Quarter, 1977.

3-4 "Steel Skylight Spans Stepped Studio", Modern Steel Construction, American Institute of Steel Construction, Volume XIII/Number 1, First Quarter 1973.

4-1 Timber Construction Manual, American Institute of Timber Construction, 2nd Edition, 1974, Wiley-Interscience.

4-2 Building Code Requirements for Reinforced Concrete, ACI 318-77, American Concrete Institute.

4-3 Specification for the Design of Cold-Formed Steel Structural Members, American Iron and Steel Institute, 1968 Edition.

4-4 Specification for the Design, Fabrication, and Erection of Structural Steel for Buildings, American Iron and Steel Institute, 7th Edition, 1970.

5-1 Blodgett, Omar. W., Design of Welded Structures, James F. Lincoln Arc Welding Foundation, 1966, section 2.10.

5-2 "ICES STRUDL II, The Structural Design Language", Engineering User's Manual, Volume I, Frame Analysis Department of Civil Engineering Massachusetts Institute of Technlogy, First Edition, November 1968.

5-3 Manual of Steel Construction, American Institute of Steel Construction (AISC), 7th Edition, 1969, Section 1.6.1.

APPENDIX C

VEDA REPORT 44112-80U/Q0401-3

METHODOLOGY FOR OPTICAL PERFORMANCE ANALYSIS

Prepared by:

VEDA INCORPORATED
400 N. Mobil, Bldg. D
Camarillo, CA 93010

7 November 1980

Prepared for:

Internal Veda Document

TABLE OF CONTENTS

LIST OF ILLUSTRATIONS

SECTION 1.0

VECTOR ANALYSIS CONCEPTS USED IN SOLUTION

1.1 Notation Conventions

The notation conventions to be used throughout this report are as follows:

1. Scalar values are represented by lower case letters, (e.g. t,z,w).

2. Vectors are represented by a capital letter with a line over it. An optional character subscript is used when differentiating like attributes from different heliostats. A numeric subscript refers to that component of the vector and is therefore a scalar, (e.g. $\overline{A}$, $\overline{B}$, $\overline{P}_i$, $\overline{P}_j$, V_3)

3. Unit vectors are represented in a similar fashion to vectors with the exception that an inverted "V" is placed over the character (e.g. $\hat{S}$, $\hat{V}_j$)

4. Magnitude of a vector is represented by vertical lines on either side (e.g. $|\overline{A}|$, $|\overline{P}_k|$).

1.2 Dot Product

The dot product of two vectors (also known as the scalar product and the inner product) is computed by summing the products of the like components of the vectors and is equal to the product of the magnitudes of the vectors and the cosine of the angle between them.

$$\overline{A} \cdot \overline{B} = A_1 B_1 + A_2 B_2 + A_3 B_3 = |\overline{A}| \, |\overline{B}| \cos \omega$$

Note that when the vectors are perpendicular, the cosine of the angle between them is zero so the dot product of perpendicular vectors is zero. Mathematically, the dot product commutes, associates, and distributes.

1.3 Cross Product

The cross product of two vectors (also known as the vector product) defines a vector that is normal to the plane containing the the original vectors. The direction of the resultant can be found by using the right hand rule. The components are:

$$\overline{A} \times \overline{B} = (A_2 B_3 - A_3 B_2, A_3 B_1 - A_1 B_3, A_1 B_2 - A_2 B_1)$$

The magnitude of the cross product is equal to the product of the magnitudes of the two vectors and the sine of the angle between them.

$$|\overline{A} \times \overline{B}| = |\overline{A}| \ |\overline{B}| \ \sin \omega$$

Note that the magnitude is equal to the area of the parallelogram whose sides are defined by the vectors $\overline{A}$ and $\overline{B}$. The cross product associates and distributes, but anti-commutes.

(i.e. $\overline{A} \times \overline{B} = -\overline{B} \times \overline{A}$)

1.4 Bisector of Angle Between Two Vectors

We will need to find a vector that bisects the angle between two non-colinear vectors. It can be shown that a vector lying along the bisector of the angle formed by two other vectors is the sum of the unit vectors along the two vectors. Given unit vectors $\hat{A}$ and $\hat{B}$, the vector $\overline{C}$ will bisect $\hat{A}$ and $\hat{B}$ if we define $\overline{C}$ as:

$$\overline{C} = \hat{A} + \hat{B}$$

1.5 Vector Representation of Line

The vector representation of a line is equivalent to a parametric representation in that we use a known point on the line and its direction to define any point on the line. (Note that the coordinates of a point in space can be also interpretted as a vector from the origin to that point).

$\overline{Q} = \overline{P} + t\,\overline{D}$

$\overline{Q}$ is any point on line

$\overline{P}$ is known point on line

$\overline{D}$ is direction of line

t is a scalar multiplier, can be any real number

Any point, $\overline{Q}$, on the line will have a unique value of t.

1.6 Vector Representation of Plane

The vector representation of a plane involves, as with the line, knowledge of two vectors. Since all points in the plane relative to a known point on the plane should be perpendicular to the normal, we write:

$(\overline{Q} - \overline{P}) \cdot \overline{N} = 0$

$\overline{Q}$ is any point on plane,

$\overline{P}$ is known point on plane,

$\overline{N}$ is normal vector to plane.

This reduces to the familiar equation of a plane if one substitutes components for the vectors and simplifies.

SECTION 2.0

COORDINATE SYSTEMS

Two systems of coordinates are used in this model. The first is a right-handed cartesian system oriented to the local tangent plane with origin at some reference point fixed to the site of the UHA. Since the conventional architectural plans are in this system, our model of the positions of the individual mirrors and the focal point of the receiver are conveniently expressed in it (see Figure 2-1). The second system is equatorial, so named because it simplifies the apparent motion of the celestial sphere caused by earth's axial spin to rotation about one axis of the coordinate system. This system is convenient for expressing the direction of the sun and, since the mirrors of the array are mounted equatorially, it can also be used for the spatial orientation of the mirror.

2.1 Horizon Coordinates

In the plan coordinates (astronomical terminology calls this "horizon coordinates"), the positive X_H axis is designated as east, the positive Y_H axis is north, and the positive Z_H axis straight up toward the zenith. The axes X_H and Y_H define the local tangent plane. The origin of coordinates is commonly specified at or near the local ground level vertically displaced from the center of the nominal focal zone of the heliostat array. However, the equations to be developed will not make this assumption for the sake of generality.

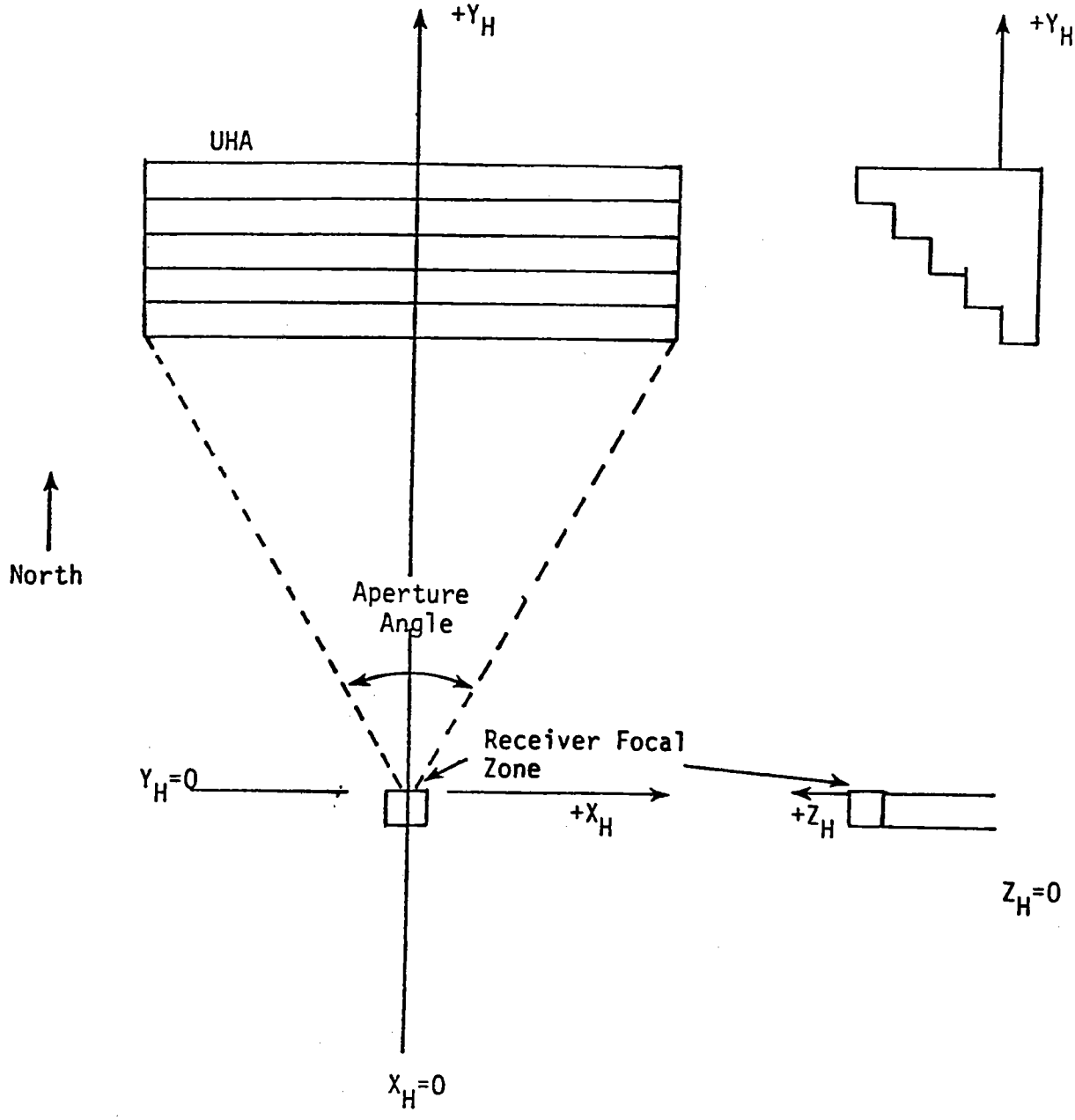

Figure 2-1. Layout of a UHA Central Power System in Horizon Coordinates.

2.2 Equatorial Coordinates

The equatorial system is oriented to the celestial sphere. The positive Y_E axis is directed toward the north pole of the celestial sphere. The positive X_E axis is situated such that it is parallel to the X_H axis at local noon. The Z_E axis is then defined from the right hand rule.

2.3 Relation Between Horizon and Equatorial Coordinates

The relation between the orientation of these two systems reduces to two rotations. One compensates for the angular difference between the horizon plane Y_H and the polar axis Y_E and is a rotation about X_E through an angle equal to the latitude of the site of the UHA. The other rotation is around Y_E and compensates for the earth's axial spin, which is assumed to be 15° per hour for the purpose of this study.

The development of this model only used the equatorial system for expressing the direction cosines of the sun. The relationship of the two systems is then used to transform this vector into the horizon system.

SECTION 3.0

DETAILS OF SOLUTION

3.1 Flowchart of Optical Performance Model

The general flow of the simulation model is illustrated in Figure 3-1. A description of each block will be given below using the number in the upper right hand corner of each block for reference.

1. Since the essence of this simulation is to model events as a function of time, the fundamental driver of the algorithm is time of both year and day. These inputs are required both to position the sun relative to the UHA and select the appropriate insolation data.
2. The solar declination is computed from the time of year. The direction of the sun at a given time of day is then computed. (Section 3.2)
3. Each of the following steps 4 through 10 will be performed for each heliostat in the subject UHA. The amount of energy delivered to the receiver by this heliostat will be summed over all heliostats for total energy. This particular heliostat will be henceforth generally referred to as the jth heliostat.

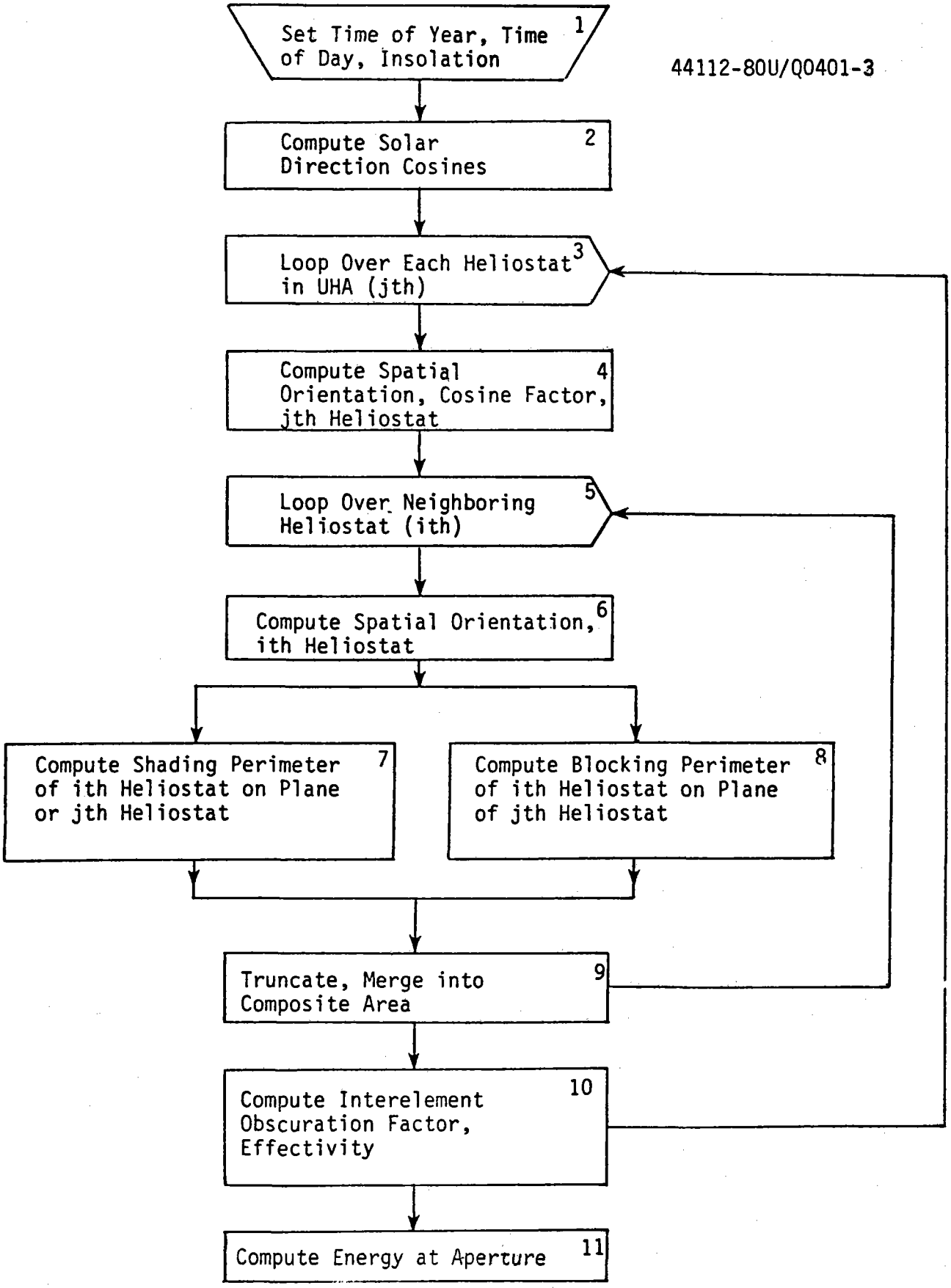

Figure 3-1. Flowchart of Optical Performance Model.

4. Knowing the location of the jth heliostat, the location of the desired focal point on the receiver, and having computed the solar direction in step 2, the spatial orientation of the mirror to accomplish the desired reflection can be computed. (Section 3.3) Knowing the spatial orientation of the heliostat, the cosine factor can be readily computed.
5. We desire to check for all shading and blocking of the heliostat. The contributions to shading and blocking of this particular heliostat by all other heliostats in the array could be evaluated and we would be assured of never missing any. That technique would be extremely wasteful of computer time and not very realistic. Some small subset of the array in the neighborhood of the jth heliostat is all that is required. Steps 6 through 9 will be executed for each heliostat, henceforth referred to as the ith heliostat, in the vicinity the jth heliostat.
6. This step is analogous to Step 4 in the computing of the spatial orientation of the ith heliostat.
7. Points on the perimeter of the shadow of the ith heliostat in the plane of the jth heliostat are computed. (Section 3.4).

8. Points on the perimeter of the area blocked by the ith heliostat in the plane of the jth heliostat are computed. (Section 3.5).

9. The actual area shaded or blocked is generated by truncating the perimeters computed in Steps 7 and 8 to only that area within the physical boundaries of the jth heliostat. This new area is checked against all other areas previously mapped on the jth heliostat so that only the additional area shaded or blocked is added to the total obscured area. (Section 3.6).

10. The total obscured area on the face of the jth heliostat is now known. Compute the power at the aperture contributed by the jth heliostat, using the formula:

$$E_j = Af_c f_r (f_s + f_b - 1) f_t I$$

where E_j is power delivered to aperture by heliostat j

A is surface area of heliostat j,

f_c is cosine factor,

f_s is shading factor,

f_r is heliostat reflectance factor,

f_b is blocking factor,

f_t is atmospheric transmittance factor,

and I is the insolation for the time and day in question.

11. Sum powers for the total energy at the aperture.

To compute daily energies and yearly energies, steps 1 through 11 should be exerised for sunlight hours of each day of the year. To reduce execution time, a sample of days and symmetry are used.

3.2 Solar Direction

The orbit of the earth about the sun is slightly elliptical. In a time measurement system based on constant time divisions, such as the current standard atomic clocks, the length of the day varies as the earth moves along the orbit. Consequently, the time of meridian passage of the sun deviates from the local fixed scale time by as much as 16.5 minutes. For the calculations of performance required here, the assumption of a circular orbit and a 24 hour day, during which meridian passage occurs at 1200, provide a suitable accuracy.

If an actual pointing direction command for a heliostat were required and a fixed rate clock were to be used, then a full implementation of the equation of time would be required. Additionally, corrections for atmospheric bending would be required for the pointing direction command, as these alone may amount to sufficient error to direct a heliostat off the receiver aperture location.

There are three steps to the computation of solar direction cosines. The sun's declination in the equatorial system is computed from the time of year. The sun's direction cosines in the equatorial system are found from the time of day. Finally, the sun's direction cosines are computed in the horizon system.

The declination of the sun, i.e., its apparent plane of constant latitude as the earth rotates on its axis, varies during the year due to tilt of the earth's axis of rotation with respect to the ecliptic (the plane of the earth's orbit about the sun) and the position of earth in its orbit. The model for computing the declination in the equatorial system uses a sinusoid with amplitude equal to the tilt of the earth's axis to the ecliptic, 23.45°. The positive peak corresponds to the summer solstice, the negative peak to the winter solstice, and each axis crossing to the corresponding equinox. Time of year then can be converted to an angle and the declination computed (see Figure 3-2).

The solar direction cosines are evaluated by a rotation about the Y_E axis by an angle computed from the time of day. True local time, in which sun passage of the local meridian is 1200, or noon, is used. At noon, the direction cosines of the solar directtion in the equatorial system are:

(0, sin D, cos D) ; where D is the solar declination

Based on the assumption of a 24 hour day, the earth's rotation rate is 15° per hour. The angle that we rotate through is then (180-15H), where H is the 24 hour clock time of day in hours, local time. We compute the solar direction cosines in the equatorial system as:

$$\begin{pmatrix} \cos(180-15H) & 0 & \sin(180-15H) \\ 0 & 1 & 0 \\ -\sin(180-15H) & 0 & \cos(180-15H) \end{pmatrix} \begin{pmatrix} 0 \\ \sin D \\ \cos D \end{pmatrix} = \begin{pmatrix} \sin(180-15H)\cos D \\ \sin D \\ \cos(180-15H)\cos D \end{pmatrix}$$

Figure 3-2. Projection of Ecliptic on Celestial Sphere.

The last step is to compute the solar direction cosines in the horizon system. This entails a rotation about the X_E axis by an angle equal to the latitude of the site.

$$\begin{pmatrix} 1 & 0 & 0 \\ 0 & \cos L & -\sin L \\ 0 & \sin L & \cos L \end{pmatrix} \begin{pmatrix} \sin(180-15H)\cos D \\ \sin D \\ \cos(180-15H)\cos D \end{pmatrix}_E = \begin{pmatrix} \sin(180-15H)\cos D \\ \cos L\sin D - \sin L\cos(180-15H)\cos D \\ \sin L\sin D + \cos L\cos(180-15H)\cos D \end{pmatrix}_H$$

After using trigonemetric identities to reduce this result, the direction cosines of the sun in the horizon system are:

$$\hat{S} = \begin{pmatrix} X \\ Y \\ Z \end{pmatrix}_H = \begin{pmatrix} \sin(15H)\cos(D) \\ \cos(L)\sin(D) + \sin(L)\cos(15H)\cos(D) \\ \sin(L)\sin(D) - \cos(L)\cos(15H)\cos(D) \end{pmatrix} \quad \text{(equation 1)}$$

The azimuth and elevation angles are computed by

$$A = \arctan(X_H/Y_H), \text{ in four quadrants}$$

$$E = \arctan\left(Z_H/\sqrt{X_H^2 + Y_H^2}\right)$$

The time of sunrise can be computed by setting the Z_H term to zero and solving for H.

$$H = \frac{1}{15} \text{ arccosine } \left[\tan(L)\tan(D)\right]$$

The arccosine in this expression is assumed to be in degrees.

3.3 Spatial Orientation of a Heliostat

The question to be discussed in this section is how we position the heliostat such that it will reflect sunlight toward the focal zone of the receiver. We assume that the position of both the receiver aim point and the pivot point of the heliostat mirror are known in the horizon system. We also know the direction cosines of the sun from equation 1 and assume them to be constant over the entire array.

If the mirror is directed such that its normal bisects the angle between the sun's line of sight and the direction to the aim point of the receiver, it can be shown that the sun's incoming energy will reflect off the mirror into the receiver aperture using geometric optics.

Let $\overline{P}_i$ denote the position of the pivot point of the ith heliostat, $\overline{C}$ denote the nominal aim point at the receiver plane, and $\hat{S}$ denote the solar direction cosines previously derived (equation 1), all vectors being in the horizon coordinate system. Then the unit normal to the ith heliostat, $\hat{N}_i$, will be

$$\hat{N}_i = \frac{\hat{Q} + \hat{S}}{|\hat{Q} + \hat{S}|} \quad ;\text{where } \hat{Q} = \frac{\overline{C} - \overline{P}_i}{|\overline{C} - \overline{P}_i|} \qquad \text{(equation 2)}$$

which is the normalized sum of the unit vectors toward the sun and toward the receiver.

The effective solar energy interception area of the heliostat is that area which it projects on the plane perpendicular to the direction

of the sun. This area is equal to the actual area of the heliostat multiplied by the cosine of the angle between the normal to the heliostat and the vector directed from the heliostat toward the sun. This angle is sometimes referred to as the "half angle" since its magnitude is one-half the angle between incident and reflected rays. This cosine factor can be computed by

$$f_{ci} = \hat{S} \cdot \hat{N}_i \qquad \text{(equation 3)}$$

where f_{ci} indicates the cosine factor of the ith heliostat.

Now that the direction of the normal is known, we can compute how the heliostat must be "rolled" about the polar axis, and "pitched" about the declination axis to bring the normal of the mirror to its desired direction. These values are not required for this analysis, but for completeness sake, we will derive them since they are the independent controllable variables, were we designing a control system for a UHA. Also the vectors defining spatial orientation will be needed later.

Defining the "semi-major" axis of the ith heliostat (the declination axis) as $\bar{X}_i$ and the "semi-minor" axis as $\bar{Y}_i$, our problem is to computed these vectors (See Figure 3-5). We shall treat the shape of all mirrors used in this model as rectangular plates. This assumption is sufficiently accurate for our purposes given the large radii of curvature when compared to the mirror dimension.

The design of the heliostat mounting is such that the polar axis is aligned to equatorial north and the declination axis is perpendicular to the polar axis. For an altazimuth mounting, the azimuth axis is aligned

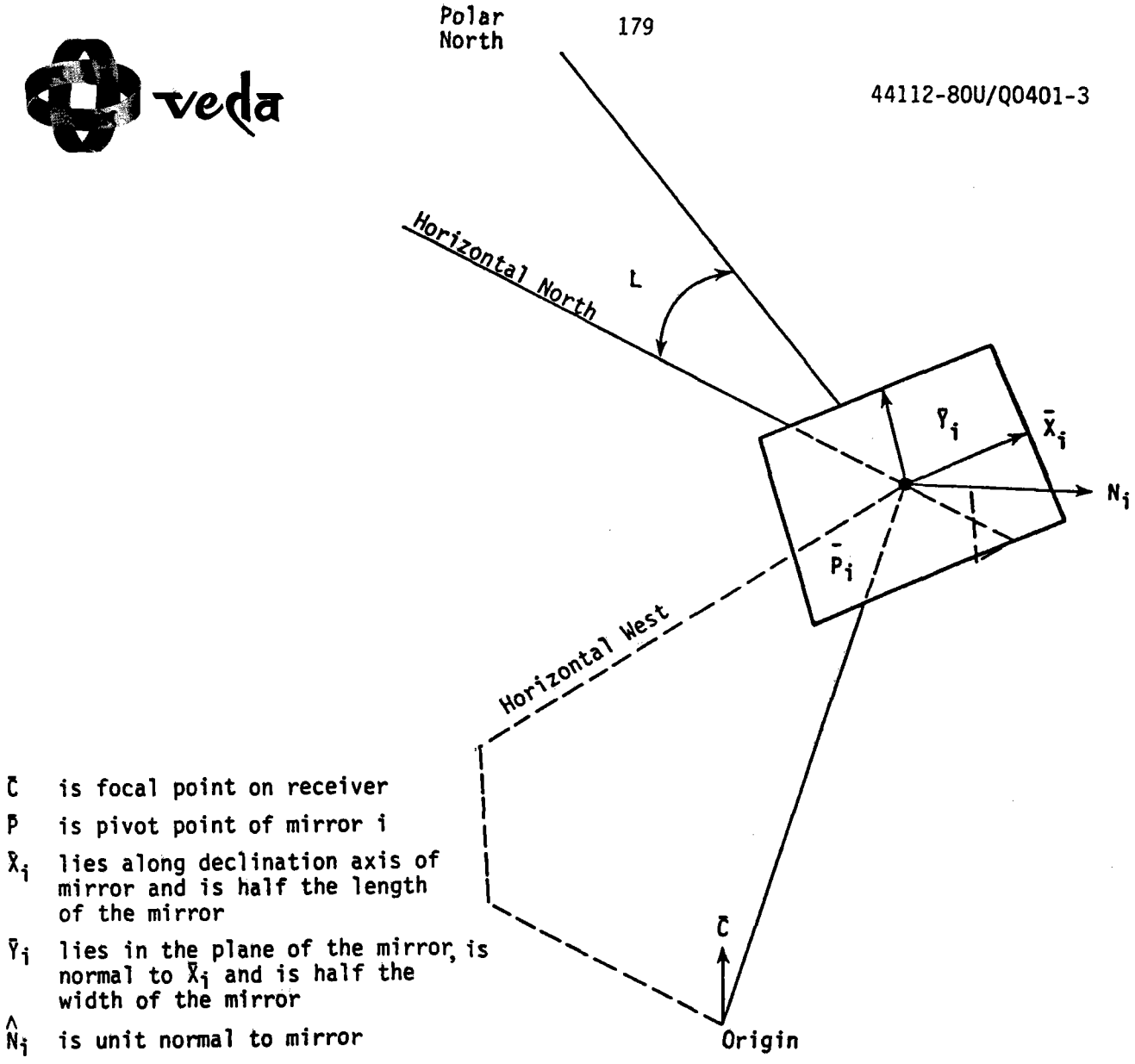

$\bar{C}$ is focal point on receiver

$\bar{P}$ is pivot point of mirror i

$\bar{X}_i$ lies along declination axis of mirror and is half the length of the mirror

$\bar{Y}_i$ lies in the plane of the mirror, is normal to $\bar{X}_i$ and is half the width of the mirror

$\hat{N}_i$ is unit normal to mirror

Figure 3-3. Geometry of Heliostat Parameters Used in Methodology.

to the horizon system vertical and the declination axis is perpendicular to the azimuth axis, lying in the horizontal plane.

To take advantage of the generality of this solution, we define a unit vector, $\hat{Z}$, to represent the "characteristic" axis of either mounting. In horizon coordinates, the vector will be

$$\hat{Z} = \begin{cases} (0, \cos L, \sin L), & \text{for an equatorial mounting} \\ (0, \quad 0, \quad 1), & \text{for an altazimuth mounting} \end{cases}$$

where L is the latitude of the site.

Since $\bar{X}_i$ coincides with the declination axis, $\bar{X}_i$ is perpendicular to $\hat{Z}$. Also, $\bar{X}_i$ lies in the plane of the mirror and so must be perpendicular to the mirror normal $\hat{N}_i$. A vector perpendicular to both $\hat{Z}$ and $\hat{N}_i$ will lie along the cross product of those vectors. Letting the desired length of $\bar{X}_i$ be denoted by x_m, we get

$$\bar{X}_i = \frac{x_m \ \hat{Z} \times \hat{N}_i}{|\hat{Z} \times \hat{N}_i|} \qquad \text{(equation 4)}$$

deliberately choosing the sequence $\hat{Z}$ cross $\hat{N}_i$ to yield $\bar{X}_i$ in the direction shown in Figure 3-3. In an analogous fashion, we note that $\bar{Y}_i$ must be perpendicular to both $\hat{N}_i$ and $\bar{X}_i$, hence:

$$\bar{Y}_i = \frac{y_m \ \hat{N}_i \times \bar{X}_i}{|\hat{N}_i \times \bar{X}_i|} \qquad \text{(equation 5)}$$

It is convenient for visualizing the heliostat orientation to reduce the $\overline{X}_i$ and $\overline{Y}_i$ vectors to a roll and pitch angle. Defining roll and pitch as in Figure 3-4, we can compute them by

$$\text{Pitch} = \arccos\left(\frac{\hat{Z} \cdot \overline{Y}_i}{y_m}\right)$$

$$\text{Roll} = \pm \arccos\left(\frac{X_{i1}}{x_m}\right) \qquad \begin{array}{l} + \text{ if } Y_{i1} > 0 \\ - \text{ if } Y_{i1} < 0 \end{array}$$

3.4 Shading Of One Heliostat By Another

We now wish to compute the shadow of one heliostat on another (see Figure 3-5). This will be accomplished in two steps. The first step will be to find the corners of the shadow of the ith heliostat on the infinite plane containing the jth heliostat. The second will be to truncate the shadow polygon to the actual boundaries of the jth heliostat.

Using our previous definitions of the vectors $\overline{P}$, $\overline{X}$, and $\overline{Y}$, the coordinates of the corners of the ith heliostat can be computed by

$$\overline{A} = \overline{P}_i + f_1\overline{X}_i + f_2\overline{Y}_i, \quad \text{where } f_1, f_2 = \begin{pmatrix} 1,1 \\ -1,1 \\ -1,-1 \\ 1,-1 \end{pmatrix}$$

This $\overline{A}$ is a point through which the edge of the shadow passes. Since the shadow will project along the reverse direction of the sun's direction, we form the vector equation of any point, $\overline{Q}$, on the line along the shadow extremity.

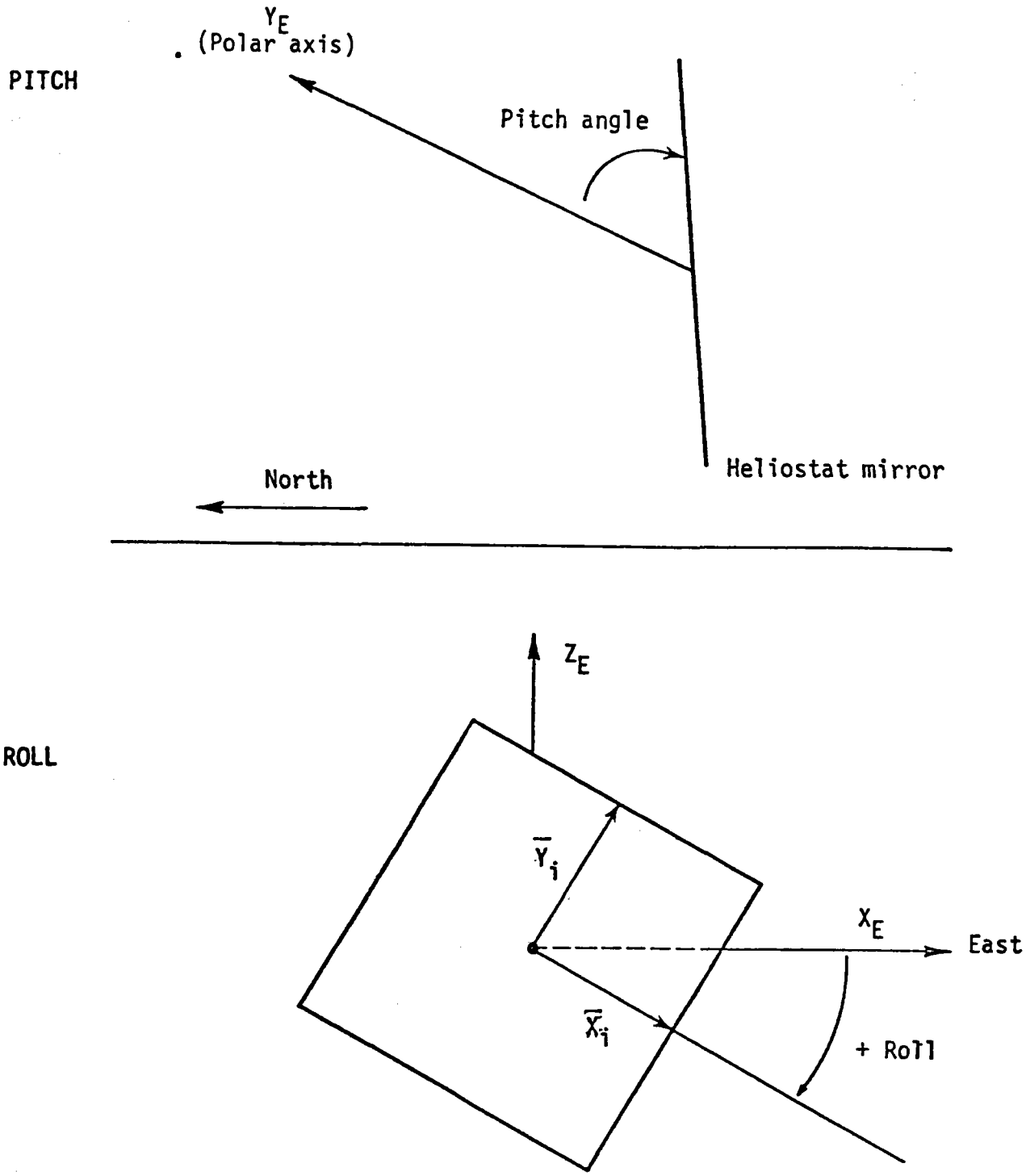

Figure 3-4. Roll and Pitch of Heliostat Mirror.

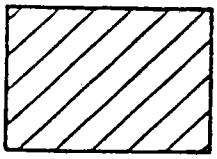

Shadowing area on infinite plane containing heliostat j

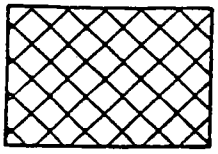

Area actually shaded by heliostat i

44112-80U/Q0401-3

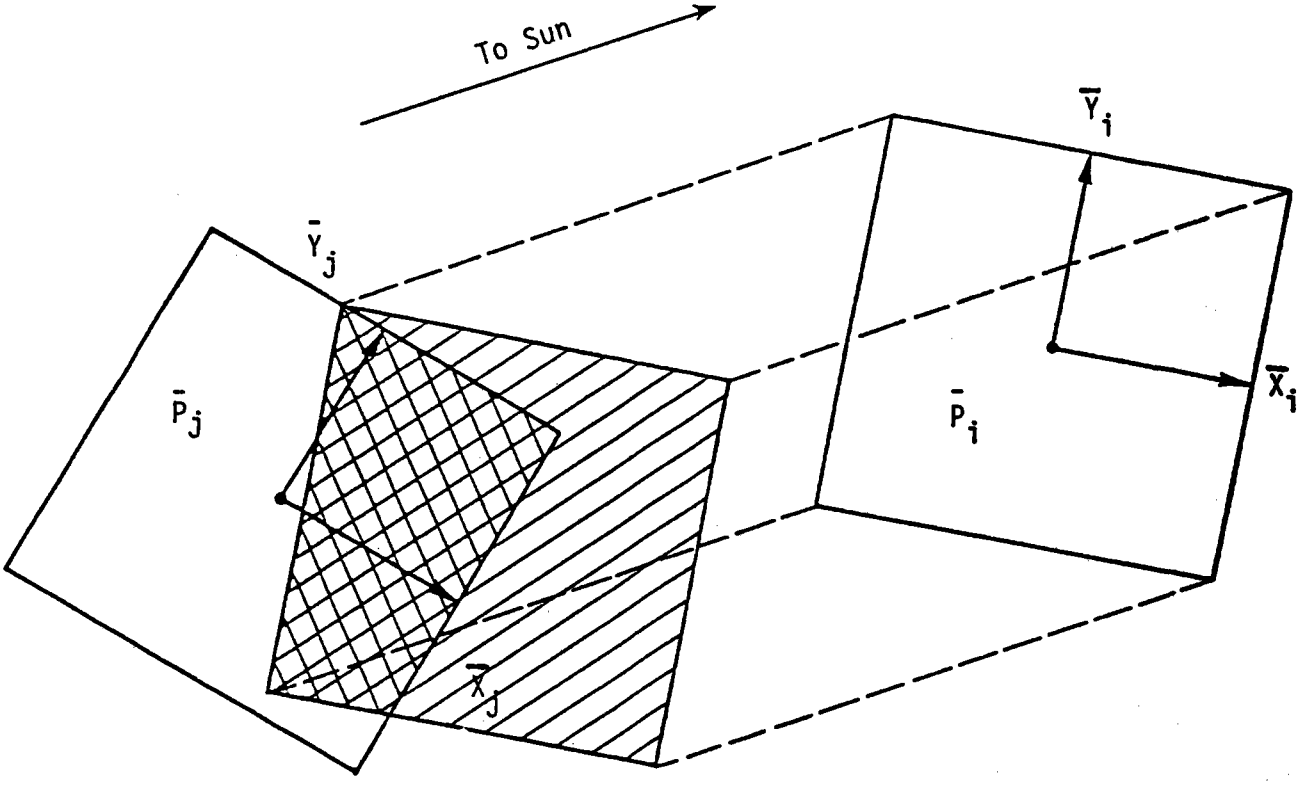

Figure 3-5. Geometry of Heliostat Shading.

$$\overline{Q} = \overline{A} - t\hat{S} = \overline{P}_i + f_1\overline{X}_i + f_2\overline{Y}_i - t\hat{S},$$

where t is real.

To compute the intercept of this line with the plane containing the jth heliostat, we find the particular value of t, r, which will satisfy the equation of the jth plane.

$$(\overline{Q} - \overline{P}_j) \cdot \hat{N}_j = 0$$

or

$$\left[(\overline{P}_i + f_1\overline{X}_i + f_2\overline{Y}_i - r\hat{S}) - \overline{P}_j\right] \cdot \hat{N}_j = 0$$

Solving for r,

$$r = \frac{\overline{P}_i \cdot \hat{N}_j + f_1\overline{X}_i \cdot \hat{N}_j + f_2\overline{Y}_i \cdot \hat{N}_j - \overline{P}_j \cdot \hat{N}_j}{\hat{S} \cdot \hat{N}_j} \qquad \text{(equation 6)}$$

Two constraints must be imposed on r to guarantee a physically meaningful solution. The value of r must be greater than zero for the shadow to really exist since a shadow cannot be thrown toward the illumination source. The term $\hat{S} \cdot \hat{N}_j$ must be greater than zero, or the shadow falls on the back or edge of the jth heliostat. This second condition is unlikely to occur. We then compute the intersection point, $\overline{I}$, as

$$\overline{I} = \overline{P}_i + f_1\,\overline{X}_i + f_2\,\overline{Y}_i - r\hat{S}.$$

We note that all of the dot products are constant for any one positioning of the two heliostats and that the perimeter of the shadow can be traced out by varying the scalars f_1 and f_2 after computing these five dot products. We shall choose them in such a way as to move counterclockwise about the perimeter of the jth heliostat.

To reduce the problem to two dimensions, each intersection point is expressed as the ordered pair (g,h) such that

$$\bar{I} = \bar{P}_i + f_1\bar{X}_i + f_2\bar{Y}_i - r\hat{S} = \bar{P}_j + g\bar{X}_j + h\bar{Y}_j$$

which yields

$$g = \frac{(\bar{I}-\bar{P}_j).\bar{X}_j}{x_m^2} \quad , \quad h = \frac{(\bar{I}-\bar{P}_j).\bar{Y}_j}{y_m^2} \qquad \text{(equation 7)}$$

If $-1 \leq (g,h) \leq 1$ is true, then the point lies within the boundary of the jth heliostat.

We now have the corners of the perimeter of the complete shadow of the ith heliostat expressed as two dimensional points in the plane of the jth heliostat. Only the area of the shadow inside the boundaries of the jth heliostat actually reduces the effective area of the mirror. Therefore, we must truncate the shadow perimeter to only the area inside the jth heliostat. A description of the algorithm is contained in Section 3.6.

3.5 Blocking Of One Heliostat By Another

To compute the area of the jth heliostat blocked from the receiver by heliostat i, we shall proceed in a manner similar to that used for shading. The difference is that the direction of the projection of the edge of heliostat i toward heliostat j is the line of sight from the focal point on the receiver through the edge (see Figure 3-6).

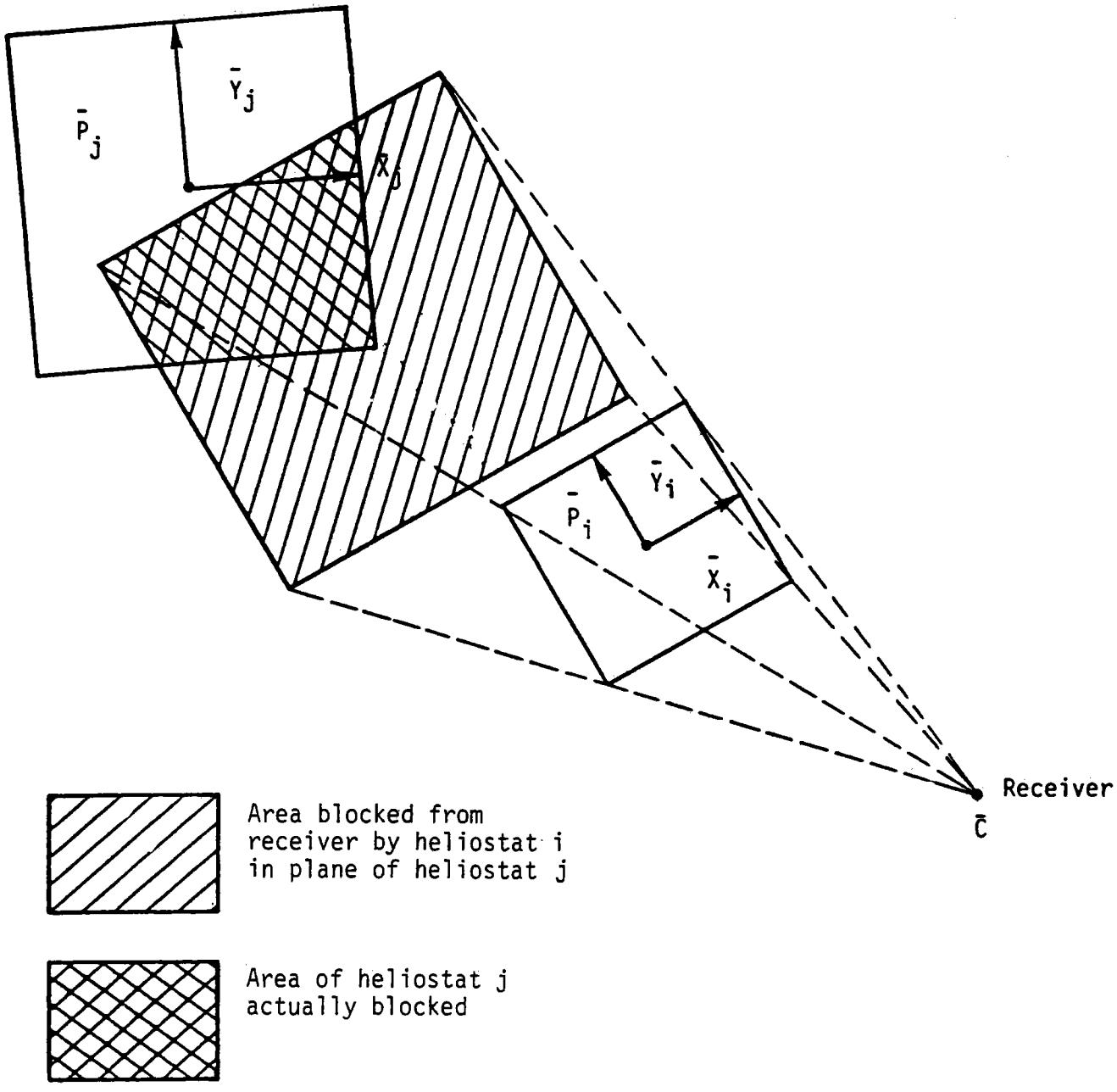

Figure 3-6. Geometry of Heliostat Blocking.

The line of sight from the receiver to an edge of heliostat i is

$\bar{P}_i + f_1\bar{X}_i + f_2\bar{Y}_i - \bar{C}$, where f_1 and f_2 are as before.

Any point on the line from the receiver through an edge of the ith heliostat is

$$\bar{Q} = \bar{C} + t \quad \bar{P}_i + f_1\bar{X}_i + f_2\bar{Y}_i - \bar{C}$$

To find the particular values of t, r, such that $\bar{Q}$ is in the plane of the jth heliostat, we substitute $\bar{Q}$ into the equation of the plane of the jth heliostat.

$$(\bar{Q} - \bar{P}_j) \cdot \hat{N}_j = 0$$

$$\left[\bar{C} + \quad (\bar{P}_i + f_1\bar{X}_i + f_2\bar{Y}_i - \bar{C}) \quad - \bar{P}_j\right] \cdot \hat{N}_j = 0$$

solving for

$$r = \frac{\bar{P}_j \cdot \hat{N}_j - \bar{C} \cdot \hat{N}_j}{\bar{P}_i \cdot \hat{N}_j + f_1\bar{X}_i \cdot \hat{N}_j + f_2\bar{Y}_i \cdot \hat{N}_j - \bar{C} \cdot \hat{N}_j} \qquad \text{(equation 8)}$$

The value of that we compute must be greater than one for the blocked heliostat to actually be behind the heliostat that is doing the blocking.

As in Section 3.4, we compute the intersection point as

$$\bar{Q} = \bar{C} + \quad (\bar{P}_i + f_1\bar{X}_i + f_2\bar{Y}_i - \bar{C}) = \quad (\bar{P}_i + f_1\bar{X}_i + f_2\bar{Y}_i) + (1 - r)\,\bar{C}.$$

Finally, we compute the blocked perimeter in the two dimensional coordinate system of the jth plane, (repeating equation 7)

$$g = \frac{(\bar{I} - \bar{P}_j) \cdot \bar{X}_j}{x_m^2}, \qquad h = \frac{(\bar{I} - \bar{P}_j) \cdot \bar{Y}_j}{y_m^2}$$

If $-1 \leq (g,h) \leq 1$ is true, the point is within the boundaries of the heliostat.

We now have the corners of the perimeter of the entire blocked area produced by the ith heliostat expressed as two dimensional points in the plane of the jth heliostat. We must reduce this area to that which is completely within the actual boundary of the jth heliostat. The algorithm for doing this is described in Section 3.6.

3.6 Polygonal Areas

3.6.1 Truncating to a Set of Boundaries

We have a set of ordered pairs defining a polygon in the plane of heliostat j. Some, none, or all of this polygon may actually be within the borders of the heliostat. Since we have chosen to express the vertices of the polygon in terms of the semi-axes of the mirror (by normalizing them), the boundaries of the jth heliostat in g,h space are unity (see Figure 3-7).

We express each boundary analogously to our expression for a plane. This way we can divide the entire plane into two half planes. Using two dimensional vectors we state the equation of the line defining the boundary.

$$(\bar{Q} - \bar{P}) \cdot \bar{N} = 0$$

$\bar{Q}$ = any point on line,

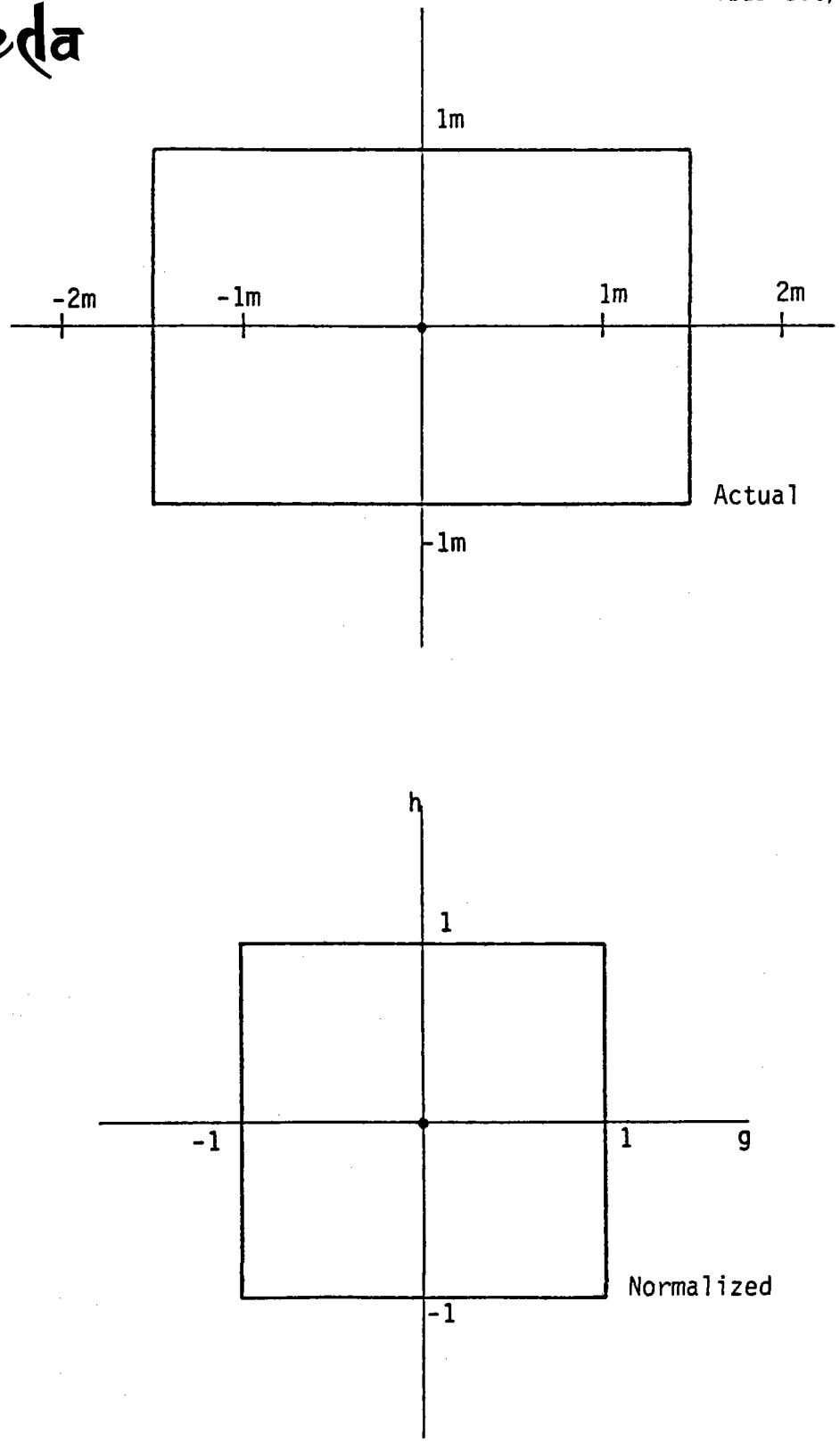

Figure 3-7. Mapping of Actual Heliostat Into Normalized Coordinates.

$\overline{P}$ = any known point on boundary,

$\overline{N}$ = a normal to the boundary.

We can find the vector equations of the boundaries quite easily by inspection of Figure 3-7.

Boundary to right: $\left[\overline{Q} - (1,0)\right] \cdot (1,0) = 0$

Boundary above: $\left[\overline{Q} - (0,1)\right] \cdot (0,1) = 0$

Boundary to left: $\left[\overline{Q} - (-1,0)\right] \cdot (-1,0) = 0$

Boundary below: $\left[\overline{Q} - (0,-1)\right] \cdot (0,-1) = 0$

These equations reduce to a more familiar form if we substitute $\overline{Q} = (g,h)$ and simplify.

$\left[(g,h) - (1,0)\right] \cdot (1,0) = 0$ becomes $g = 1$

$\left[(g,h) - (0,1)\right] \cdot (0,1) = 0$ becomes $h = 1$

$\left[(g,h) - (-1,0)\right] \cdot (-1,0) = 0$ becomes $g = -1$

$\left[(g,h) - (0,-1)\right] \cdot (0,-1) = 0$ becomes $h = -1$

which is what we asserted earlier.

The point where a line intersects a given boundary can be computed using a two dimensional analog to the three dimensional solutions. Let $\overline{R}$ and $\overline{S}$ be two points in a plane. Any point, $\overline{Q}$, on the line through the points $\overline{R}$ and $\overline{S}$ can be expressed as

$$\overline{Q} = \overline{R} + t\ (\overline{S} - \overline{R}) \qquad \text{(equation 9)}$$

To find which t gives us a point on the boundary, we substitute into the equation of the boundary

$$(\overline{Q} - \overline{P}) \cdot \overline{N} = 0$$

$$\left[\overline{R} + r\,(\overline{S}-\overline{R})-\overline{P}\right] \cdot \overline{N} = 0$$

solving for r,

$$r = \frac{\overline{P}.\overline{N} - \overline{R}.\overline{N}}{\overline{S}.\overline{N} - \overline{R}.\overline{N}} \qquad \text{(equation 10)}$$

Note that for each boundary we will need to consider, the dot product $\overline{P}.\overline{N} = 1$. We now have the tools to truncate a polygon to only the area within given boundaries. For each boundary, $\overline{N}$, we perform the following steps to generate the bounded perimeter list (see Figure 3-8). Starting at the first vertex, the ordered pair $(g,h)_1$ of the polygon, we creep around the perimeter keeping any vertex found to be within the boundary. For each line segment between vertices, we solve equation 10 for r substituting $(g,h)_i$ for $\overline{R}$ and $(g,h)_{i+1}$ for $\overline{S}$. If the value of r is greater than zero and less than one, the intersection point is computed from equation 9 and the new point added.

After generating a new list of vertices for the obscuration polygon successively for each of the four boundaries, the remaining polygon will lie entirely within the borders. We can compute the area of this

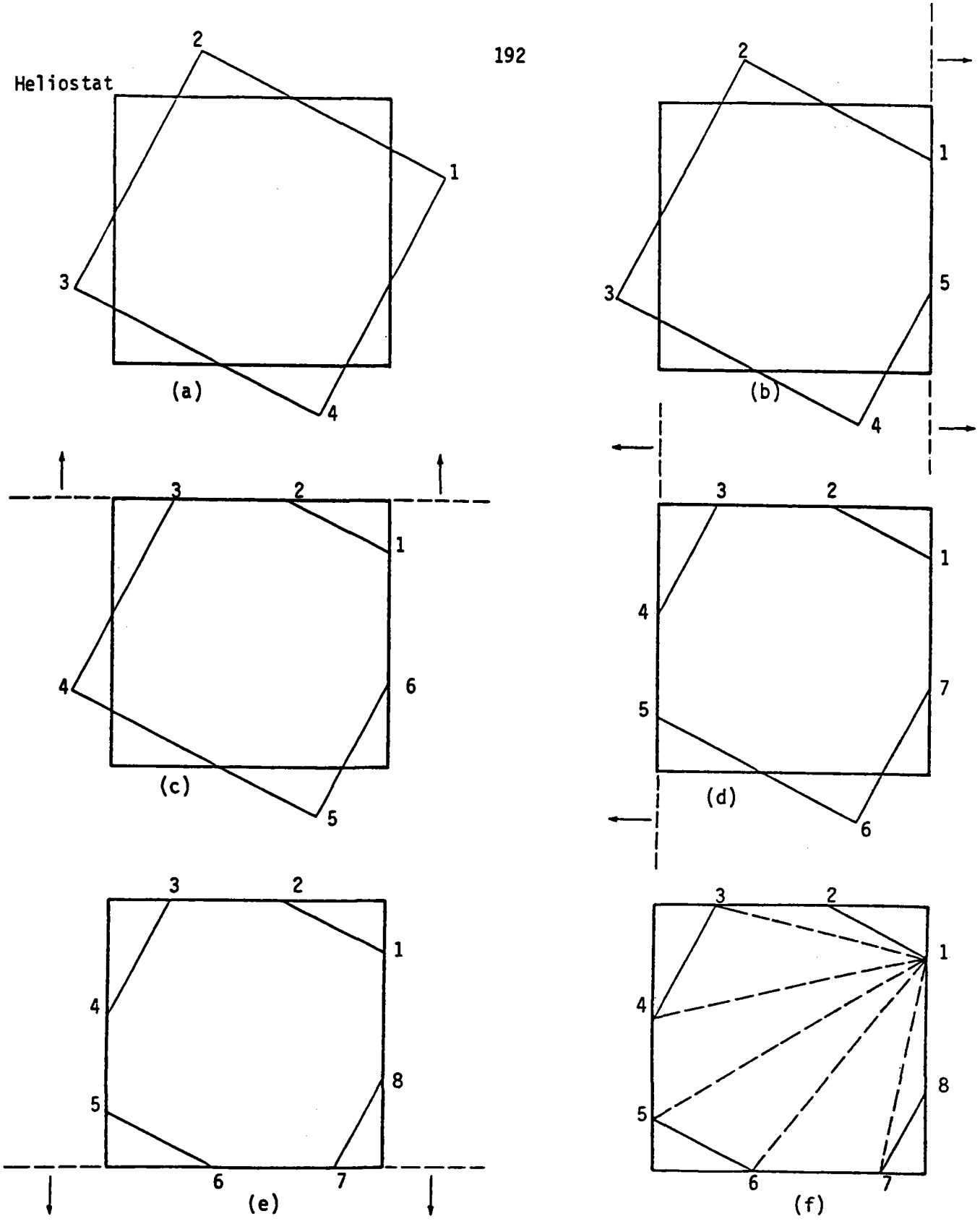

Figure 3-8. Illustration of Successive Truncation of Obscuration Polygon and Area Computation.

directly by cutting the area into triangles, computing the area of each triangle, then summing.

3.6.2 Computing Polygon Area

The exact formula for computing the area enclosed by a polygon is now developed. Recalling that the area will be in normalized heliostat coordinates, we must multiply the resultant area by the magnitudes of the true dimensions to convert to physical measure of area.

The area of any triangle with sides $\overline{A}$ and $\overline{B}$ can be computed from the cross product. Since these vectors lie in the plane of the jth heliostat, we simplify the cross product:

$$1/2\ \overline{A} \times \overline{B} = 1/2\ \left[(g_2-g_1, h_2-h_1, 0) \times (g_3-g_1, h_3-h_1, 0)\right]$$
$$= 1/2\ \left[(g_2-g_1)\ (h_3-h_1)-(h_2-h_1)(g_3-g_1)\right]$$

Generalizing to a polygon,

$$\text{Area} = 1/2\ x_m y_m \sum_{i=3}^{N} (g_{i-1}-g_1)\ (h_i-h_1)-(h_{i-1}-h_1)-(g_i-g_1) \qquad \text{(equation 12)}$$

3.6.3 Merging Areas

Up to now, the problem has been the simplest case of one heliostat shading or blocking another. In a Unified Heliostat Array, several heliostats may shade or block a given heliostat and the areas shaded or blocked by each may overlap. If we were to merely sum the areas on one heliostat that are shaded and blocked by other heliostats without taking

into account potential overlapping, we are sure to overestimate system degradation due to these effects.

The algorithm to accumulate obscured areas on a heliostat uses the truncation technique described in Section 3.6.1. The area of intersection between each new polygonal area is found by truncating the new area to within the boundaries of each of the old ones. The area of intersection (or overlapped area) found each time is subtracted from the whole area of the new polygon. Only the net increase in obscured area contributed by the new polygon is actually added to the total obscuration.

New points in the perimeter are compiled using equation 10. The endpoints of the segment $\overline{R}$ and $\overline{S}$ are as before. The boundary parameters, $\overline{P}$ and $\overline{N}$, are different. Since the truncation boundaries are the edges of the older polygons, we can represent these values with the endpoints of these edges letting $(g,h)_i$ and $(g,h)_{i+1}$ denote these endpoints, we find

$$\overline{P} = (g,h)_i \qquad \overline{N} = (-(h_{i+1} - h_i),\ g_{i+1} - g_i)$$
$$= (h_i - h_{i+1},\ g_{i+1} - g_i)$$

3.7 Outputs of Simulation

The primary output from the simulation as so far described is a total power delivered to the aperture at the selected time of day and year. The simulation sums this power on an hourly basis from 0700 to 1700 local time and a daily basis for 24 days spaced throughout the year. To compute an annualized energy, we multiply the summed energy by the

factor 330/24. This factor derives from our desire to find total annual energy assuming 330 days of operation per year and using the simulation's estimate of average daily energy.

Additional performance indicators that are computed at each hour are average cosine factor for the array, the effective shading factor, and the effective blocking factor. The average cosine factor is averaged over the entire array. The effective shading and blocking factors are computed by

$$\text{effective shading} = \frac{\sum f_{si} f_{ci}}{\sum f_{ci}}, \quad \text{effective blocking} = \frac{\sum f_{ci} f_{bi}}{\sum f_{ci}}$$

where the sums are taken over each heliostat in the array, f_{ci} the cosine factor for the ith heliostat, f_{si} the shading factor, and f_{bi} the blocking factor. The effective factors are used in place of average factors to weight shading or blocking loss by the contribution to total energy made by an individual heliostat.

3.8 Flux Density

We have computed the total energy delivered at the receiver. This does not take into account any spillage losses or reradiative losses. Also, it is possible to optimize the receiver design given a method of predicting the actual distribution of the incident energy. The model used by the simulation to compute energy density in the receiver plane is described below.

The basic approach is to divide each mirror into a collection of smaller flat mirror segments, project an image of the solar disk from the center of each segment to the aperture plane, and sum the incident energy into the appropriate elements of a grid superimposed on the plane of the aperture.

We start by finding the local normal at any point on the face of a toroidal segment mirror. Referring to Figure 3-9, the point at which the local normal is desired can be represented by

$$\overline{W} = \overline{P}_j + f_1\overline{X}_j + f_2\overline{Y}_j.$$

Assume also that the long radius of curvature, r_1, lies along the $\overline{Y}_j$ axis. If the long radius lies instead in the $\overline{X}_j$ direction, the vectors $f_1\overline{X}_j$ and $f_2\overline{Y}_j$ in the following derivation should be interchanged.

Considering only the long axis, the center of curvature will be along the $\hat{V}_j$ vector. The local normal will be along the line of sight to this center, hence:

$\overline{Q}$ = center of curvature - point on a mirror

$$\overline{Q} = (\overline{P}_j + r_1\hat{V}_j) - (\overline{P}_j + f_2\overline{Y}_j)$$

$$\overline{Q} = r_1\hat{V}_j - f_2\overline{Y}_j$$

After converting $\overline{Q}$ to a unit vector, we find the normal at $\overline{W}$ using the shorter radius of curvature, r_s, as before

$$\overline{N} = (\overline{P}_j + f_2\overline{Y}_j + r_s\hat{Q}) - (\overline{P}_j + f_2\overline{Y}_j + f_1\overline{X}_j)$$

$$\overline{N} = r_s\hat{Q} - f_1\overline{X}_j.$$

3.8.2 Reflection Direction

To find the direction of geometric reflection, we wish to find the vector $\overline{R}$ given the solar direction cosines, $\hat{S}$, and the normal to the surface $\overline{N}$, such that the angle between $\overline{R}$ and $\overline{N}$ is equal to the angle between between $\hat{S}$ and $\overline{N}$, and $\overline{R}$ is coplanar with $\hat{S}$ and $\overline{N}$. The component of $\hat{S}$ along

$\overline{N}$ is

$$\frac{\hat{S}.\overline{N}}{|\overline{N}|} .$$

The component of S normal to $\overline{N}$ is thus

$$\hat{S} - \frac{\hat{S}.\overline{N}}{|\overline{N}|} \overline{N}.$$

Subtracting twice this vector from $\hat{S}$ will give us $\overline{R}$.

$$\overline{R} = \hat{S} - 2\left[\hat{S} - \frac{\hat{S}.\overline{N}}{|\overline{N}|} \overline{N}\right]$$

$$\overline{R} = 2\left(\frac{\hat{S}.\overline{N}}{|\overline{N}|}\right)\overline{N} - \hat{S}$$

If the vector $\overline{N}$ computed earlier was converted to a unit vector, then

$$R = 2\ (\hat{S}.\hat{N})\ \hat{N} - \hat{S}$$

3.8.3 Intercept at Aperture

Substituting known values into the vector equation of a line, any point on the reflected ray can be represented by:

$$\overline{G} = (\overline{P}_j + f_1 X_j + f_2 Y_j) + t\left[2\ (\hat{S}.\hat{N})\hat{N} - \hat{S}\right]$$

To find the intercept on the aperture, we solve for the value of t, r, that satisfies the equation of the aperture plane. For this model, a northward facing receiver is assumed. The normal to the receiver is (0,1,0)

and, for a point on the receiver, we use the nominal aim point, $\bar{C}$. Therefore, the equation solved for r reduces to

$$r = \frac{C_2 - P_{j2} - f_1 X_{j2} - f_2 Y_{j2}}{2(\hat{S}.\hat{N})N_2 - S_2}$$

Note that we are using the components instead of the vectors.

The intercept of the center of the solar image from point $\bar{W}$ at the aperture, $\bar{I}$, is thus

$$\bar{I} = \begin{pmatrix} X_I \\ Y_I \\ Z_I \end{pmatrix} = \begin{cases} P_{j1} + f_1 X_{j1} + f_2 Y_{j1} + r\left[2(\hat{S}.\hat{N})\, N_1 - S_1\right] \\ C_2 \\ P_{j3} + f_1 X_{j3} + f_2 Y_{j3} + r\left[2(\hat{S}.\hat{N})\, N_3 - S_3\right] \end{cases}$$

3.8.4 Image Shape

The reflected circular image will strike the aperture plane at some oblique angle so that the image will be an ellipse. We wish to compute the semi-axes and the center of this ellipse.

The direction of the semi-minor axis, $\bar{S}_n$, will be normal to the plane formed by the reflected ray direction and the normal to the aperture plane. Its magnitude will be the angular radius of the sun times the throw distance. Therefore,

$$\bar{S}_n = \frac{\gamma d\ (\hat{R} \times \bar{H})}{\hat{R} \times \bar{H}}$$

where γ is the angular radius of the sun, d the throw distance, $\hat{R}$ the direction of the reflected ray, and $\bar{H}$ the normal to the receiver plane, (0,1,0).

The semi-major axis of the ellipse, $\bar{S}_j$, will be perpendicular to the receiver normal and $\bar{S}_n$. Its direction is thus found by $\bar{S}_n \times \bar{H}$. Due to the angle of intercept, the image will not be symmetric about the reflection direction (see Figure 3-10).

The angle α can be computed from the dot product

$$\cos \alpha = \hat{R} \cdot \hat{S}_j$$

where $\hat{S}_j$ is the normalized vector $\bar{S}_n \times \bar{H}$ and is the direction of the semi-major axis. The two line segment lengths, δ_1 and δ_2, are computed from the law of sines,

$$\frac{\delta_1}{\sin\gamma} = \frac{d}{\sin(\pi - \gamma - \alpha)}, \quad \frac{\delta_2}{\sin\gamma} = \frac{d}{\sin(\alpha - \gamma)}$$

Using γ = 0.0046 radians, and using trigonometric identities and the small angle approximation, we get

$$\delta_1 = \frac{d}{\frac{1}{\gamma}\sin\alpha - \cos\alpha}, \quad \delta_2 = \frac{d}{\frac{1}{\gamma}\sin\alpha + \cos\alpha}$$

We then compute the actual center of the ellipse, $\bar{C}$,

$$\bar{C} = \bar{I} + \left(\frac{\delta_2 - \delta_1}{2}\right)\hat{S}_j$$

The semi-major axis is then found by multiplying the length times the unit vector

$$\bar{S}_j = \left(\frac{\delta_1 + \delta_2}{2}\right)\hat{S}_j$$

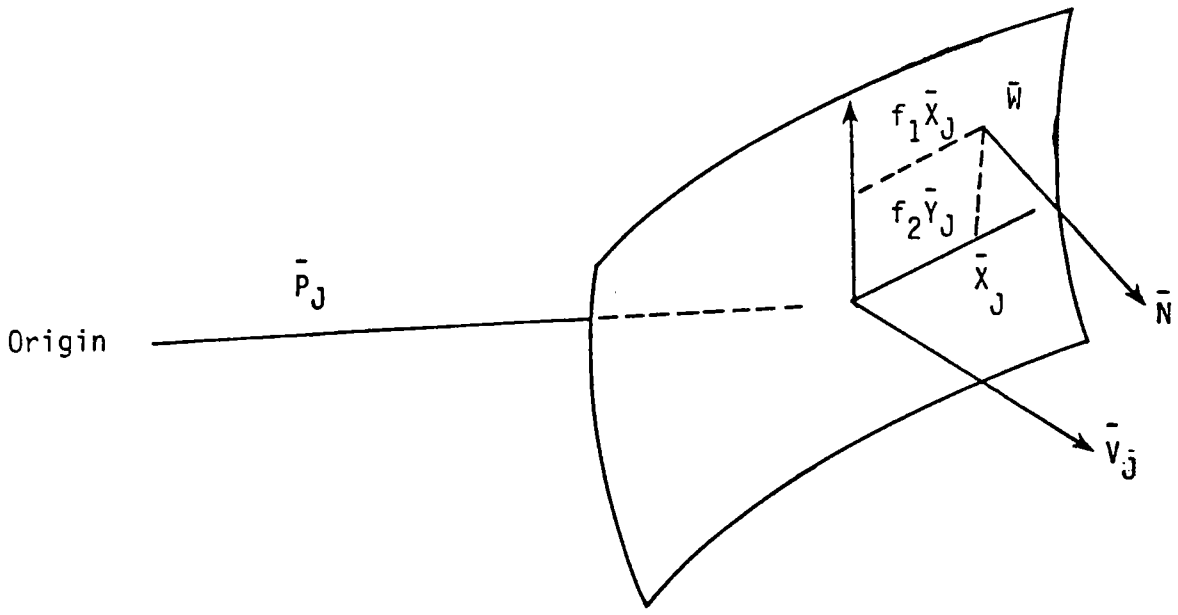

Figure 3-9. Geometry of Toroidal Segment Mirror.

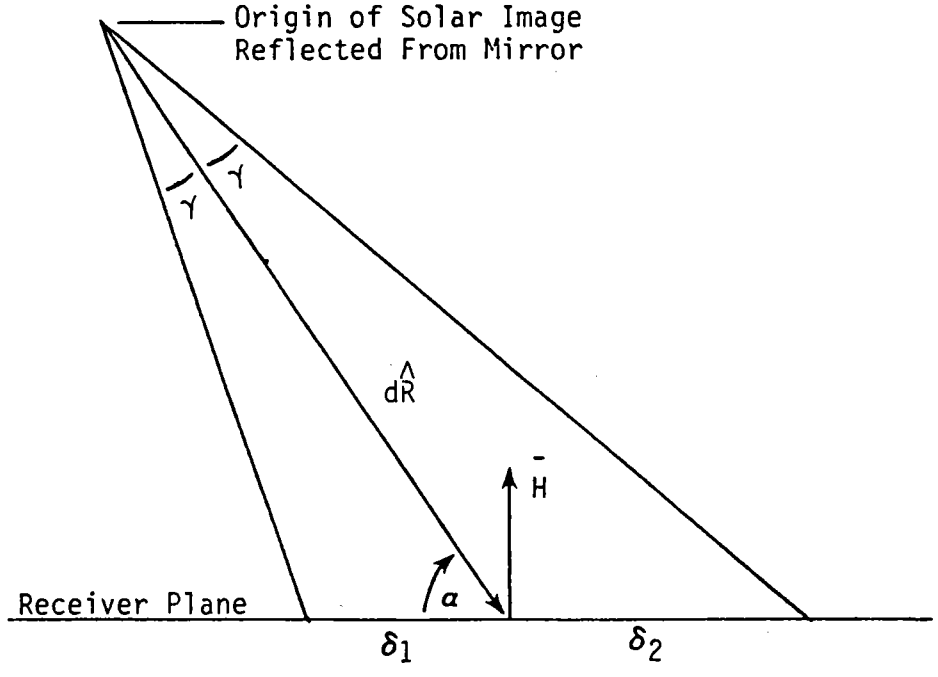

Figure 3-10. Distortion of Solar Image on Receiver Plane.

Any point on the ellipse can then be represented by

$$\bar{U} = \bar{L} + a\,\bar{S}_j + b\,\bar{S}_n,\ a^2 + b^2 = 1.$$

The area of the ellipse will be

$$\text{Area} = \pi \quad |\bar{S}_j| \quad |\bar{S}_n|$$

3.8.5 Computing Energy Density at Aperture

We divide the power at the aperture contributed by an individual heliostat into n equal parts, n being the number of segments into which the mirror is divided. This unit energy is assumed to be concentrated into the solar image coming from the center of each segment. If the segment is shaded or blocked, no contribution to flux density is computed.

Pointing inaccuracies are modeled by computing a random displacement to the $\bar{L}$ vector (center of the ellipse) sampled from a uniform distribution whose maximum magnitude is equal to an input angle times the throw distance.

A grid is overlaid on the receiver. Each bin is square with the length of a side an input variable. This grid is centered on the nominal aimpoint for the array. The number of bins within the ellipse can be computed from the area of the ellipse and the area of each bin. We then divide the unit energy delivered by the segment of the mirror by this number of bins. Each bin inside the ellipse is incremented by this energy per bin value.

SECTION 4.0

COMPUTER IMPLEMENTATION CONSIDERATIONS

A major bottleneck to speed of execution of the shading and blocking algorithm on a digital computer is defining the actual limits of the local search matrices to minimize the number of times the complete blocking or shading computations must be done between individual heliostats. This was accomplished in two steps.

A technique to check whether or not it is necessary to proceed with a full shading or blocking analysis was developed. Both involve projecting the pivot point of the ith heliostat onto the plane of the jth heliostat along the appropriate direction. If the distance between the pivot point of the jth heliostat and this projected point was greater than the maximum dimension of the mirror, the full scale analysis would not be needed.

Using the nomenclature defined in Section 3.4, the equations for shading are:

$$\left[(\overline{P}_i - t\hat{S}) - \overline{P}_j\right] \cdot \hat{N}_j = 0$$

$$t = \frac{\overline{P}_j \cdot \hat{N}_j - \overline{P}_i \cdot \hat{N}_j}{\hat{S} \cdot \hat{N}_j}$$

$$\text{distance} = \left|\overline{P}_i - t\hat{S} - \overline{P}_j\right|$$

If distance is less than or equal to the maximum dimension, then proceed with shading analysis of this pair of heliostats.

Similarly, for blocking:

$$\left\{\left[\overline{P}_i + t\,(\overline{P}_i - \overline{C})\right] - \overline{P}_j\right\} \cdot \hat{N}_j = 0$$

$$t = \frac{\overline{P}_j \cdot \hat{N}_j - \overline{P}_i \cdot \hat{N}_j}{\overline{P}_i \cdot \hat{N}_j - \overline{C} \cdot \hat{N}_j}$$

$$\text{distance} = \left|\overline{P}_i + t\,(\overline{P}_i - \overline{C}) - \overline{P}_j\right|$$

If distance is less than the maximum dimension, then proceed with full blocking analysis for this pair of heliostats. The resultant distances are checked against the maximum dimension of the mirror. Only those heliostat pairings that pass these criteria are checked further.

Notice the several time saving features of this initial screening. The dot products $\overline{P}_i \cdot \hat{N}_j, \overline{P}_j \cdot \hat{N}_j, \hat{S} \cdot \hat{N}_j$, and $\overline{C} \cdot \hat{N}_j$ are required in the full scale analysis anyway and so can be computed once and used in both as required. Only the position of the pivot points of the ith heliostat is required for this screening, eliminating the need for a computation (or storage retrieval) of the spatial orientation until really needed.

Using these equations and the interelement spacing set forth in the specifications (Veda Report #43342-80U/P0069) of the UHA, the maximum boundary of an area containing potential shading heliostats was independently developed over the times and dates of interest. A similar boundary was developed for blocking. The boundaries were reduced to a "search" matrix of neighboring heliostats containing potential shading or blocking mirrors which was implemented in the FORTRAN simulation of UHA performance.

Another decision was made concerning how to treat the spatial orientation information. This position information is considered constant for each heliostat for any given time of day or year. The option of computing them once and accessing the data when needed was unavailable due to limited memory size and slow peripheral memory access times. The overhead to perform a "sliding area" computation to minimize the number of times we recompute spatial orientations turned out to require almost as much time as the brute force method. For this reason, Veda's implementation of the algorithm computes spatial orientations whenever needed.

APPENDIX D

PERFORMANCE ANALYSIS:

SAMPLE COMPUTER OUTPUT

INDEX

The data in this Appendix is representative of the computer generated data developed for the optical performance analysis.

Computer outputs were generated for each of four UHA designs. The computational process assumed a circular earth orbit about the sun. Thus, the heliostat field performance factors, other than insolation level, are symmetrical about local noon for each day, and symmetrical annually for the period between winter and summer solstices. That is, field conditions at 1000 are symmetrical to 1400 on the same day and these hours then correspond to the same hours on the annually symmetric day. Thus, the vernal equinox day is symmetric to the autumnal equinox day. There is no daily symmetry for local noon, and no annual symmetry for the solstice days. The 1976 Barstow insolation data base was used for insolation values. Insolation symmetry was not assumed. The appropriate insolation values were used for each hour of each day analyzed.

Calculations for performance were made on a heliostat by heliostat basis and integrated for the entire field. This results in a net field effectivity factor, which considers cosine factor, shading factor, blocking factor, reflectivity of the heliostat, and atmospheric transmission factor. This effectivity multiplied by the product of insolation and heliostat area yields power delivered to the aperture plane. Similarly, the image plane flux distribution is computed on a heliostat by heliostat basis and integrated over the entire heliostat field. The increment of heliostat area for each calculation, and the increment of aperture plane area were chosen so as to give a reasonable resolution of the flux density.

Both circular and rectangular apertures were selected for investigation. In this appendix, only design point aperture data is included, but similar data were generated for other apertures in order to calculate the performance and cost of energy results shown in the main body of this report. The calculated data include:

aperture plane image flux distribution;

total power to the aperture:

cosine factor, cosine weighted shading factor, and cosine weighted blocking factor by heliostat, and integrated over the heliostat field;

aperture dimensions;

aperture flux distribution;

power into the aperture;

aperture capture efficiency;

annual tabulation of power through the aperture;

annual tabulation of power in excess of power lost through the aperture by reradiation, at 250°K intervals over the range of 1000-2000°K.

In the tabulations, the column labeled ER1 is power for the day and hour specified. The column labeled ER2 is for the symmetrical hour after noon of the same day. The column labeled ER3 is for the designated hour of the symmetrical half of the year, and ER4 corresponds to the symmetrical hour after noon of that day. Day 1 is winter solstice, day 7 is vernal equinox, and day 13 is summer solstice.

The shading and blocking patterns will at first appear to have significant amounts of power deterioration. A factor of 1.000 indicates a cosine weighted value equal to less than 1/2 of 1 percent loss for the entire field,

i.e., the transfer function is greater than 0.995. The net annual losses are very small, even though field optimization has not been performed. The most severe loss, for the designs studied, occurs early on the summer solstice for the UHA using the repowering heliostat. The shading and blocking factors are essentially unity (i.e. no shading or blocking) within the time frame of local noon plus and minus three hours throughout the year. Shading degradation, which varies with both heliostat design and sun position, occurs beyond that six hour time.

Each of the sections, D-1 through D-4, consists of a group of data concerning design point apertures. The total image at the aperture plane at noon of the winter solstice is presented in terms of flux density in watts/m^2. Cosine, shading, and blocking factors for that image then follow. The rectangular receiver aperture chosen for design point is then shown. "Power per bin" is tabulated. For the 1 MWt UHA, a "bin" is a square 0.01m^2 in area at the receiver aperture; for the three remaining UHA's the area of each square bin is 0.1m^2. Three tables then follow. The first is the tabulation of power through the aperture throughout the year based on a lossless receiver. The next two tables show the net power after reradiation losses at 1000°K and 1500°K respectively. Similar data are provided for the design point round aperture.

Inspection of these tables allows a direct comparison between different UHA's and different apertures for the same UHA. The round aperture is shown to be more efficient than the rectangular aperture of the same area; the effect being more pronounced at the higher temperatures.

```
LATITUDE OF SITE :     35.0,   SOLAR DECLINATION : -23.45,   TIME OF DAY 12:00,   TOTAL ENERGY IS :      1031199.00

                          FLUX CONTOUR
MAXIMUM SPOT DIMENSIONS, HORIZONTAL: -1.14   1.18   VERTICAL:     -1.01      1.02
HOTTEST SPOT IS    1469642.00   AT        .05      -.05
 1                                                                  RANGES (W/SQ.M)
 2                                                          A    1413117.0  TO     1469642.0
 3                                                          B    1356592.0  TO     1413117.0
 4                                                          C    1300067.0  TO     1356592.0
 5                                                          D    1243542.0  TO     1300067.0
 6                                                          E    1187017.0  TO     1243542.0
 7                                                          F    1130492.0  TO     1187017.0
 8                                                          G    1073967.0  TO     1130492.0
 9                                                          H    1017442.0  TO     1073967.0
10                                                          I     960917.6  TO     1017442.0
11                                                          J     904392.8  TO      960917.6
12                                                          K     847868.1  TO      904392.8
13              ZZZZZZZZZZ                                  L     791343.3  TO      847868.1
14            ZZZZZZZZZZZZZ                                 M     734818.6  TO      791343.3
15          ZZZZZZZZYYYYZZZZZ                               N     678293.8  TO      734818.6
16        ZZZZZZYXXWWWXYZZZZZ                               O     621769.1  TO      678293.8
17        ZZZZZYXVTSSTUWYZZZZZ                              P     565244.3  TO      621769.1
18      ZZZZZYXURONNOQTWYZZZZZ                              Q     508719.6  TO      565244.3
19      ZZZZZXURNKIIJLPTWYZZZZZ                             R     452194.8  TO      508719.6
20      ZZZZYWSNIFEEFHLQVYZZZZZ                             S     395670.1  TO      452194.8
21      ZZZZYVQKFC99CEIOUXZZZZZ                             T     339145.3  TO      395670.1
22      ZZZZXUPJDAAAACHNTXYZZZZZ                            U     282620.6  TO      339145.3
23      ZZZZXUPJDAAAACHNTXYZZZZZ                            V     226095.8  TO      282620.6
24      ZZZZYVQKFCB9CEJOUXZZZZZ                             W     169571.1  TO      226095.8
25      ZZZZYWSNIFEEFHMRVYZZZZZ                             X     113046.3  TO      169571.1
26       ZZZYXUQMKIIJLPTXYZZZZZ                             Y      56521.6  TO      113046.3
27       ZZZZYWUPONNOQTWYZZZZZ                              Z         -3.1  TO       56521.6
28        ZZZZYWVTSSTUWYZZZZ
29         ZZZZYXXWWWXYZZZZZ
30          ZZZZZZYYZZZZZZZ
31            ZZZZZZZZZZZZ
32               ZZZZZZZZ
33
34
35
36
37
38
39
40
41
42
43
44
45
  12345678901234567890123456789012345678901234567890123345                AREA =   3.66
          A   B   C   D   E   F   G   H   I   J   K   L   M   N   O   P   Q   R   S   T   U   V   W   X   Y   Z
   PERCENT   2   1   2   1   2   2   0   1   2   1   1   1   1   2   2   1   2   1   2   3   3   2   4   5   8  51
CUMULATIVE 100  98  97  95  95  93  91  91  90  88  87  86  85  84  82  80  79  78  77  75  72  69  68  64  59  51
HELIOSTAT X, Y =         50.000       96.605 ; FIELD RADIUS AND =    0 ; REC. HT =    9.00
MIR. RADII =    275.00     180.00   ; HELIO SIZE WD, HT =      3.000     2.000    BIN SIZE =   .10  METER
JITTER (MRAD) = 3.0  DISKFILE  = Y
```

Figure D-1-1. 1 MWt VIH Design Point Solar Image Characteristics at Aperture Plane.


```
VEDA 1 MWT     DAY =  1   HOUR = 12
.....................
.....................
.....................
.....................
.....................
.....................
.....................
.....................
.....................
.....................

AVERAGE COSINE FACTOR      =

WEIGHTED SHADING FACTOR    =

WEIGHTED BLOCKING FACTOR   =


LEGEND (.) NO SHADING, NO BLOCKING
       (S) SHADING, NO BLOCKING
       (B) BLOCKING, NO SHADING
       (X) SHADING AND BLOCKING
```

Figure D-1-2. 1 MWt VIH Design Point Shading and Blocking Matrix.

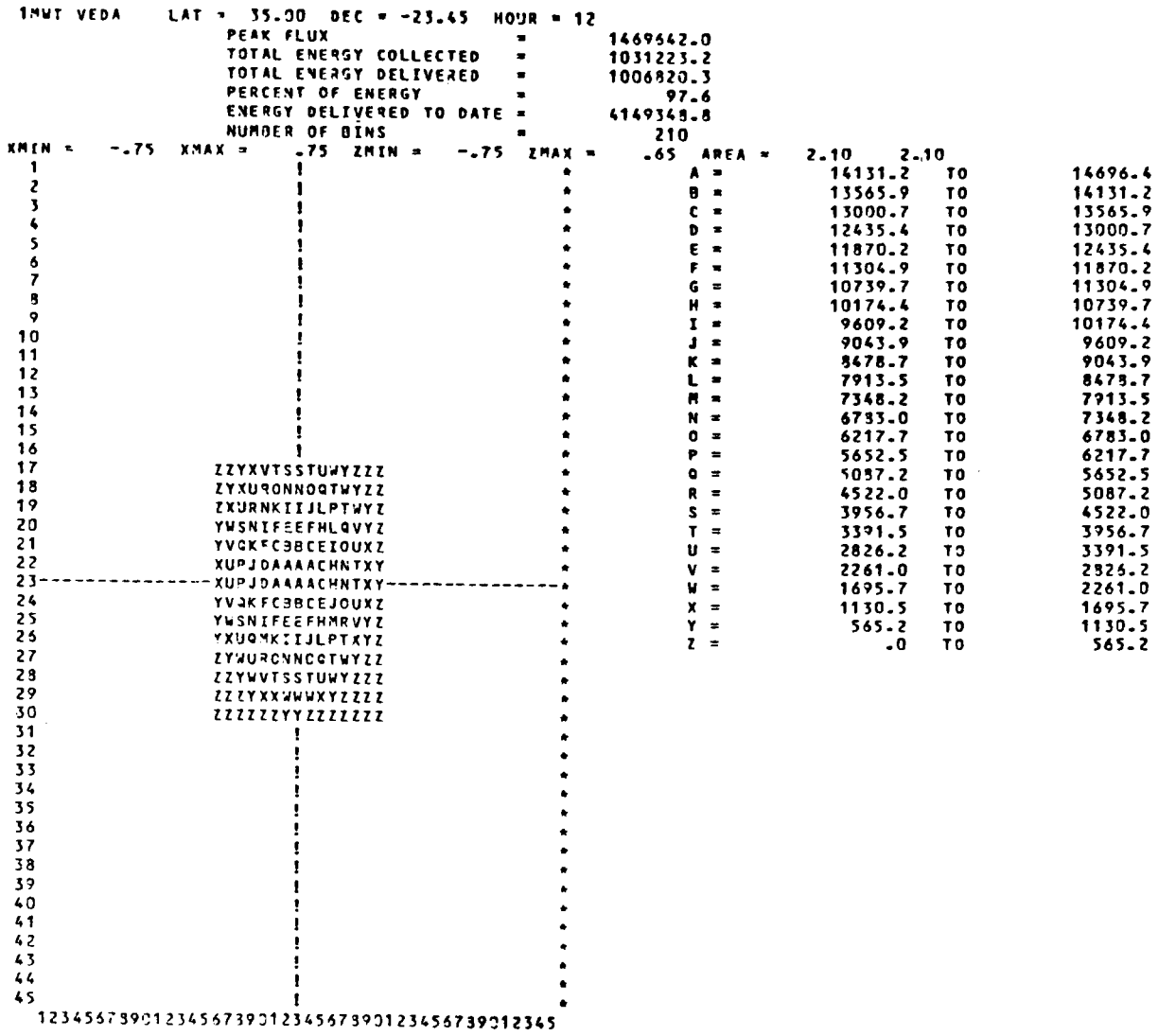

Figure D-1-3. 1 MWt VIH Design Point Rectangular Aperture Characteristics.

Table D-1-1. 1 MWt VIH Power Through the Rectangular Aperture.

DAY	HR	ER1	ER2	ER3	ER4
1	8	591241.7	529192.4	.0	.0
1	9	615534.0	546473.5	.0	.0
1	10	935766.1	832080.9	.0	.0
1	11	996326.5	884999.6	.0	.0
1	12	1036820.7	.0	.0	.0
2	8	529030.1	516963.6	659129.2	497152.5
2	9	758903.5	573108.9	847556.1	779218.0
2	10	896514.1	805680.6	935979.6	911242.0
2	11	967947.2	962134.1	979573.2	967943.8
2	12	961445.5	.0	990798.5	.0
3	8	439239.7	619351.1	625295.8	457924.2
3	9	730084.1	502979.6	812135.9	744375.7
3	10	892649.4	913445.4	908722.3	873737.0
3	11	946571.5	963909.9	934082.3	938876.7
3	12	959711.6	.0	962632.0	.0
4	8	422209.1	604935.6	606913.9	485708.7
4	9	947393.1	857954.6	963295.9	794336.1
4	10	892383.5	964376.9	942839.6	909197.9
4	11	1009242.3	1004330.5	976740.8	948096.4
4	12	1020108.9	.0	987445.1	.0
5	8	554726.9	668389.6	528864.9	468130.0
5	9	752675.0	786332.8	688924.1	731497.9
5	10	834165.5	942992.8	777551.4	807875.5
5	11	962592.3	897841.6	829975.0	844953.1
5	12	939732.9	.0	844162.3	.0
6	8	277093.0	599447.4	668715.9	624947.5
6	9	602105.9	787237.4	965098.8	906226.2
6	10	739249.2	962408.1	933601.2	913792.8
6	11	891443.5	908904.5	974575.7	964412.8
6	12	930162.5	.0	984161.1	.0
7	7	227552.3	234098.3	191350.1	149281.0
7	8	601983.2	603903.0	527945.7	557702.3
7	9	809819.5	809619.5	725718.7	776059.2
7	10	890137.1	887494.3	834775.1	857613.4
7	11	929465.7	930367.3	888029.2	904248.8
7	12	941002.1	.0	903795.4	.0
8	7	229096.5	207207.5	257186.2	135708.9
8	8	412672.3	541714.5	564562.4	547090.1
8	9	747003.2	754315.0	740513.7	717779.6
8	10	838990.3	800047.7	200899.9	746432.1
8	11	881234.6	889048.6	954760.1	857390.4
8	12	897220.4	.0	862711.8	.0
9	7	332953.4	303407.3	352584.8	333295.8
9	8	567300.3	542489.2	572771.9	566847.2
9	9	727742.2	715421.3	737337.0	758469.1
9	10	824487.1	792533.6	813950.5	826313.0
9	11	853381.5	834897.0	854732.0	864929.8
9	12	862352.2	.0	866286.8	.0
10	7	340793.2	313442.7	365172.3	323438.6
10	8	580348.6	553187.2	613780.4	568821.2
10	9	716810.1	691229.0	753170.6	723708.4
10	10	781611.0	764843.7	824729.1	752072.6
10	11	822822.4	814569.3	869046.1	862436.5
10	12	838302.3	.0	877379.1	.0
11	7	268727.6	260939.1	273384.6	286215.1
11	8	511933.4	511833.2	518267.7	506244.7
11	9	639165.7	641372.2	656355.1	623149.2
11	10	704606.5	706155.5	741157.6	717047.0
11	11	750552.6	753772.4	774694.1	775970.6
11	12	769124.7	.0	793594.0	.0
12	7	299234.2	267067.6	302946.9	271390.9
12	8	563440.9	429372.3	551620.7	506002.7
12	9	686905.3	593502.6	687626.6	655220.6
12	10	743389.0	703170.0	740122.7	715963.2
12	11	772468.3	741493.6	774073.1	759827.4
12	12	778609.6	.0	784414.0	.0
13	7	295864.7	260371.8	.0	.0
13	8	571625.0	507976.9	.0	.0
13	9	715512.0	644030.2	.0	.0
13	10	775936.9	708430.0	.0	.0
13	11	824577.9	813171.6	.0	.0
13	12	835773.7	.0	.0	.0

Table D-1-2. 1 MWt VIH Usable Power at 1000°K, Rectangular Aperture.

TEMPERATURE (KELVIN) = 1000.
AREA (SQ. M.) = 2.1

DAY	HOUR	EP1	EP2	EP3	EP4
1	8	472179.9	410130.6	.0	.0
1	9	486022.2	597411.7	.0	.0
1	10	599704.5	813019.1	.0	.0
1	11	677874.7	975937.9	.0	.0
1	12	687758.5	.0	.0	.0
2	8	409983.5	397601.5	540067.9	378090.7
2	9	496861.7	609047.1	728494.3	660176.2
2	10	727450.6	786618.8	816919.1	792180.2
2	11	846382.0	943072.3	860511.4	648882.0
2	12	842881.7	.0	877726.7	.0
3	8	330477.9	500289.3	506234.0	338862.4
3	9	494022.3	683917.8	673074.1	625313.9
3	10	773587.6	794383.6	789662.5	754675.2
3	11	827516.7	844848.1	865020.5	819814.9
3	12	842649.8	.0	843570.2	.0
4	8	527147.3	575873.8	580852.1	366646.9
4	9	728476.5	734792.8	744234.1	675264.3
4	10	772221.7	945315.0	823776.3	787136.1
4	11	5461e3.5	887268.7	557679.0	829034.6
4	12	621047.1	.0	568383.3	.0
5	8	438365.1	549127.5	399803.1	369068.2
5	9	638617.2	667271.0	569362.7	612366.1
5	10	765108.5	822621.0	658489.6	688817.7
5	11	842636.5	778779.9	710813.2	725891.3
5	12	870677.1	.0	725100.5	.0
6	8	176031.2	480391.6	569654.1	505835.7
6	9	421044.1	663175.6	746027.0	789164.4
6	10	630798.0	743346.3	814539.4	754721.0
6	11	772861.7	769932.7	855513.9	845351.0
6	12	801100.7	.0	865299.3	.0
7	7	130390.5	115036.5	72288.3	30219.2
7	8	432721.4	499841.2	408983.9	435640.5
7	9	690557.7	690557.7	606656.9	656997.4
7	10	771371.3	763432.5	715708.3	733551.6
7	11	810403.9	811705.5	768967.4	785187.0
7	12	821963.3	.0	784733.6	.0
8	7	110324.7	88145.7	138124.4	16647.0
8	8	293613.7	422652.7	445500.6	428028.3
8	9	627946.2	635263.2	621451.9	598717.9
8	10	709923.5	690985.9	691238.1	682737.3
8	11	761972.3	769936.8	735699.3	736328.6
8	12	778155.6	.0	743550.0	.0
9	7	213891.6	194345.5	234523.0	216234.0
9	8	468444.5	423427.4	453710.1	447735.4
9	9	618880.4	596759.5	618275.2	635407.3
9	10	695035.5	673471.8	694888.7	707251.2
9	11	734119.5	717835.2	735670.2	745868.0
9	12	743790.4	.0	747335.0	.0
10	7	221731.4	194380.9	246110.5	204376.8
10	8	481486.8	434125.4	494718.6	447759.4
10	9	597848.3	572167.2	634108.8	604646.6
10	10	682549.2	645751.9	705866.3	673010.8
10	11	723763.8	695507.5	749984.3	743374.7
10	12	711740.5	.0	754317.3	.0
11	7	149365.9	141877.3	154322.8	167153.3
11	8	392877.6	394771.4	399205.9	367182.9
11	9	520103.9	522310.4	547293.3	509087.5
11	10	595544.7	597093.7	620395.8	597985.2
11	11	631467.8	634710.6	655632.3	656908.8
11	12	650062.9	.0	674522.2	.0
12	7	130172.4	48005.8	103385.1	152329.1
12	8	434378.3	312310.5	432558.9	386940.9
12	9	567844.3	463440.8	568564.9	536158.8
12	10	634527.2	583105.2	621272.9	599901.4
12	11	633426.5	622431.8	655011.3	642765.6
12	12	617347.8	.0	665353.3	.0
13	7	176902.9	141310.0	.0	.0
13	8	436563.2	399815.1	.0	.0
13	9	594452.7	524968.4	.0	.0
13	10	698375.1	599268.2	.0	.0
13	11	735616.1	700110.0	.0	.0
13	12	718711.6	.0	.0	.0

Table D-1-3. 1 MWt VIH Usable Power at 15000K, Rectangular Aperture.

TEMPERATURE (KELVIN) = 1500.
AREA (SQ. M.) = 2.1

DAY	HOUR	EP1	EP2	EP3	EP4
1	8	.0	.0	.0	.0
1	9	12833.8	213723.1	.0	.0
1	10	236015.9	329330.5	.0	.0
1	11	394186.1	392249.2	.0	.0
1	12	404367.9	.0	.0	.0
2	8	.0	.0	56378.9	.0
2	9	156173.1	.0	244205.7	176487.6
2	10	283783.9	302930.2	333229.5	308491.6
2	11	365191.4	359383.7	376822.8	365193.4
2	12	386695.1	.0	388033.1	.0
3	8	.0	16600.7	22545.4	.0
3	9	177333.7	202229.2	229385.5	141625.7
3	10	246369.0	310695.0	305971.9	270986.4
3	11	342928.1	361159.5	381331.9	336126.3
3	12	356961.2	.0	359381.6	.0
4	8	17453.7	97185.2	97163.5	.0
4	9	240147.9	255104.2	260545.5	191575.7
4	10	336523.1	361496.4	340058.2	305447.5
4	11	405491.9	403590.1	373990.4	345346.0
4	12	417358.5	.0	394694.7	.0
5	8	.0	65639.2	.0	.0
5	9	146324.6	192582.4	86173.7	128677.5
5	10	281414.9	340232.4	174901.0	205125.1
5	11	359947.9	396091.2	227124.6	243203.7
5	12	386938.6	.0	241411.9	.0
6	8	.0	.0	85965.5	22197.1
6	9	.0	184487.0	262349.4	305475.8
6	10	137099.4	259657.7	330350.9	311032.4
6	11	288693.1	306244.1	371225.3	361662.4
6	12	317413.1	.0	381510.7	.0
7	7	.0	.0	.0	.0
7	8	.0	5152.6	.0	.0
7	9	206369.1	206859.1	122968.3	173208.8
7	10	237582.7	284743.9	232019.7	254563.0
7	11	326716.3	327616.9	285275.8	301498.4
7	12	335251.7	.0	301045.0	.0
8	7	.0	.0	.0	.0
8	8	.0	.0	.0	.0
8	9	144257.3	151564.6	137763.3	115029.2
8	10	226239.9	197297.3	198149.5	143651.7
8	11	278364.2	285298.2	252009.7	254640.0
8	12	294470.0	.0	259961.4	.0
9	7	.0	.0	.0	.0
9	8	.0	.0	.0	.0
9	9	125191.9	112670.9	134586.6	155718.7
9	10	202136.7	199753.2	211200.1	223562.6
9	11	251132.9	234146.6	251981.6	262179.4
9	12	260101.9	.0	263536.4	.0
10	7	.0	.0	.0	.0
10	8	.0	.0	11030.0	.0
10	9	114159.7	89478.6	150420.2	120958.0
10	10	178360.6	162093.3	221977.7	149322.2
10	11	230272.0	211918.9	256295.7	259656.1
10	12	238051.9	.0	270628.7	.0
11	7	.0	.0	.0	.0
11	8	.0	.0	.0	.0
11	9	36415.7	38621.8	83604.7	25398.9
11	10	101856.1	103405.1	138407.2	114296.6
11	11	147309.2	151022.0	171943.7	173220.2
11	12	160174.3	.0	190843.6	.0
12	7	.0	.0	.0	.0
12	8	.0	.0	.0	.0
12	9	34155.4	.0	84976.2	52470.2
12	10	140638.6	99419.6	137582.3	116212.8
12	11	186737.9	136743.2	171132.7	157077.0
12	12	173659.2	.0	181663.6	.0
13	7	.0	.0	.0	.0
13	8	.0	.0	.0	.0
13	9	111761.6	41279.8	.0	.0
13	10	173189.5	105679.6	.0	.0
13	11	221927.5	156421.4	.0	.0
13	12	237302.9	.0	.0	.0

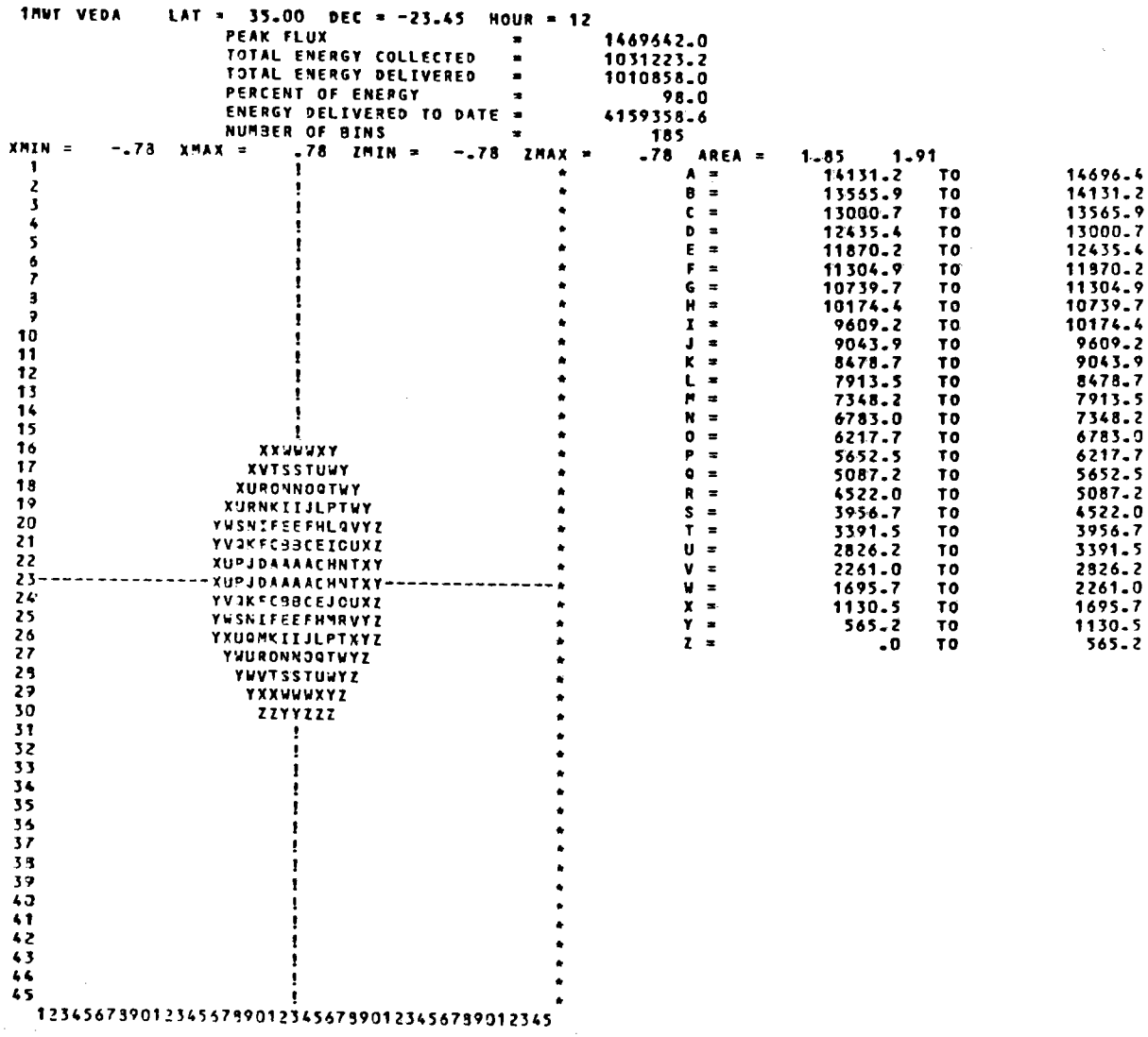

Figure D-1-4. 1 MWt VIH Design Point Round Aperture Characteristics.

Table D-1-4. 1 MWt VIH Power Through the Round Aperture.

DAY	HR	ER1	ER2	ER3	ER4
1	8	590548.6	528572.0	.0	.0
1	9	616944.3	818277.7	.0	.0
1	10	940912.9	934212.3	.0	.0
1	11	1000094.8	993151.8	.0	.0
1	12	1010858.0	.0	.0	.0
2	8	527612.1	515577.7	657362.2	495819.7
2	9	759537.9	528536.4	848242.2	779868.7
2	10	898655.9	907868.5	938241.0	913443.4
2	11	971542.1	965710.9	983214.8	971542.1
2	12	965623.2	.0	995093.7	.0
3	8	438762.1	618677.7	624615.9	457426.3
3	9	781628.4	804569.2	813743.7	745849.3
3	10	894697.2	915540.8	910806.9	875741.4
3	11	951031.2	968444.2	988711.5	943293.2
3	12	962303.6	.0	965231.8	.0
4	8	619630.3	694287.0	699260.7	485255.4
4	9	847818.1	857773.4	863214.2	794250.8
4	10	894809.4	967106.7	945507.6	910768.8
4	11	1011921.8	1010003.0	980305.3	951556.4
4	12	1024417.8	.0	991616.0	.0
5	8	553673.7	667601.9	508265.3	487554.8
5	9	753948.1	787662.8	690089.3	732665.0
5	10	887548.4	946591.0	780526.6	810966.7
5	11	967448.4	902271.7	833969.8	849122.2
5	12	994372.8	.0	848541.1	.0
6	8	297087.2	599431.6	688702.3	624935.1
6	9	604092.4	789834.7	867953.0	911222.6
6	10	743497.0	866659.5	938203.5	918287.4
6	11	893927.1	911527.0	977290.9	967099.7
6	12	923712.3	.0	988158.5	.0
7	7	229922.4	236432.6	193258.1	150769.6
7	8	603859.4	610799.7	529590.3	559439.6
7	9	812796.3	812796.3	728566.3	779104.3
7	10	893154.8	890506.9	837603.8	860524.6
7	11	932739.1	933642.9	891155.7	907432.4
7	12	944982.4	.0	907618.2	.0
8	7	231873.8	209719.5	260304.1	137354.0
8	8	414241.9	543774.6	566709.4	549170.7
8	9	749250.0	756579.0	742736.3	719933.9
8	10	830768.1	801763.4	802617.4	748032.8
8	11	883481.1	890514.5	857133.6	859771.2
8	12	898929.4	.0	864355.1	.0
9	7	335221.3	305473.9	355993.2	337579.6
9	8	570483.7	545335.4	575777.0	569821.2
9	9	730128.2	717569.7	739551.2	760746.8
9	10	806127.5	793754.8	815204.8	827586.2
9	11	854231.9	837240.7	855083.0	865285.0
9	12	863907.1	.0	867345.9	.0
10	7	343499.2	316302.8	368504.4	326389.9
10	8	583353.0	555859.4	616745.4	571569.0
10	9	718945.1	693191.1	755308.5	725762.7
10	10	781856.9	765084.3	824987.6	752309.2
10	11	823053.5	814798.0	869290.2	862678.6
10	12	829630.3	.0	872147.1	.0
11	7	271100.1	263635.2	276209.3	289172.4
11	8	512932.8	514830.3	519273.4	507227.0
11	9	639602.2	641810.2	666810.1	628578.2
11	10	704035.3	705583.0	740556.8	716465.7
11	11	749384.9	752592.7	773481.6	774756.1
11	12	768172.5	.0	792611.6	.0
12	7	302248.3	168750.4	305998.4	274124.5
12	8	555535.9	430997.7	553708.9	507918.2
12	9	687563.1	583060.0	688284.6	655847.6
12	10	742347.5	701186.3	739295.5	717955.9
12	11	771589.9	740631.3	773172.9	758943.8
12	12	775980.5	.0	783980.5	.0
13	7	298966.3	263368.3	.0	.0
13	8	574689.5	508819.3	.0	.0
13	9	715007.2	643575.8	.0	.0
13	10	775042.4	707613.3	.0	.0
13	11	822761.4	817268.1	.0	.0
13	12	834299.8	.0	.0	.0

Table D-1-5. 1 MWt VIH Usable Power at 1000°K, Round Aperture.

TEMPERATURE (KELVIN) = 1000.
AREA (SQ. M.) = 1.9

DAY	HOUR	ER1	ER2	ER3	ER4
1	8	432826.0	420849.4	.0	.0
1	9	529231.7	710555.1	.0	.0
1	10	533193.3	826459.7	.0	.0
1	11	892373.2	890429.2	.0	.0
1	12	903136.4	.0	.0	.0
2	8	419893.9	407855.1	549639.6	388097.1
2	9	651815.3	420813.8	740519.6	672146.1
2	10	780732.7	800145.9	830518.4	805720.8
2	11	9[illegible]	857948.3	875492.2	962819.5
2	12	887900.6	.0	887371.1	.0
3	8	331039.5	510955.1	516893.2	349702.7
3	9	673935.3	696946.6	706021.1	638126.7
3	10	756774.6	807615.2	803384.3	769012.8
3	11	843309.6	860721.6	880988.9	935570.6
3	12	854561.0	.0	857509.2	.0
4	8	511907.7	586564.4	591538.1	377532.8
4	9	740096.5	750050.8	755491.6	686528.2
4	10	752086.8	859394.1	827765.0	803046.2
4	11	904169.2	902280.4	872582.7	843833.8
4	12	916695.2	.0	883993.4	.0
5	8	445951.1	559879.3	400542.7	379822.2
5	9	646225.5	679940.2	592766.7	624942.4
5	10	779325.3	832868.4	672904.0	703244.1
5	11	859725.6	794549.1	726247.2	741399.6
5	12	897150.2	.0	740818.5	.0
6	8	139364.6	491709.0	560979.7	517212.5
6	9	495567.8	682112.1	760230.4	803500.0
6	10	635774.4	759936.9	830480.9	810564.8
6	11	736204.5	803804.4	869568.3	859377.1
6	12	815987.7	.0	880425.9	.0
7	7	122193.9	129710.0	85535.5	43047.0
7	8	496135.9	503077.1	421367.7	451717.0
7	9	705071.7	705073.7	620843.7	671381.7
7	10	735432.2	752764.3	729881.2	752602.0
7	11	825015.9	825920.3	793433.1	799709.8
7	12	837259.6	.0	799395.6	.0
8	7	124151.2	101996.9	152581.5	29631.4
8	8	206519.7	436052.0	458986.8	441448.1
8	9	641527.4	643856.4	635013.7	612211.3
8	10	723045.5	694040.6	694894.8	640310.2
8	11	779758.5	782791.9	749411.0	752048.6
8	12	791204.8	.0	756532.5	.0
9	7	227498.7	197751.3	248270.6	229857.0
9	8	462761.1	437612.8	466054.4	462098.1
9	9	622405.6	609847.1	671328.6	653024.2
9	10	698404.9	686032.2	707482.2	719863.5
9	11	746509.2	729518.1	747360.4	757562.4
9	12	756184.5	.0	759623.3	.0
10	7	235776.6	208530.2	260781.8	218667.3
10	8	475620.4	448176.9	509022.8	463846.4
10	9	611223.5	585468.5	647585.9	618040.1
10	10	694124.1	657361.7	717265.0	644536.6
10	11	715330.9	707075.4	761567.6	754956.0
10	12	721907.7	.0	764424.5	.0
11	7	163277.5	155912.6	168486.7	181449.8
11	8	405210.2	407107.7	411550.8	399504.4
11	9	534479.0	534037.6	559087.5	520855.6
11	10	596312.7	597880.4	632234.2	603743.1
11	11	644668.3	644870.1	665759.0	667033.5
11	12	660449.2	.0	684969.0	.0
12	7	194526.7	61027.8	198275.8	166401.9
12	8	447511.2	323275.1	445934.3	400195.6
12	9	579940.9	475337.4	590562.0	544125.0
12	10	634826.8	593463.7	631572.9	610233.3
12	11	663867.3	672906.7	665450.3	651221.2
12	12	668257.8	.0	676257.9	.0
13	7	194243.7	155665.7	.0	.0
13	8	466466.8	401096.7	.0	.0
13	9	607354.6	535552.2	.0	.0
13	10	667343.6	599690.7	.0	.0
13	11	715030.6	709545.5	.0	.0
13	12	728577.2	.0	.0	.0

Table D-1-6. 1 MWt VIH Usable Power at 1500°K, Round Aperture.

TEMPERATURE (KELVIN) = 1500.
AREA (SQ. M.) = 1.0

DAY	HOUR	ER1	ER2	ER3	ER4
1	8	45203.0	.0	.0	.0
1	9	71594.7	272932.1	.0	.0
1	10	395567.1	399860.7	.0	.0
1	11	434749.2	452806.2	.0	.0
1	12	465012.4	.0	.0	.0
2	8	.0	.0	112016.6	.0
2	9	214192.3	.0	302896.6	234523.1
2	10	343310.3	362522.9	392895.4	384097.9
2	11	426196.5	420765.3	437969.2	426196.5
2	12	430277.6	.0	449748.1	.0
3	8	.0	73332.1	79270.3	.0
3	9	236252.9	259223.6	268398.1	200503.7
3	10	349351.8	370195.2	365461.3	332395.8
3	11	405655.6	423098.6	443365.9	397947.6
3	12	415998.0	.0	419886.2	.0
4	8	24284.7	148941.4	157915.1	.0
4	9	302473.5	312477.8	317968.6	249905.2
4	10	349463.6	421741.1	400162.0	368423.2
4	11	466576.2	464457.4	434959.7	406210.8
4	12	479072.2	.0	446270.4	.0
5	8	8428.1	122256.3	.0	.0
5	9	208602.5	242317.2	144743.7	187319.4
5	10	342202.8	401245.4	235181.0	265621.1
5	11	422102.9	356926.1	288624.2	303776.6
5	12	449527.2	.0	303195.5	.0
6	8	.0	54086.0	143356.7	79589.5
6	9	58746.9	244489.1	322407.4	365877.0
6	10	199151.4	321313.9	292857.9	372941.8
6	11	348581.3	366181.4	431945.3	421754.1
6	12	378366.7	.0	442812.9	.0
7	7	.0	.0	.0	.0
7	8	58612.8	65454.1	.0	14094.0
7	9	267450.7	267450.7	183220.7	223758.7
7	10	347809.2	345161.3	272258.2	315179.0
7	11	387392.5	389297.3	345310.1	362086.8
7	12	399838.9	.0	362272.6	.0
8	7	.0	.0	.0	.0
8	8	.0	.0	21363.8	3825.1
8	9	203904.4	211233.4	197390.7	174588.3
8	10	295423.6	296417.8	257271.8	202697.2
8	11	335176.5	345168.9	311788.0	314425.6
8	12	353393.3	.0	319009.5	.0
9	7	.0	.0	.0	.0
9	8	25138.1	.0	30431.4	24475.6
9	9	184782.9	172224.1	194205.6	215401.2
9	10	260791.3	248439.2	269959.2	222240.6
9	11	308286.3	291995.1	309737.4	319939.4
9	12	318561.5	.0	322000.3	.0
10	7	.0	.0	.0	.0
10	8	38007.4	10513.8	71399.8	28223.4
10	9	172593.5	147845.5	209962.9	180417.1
10	10	236511.7	219736.7	279642.0	206963.6
10	11	277707.9	269452.4	323944.6	317333.0
10	12	284284.7	.0	326801.5	.0
11	7	.0	.0	.0	.0
11	8	.0	.0	.0	.0
11	9	94256.5	95464.6	121464.5	83232.6
11	10	159689.7	140237.4	195211.2	171120.1
11	11	204239.3	227247.1	228136.0	229410.5
11	12	220426.9	.0	247266.0	.0
12	7	.0	.0	.0	.0
12	8	10192.3	.0	8363.3	.0
12	9	142017.5	37714.4	142939.0	110502.0
12	10	197201.9	155840.7	193949.9	172610.3
12	11	226244.3	195295.7	227927.3	213598.2
12	12	230634.9	.0	238634.9	.0
13	7	.0	.0	.0	.0
13	8	29743.8	.0	.0	.0
13	9	169661.0	98230.2	.0	.0
13	10	229692.5	162267.7	.0	.0
13	11	277415.8	271622.5	.0	.0
13	12	285954.2	.0	.0	.0

```
LATITUDE OF SITE :     35.0,   SOLAR DECLINATION : -23.45,   TIME OF DAY 12:00,   TOTAL ENERGY IS :     10266000.00

                        FLUX CONTOUR
MAXIMUM SPOT DIMENSIONS, HORIZONTAL: -3.30  3.30   VERTICAL:     -2.95     2.95
HOTTEST SPOT IS   1318825.00   AT        .16       .16                          RANGES (W/SQ.M)
 1                                                                 A   1268101.0  TO     1318825.0
 2                                                                 B   1217377.0  TO     1268101.0
 3                                                                 C   1166653.0  TO     1217377.0
 4                                                                 D   1115929.0  TO     1166653.0
 5                                                                 E   1065205.0  TO     1115929.0
 6                                                                 F   1014481.0  TO     1065205.0
 7                                                                 G    963756.9  TO     1014481.0
 8                                                                 H    913032.9  TO      963756.9
 9                                                                 I    862308.8  TO      913032.9
10                                                                 J    811584.7  TO      862308.8
11                                                                 K    760860.7  TO      811584.7
12                                                                 L    710136.6  TO      760860.7
13                                                                 M    659412.6  TO      710136.6
14                ZZZZZZZZZZZZZ                                    N    608688.5  TO      659412.6
15              ZZZZZZZZZZZZZZZZ                                   O    557964.4  TO      608688.5
16             ZZZZZZZYXXXXYZZZZZZ                                 P    507240.4  TO      557964.4
17             ZZZZYXVTSSTVXYZZZZZ                                 Q    456516.3  TO      507240.4
18            ZZZZYWTQNLLNQTWYZZZZZ                                R    405792.2  TO      456516.3
19            ZZZYWTOKGFFGKOTWYZZZ                                 S    355068.2  TO      405792.2
20            ZZZYUPKFCBBCFJPUYZZZ                                 T    304344.1  TO      355068.2
21            ZZZXSPGCAAAACGPSXZZZZ                                U    253620.1  TO      304344.1
22            ZZYWRLFBAAAABFLRWYZZZ                                V    202896.0  TO      253620.1
23           ZZZYWRLFBAAAABELRWYZZ                                 W    152171.9  TO      202896.0
24           ZZZZXSPGCAAAACGPTXZZZZ                                X    101447.9  TO      152171.9
25            ZZZYUPKFCBBCFJPUYZZZZ                                Y     50723.8  TO      101447.9
26            ZZZYWTOKFFFHKOTWYZZZ                                 Z        -.2  TO       50723.8
27            ZZZZYWTGNMMNGTWYZZZZ
28             ZZZZYXVTSSTVXYZZZZZ
29             ZZZZZZYXXXXYZZZZZZ
30              ZZZZZZZZZZZZZZZZ
31                ZZZZZZZZZZZZ
32
33
34
35
36
37
38
39
40
41
42
43
44
45
  12345678901234567890123456789012345678901234567890123456789012345          AREA =  33.55
          A  B  C  D  E  F  G  H  I  J  K  L  M  N  O  P  Q  R  S  T  U  V  W  X  Y  Z
  PERCENT  5  2  2  0  0  3  2  1  0  1  2  2  2  1  1  1  1  1  2  4  1  1  4  5  7 49
CUMULATIVE 100 95 93 90 90 90 87 85 85 85 84 82 80 79 77 76 75 74 73 71 67 65 64 61 56 49
HELIOSTAT X, Y =      167.500     290.127 ; FIELD RADIUS AND =   0 ; REC. HT =   8.00
MIR. RADII =  1200.00    500.00   ; HELIO SIZE WD, HT =     3.000    2.000    BIN SIZE =   .32  METER
JITTER (MRAD) = 3.0  DISKFILE  = Y
```

Figure D-2-1. 10 MWt VIH Design Point Solar Image Characteristics at Aperture Plane.

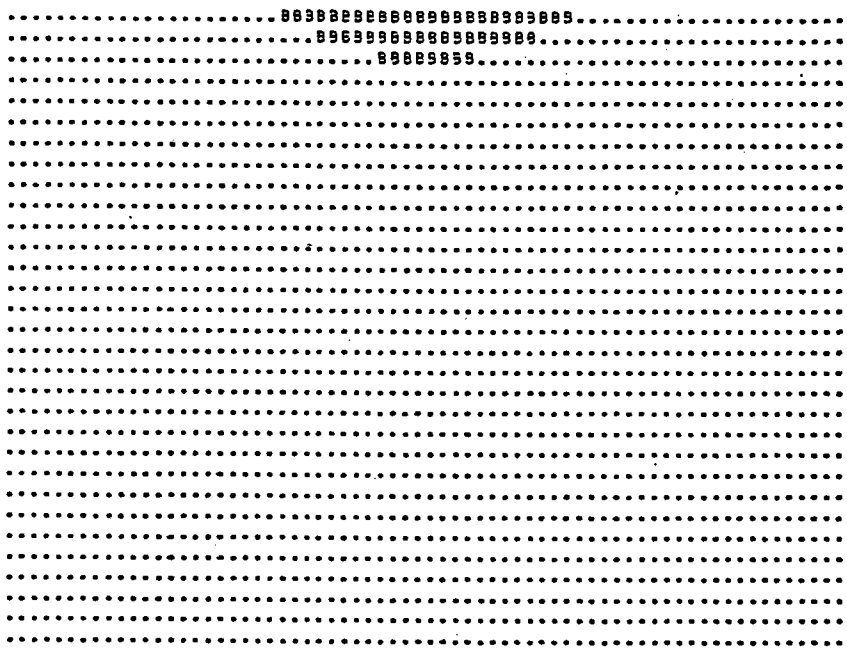

AVERAGE COSINE FACTOR = .942

WEIGHTED SHADING FACTOR = 1.000

WEIGHTED BLOCKING FACTOR = 1.000

LEGEND (.) NO SHADING, NO BLOCKING
(S) SHADING, NO BLOCKING
(B) BLOCKING, NO SHADING
(X) SHADING AND BLOCKING

Figure D-2-2. 10 MWt VIH Design Point Shading and Blocking Matrix.

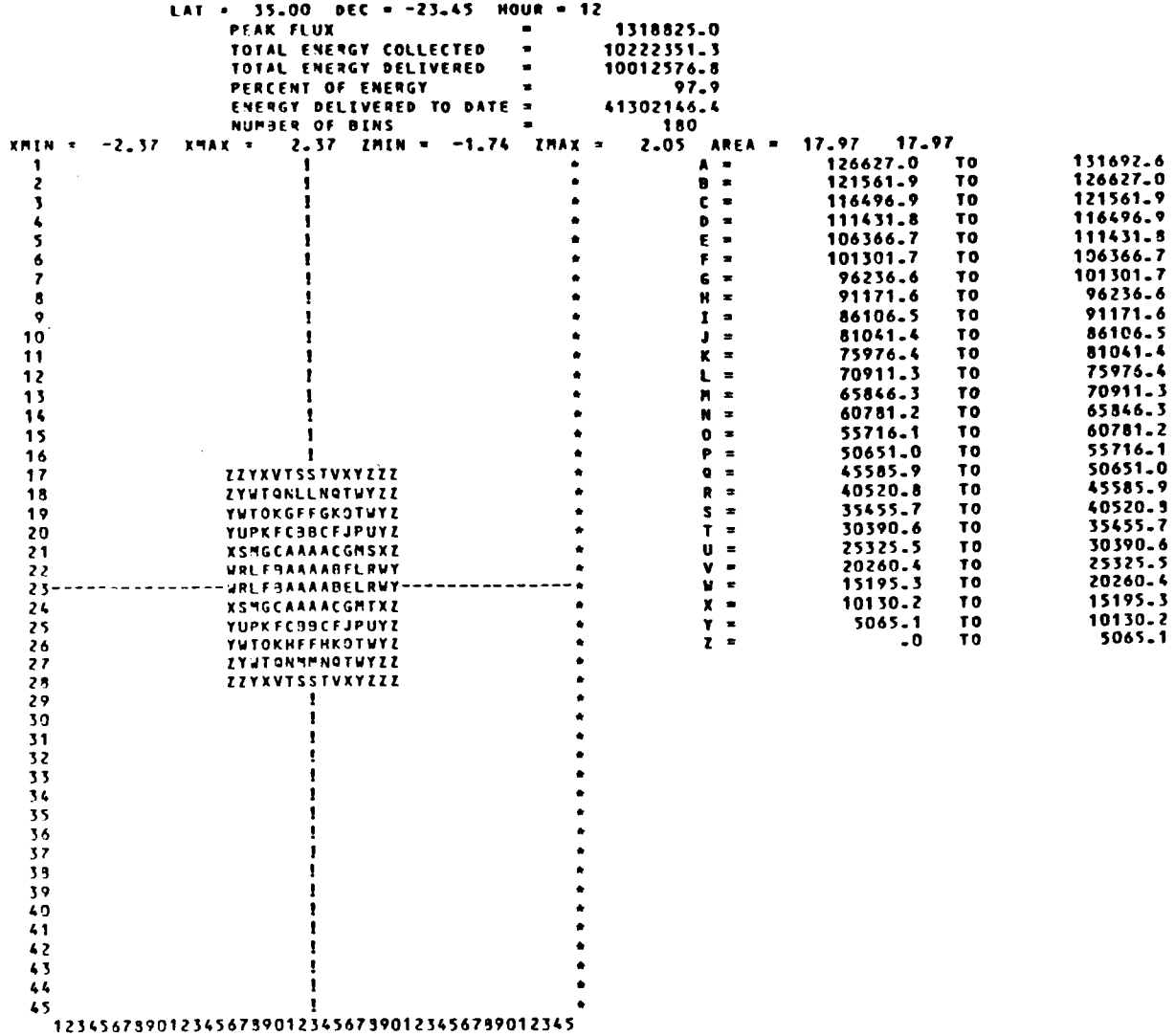

Figure D-2-3. 10 MWt VIH Design Point Rectangular Aperture Characteristics.

Table D-2-1. 10 MWt VIH Power Through the Rectangular Aperture.

DAY	HR	ER1	ER2	ER3	ER4
1	8	5884024.1	5266510.2	.0	.0
1	9	6119447.4	8116466.5	.0	.0
1	10	9381982.7	9315169.7	.0	.0
1	11	9904115.3	9884873.1	.0	.0
1	12	10012576.8	.0	.0	.0
2	8	5251596.0	5131811.6	6543066.3	4935150.4
2	9	7523287.5	5235197.8	8401911.4	7724666.6
2	10	8863248.1	9054869.8	9357798.5	9110472.6
2	11	9645821.3	9587926.4	9761711.6	9645821.3
2	12	9533201.4	.0	9824151.2	.0
3	8	4377127.4	6171980.2	6231220.2	4563322.3
3	9	7747077.9	7974454.4	8065387.1	7392454.3
3	10	8927133.3	9135107.9	9087873.9	8737995.7
3	11	9423790.5	9596335.9	9797165.3	9347114.5
3	12	9502853.6	.0	9531770.2	.0
4	8	6164718.7	6907480.4	6956963.9	4827819.2
4	9	8429156.2	8528133.8	8582227.2	7896581.4
4	10	8894807.6	9613475.5	9398770.7	9053451.4
4	11	10002776.2	9983809.5	9690249.6	9406068.4
4	12	10112850.3	.0	9789037.8	.0
5	8	5522642.7	6659025.2	5069714.4	4863136.6
5	9	7542077.6	7879340.5	6903270.0	7329173.2
5	10	8816215.0	9402698.8	7753144.0	8055512.2
5	11	9527047.8	8885214.2	8212603.3	8361819.0
5	12	9812878.8	.0	9369543.3	.0
6	8	2965094.8	5982659.4	6873630.9	6237199.3
6	9	6060570.3	7924033.7	8707757.0	9141861.0
6	10	7362128.9	8581697.3	9290118.2	9092908.2
6	11	8802529.8	8975837.4	9623416.5	9523063.6
6	12	9068067.2	.0	9700734.9	.0
7	7	2334657.7	2400763.5	1962365.1	1530931.7
7	8	6034182.0	6103544.0	5292042.0	5590317.3
7	9	8152720.0	8152720.0	7307854.0	7814773.6
7	10	8823906.4	8797747.5	8275091.7	8501537.6
7	11	9156137.3	9165018.7	8747946.9	8907726.4
7	12	9263821.4	.0	8897534.6	.0
8	7	2483076.0	2245831.2	2787528.6	1470888.3
8	8	4166252.5	5469033.1	5699700.1	5523303.6
8	9	7507269.7	7580703.8	7442004.2	7213531.2
8	10	8222166.8	7935105.0	7943557.6	7403329.8
8	11	8662472.1	8731434.6	8404137.1	8429998.6
8	12	8786728.3	.0	8448776.1	.0
9	7	3529441.7	3216241.0	3748142.8	3554272.2
9	8	5811911.7	5555708.1	5865838.2	5805162.4
9	9	7331928.8	7205817.2	7426554.6	7639400.0
9	10	7969704.4	7847382.9	8059445.4	8181853.8
9	11	8379159.6	8212492.6	8337507.9	8487579.2
9	12	8453940.2	.0	8487591.4	.0
10	7	3517095.6	3238631.0	3773124.6	3341913.6
10	8	6033393.6	5749037.8	6378757.7	5911516.0
10	9	7234054.0	6974916.6	7599944.3	7302653.2
10	10	7747806.5	7581598.7	8175210.3	7455004.0
10	11	8066370.0	7985461.7	8519514.4	8454717.9
10	12	8107781.4	.0	8523288.1	.0
11	7	2736072.4	2660733.8	2787636.7	2918466.7
11	8	5303714.6	5323334.3	5369276.2	5244717.2
11	9	6458383.9	6480679.3	6733116.3	6347069.2
11	10	6985548.5	7000904.8	7347920.1	7109884.4
11	11	7366085.0	7397615.8	7602943.3	7615471.4
11	12	7504816.0	.0	7743578.2	.0
12	7	3073958.7	1716243.9	3112097.9	2787931.0
12	8	5780796.9	4484876.7	5761785.7	5285296.2
12	9	6954020.9	5897075.0	6961317.7	6633249.5
12	10	7386821.2	6977241.3	7356452.0	7144109.6
12	11	7577064.6	7273049.2	7592609.5	7452878.7
12	12	7587725.0	.0	7665950.6	.0
13	7	3071320.5	2705617.9	.0	.0
13	8	5972721.0	5288135.8	.0	.0
13	9	7247625.8	6523565.6	.0	.0
13	10	7701963.4	7031898.8	.0	.0
13	11	8089575.2	8035564.2	.0	.0
13	12	8162015.6	.0	.0	.0

Table D-2-2. 10 MWt VIH Usable Power at 1000°K, Rectangular Aperture.

TEMPERATURE (KELVIN) = 1000.
AREA (SQ. M.) = 13.0

DAY	HOUR	ER1	ER2	ER3	ER4
1	8	48e3[illegible].3	4245990.4	.0	.0
1	9	50[illegible].[illegible]	7395916.7	.0	.0
1	10	[illegible]1462.9	8294639.9	.0	.0
1	11	[illegible]553.7	9864343.3	.0	.0
1	12	[illegible]047.3	.0	.0	.0
2	8	[illegible]369.2	4111281.8	5522536.5	3914620.6
2	9	[illegible]757.7	4214668.0	7381381.6	e704136.8
2	10	[illegible]773.3	8074740.0	8337269.7	8089942.8
2	11	[illegible]391.5	85e739e.6	8741181.8	8625291.5
2	12	[illegible]71.6	.0	8803621.4	.0
3	8	[illegible]7.6	5151450.4	5210690.4	3542792.5
3	9	[illegible]548.1	6953024.6	7044857.3	e371924.5
3	10	[illegible]03.5	8114578.1	80e7344.1	7717465.9
3	11	[illegible]3e3.7	8575806.1	8776e35.5	8326554.7
3	12	[illegible]73.9	.0	8511240.4	.0
4	8	[illegible]8.7	5886950.6	5936434.0	3307239.4
4	9	[illegible]4.4	7507604.0	7561697.4	e376051.6
4	10	[illegible]77.3	9592945.7	9678240.9	8032921.6
4	11	[illegible]46.4	89e3279.7	8669719.8	8385538.6
4	12	[illegible]330.5	.0	8768508.0	.0
5	8	[illegible]13.9	5639495.4	4049184.6	3842606.8
5	9	[illegible]47.8	4358810.7	5882740.2	e303643.4
5	10	[illegible]8.0	8382169.0	6732614.2	7034922.4
5	11	[illegible]14.0	7864694.4	7192073.5	7341289.2
5	12	[illegible]43.7	.0	7349013.5	.0
6	8	[illegible]3	4962129.6	5553101.1	5216669.5
6	9	[illegible]42.5	6903533.9	7687227.2	8121331.2
6	10	[illegible]99.1	7561157.5	8269588.4	e072378.4
6	11	[illegible]00.0	7955307.6	8602386.7	8502533.8
6	12	[illegible]7.4	.0	8e90205.1	.0
7	7	[illegible]127.3	1180232.7	941935.3	510401.9
7	8	[illegible]52.2	5263014.7	4271512.2	4569787.5
7	9	[illegible]92.7	7132190.2	6257324.2	6794243.8
7	10	[illegible]74.8	7777217.7	7254561.9	7461007.8
7	11	[illegible]07.7	8144488.9	7727417.1	7887196.6
7	12	[illegible]91.6	.0	7877004.8	.0
8	7	[illegible]46.3	1225301.4	1766998.5	450358.5
8	8	[illegible]20.7	4448503.3	4679170.3	4502773.8
8	9	[illegible]09.9	6603174.0	6421474.4	e193001.4
8	10	[illegible]77.0	4914575.2	6923027.8	6382800.0
8	11	[illegible]43.3	7710904.8	7353607.3	7409468.8
8	12	[illegible]94.5	.0	7428246.3	.0
9	7	[illegible]11.8	919e711.2	2727613.0	2533742.4
9	8	[illegible]81.9	4535179.3	4845308.4	4784632.6
9	9	[illegible]99.0	6185287.4	6406024.8	6e15870.2
9	10	[illegible]74.0	692e853.1	7038715.6	71e1324.0
9	11	[illegible]78.9	7191662.8	7366978.1	74e7049.4
9	12	[illegible]13.6	.0	7467061.6	.0
10	7	[illegible]56.5	2211101.2	2752594.8	2321383.8
10	8	[illegible]41.4	4728538.0	5258227.9	4892936.2
10	9	[illegible]34.3	6754756.8	6579414.5	6282123.4
10	10	[illegible]74.7	6561e38.9	7154680.5	6434474.2
10	11	[illegible]84.1	696.931.9	7498984.6	7434193.1
10	12	[illegible]51.6	.0	7502759.3	.0
11	7	[illegible]43.4	1e4024.0	1767126.9	1997936.9
11	8	[illegible]54.4	4102e04.5	4249746.4	4224187.4
11	9	[illegible]52.1	5460149.5	5712586.5	5326539.4
11	10	[illegible]43.7	5980375.0	6327392.3	e088354.6
11	11	[illegible]45.2	6370e4.0	6592413.5	6594941.6
11	12	[illegible]3.9	.0	6723748.4	.0
12	7	[illegible]3.3	695714.1	20915e5.1	1767401.2
12	8	[illegible]7.9	3466346.6	4741355.3	4264756.4
12	9	[illegible]1.1	6432545.2	5940787.9	5e12719.7
12	10	[illegible]1.4	5956711.5	6275922.3	6123579.8
12	11	[illegible]74.7	6753519.4	6573279.7	6438348.9
12	12	[illegible]68.2	.0	6645420.9	.0
13	7	[illegible]3.7	1695245.1	.0	.0
13	8	[illegible]1.1	4067e0e.0	.0	.0
13	9	[illegible]3.0	[illegible]16.6	.0	.0
13	10	[illegible]3.0	[illegible]59.0	.0	.0
13	11	[illegible]4.2	7015214.4	.0	.0
13	12	[illegible]6.2	.0	.0	.0

Table D-2-3. 10 MWt VIH Usable Power at 1500°K, Rectangular Aperture.

TEMPERATURE (KELVIN) = 1500.
AREA (SQ. M.) = 13.7

DAY	HOUR	EF1	EF2	EF3	EF4
1	8	7175[illegible].0	130078.1	.0	.0
1	9	6[illegible]3[illegible].9	2950034.4	.0	.0
1	10	[illegible]	4145737.6	.0	.0
1	11	[illegible]	4713441.0	.0	.0
1	12	[illegible]	.0	.0	.0
2	8	[illegible]	.0	1376634.2	.0
2	9	[illegible]	64765.7	3235479.3	2558234.5
2	10	[illegible]	3688437.7	4191366.4	3744040.5
2	11	[illegible]	4421494.3	4595279.5	4474389.2
2	12	[illegible]	.0	4657719.1	.0
3	8	.0	1005548.1	1064788.1	.0
3	9	[illegible]	2804072.7	2899955.0	2226022.2
3	10	[illegible]	3966675.8	3901441.8	3571563.6
3	11	[illegible]	4429003.8	4630733.2	4182692.4
3	12	[illegible]	.0	4365738.1	.0
4	8	[illegible]	1741048.3	1790571.7	.0
4	9	[illegible]	3361701.7	3415795.1	2730149.3
4	10	[illegible]	4447047.4	4232338.6	3957019.3
4	11	[illegible]	4817377.4	[illegible]	4239636.3
4	12	[illegible]	.0	4622605.7	.0
5	8	[illegible]	1492593.1	.0	.0
5	9	[illegible]	2712028.4	1736937.9	2162741.1
5	10	[illegible]	4236266.7	2586711.9	2859080.1
5	11	[illegible]	3718792.1	3046171.2	3195386.9
5	12	[illegible]	.0	3203111.2	.0
6	8	.0	816237.3	1707198.3	1070767.2
6	9	[illegible]	2757601.6	3541324.9	3375428.9
6	10	[illegible]	3415255.2	4123586.1	3726476.1
6	11	[illegible]	3909405.3	4456984.4	4356631.5
6	12	[illegible]	.0	4534302.8	.0
7	7	.0	.0	.0	.0
7	8	[illegible]	937111.9	1256809.9	427895.2
7	9	[illegible]	2986287.9	2141471.9	2643341.5
7	10	[illegible]	3631315.4	3108659.6	3335105.5
7	11	[illegible]	3998566.6	3581514.8	3741294.3
7	12	[illegible]	.0	3731102.5	.0
8	7	.0	.0	.0	.0
8	8	.0	302621.0	533268.0	156871.5
8	9	[illegible]	2414271.7	2275572.1	2047099.1
8	10	[illegible]	2769672.9	2777125.5	2236897.7
8	11	[illegible]	3165002.5	3237705.0	2963566.5
8	12	[illegible]	.0	3252344.0	.0
9	7	.0	.0	.0	.0
9	8	[illegible]	389276.0	699406.1	438730.3
9	9	[illegible]	2079785.1	2260122.5	2472967.9
9	10	[illegible]	2680950.9	2993013.3	3015421.7
9	11	[illegible]	3044080.5	3221075.9	3321147.1
9	12	[illegible]	.0	3321159.3	.0
10	7	.0	.0	.0	.0
10	8	[illegible]	783605.7	1212725.6	745093.9
10	9	[illegible]	1609496.5	2432512.2	2126221.1
10	10	[illegible]	2415166.6	3005778.2	2283571.9
10	11	[illegible]	2819039.6	3353083.3	3293285.8
10	12	[illegible]	.0	[illegible]	.0
11	7	.0	.0	.0	.0
11	8	[illegible]	156932.2	232844.1	78235.1
11	9	[illegible]	1114247.2	[illegible]	1182637.1
11	10	[illegible]	1674472.7	2131488.0	1942452.3
11	11	[illegible]	2271187.7	2436511.2	2449039.3
11	12	[illegible]	.0	2577146.1	.0
12	7	.0	.0	.0	.0
12	8	[illegible]	.0	595353.6	115864.1
12	9	[illegible]	770640.6	1794598.6	1466817.4
12	10	[illegible]	1410839.2	2190219.2	1977677.5
12	11	[illegible]	1906617.1	2426177.4	2286446.6
12	12	[illegible]	.0	2496518.5	.0
13	7	.0	.0	.0	.0
13	8	[illegible]	101703.7	.0	.0
13	9	[illegible]	1157133.5	.0	.0
13	10	[illegible]	1865456.7	.0	.0
13	11	[illegible]	2269132.1	.0	.0
13	12	[illegible]	.0	.0	.0

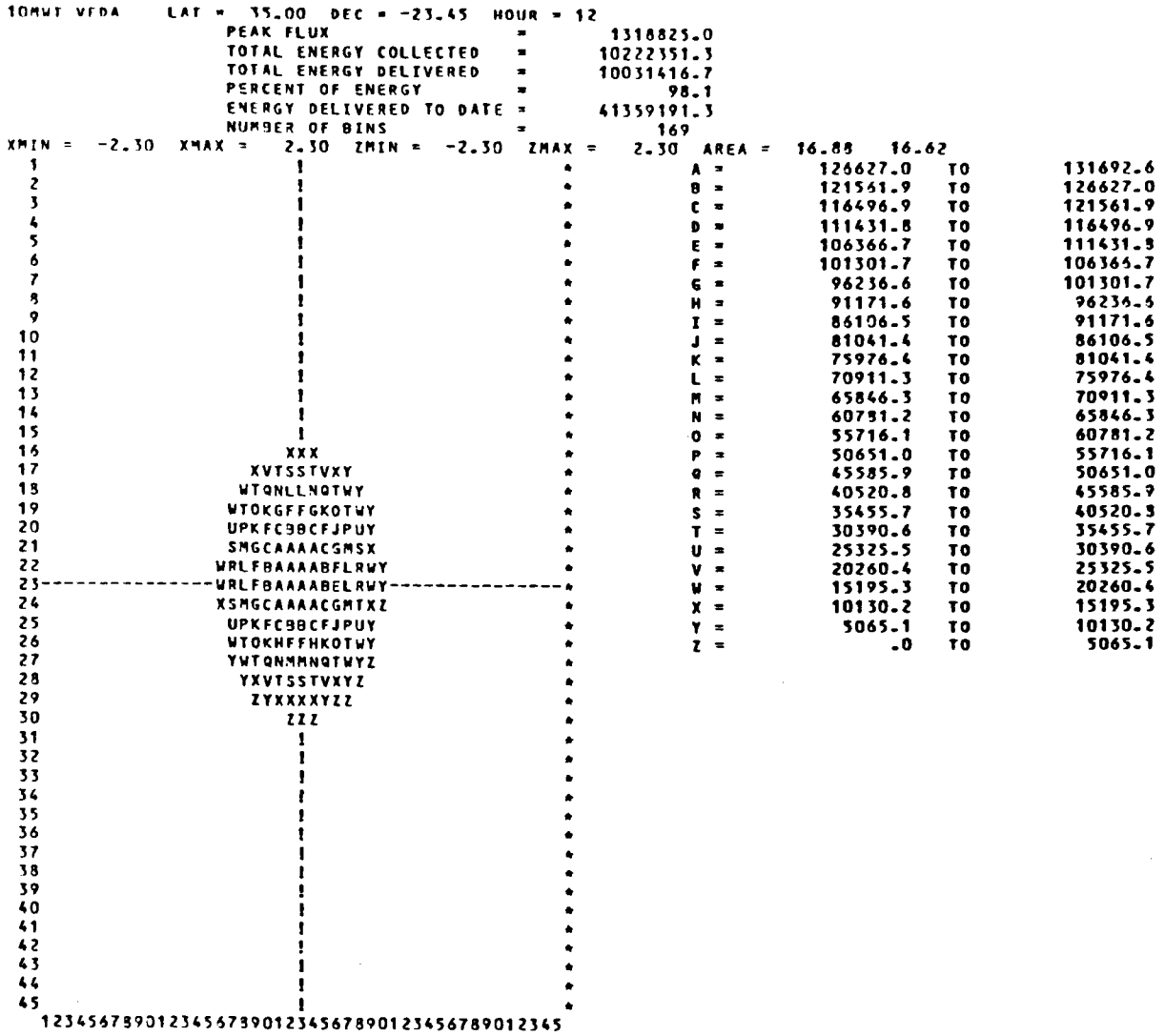

Figure D-2-4. 10 MWt VIH Design Point Round Aperture Characteristics.

Table D-2-4. 10 MWt VIH Power Through the Round Aperture.

DAY	HR	ER1	ER2	ER3	ER4
1	8	5882744.1	5265364.5	.0	.0
1	9	6122974.3	8121144.4	.0	.0
1	10	9398299.1	9331369.9	.0	.0
1	11	9923757.1	9904476.7	.0	.0
1	12	10031416.7	.0	.0	.0
2	8	5250979.1	5131208.8	6542297.7	4934570.6
2	9	7532264.3	5241444.5	8411936.6	7733883.7
2	10	8875758.0	9067650.1	9371006.3	9123331.4
2	11	9662030.0	9604037.8	9778115.0	9662030.0
2	12	9552624.1	.0	9844166.6	.0
3	8	4378531.2	6173959.7	6233218.7	4564785.9
3	9	7750096.5	7977561.7	8068529.8	7395334.7
3	10	8941625.6	9149937.8	9102627.2	8752180.9
3	11	9444310.4	9617231.5	9818498.1	9367467.4
3	12	9528551.4	.0	9557546.2	.0
4	8	6164276.9	6906985.4	6956465.2	4827473.3
4	9	8437459.2	8536534.4	8590681.0	7904359.9
4	10	8908974.6	9628787.1	9413740.3	9067871.0
4	11	10029812.3	10010794.3	9716440.9	9431491.7
4	12	10135028.6	.0	9810505.9	.0
5	8	5525995.5	6663068.0	5072792.3	4866089.1
5	9	7551472.4	7889155.4	6911869.1	7338302.8
5	10	8840163.3	9428240.2	7774204.6	8077394.1
5	11	9552570.7	8909017.6	8234604.8	8384220.2
5	12	9838024.7	.0	8390990.6	.0
6	8	2968856.5	5990249.3	6882351.1	6245112.1
6	9	6075305.8	7943299.9	8728928.7	9164088.2
6	10	7379366.6	8601780.5	9311870.1	9114198.3
6	11	8829106.4	9002937.3	9652471.6	9551815.7
6	12	9100301.2	.0	9735217.8	.0
7	7	2343392.8	2409745.9	1969707.2	1536659.7
7	8	6048073.8	6117595.5	5304225.3	5603187.2
7	9	8172311.3	8172311.3	7325415.1	7833552.8
7	10	8852394.7	8526151.3	8301808.1	8528985.1
7	11	9192351.5	9201268.0	8782546.6	8942958.0
7	12	9296096.9	.0	8928533.9	.0
8	7	2484175.0	2246825.2	2788762.3	1471539.3
8	8	4190309.6	5487485.7	5718931.0	5541939.4
8	9	7531550.0	7605221.6	7466073.3	7236861.4
8	10	8252385.2	7964268.4	7972752.0	7430538.8
8	11	8696248.8	8765480.1	8436906.4	8462868.8
8	12	8824411.7	.0	8485010.2	.0
9	7	3530034.7	3216781.5	3748772.6	3554869.4
9	8	5827216.7	5570338.4	5881285.2	5820449.6
9	9	7363678.8	7237021.0	7458714.3	7672481.4
9	10	8006778.0	7883887.5	8096936.4	8219914.3
9	11	8412178.1	8244854.3	8420559.3	8521025.0
9	12	8485861.9	.0	8519640.1	.0
10	7	3524330.7	3245293.2	3780886.3	3348788.3
10	8	6057839.1	5772331.2	6404602.5	5935467.7
10	9	7267238.8	7006912.6	7634807.5	7336152.7
10	10	7784978.4	7617973.2	8214432.8	7490771.1
10	11	8098223.5	8016995.6	8553157.3	8488104.9
10	12	8145498.0	.0	8562937.6	.0
11	7	2745297.1	2669704.5	2797035.3	2929306.4
11	8	5328584.9	5348296.6	5394454.0	5269310.9
11	9	6491643.6	6514053.8	6767790.8	6379755.6
11	10	7022624.4	7038062.2	7386919.3	7146614.9
11	11	7396003.1	7427661.9	7633823.4	7646402.4
11	12	7535488.9	.0	7775226.9	.0
12	7	3087501.4	1723805.0	3125808.6	2800213.5
12	8	5816089.3	4512256.6	5796960.9	5317562.6
12	9	6992552.8	5929750.5	6999890.1	6670004.0
12	10	7422668.4	7011100.8	7392151.7	7178778.9
12	11	7610771.5	7305403.6	7626385.6	7486033.1
12	12	7620541.9	.0	7699105.9	.0
13	7	3086645.6	2719118.2	.0	.0
13	8	6038655.6	5319951.7	.0	.0
13	9	7289070.8	6560870.2	.0	.0
13	10	7740953.4	7067486.6	.0	.0
13	11	8123764.9	8069525.5	.0	.0
13	12	8197200.9	.0	.0	.0

Table D-2-5. 10 MWt VIH Usable Power at 1000^{O}K, Round Aperture.

TEMPERATURE (KELVIN) = 1000.
AREA (SQ. M.) = 14.6

DAY	HOUR	ER1	ER2	ER3	ER4
1	8	[illegible]	4324209.2	.0	.0
1	9	[illegible]	7179959.1	.0	.0
1	10	[illegible]	8390214.6	.0	.0
1	11	[illegible]	9963321.4	.0	.0
1	12	[illegible]	.0	.0	.0
2	8	[illegible]	4190053.5	5601142.4	3993415.3
2	9	[illegible]	4700239.2	7470781.3	6792728.4
2	10	[illegible]	9126494.8	8429351.0	8182176.1
2	11	[illegible]	9562882.5	9836959.7	6720874.7
2	12	[illegible]	.0	8903011.3	.0
3	8	[illegible]	5232804.4	5292063.4	3623630.6
3	9	[illegible]	7036406.4	7127374.5	6454179.4
3	10	[illegible]	9209782.5	8161471.9	7811025.6
3	11	[illegible]	9676076.2	9577342.8	8426312.1
3	12	[illegible]	.0	8616790.9	.0
4	8	[illegible]	5965830.1	6015309.9	3556318.0
4	9	[illegible]	7595379.1	7649325.7	6963204.6
4	10	[illegible]	8697631.5	3472595.0	5126715.7
4	11	[illegible]	9069639.0	9775285.6	8490336.4
4	12	[illegible]	.0	3869350.6	.0
5	8	[illegible]	5721912.7	4131637.0	3924933.8
5	9	[illegible]	6949000.1	5970713.8	6397147.5
5	10	[illegible]	8487084.9	6833049.7	7136238.8
5	11	[illegible]	7967862.3	7293449.5	7443064.9
5	12	[illegible]	.0	7449935.3	.0
6	8	[illegible]	5049094.0	5941195.6	5303956.8
6	9	[illegible]	7002144.6	7737773.4	8222932.9
6	10	[illegible]	7660625.2	9370714.8	8173043.0
6	11	[illegible]	8061782.0	9711316.3	8610660.4
6	12	[illegible]	.0	8794062.5	.0
7	7	[illegible]	1468590.6	1028551.9	595504.4
7	8	[illegible]	5176440.2	4363070.0	4662031.9
7	9	[illegible]	7231156.0	6384259.8	6592397.5
7	10	[illegible]	7984996.0	7360652.8	7587829.8
7	11	[illegible]	9260112.7	7841391.3	8001802.7
7	12	[illegible]	.0	7957376.5	.0
8	7	[illegible]	1305669.9	1847607.0	530384.0
8	8	[illegible]	4544330.4	4777775.7	4600734.1
8	9	[illegible]	6664056.3	6524918.0	6295706.1
8	10	[illegible]	7023113.1	7031596.7	6459333.5
8	11	[illegible]	7824324.8	7495751.1	7521713.5
8	12	[illegible]	.0	7543854.9	.0
9	7	[illegible]	2275626.2	2807617.3	2613714.1
9	8	[illegible]	4629183.1	4940129.9	4879294.3
9	9	[illegible]	6295865.7	6517589.0	6731326.1
9	10	[illegible]	6942732.2	7155781.1	7273759.0
9	11	[illegible]	7703499.0	7479404.0	7579869.7
9	12	[illegible]	.0	7578484.8	.0
10	7	[illegible]	2304137.9	2839731.0	2407633.0
10	8	[illegible]	4971175.9	5463447.2	4994312.4
10	9	[illegible]	6065757.3	6693652.2	6394997.4
10	10	[illegible]	6576917.9	7273277.5	6549615.5
10	11	[illegible]	7075840.3	7612002.0	7546949.6
10	12	[illegible]	.0	7621782.3	.0
11	7	[illegible]	1708549.2	1855880.0	1987151.1
11	8	[illegible]	4407141.3	4453298.7	4328155.6
11	9	[illegible]	5572899.5	5826635.5	5438600.3
11	10	[illegible]	6094906.9	6445764.0	6205459.6
11	11	[illegible]	6486506.6	6692668.1	6705247.1
11	12	[illegible]	.0	6874071.6	.0
12	7	[illegible]	729649.7	[illegible]	1359058.2
12	8	[illegible]	3571121.3	4575805.6	4176407.3
12	9	[illegible]	4959595.2	6059734.8	5728248.7
12	10	[illegible]	5069545.5	6450996.4	6237623.6
12	11	[illegible]	6364248.3	6655230.3	6544877.8
12	12	[illegible]	.0	6757950.6	.0
13	7	[illegible]	1777962.9	.0	.0
13	8	[illegible]	4373776.4	.0	.0
13	9	[illegible]	5619714.9	.0	.0
13	10	[illegible]	6176331.3	.0	.0
13	11	[illegible]	7124370.2	.0	.0
13	12	[illegible]	.0	.0	.0

Table D-2-6. 10 MWt VIH Usable Power at 1500°K, Round Aperture.

TEMPERATURE (KELVIN) = 1500.
AREA (SQ. M.) = 16.0

DAY	HOUR	EP1	EP2	EP3	EP4
1	8	1118145.0	500766.0	.0	.0
1	9	1356525.8	3356545.9	.0	.0
1	10	4e32700.0	4665771.4	.0	.0
1	11	5159158.5	5139878.2	.0	.0
1	12	5166915.2	.0	.0	.0
2	8	4847e10.5	7466e10.3	1777699.2	169972.1
2	9	3787665.8	4766546.0	3647338.1	2969285.2
2	10	4111159.5	4307051.6	460e407.8	4354732.9
2	11	4897471.5	4814479.3	5013516.5	4897431.5
2	12	4736326.1	.0	5079568.1	.0
3	8	.0	1409361.9	1466620.2	.0
3	9	2963498.0	3912963.2	3303951.3	2e30736.2
3	10	4177327.1	4795179.3	4338029.7	3987582.4
3	11	4e78711.9	4972e33.0	5053899.6	4602868.9
3	12	4781103.9	.0	4792947.7	.0
4	8	1116678.4	2142396.9	2191966.7	62874.8
4	9	2e30161.7	3771935.9	352e082.5	3139761.4
4	10	4144778.1	4864189.6	4649141.8	4303272.5
4	11	4e5213.3	5246145.8	4951842.4	4666893.2
4	12	4770433.1	.0	5045907.4	.0
5	8	7e1597.0	1398469.5	309193.8	101490.6
5	9	2736623.9	3124556.9	2147270.6	2573704.3
5	10	4077344.9	4463641.7	3809606.1	3312795.6
5	11	47e7972.0	4144419.1	3470006.3	3619621.7
5	12	5071426.2	.0	3626392.1	.0
6	8	.0	1225650.8	2117752.6	1480513.6
6	9	1310707.7	2179701.4	3964330.2	4399489.7
6	10	3e14748.1	3837152.0	4547271.6	4349599.8
6	11	4044707.3	4238238.8	4687873.1	4767217.2
6	12	4215722.7	.0	4970619.3	.0
7	7	.0	.0	.0	.0
7	8	12e3475.7	1352997.0	539626.8	538588.7
7	9	2407712.9	3407712.8	2560916.6	3066954.3
7	10	4037796.2	4261552.8	3537209.6	3764386.6
7	11	4e37767.2	4436e69.5	4017949.1	4173359.5
7	12	4531498.6	.0	4143935.4	.0
8	7	.0	.0	.0	.0
8	8	.0	722837.2	954332.5	777340.9
8	9	37e8951.9	2940623.1	2701474.8	2472262.0
8	10	4487766.7	3199e69.5	3202153.5	2665940.7
8	11	3971e50.7	4000881.6	3672307.9	3659270.3
8	12	4039813.2	.0	3720411.7	.0
9	7	.0	.0	.0	.0
9	8	10e2e13.2	805739.9	1116686.7	1055851.1
9	9	2595091.3	2472422.5	2694115.8	2907232.9
9	10	3e4e179.5	3119239.0	3332337.9	2456315.9
9	11	3e47779.8	3480255.8	3655960.8	3756426.5
9	12	3771e63.4	.0	3755041.6	.0
10	7	.0	.0	.0	.0
10	8	1093340.6	1007732.7	1640004.0	1170869.2
10	9	2e20e40.2	2242314.1	2870209.0	2571554.2
10	10	3010779.6	2953374.7	3449934.3	2726172.6
10	11	3330605.0	3252397.1	3788559.8	3723506.4
10	12	3360899.5	.0	3798339.1	.0
11	7	.0	.0	.0	.0
11	8	5e7959.4	593e98.1	629955.5	504712.4
11	9	1727340.1	1749455.3	2003192.3	1615157.1
11	10	2e59e90.2	2273443.7	2622320.8	2382016.4
11	11	2e71e04.6	2667063.4	2869224.9	2981803.9
11	12	2770960.4	.0	3010628.4	.0
12	7	.0	.0	.0	.0
12	8	1051e50.3	.0	1270362.4	552964.1
12	9	1937954.7	11e5152.0	2335791.6	1905405.5
12	10	2e59e04.8	2246502.7	2e27653.2	2414180.4
12	11	28ae173.2	2640506.1	2961787.1	2721434.6
12	12	2835443.4	.0	2934307.4	.0
13	7	.0	.0	.0	.0
13	8	1244057.6	555353.2	.0	.0
13	9	2534479.3	1756271.7	.0	.0
13	10	2e7e354.9	2302598.1	.0	.0
13	11	3259166.4	3304927.0	.0	.0
13	12	3402e83.4	.0	.0	.0

```
LATITUDE OF SITE :    35.0,   SOLAR DECLINATION : -23.45,   TIME OF DAY 12:00,   TOTAL ENERGY IS :    10451690.00

                          FLUX CONTOUR
MAXIMUM SPOT DIMENSIONS, HORIZONTAL: -3.33  3.26   VERTICAL:    -3.36     3.30
HOTTEST SPOT IS    953826.90   AT       .16     -.16                    RANGES (W/SQ.M)
 1                                                                A    917141.2  TO      953826.9
 2                                                                B    880455.6  TO      917141.2
 3                                                                C    843769.9  TO      880455.6
 4                                                                D    807084.2  TO      843769.9
 5                                                                E    770398.5  TO      807084.2
 6                                                                F    733712.8  TO      770398.5
 7                                                                G    697027.1  TO      733712.8
 8                                                                H    660341.4  TO      697027.1
 9                                                                I    623655.7  TO      660341.4
10                                                                J    586970.1  TO      623655.7
11                                                                K    550284.4  TO      586970.1
12                    Z                                           L    513598.7  TO      550284.4
13                  ZZZZZZZZ                                      M    476913.0  TO      513598.7
14                ZZZZZZZZZZZZ                                    N    440227.3  TO      476913.0
15              ZZZZZYYXXYYZZZZ                                   O    403541.6  TO      440227.3
16            ZZZZYXVUTTUVXYZZZ                                   P    366855.9  TO      403541.6
17            ZZYXVTQOMMNPSVYZZ                                   Q    330170.2  TO      366855.9
18          ZZZXVRNKHHHIKNRVYZZ                                   R    293484.6  TO      330170.2
19          ZZYVSNIEDCCDFINRWYZ                                   S    256798.9  TO      293484.6
20          ZZXTOJEBAAAAACFJOTXZZ                                 T    220113.2  TO      256798.9
21          ZYWSMGCAAAAAADGMRWZZ                                  U    183427.5  TO      220113.2
22        ZZYVRLF3AAAAAAACFL9VZZ                                  V    146741.8  TO      183427.5
23        ZZYV9KF3AAAAAAACFL3VYZ                                  W    110056.1  TO      146741.8
24        ZZZWRMGCAAAAAAACGMRWZZ                                  X     73370.4  TO      110056.1
25          ZZXTOID9AAAAA9EIOTXZZ                                 Y     36684.8  TO       73370.4
26          ZZYVRMHDB93CEHMRVYZZ                                  Z        -.9   TO      36684.8
27          ZZZXVRMJGFFHJNRUXZZZ
28           ZZZXVSPNLMNPSVXZZZZ
29           ZZZZYWVTSSTVWYZZZZZ
30            ZZZZZYYXXXYZZZZZZ
31            ZZZZZZZZZZZZZZZZ
32              ZZZZZZZZZZZZZ
33                  ZZZZ
34
35
36
37
38
39
40
41
42
43
44
45
  12345678901234567890123456789012345678901234567890123456789012345              AREA =  35.65
          A   B   C   D   E   F   G   H   I   J   K   L   M   N   O   P   Q   R   S   T   U   V   W   X   Y   Z
  PERCENT   9   2   3   1   1   2   1   2   1   1   1   1   3   2   1   1   1   3   2   3   1   5   2   5   6  39
CUMULATIVE 100  91  89  86  85  84  82  80  78  77  76  75  74  71  69  68  67  66  62  61  59  57  52  50  45  39
HELIOSTAT X, Y =      205.800     356.466 ; FIELD RADIUS AND =    0 ; REC. HT =    8.00
MIR. RADII =    950.00    850.00   ; HELIO SIZE WD, HT =     7.010     7.320    BIN SIZE =   .32  METER
JITTER (MRAD) = 3.0  DISKFILE  = Y
```

Figure D-3-1. 10 MWt Repowering Heliostat Design Point Solar Image Characteristics at Aperture Plane.

10 MWT 1:5, DAY 1, HOUR 12

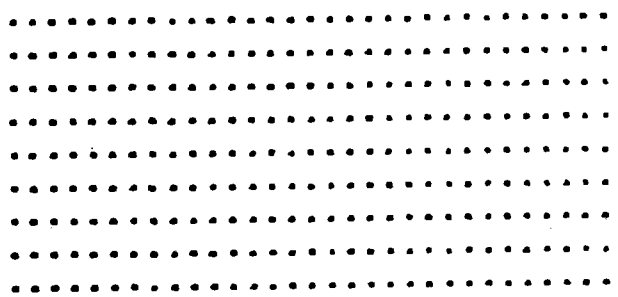

AVERAGE COSINE FACTOR = .941

WEIGHTED SHADING FACTOR = 1.000

WEIGHTED BLOCKING FACTOR = 1.000

LEGEND (.) NO SHADING, NO BLOCKING
(1) SHADING, NO BLOCKING
(2) BLOCKING, NO SHADING
(4) SHADING AND BLOCKING

Figure D-3-2. 10 MWt Repowering Heliostat Design Point Shading and Blocking Matrix.

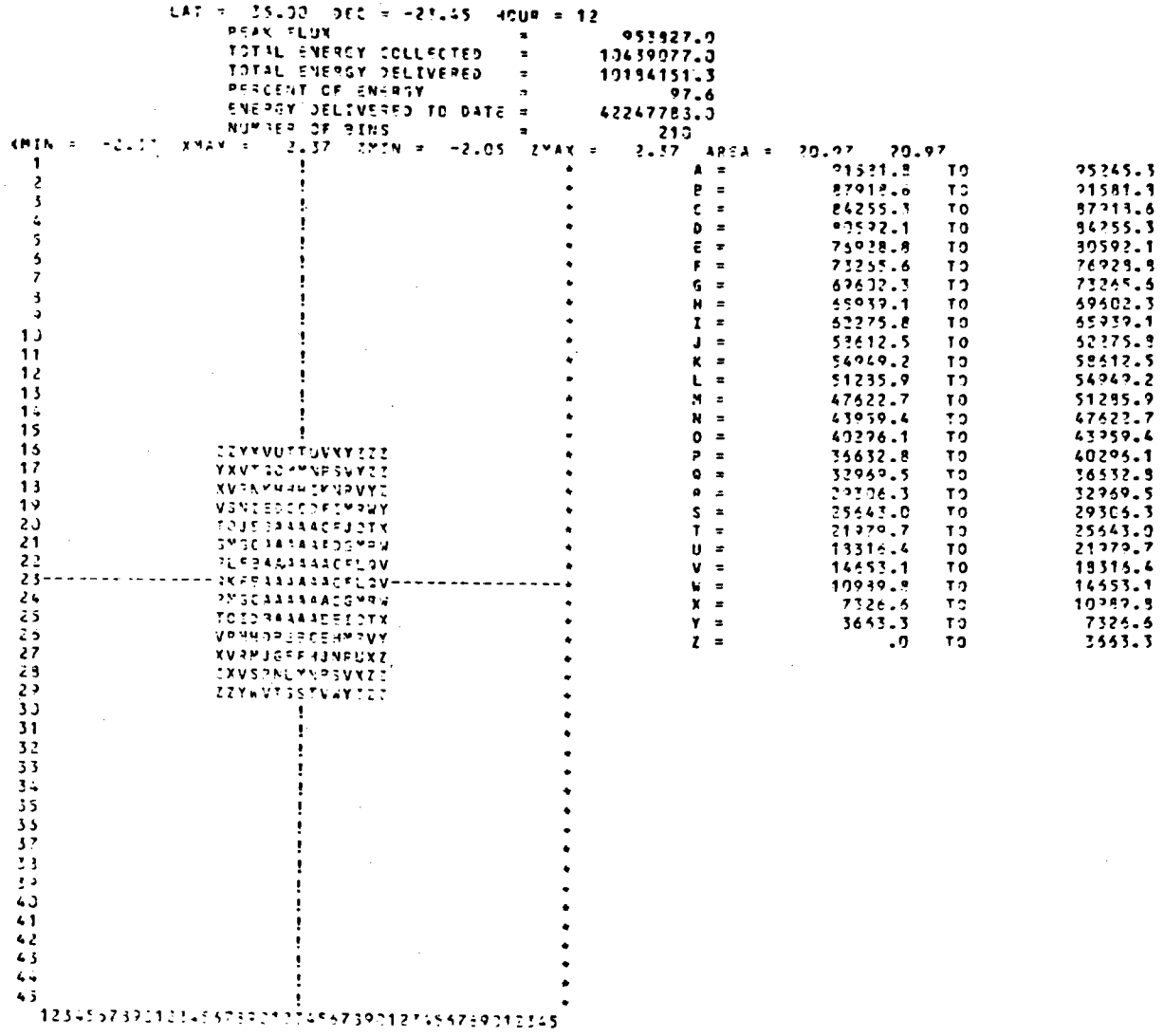

Figure D-3-3. 10 MWt Repowering Heliostat Design Point Rectangular Aperture Characteristics.

Table D-3-1. 10 MWt Repowering Heliostat Power Through the Rectangular Aperture.

DAY	HR	ER1	ER2	ER3	ER4
1	8	8205595.7	5557018.4	.0	.0
1	9	8270302.4	8316419.9	.0	.0
1	10	9506511.1	9439811.2	.0	.0
1	11	10079328.1	10055747.4	.0	.0
1	12	10144151.7	.0	.0	.0
2	8	9539359.1	5413010.2	6901594.8	5205572.8
2	9	7696740.3	5355937.7	8595621.3	7903762.4
2	10	8963863.1	9176560.0	9483559.8	9232910.1
2	11	9793569.7	9734794.0	9911235.2	9793569.7
2	12	9792567.3	.0	9988383.5	.0
3	8	6621625.4	6516735.9	6579284.9	4813221.3
3	9	7900366.8	8132160.1	8224891.1	7538650.1
3	10	9031600.1	9242036.5	9194221.8	8840249.2
3	11	9531701.7	9706292.9	9909352.0	9454147.6
3	12	9678792.1	.0	9705834.7	.0
4	8	8534902.8	7322866.5	7374721.3	5117724.1
4	9	8549567.9	8650060.6	8704927.4	8009478.9
4	10	9870393.8	9695060.7	9478533.7	9132223.9
4	11	10115684.9	10094504.1	9799633.5	9512241.6
4	12	10241354.6	.0	9913456.4	.0
5	8	5915324.5	7132506.3	5430191.2	5209924.9
5	9	7535604.5	7324813.8	6943110.2	7371471.4
5	10	8877974.7	9463567.0	7807456.7	8111943.0
5	11	9591107.7	9944958.4	8267824.9	8418043.9
5	12	9940355.6	.0	8478270.1	.0
6	8	3179758.2	6415784.8	7371259.7	6683752.5
6	9	6020979.2	7373269.4	8650873.0	9082141.2
6	10	7364303.7	8594028.5	9292869.2	9395600.8
6	11	8856547.6	9031030.6	9682581.1	9581611.2
6	12	9109740.4	.0	9744887.6	.0
7	7	3177767.9	3267745.9	2671029.7	2083793.7
7	8	6482553.1	6557371.4	5685530.4	6005983.9
7	9	8030297.8	8030297.8	7198118.5	7697426.1
7	10	8771754.5	8745750.2	8226183.5	8451291.0
7	11	9144101.4	9152971.3	8736447.7	8896017.1
7	12	9249686.5	.0	8883957.6	.0
8	7	2730156.0	2469937.2	3065689.2	1617664.6
8	8	4292535.7	5434804.9	5872463.6	5690720.4
8	9	7211814.6	7403532.4	7268074.4	7044941.1
8	10	8035364.2	7302806.4	7811120.0	7279899.1
8	11	8564149.2	8532349.0	8308765.8	8334333.8
8	12	8717569.4	.0	8382260.9	.0
9	7	2702163.4	2507937.9	2922700.6	2771525.5
9	8	5602472.7	5550508.9	5260348.7	5799729.7
9	9	7055412.2	6943892.8	7156596.3	7361704.6
9	10	7752944.8	7648627.3	7855314.6	7974622.7
9	11	8007551.5	8044395.9	8215829.0	8313852.0
9	12	8088147.8	.0	8331178.6	.0
10	7	2426221.3	2334679.8	2602483.3	2305944.6
10	8	5277469.3	5600650.0	6214116.3	5753934.5
10	9	6926893.8	6659475.8	7256236.6	6972390.6
10	10	7478393.4	7318454.4	7891462.7	7196253.5
10	11	7637735.4	7759120.3	8278035.8	8215075.9
10	12	7695738.9	.0	8330378.8	.0
11	7	1675802.4	1629464.2	1707181.0	1787302.8
11	8	5021309.4	5039884.4	5083380.1	4965453.5
11	9	6835946.7	6106956.4	6344836.0	5981051.2
11	10	6689810.7	6703514.6	7035894.0	6807008.8
11	11	7071456.4	7101726.0	7298840.8	7310867.8
11	12	7245395.0	.0	7475300.6	.0
12	7	1530749.7	862559.4	1600361.9	1433662.7
12	8	5136717.1	4923975.8	5169556.6	4742138.0
12	9	6824089.0	6572471.8	6530914.7	6223130.2
12	10	7014103.7	6825378.2	6955465.2	6783831.8
12	11	7089033.0	6990683.1	7276937.7	7143015.9
12	12	7140450.5	.0	7335100.2	.0
13	7	1617164.9	1424678.5	.0	.0
13	8	5038541.2	4691229.6	.0	.0
13	9	6777352.3	6103273.6	.0	.0
13	10	7299471.1	6684534.6	.0	.0
13	11	7720913.3	7171051.3	.0	.0
13	12	7834447.9	.0	.0	.0

Table D-3-2. 10 MWt Repowering Heliostat Usable Power at 1000^{o}K, Rectangular Aperture.

TEMPERATURE (KELVIN) = 1000.
AREA (SQ. M.) = [illegible]

DAY	HOUR	ER1	ER2	ER3	ER4
1	8	[illegible]	4366400.3	.0	.0
1	9	[illegible]	7125800.8	.0	.0
1	10	[illegible]	5749193.1	.0	.0
1	11	[illegible]	7963129.3	.0	.0
1	12	[illegible]	.0	.0	.0
2	8	[illegible]	4222392.1	5710976.7	4014954.7
2	9	[illegible]	4165279.6	7405003.2	6713144.3
2	10	[illegible]	7985941.9	8292941.7	8042292.0
2	11	[illegible]	8544169.9	8720617.1	8602951.6
2	12	[illegible]	.0	8727765.4	.0
3	8	[illegible]	5329117.8	5388666.8	3627603.2
3	9	[illegible]	6941542.0	7034273.0	6348032.0
3	10	[illegible]	9051390.4	8003603.7	7649631.1
3	11	[illegible]	8515604.8	8718733.9	8263529.5
3	12	[illegible]	.0	8515216.6	.0
4	8	[illegible]	6131648.4	6184103.2	3927106.0
4	9	[illegible]	7459442.5	7514309.3	6818860.8
4	10	[illegible]	8504442.6	8287915.6	7939665.8
4	11	[illegible]	8905886.0	9609012.4	8321623.5
4	12	[illegible]	.0	8722839.3	.0
5	8	[illegible]	5941890.2	4239573.1	4018306.8
5	9	[illegible]	6734195.7	5752492.1	6160853.3
5	10	[illegible]	8277948.9	6616938.6	6921324.9
5	11	[illegible]	7754340.3	7077206.8	7227425.8
5	12	[illegible]	.0	7287652.0	.0
6	8	[illegible]	5225166.7	6150641.6	5498134.4
6	9	[illegible]	6591651.3	7460254.9	7891523.1
6	10	[illegible]	7393610.4	8102251.1	7904952.7
6	11	[illegible]	7840402.5	8491963.0	8390993.1
6	12	[illegible]	.0	8554269.5	.0
7	7	[illegible]	2077127.2	1480411.6	893175.6
7	8	[illegible]	5366753.3	4494912.3	4815365.9
7	9	[illegible]	6879679.7	6007500.4	6506808.0
7	10	[illegible]	7555132.1	7035565.4	7260672.9
7	11	[illegible]	7962353.2	7545929.6	7705399.0
7	12	[illegible]	.0	7693339.5	.0
8	7	[illegible]	1279119.1	1875071.1	427046.5
8	8	[illegible]	4444156.8	4681545.5	4500102.3
8	9	[illegible]	6212914.3	6077456.3	5854323.0
8	10	[illegible]	6613190.3	6620501.9	6089281.0
8	11	[illegible]	7441730.9	7118147.7	7143715.7
8	12	[illegible]	.0	7191642.8	.0
9	7	[illegible]	1317319.8	1732082.5	1560907.4
9	8	[illegible]	4359990.8	4669730.6	4609111.6
9	9	[illegible]	5753264.7	5965978.2	6171086.5
9	10	[illegible]	6453005.2	6664696.5	6784004.6
9	11	[illegible]	6953777.8	7035210.9	7123233.9
9	12	[illegible]	.0	7140560.5	.0
10	7	[illegible]	1044060.7	1412865.2	1115326.5
10	8	[illegible]	4410031.9	5023498.2	4568316.4
10	9	[illegible]	5468957.7	6065618.5	5781772.5
10	10	[illegible]	6127936.3	6700544.6	6003635.4
10	11	[illegible]	6563592.2	7097417.7	7024437.8
10	12	[illegible]	.0	7109760.7	.0
11	7	[illegible]	433846.1	516562.9	596694.7
11	8	[illegible]	3349256.3	3992762.0	3774835.4
11	9	[illegible]	4916336.3	5154217.9	4790433.1
11	10	[illegible]	5512996.5	5545275.9	5616390.7
11	11	[illegible]	5911107.9	6102272.7	6120249.7
11	12	[illegible]	.0	6235182.5	.0
12	7	[illegible]	.0	409743.9	243044.6
12	8	[illegible]	2333357.7	3979041.5	3551519.9
12	9	[illegible]	4341853.7	5340296.4	5032512.1
12	10	[illegible]	5434750.1	5794547.1	5593213.2
12	11	[illegible]	5790045.0	6006719.2	5952397.8
12	12	[illegible]	.0	6144432.1	.0
13	7	[illegible]	233990.4	.0	.0
13	8	[illegible]	2500611.5	.0	.0
13	9	[illegible]	4909465.5	.0	.0
13	10	[illegible]	5473586.7	.0	.0
13	11	[illegible]	5492473.2	.0	.0
13	12	[illegible]	.0	.0	.0

Table D-3-3. 10 MWt Repowering Heliostat Usable Power at 1500°K, Rectangular Aperture.

TEMPERATURE (KELVIN) = 1500.
AREA (SQ. M.) = 21.0

DAY	HOUR	ER1	ER2	ER3	ER4
1	8	131091.1	.0	.0	.0
1	9	1[illegible]2698.3	2038914.8	.0	.0
1	10	3[illegible]9207.2	3411377.1	.0	.0
1	11	4[illegible]934.0	4031243.3	.0	.0
1	12	4[illegible]647.2	.0	.0	.0
2	8	.0	.0	874390.7	.0
2	9	1[illegible]735.2	.0	2568117.2	1375258.3
2	10	2934[illegible]57.0	3149055.9	3456055.7	3205406.0
2	11	3[illegible]065.9	3707282.9	3953731.1	3766065.6
2	12	3[illegible]065.8	.0	3960879.4	.0
3	8	.0	499231.8	551780.8	.0
3	9	1[illegible]782.8	2104664.0	2197387.0	1511146.0
3	10	7[illegible]4096.0	3114504.4	3166717.7	2812745.1
3	11	3[illegible]4197.6	3678218.8	3891547.9	3426643.5
3	12	3[illegible]86.0	.0	3678370.6	.0
4	9	537393.7	1294762.4	1347217.2	.0
4	7	2[illegible]1e1.8	2622556.5	2677423.3	1981974.8
4	10	2[illegible]759.7	3567556.6	3451039.6	3102779.8
4	11	4[illegible]180.6	4069000.0	3772126.4	3484737.5
4	12	4[illegible]882.5	.0	3885952.3	.0
5	8	.0	1105024.2	.0	.0
5	9	1[illegible]100.4	1597339.7	915606.1	1343867.3
5	10	2[illegible]470.6	3441062.9	1779953.6	2084438.9
5	11	3[illegible]03.6	3917454.3	2240320.8	2390839.8
5	12	3[illegible]51.5	.0	2450766.0	.0
6	8	.0	388280.7	1343755.6	661248.4
6	9	.0	1844765.3	2623368.9	2054637.1
6	10	133[illegible]04.6	2556724.4	3265365.1	3068096.7
6	11	2[illegible]143.9	3003516.5	3655277.0	3554127.1
6	12	3[illegible]36.3	.0	3717383.5	.0
7	7	.0	.0	.0	.0
7	8	455348.0	529867.3	.0	.0
7	9	2002963.7	2002793.7	1170614.4	1669922.0
7	10	2744260.4	2718246.1	2196679.4	2423786.9
7	11	3116597.5	3125467.2	2709943.6	2663513.0
7	12	3222151.4	.0	2856453.5	.0
8	7	.0	.0	.0	.0
8	8	.0	.0	.0	.0
8	9	1304310.6	1370038.3	1240570.3	1017437.0
8	10	2057580.1	1775704.3	1783615.9	1252395.0
8	11	2536665.1	2604844.9	2281261.7	2306829.7
8	12	2690045.7	.0	2354756.6	.0
9	7	.0	.0	.0	.0
9	8	.0	.0	.0	.0
9	9	1037906.1	916378.7	1129092.2	1334200.5
9	10	1740340.5	1621119.2	1827910.5	1947118.6
9	11	2130147.4	2216691.8	2128324.9	2286347.9
9	12	2270643.5	.0	2303674.5	.0
10	7	.0	.0	.0	.0
10	8	.0	.0	186612.2	.0
10	9	879589.7	831971.7	1229732.5	944836.5
10	10	1451347.3	1390950.3	1863958.6	1163749.4
10	11	1810721.3	1731816.2	2250531.7	2187571.8
10	12	1[illegible]827.8	.0	2272974.7	.0
11	7	.0	.0	.0	.0
11	8	.0	.0	.0	.0
11	9	[illegible]2.5	79452.7	317331.9	.0
11	10	[illegible]03.0	676110.6	1008384.6	779504.7
11	11	[illegible]69.7	1074231.9	1271[illegible]6.7	1283363.7
11	12	1[illegible]90.8	.0	1448296.5	.0
12	7	.0	.0	.0	.0
12	8	.0	.0	.0	.0
12	9	49[illegible]4.9	.0	503410.9	195626.1
12	10	8[illegible]8.8	597574.1	957[illegible]1.1	756327.2
12	11	1[illegible]3.5	943159.0	1249437.2	1115511.8
12	12	1[illegible]6.5	.0	1307596.1	.0
13	7	.0	.0	.0	.0
13	8	.0	.0	.0	.0
13	9	7[illegible]7.9	72746.5	.0	.0
13	10	1[illegible]6.7	477010.7	.0	.0
13	11	1[illegible]9.7	1647547.2	.0	.0
13	12	1[illegible]3.8	.0	.0	.0

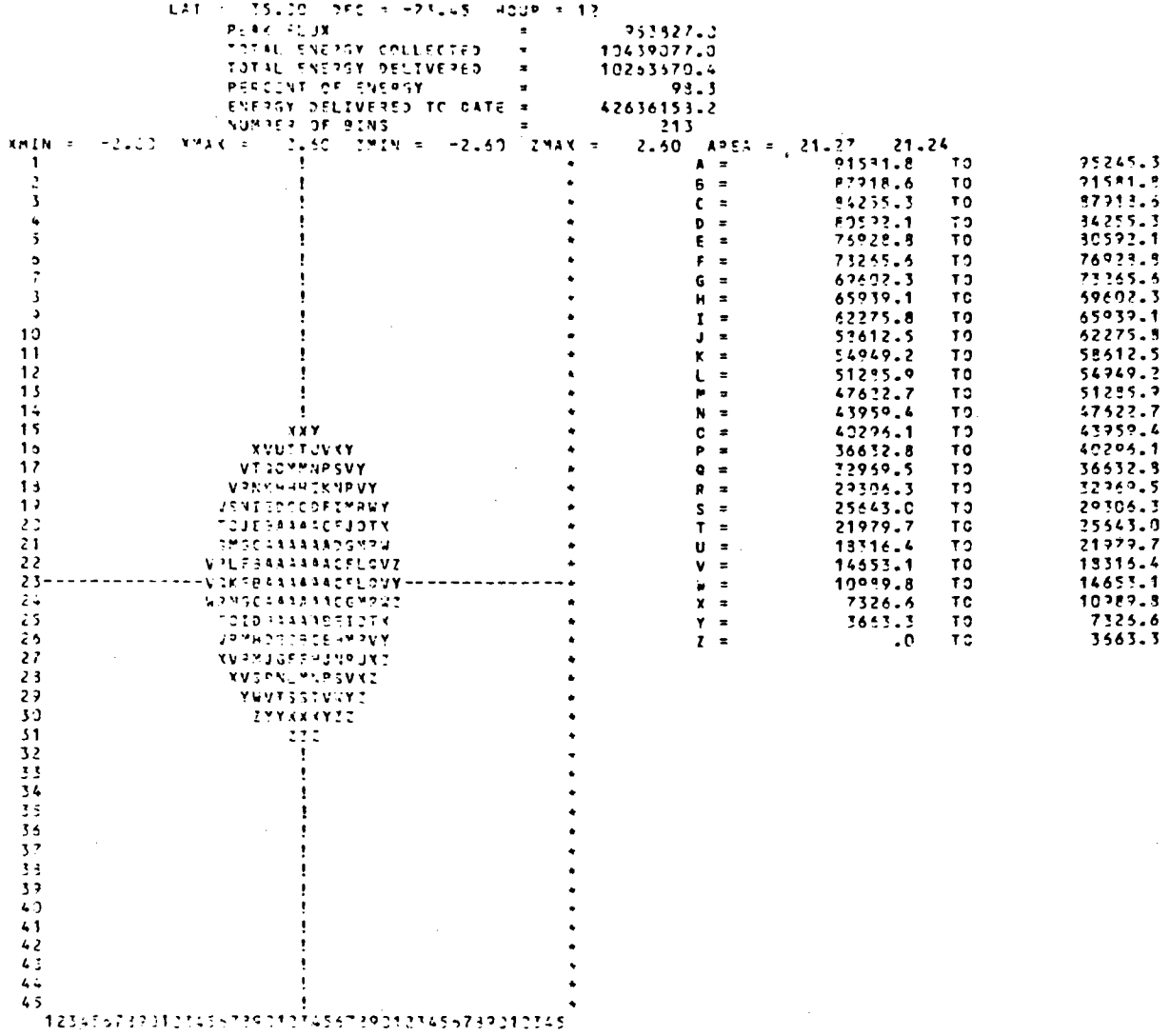

Figure D-3-4. 10 MWt Repowering Heliostat Design Point Round Aperture Characteristics.

Table D-3-4. 10 MWt Repowering Heliostat Power Through the Round Aperture.

DAY	HR	ER1	ER2	ER3	ER4
1	8	[illegible]	[illegible]	.0	.0
1	9	[illegible]	[illegible]	.0	.0
1	10	[illegible]	[illegible]	.0	.0
1	11	[illegible]	[illegible]	.0	.0
1	12	[illegible]	.0	.0	.0
2	8	[illegible]	5479024.0	5935762.5	5269056.9
2	9	[illegible]	9417947.4	3695204.1	7994318.2
2	10	[illegible]	9245772.6	9555098.1	9302547.9
2	11	[illegible]	9824215.7	10002283.8	9893537.5
2	12	[illegible]	.0	10075536.9	.0
3	8	[illegible]	6601154.2	6664513.4	4880636.8
3	9	[illegible]	8216633.1	8310217.2	7816948.7
3	10	[illegible]	9331532.3	9293262.7	8925881.4
3	11	[illegible]	9796736.0	10001761.3	9542312.0
3	12	[illegible]	.0	9796293.2	.0
4	8	[illegible]	7401707.4	7454731.9	5173247.8
4	9	[illegible]	8749678.9	8804171.2	8100794.0
4	10	[illegible]	9773497.8	9555219.0	9204151.7
4	11	[illegible]	10191959.1	9832572.9	9592751.6
4	12	[illegible]	.0	9919297.9	.0
5	8	[illegible]	7224410.0	5530153.7	5276041.4
5	9	[illegible]	8211532.1	7020855.9	7454013.7
5	10	[illegible]	9568272.0	7893065.7	8190500.2
5	11	[illegible]	9030000.0	8346428.9	8498076.0
5	12	[illegible]	.0	8541840.6	.0
6	8	[illegible]	6492761.3	7459700.0	6769004.1
6	9	[illegible]	7945771.5	8771644.8	9166939.6
6	10	[illegible]	8966789.0	9332223.5	9183058.2
6	11	[illegible]	9106937.7	9765975.3	9662156.6
6	12	[illegible]	.0	9846031.3	.0
7	7	[illegible]	3292637.9	2691376.2	2099667.0
7	8	[illegible]	6633577.9	5751604.9	6075782.4
7	9	[illegible]	8106561.4	7266478.8	7770528.4
7	10	[illegible]	8844174.9	8318760.9	8546401.8
7	11	[illegible]	9227433.7	8807521.6	8968389.1
7	12	[illegible]	.0	8952887.5	.0
8	7	[illegible]	2476919.0	3074355.1	1622237.3
8	8	[illegible]	5694234.5	5934389.3	5750729.6
8	9	[illegible]	7492330.6	7355248.1	7129438.5
8	10	[illegible]	7882598.3	7890994.9	7354341.8
8	11	[illegible]	8726892.6	8399765.4	8425613.4
8	12	[illegible]	.0	8456010.8	.0
9	7	[illegible]	2515436.8	2931439.6	2779812.5
9	8	[illegible]	5614345.9	5927749.2	5869473.0
9	9	[illegible]	7026065.6	7241296.6	7445832.5
9	10	[illegible]	7731126.3	7940247.1	8063642.1
9	11	[illegible]	8121005.1	8294279.8	8393027.3
9	12	[illegible]	.0	8409730.9	.0
10	7	[illegible]	2267876.5	2610703.8	2312339.9
10	8	[illegible]	5679119.3	6301160.7	5979521.4
10	9	[illegible]	6742099.2	7346263.9	7053896.2
10	10	[illegible]	7413457.1	7990884.6	7286916.7
10	11	[illegible]	7834600.1	8356563.5	8294991.1
10	12	[illegible]	.0	8400920.9	.0
11	7	[illegible]	1632180.9	1710027.3	1790282.7
11	8	[illegible]	5103576.1	5146612.9	5027219.3
11	9	[illegible]	[illegible]	6424621.5	[illegible]
11	10	[illegible]	[illegible]	7112733.4	6881348.6
11	11	[illegible]	[illegible]	7386286.8	7396457.9
11	12	[illegible]	.0	7576137.1	.0
12	7	[illegible]	864862.1	1604537.4	1437403.2
12	8	[illegible]	[illegible]	5236863.7	[illegible]
12	9	[illegible]	[illegible]	6619232.1	[illegible]
12	10	[illegible]	[illegible]	[illegible]	[illegible]
12	11	[illegible]	[illegible]	[illegible]	[illegible]
12	12	[illegible]	.0	[illegible]	.0
13	7	[illegible]	[illegible]	.0	.0
13	8	[illegible]	[illegible]	.0	.0
13	9	[illegible]	[illegible]	.0	.0
13	10	[illegible]	[illegible]	.0	.0
13	11	[illegible]	[illegible]	.0	.0
13	12	[illegible]	.0	.0	.0

Table D-3-5. 10 MWt Repowering Heliostat Usable Power at 1000^{o}K, Round Aperture.

TEMPERATURE (KELVIN) = 1000.
AREA (SQ. M.) = 31.2

DAY	HOUR	ER1	ER2	ER3	ER4
1	8	5094508.6	4433709.9	.0	.0
1	9	[illegible]	7199348.4	.0	.0
1	10	[illegible]	8312772.5	.0	.0
1	11	[illegible]	8931118.8	.0	.0
1	12	[illegible]	.0	.0	.0
2	8	[illegible]	4277066.7	5783805.3	4067099.6
2	9	[illegible]	4215990.1	7493246.8	6792360.9
2	10	[illegible]	8043915.5	8353130.3	8100590.6
2	11	[illegible]	8622258.4	8800326.5	8681580.2
2	12	[illegible]	.0	8873581.5	.0
3	8	[illegible]	5399196.9	5462556.1	3673679.5
3	9	[illegible]	7014655.8	7108359.9	6414991.4
3	10	[illegible]	8129575.0	8091325.4	7723924.1
3	11	[illegible]	8594780.7	8799804.0	8340354.7
3	12	[illegible]	.0	8534335.9	.0
4	8	[illegible]	6199750.6	6252774.6	3971290.5
4	9	[illegible]	7546721.6	7622213.9	6898836.7
4	10	[illegible]	8571540.5	9353261.7	8302194.4
4	11	[illegible]	8980031.8	9680615.6	8393794.3
4	12	[illegible]	.0	3796340.6	.0
5	8	[illegible]	6022452.7	4298201.4	4074084.1
5	9	[illegible]	6811594.8	5818898.5	6252056.4
5	10	[illegible]	8158304.7	6691108.0	6988543.0
5	11	[illegible]	7329042.7	7144471.6	7296118.7
5	12	[illegible]	.0	7339883.3	.0
6	8	[illegible]	5290804.0	6257742.7	5567046.8
6	9	[illegible]	6743814.2	7529687.5	7964982.3
6	10	[illegible]	7464811.7	8190266.2	7981100.9
6	11	7729141.5	7904950.4	9562018.0	8460199.3
6	12	[illegible]	.0	9644074.0	.0
7	7	[illegible]	2090680.6	1489418.9	897709.7
7	8	[illegible]	5431620.6	4549647.5	4373825.1
7	9	[illegible]	6904604.1	6064521.5	6568571.1
7	10	[illegible]	7442217.5	7118803.6	7344444.5
7	11	[illegible]	8025476.4	7605564.3	7766431.8
7	12	[illegible]	.0	7750930.2	.0
8	7	[illegible]	1274961.7	1872397.8	420290.0
8	8	[illegible]	4492767.2	4732432.0	4548772.3
8	9	[illegible]	6790373.5	6153290.8	5927431.2
8	10	[illegible]	6550641.0	5699037.6	6152384.5
8	11	[illegible]	7524935.3	7197308.1	7223656.1
8	12	[illegible]	.0	7254053.5	.0
9	7	[illegible]	1313479.5	1729482.3	1577855.2
9	8	[illegible]	4412358.6	4735791.9	4604475.7
9	9	[illegible]	5924103.3	6039339.3	6246875.2
9	10	[illegible]	6529159.0	5738099.5	6359634.8
9	11	[illegible]	6919047.8	7092113.5	7191070.0
9	12	[illegible]	.0	7237773.6	.0
10	7	[illegible]	1038919.2	1408745.5	1110382.6
10	8	[illegible]	4477162.0	5099223.4	4637664.1
10	9	[illegible]	5540141.9	6144306.6	5856938.9
10	10	[illegible]	6238699.8	6758927.3	6084959.4
10	11	[illegible]	6632642.5	7156606.2	7093033.8
10	12	[illegible]	.0	7198963.6	.0
11	7	[illegible]	430223.6	508070.0	568325.4
11	8	[illegible]	3902613.5	3944655.6	3525262.0
11	9	[illegible]	4991773.3	5222664.2	4954304.9
11	10	[illegible]	5574967.9	5910776.1	5679391.3
11	11	[illegible]	6054957.1	6184729.5	6196500.6
11	12	[illegible]	.0	6374179.5	.0
12	7	[illegible]	.0	402082.1	275445.9
12	8	[illegible]	2364545.2	4024909.4	3592654.1
12	9	[illegible]	4405110.0	5417274.9	5103729.1
12	10	[illegible]	5609456.0	5863675.4	5659727.5
12	11	[illegible]	5947376.1	6157106.9	6021674.1
12	12	[illegible]	.0	6021439.7	.0
13	7	[illegible]	225827.0	.0	.0
13	8	[illegible]	3551275.5	.0	.0
13	9	[illegible]	4971191.1	.0	.0
13	10	[illegible]	5742858.6	.0	.0
13	11	[illegible]	6564374.2	.0	.0
13	12	[illegible]	.0	.0	.0

Table D-3-6. 10 MWt Repowering Heliostat Usable Power at 1500°K, Round Aperture.

TEMPERATURE (KELVIN) = 1500.
AREA (SQ. M.) = 21.2

DAY	HOUR	ER1	ER2	ER3	ER4
1	8	211557.2	.0	.0	.0
1	9	2462[illegible]	2316396.8	.0	.0
1	10	[illegible]	[illegible]	.0	.0
1	11	[illegible]	[illegible]	.0	.0
1	12	[illegible]	.0	.0	.0
2	8	.0	.0	930853.6	.0
2	9	1721000.4	.0	2610295.2	1909409.3
2	10	[illegible]	[illegible]	[illegible]	[illegible]
2	11	[illegible]	[illegible]	[illegible]	[illegible]
2	12	[illegible]	.0	[illegible]	.0
3	8	.0	[illegible]	[illegible]	.0
3	9	[illegible]	[illegible]	[illegible]	[illegible]
3	10	[illegible]	[illegible]	[illegible]	[illegible]
3	11	[illegible]	[illegible]	[illegible]	[illegible]
3	12	[illegible]	.0	[illegible]	.0
4	8	[illegible]	[illegible]	[illegible]	.0
4	9	[illegible]	[illegible]	[illegible]	[illegible]
4	10	[illegible]	[illegible]	[illegible]	[illegible]
4	11	[illegible]	[illegible]	[illegible]	[illegible]
4	12	[illegible]	.0	[illegible]	.0
5	8	.0	[illegible]	.0	.0
5	9	[illegible]	[illegible]	[illegible]	[illegible]
5	10	[illegible]	[illegible]	[illegible]	[illegible]
5	11	[illegible]	[illegible]	[illegible]	[illegible]
5	12	[illegible]	.0	[illegible]	.0
6	8	.0	[illegible]	[illegible]	[illegible]
6	9	.0	[illegible]	[illegible]	[illegible]
6	10	[illegible]	[illegible]	[illegible]	[illegible]
6	11	[illegible]	[illegible]	[illegible]	[illegible]
6	12	[illegible]	.0	[illegible]	.0
7	7	.0	.0	.0	.0
7	8	[illegible]	[illegible]	.0	.0
7	9	[illegible]	[illegible]	[illegible]	[illegible]
7	10	[illegible]	[illegible]	[illegible]	[illegible]
7	11	[illegible]	[illegible]	[illegible]	[illegible]
7	12	[illegible]	.0	[illegible]	.0
8	7	.0	.0	.0	.0
8	8	.0	.0	.0	.0
8	9	[illegible]	[illegible]	[illegible]	[illegible]
8	10	[illegible]	[illegible]	[illegible]	[illegible]
8	11	[illegible]	[illegible]	[illegible]	[illegible]
8	12	[illegible]	.0	[illegible]	.0
9	7	.0	.0	.0	.0
9	8	.0	.0	.0	.0
9	9	[illegible]	[illegible]	[illegible]	[illegible]
9	10	[illegible]	[illegible]	[illegible]	[illegible]
9	11	[illegible]	[illegible]	[illegible]	[illegible]
9	12	[illegible]	.0	[illegible]	.0
10	7	.0	.0	.0	.0
10	8	.0	.0	216271.8	.0
10	9	[illegible]	[illegible]	[illegible]	[illegible]
10	10	[illegible]	[illegible]	[illegible]	[illegible]
10	11	[illegible]	[illegible]	[illegible]	[illegible]
10	12	[illegible]	.0	[illegible]	.0
11	7	.0	.0	.0	.0
11	8	.0	.0	.0	.0
11	9	[illegible]	[illegible]	[illegible]	.0
11	10	[illegible]	[illegible]	[illegible]	[illegible]
11	11	[illegible]	[illegible]	[illegible]	[illegible]
11	12	[illegible]	.0	[illegible]	.0
12	7	.0	.0	.0	.0
12	8	.0	.0	.0	.0
12	9	[illegible]	.0	[illegible]	[illegible]
12	10	[illegible]	[illegible]	[illegible]	[illegible]
12	11	[illegible]	[illegible]	[illegible]	[illegible]
12	12	[illegible]	.0	[illegible]	.0
13	7	.0	.0	.0	.0
13	8	.0	.0	.0	.0
13	9	[illegible]	[illegible]	.0	.0
13	10	[illegible]	[illegible]	.0	.0
13	11	[illegible]	[illegible]	.0	.0
13	12	[illegible]	.0	.0	.0

```
LATITUDE OF SITE :    35.0,   SOLAR DECLINATION : -23.45,   TIME OF DAY 12:00,   TOTAL ENERGY IS :    25731740.00

                          FLUX CONTOUR
MAXIMUM SPOT DIMENSIONS, HORIZONTAL: -6.81   6.75   VERTICAL:    -6.42     6.36
HOTTEST SPOT IS   1321757.00   AT       .79     -.16
                                                                          RANGES (W/SQ.M)
 1                                                          A   1270920.0   TO     1321757.0
 2                                                          B   1220083.0   TO     1270920.0
 3                                                          C   1169246.0   TO     1220083.0
 4                                                          D   1118409.0   TO     1169246.0
 5                                                          E   1067572.0   TO     1118409.0
 6                                                          F   1016735.0   TO     1067572.0
 7                                                          G    965898.4   TO     1016735.0
 8                                                          H    915061.6   TO      965898.4
 9                 ZZZZZZZZZZZZZ                            I    864224.8   TO      915061.6
10              ZZZZZZZZZZZZZZZZZZZ                         J    813388.0   TO      864224.8
11             ZZZZZZZZZZZZZZZZZZZZZ                        K    762551.2   TO      813338.0
12           ZZZZZZZZZYYYYYYZZZZZZZZZ                       L    711714.4   TO      762551.2
13         ZZZZZZZZYYXWWVVWWXYYZZZZZZZ                      M    660877.6   TO      711714.4
14         ZZZZZZYXWUTSRRSTUWXYZZZZZZZ                      N    610040.7   TO      660877.6
15        ZZZZZZYWVTRPONNOPRTVWYZZZZZZ                      O    559203.9   TO      610040.7
16        ZZZZZYWURPNKJIIJKNPRUWYZZZZZZ                     P    508367.1   TO      559203.9
17       ZZZZZYXUROLIGFEEFGILORUXYZZZZZ                     Q    457530.3   TO      508367.1
18       ZZZZZXVSOKHEC3B3BCEHLOSVXZZZZZ                     R    406693.5   TO      457530.3
19       ZZZZYXUQLHECAAAAAACEIMQUXYZZZZ                     S    355856.7   TO      406693.5
20       ZZZZYWSOJFCAAAAAAAACFJOSWYZZZZ                     T    305019.9   TO      355856.7
21       ZZZZYVRMIE@AAAAAAAABEIMRVYZZZZ                     U    254183.1   TO      305019.9
22       ZZZZXUQMHD@AAAAAAAABEHMQUXZZZZ                     V    203346.2   TO      254183.1
23      ZZZZZXUQMHD@AAAAAAAABEHMQUXZZZZ                     W    152509.4   TO      203346.2
24      ZZZZZYVRMIE@AAAAAAAABEIMRVYZZZZ                     X    101672.6   TO      152509.4
25      ZZZZZYWSOJFCAAAAAAAACFJOSWYZZZZ                     Y     50835.8   TO      101672.6
26       ZZZZYWUQLHECAAAAAACEIMQTWYZZZZ                     Z        -1.0   TO       50835.8
27       ZZZZZXVSOKHEC3B9BCEHKOSVXZZZZZ
28       ZZZZZYWUROLIGFEEFGILORUXYZZZZZ
29        ZZZZZYWURPNKJIIJKMPRUWYZZZZZ
30        ZZZZZZYWUSRPNNNNPRSUWYZZZZZZ
31         ZZZZZZYXWUTSRRSTUWXYZZZZZZ
32         ZZZZZZZYYXWWVVVWWXYYZZZZZZ
33          ZZZZZZZZZYYYYYYYZZZZZZZZZ
34           ZZZZZZZZZZZZZZZZZZZZZZZ
35            ZZZZZZZZZZZZZZZZZZZ
36               ZZZZZZZZZZZZZ
37
38
39
40
41
42
43
44
45
  1234567890123456789012345678901234567890123456789012345              AREA =  73.19
          A  B  C  D  E  F  G  H  I  J  K  L  M  N  O  P  Q  R  S  T  U  V  W  X  Y  Z
   PERCENT  8  2  2  0  2  1  1  1  2  1  1  1  2  1  2  1  1  2  2  1  3  2  4  3  7 47
CUMULATIVE 100 92 90 88 88 86 85 84 84 82 80 79 78 77 75 75 73 72 70 68 66 65 62 60 56 54 47
HELIOSTAT X, Y =      262.500     454.676 ; FIELD RADIUS AND =   0 ; REC. HT =   8.00
MIR. RADII =  1800.00    800.00   ; HELIO SIZE WD, HT =     3.000    2.000    BIN SIZE =  .32  METER
JITTER (MRAD) = 3.0  DISKFILE  = Y
```

Figure D-4-1. 25 MWt VIH Design Point Solar Image Characteristics at Aperture Plane.

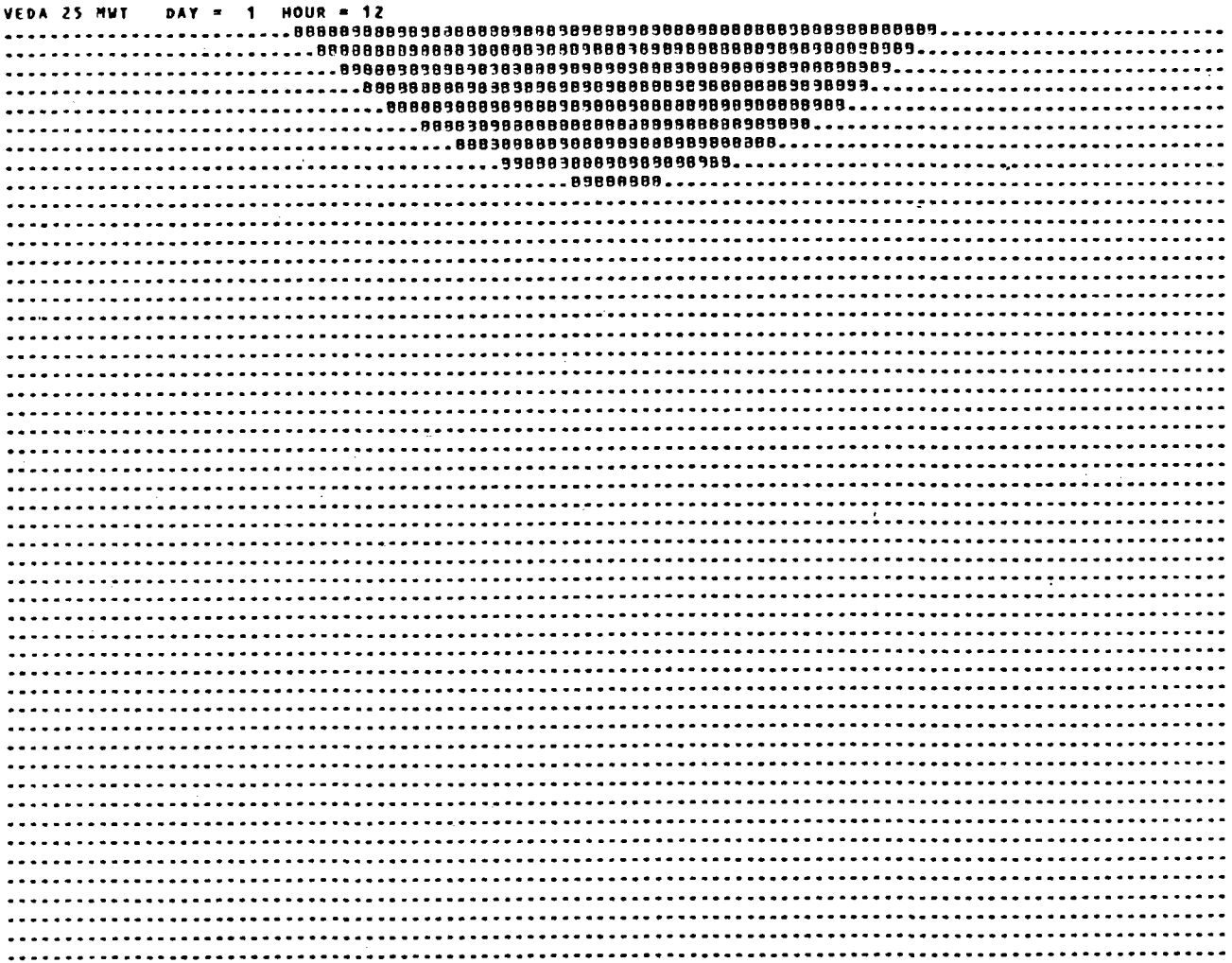

AVERAGE COSINE FACTOR = .960

WEIGHTED SHADING FACTOR = 1.000

WEIGHTED BLOCKING FACTOR = .999

LEGEND (.) NO SHADING, NO BLOCKING

(S) SHADING, NO BLOCKING

(B) BLOCKING, NO SHADING

(X) SHADING & BLOCKING

Figure D-4-2. 25 MWt VIH Design Point Shading and Blocking Matrix.

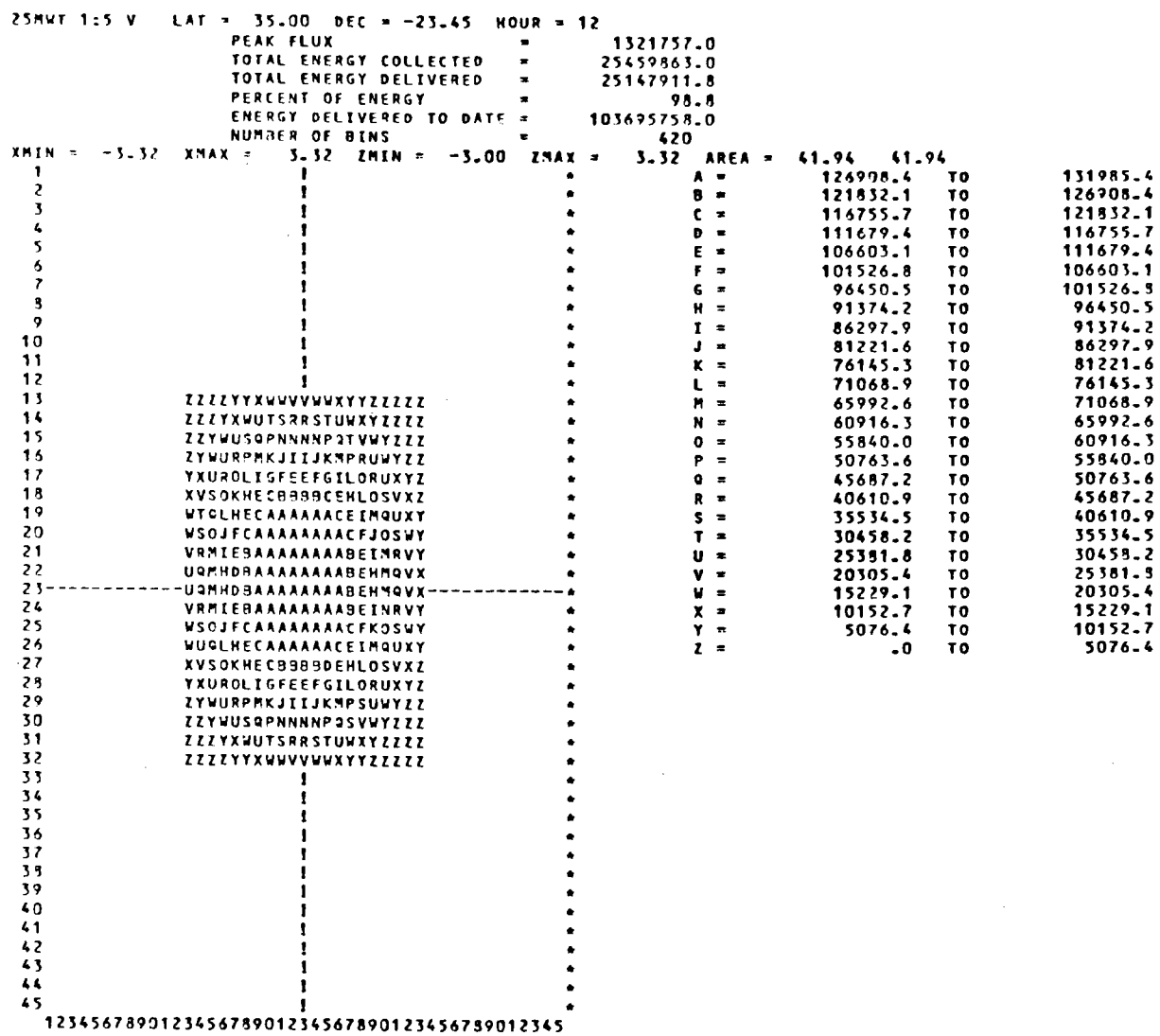

Figure D-4-3. 25 MWt VIH Design Point Rectangular Aperture Characteristics.

Table D-4-1. 25 MWt VIH Power Through the Rectangular Aperture.

DAY	HR	ER1	ER2	ER3	ER4
1	8	14709256.7	13165556.3	.0	.0
1	9	15338934.5	20344638.9	.0	.0
1	10	23592592.5	23424579.8	.0	.0
1	11	24907062.5	24858671.9	.0	.0
1	12	25147911.8	.0	.0	.0
2	8	13153181.5	12853168.9	16387906.5	12360609.8
2	9	18822140.0	13097681.9	21020325.5	19325960.4
2	10	22301703.4	22783861.8	23546090.8	22923769.6
2	11	24215310.3	24069968.2	24506246.6	24215310.3
2	12	23945831.4	.0	24676649.3	.0
3	8	10974449.3	15474551.7	15623079.6	11441282.1
3	9	19381986.6	19950847.5	20178346.9	18494773.4
3	10	22420566.4	22942896.3	22824267.8	21945545.8
3	11	23674166.9	24107630.4	24612148.0	23481543.6
3	12	23874003.3	.0	23946650.3	.0
4	8	15405290.5	17261410.9	17385067.1	12064452.8
4	9	21068699.3	21316094.2	21451300.8	19737527.3
4	10	22344154.3	24149480.2	23610132.0	22742674.5
4	11	25125710.4	25078068.3	24340683.0	23626855.7
4	12	25387111.5	.0	24574218.5	.0
5	8	13793796.7	16632117.2	12662526.7	12146561.3
5	9	18877742.0	19721907.6	17278813.3	18344844.7
5	10	22152747.3	23626421.4	19481539.4	20241308.3
5	11	23896009.9	22286144.8	20599083.2	20973350.2
5	12	24611598.4	.0	20991581.0	.0
6	8	7418319.6	14967912.3	17197018.4	15604741.3
6	9	15204049.9	19878888.9	21845002.2	22934031.5
6	10	18485803.1	21548031.2	23326852.8	22831671.8
6	11	22055267.9	22489500.5	24112049.0	23860608.7
6	12	22735127.0	.0	24321328.3	.0
7	7	5857588.4	6023445.8	4923517.0	3841063.2
7	8	15086353.4	15259768.6	13230892.9	13976625.5
7	9	20466488.3	20466488.3	18345547.1	19618111.8
7	10	22124268.4	22059679.8	20748219.8	21315989.8
7	11	22935331.2	22957578.3	21912849.6	22313083.2
7	12	23194257.8	.0	22277168.5	.0
8	7	6311799.6	5708740.6	7085696.0	3738891.6
8	8	10457723.5	13727837.1	14306835.1	13864061.8
8	9	18858462.0	19042930.4	18694513.1	18120582.9
8	10	20595998.7	19876927.4	19898100.5	18544864.8
8	11	21677198.6	21849772.1	21030734.2	21095450.7
8	12	21989882.1	.0	21144114.8	.0
9	7	8884555.2	8096144.8	9435084.7	8947060.2
9	8	14573502.7	13931066.2	14708724.5	14556578.6
9	9	18399797.5	18083314.8	18637264.9	19171409.8
9	10	19971455.9	19664927.8	20196339.8	20503085.8
9	11	20959670.8	20542769.1	20980553.3	21230872.1
9	12	21127215.7	.0	21211313.3	.0
10	7	8781069.2	8085831.4	9420292.0	8343695.3
10	8	15177675.3	14462346.6	16046477.3	14871078.6
10	9	18162854.6	17512226.9	19081511.3	18335089.6
10	10	19387231.0	18971331.5	20456717.8	18654555.2
10	11	20168124.4	19965831.5	21301109.0	21139100.0
10	12	20266456.9	.0	21305070.1	.0
11	7	6823249.3	6635369.1	6951841.0	7278106.5
11	8	13371939.3	13421405.4	13537236.1	13223192.9
11	9	16218897.0	16274887.2	16908830.6	15939353.1
11	10	17499227.1	17537695.7	18406990.2	17808191.1
11	11	18413779.5	18492600.2	19005879.0	19037196.9
11	12	18738396.5	.0	19334549.6	.0
12	7	7665133.2	4279575.4	7760236.0	6951902.8
12	8	14579103.3	11310807.4	14531157.0	13329456.2
12	9	17443582.5	14792321.9	17461886.0	16638954.1
12	10	18478830.1	17454227.3	18402858.5	17871664.1
12	11	18925417.6	18166071.0	18964244.6	18615235.6
12	12	18949131.9	.0	19144488.0	.0
13	7	7695469.4	6779168.7	.0	.0
13	8	15047449.9	13322731.7	.0	.0
13	9	18179016.2	16362876.4	.0	.0
13	10	19280899.4	17603451.7	.0	.0
13	11	20186987.4	20052206.4	.0	.0
13	12	20359259.8	.0	.0	.0

Table D-4-2. 25 MWt VIH Usable Power at 1000°K, Rectangular Aperture.

TEMPERATURE (KELVIN) = 1000.
AREA (SQ. M.) = 41.9

DAY	HOUR	ER1	ER2	ER3	ER4
1	8	[illegible]	10789989.7	.0	.0
1	9	[illegible]	17969072.3	.0	.0
1	10	[illegible]	21049013.2	.0	.0
1	11	[illegible]	22483105.3	.0	.0
1	12	[illegible]	.0	.0	.0
2	8	[illegible]	10477602.3	14012239.9	9965043.2
2	9	[illegible]	10722115.3	18644758.9	16950393.8
2	10	[illegible]	20409295.2	21170524.2	20548203.0
2	11	21839743.7	21694401.6	22130680.0	21539743.7
2	12	[illegible]	.0	22301082.7	.0
3	8	[illegible]	13098985.1	13247513.0	9365715.5
3	9	[illegible]	17575280.9	17802780.3	16119206.8
3	10	[illegible]	20567329.7	20448701.2	19569979.2
3	11	[illegible]	21772067.8	22236581.4	21105977.0
3	12	[illegible]	.0	21571083.7	.0
4	8	[illegible]	14885944.3	15009500.5	9683686.2
4	9	[illegible]	19940527.6	19075734.2	17361960.7
4	10	[illegible]	21773917.6	21234565.4	20367107.9
4	11	[illegible]	22700501.7	21965116.4	21251289.1
4	12	[illegible]	.0	22199651.9	.0
5	8	[illegible]	14256550.6	10286960.1	9770994.7
5	9	[illegible]	17346341.0	14903246.7	15969278.1
5	10	[illegible]	21250854.8	17135972.8	17365741.7
5	11	[illegible]	19910578.2	13223516.6	18597783.6
5	12	[illegible]	.0	18616014.4	.0
6	8	[illegible]	12592345.7	14821451.8	13229174.7
6	9	[illegible]	17503322.3	19469435.6	20558464.9
6	10	[illegible]	19172454.6	20951286.2	20456105.2
6	11	[illegible]	20113973.9	21736452.4	21485042.1
6	12	[illegible]	.0	21945761.7	.0
7	7	[illegible]	3647879.2	2547950.4	1465496.6
7	8	[illegible]	12884207.0	10855326.3	11601058.9
7	9	[illegible]	18090921.7	15969980.5	17242545.2
7	10	[illegible]	19683113.2	18372653.2	18940423.2
7	11	[illegible]	20582011.7	19537283.0	19937516.6
7	12	[illegible]	.0	19901601.9	.0
8	7	[illegible]	3333174.0	4710129.4	1363325.0
8	8	[illegible]	11352270.5	11931268.5	11488495.2
8	9	[illegible]	16667763.9	16318946.5	15745016.3
8	10	[illegible]	17301360.8	17572533.9	16169298.2
8	11	[illegible]	19474205.5	18655167.6	18719834.1
8	12	[illegible]	.0	19765543.2	.0
9	7	[illegible]	5720578.2	7059518.1	6571493.6
9	8	[illegible]	11555499.6	12333157.9	12181012.0
9	9	[illegible]	15707748.2	16261698.3	16795643.2
9	10	[illegible]	17259361.2	17820773.2	18127519.2
9	11	[illegible]	18167202.5	18604986.7	18555305.5
9	12	[illegible]	.0	18835746.7	.0
10	7	[illegible]	5710264.8	7044725.4	5965128.7
10	8	12502103.7	12086780.0	13670910.7	12495512.0
10	9	[illegible]	15135660.3	16705944.7	15959523.0
10	10	[illegible]	16595764.9	13081151.2	16275938.6
10	11	[illegible]	17592264.9	13925542.4	18763533.4
10	12	[illegible]	.0	18929503.5	.0
11	7	[illegible]	4259502.5	4576274.4	4902539.9
11	8	[illegible]	11045839.8	11161669.5	10647626.3
11	9	[illegible]	13999320.6	14537264.0	13563786.5
11	10	[illegible]	15162179.1	16031423.6	15432624.5
11	11	[illegible]	16117073.6	16630312.4	16661630.3
11	12	[illegible]	.0	16958763.0	.0
12	7	[illegible]	1924009.9	5384669.4	4576336.2
12	8	[illegible]	9775240.9	12155590.4	10953839.6
12	9	[illegible]	12416755.3	15056319.4	14267337.5
12	10	[illegible]	15073660.7	16027291.9	15496097.5
12	11	[illegible]	15790504.4	16598679.0	16239669.0
12	12	[illegible]	.0	16769921.4	.0
13	7	[illegible]	4403602.1	.0	.0
13	8	[illegible]	10947165.1	.0	.0
13	9	[illegible]	13957709.8	.0	.0
13	10	[illegible]	16027885.1	.0	.0
13	11	[illegible]	17676639.5	.0	.0
13	12	[illegible]	.0	.0	.0

Table D-4-3. 25 MWt VIH Usable Power at 1500°K, Rectangular Aperture.

TEMPERATURE (KELVIN) = 1500.
AREA (SQ. M.) = 41.9

DAY	HOUR	ER1	ER2	ER3	ER4
1	8	2e828950.2	1139250.4	.0	.0
1	9	7311e028.5	5914333.0	.0	.0
1	10	11596256.5	11799273.9	.0	.0
1	11	12832756.4	12932766.0	.0	.0
1	12	13121405.9	.0	.0	.0
2	8	1126875.6	426843.0	4361500.6	374303.9
2	9	8798834.1	10711776.0	8904019.6	7299e54.5
2	10	10275567.5	10752555.9	11519784.9	10897463.7
2	11	10186004.4	12047662.3	12479943.7	12189004.4
2	12	11919525.3	.0	12650343.4	.0
3	8	.0	2448245.8	7596773.7	.0
3	9	7055690.7	7924541.6	9152041.0	6468467.5
3	10	10394260.5	10915590.4	10737961.9	9919239.9
3	11	11847341.0	12091224.5	12585842.1	11455237.7
3	12	11847597.4	.0	11920344.4	.0
4	8	3778804.6	5275105.0	5358761.2	33146.9
4	9	9042533.4	9997998.3	9424994.9	7711221.4
4	10	10317842.4	13123174.3	11583826.1	10716368.6
4	11	13099404.5	13751762.4	12314377.1	11e00549.8
4	12	13360805.4	.0	12547912.6	.0
5	8	1767490.9	4405811.3	636220.8	120255.4
5	9	6851436.1	7e95e01.7	5252507.4	6313538.8
5	10	10126441.4	11600115.5	7455233.5	8215002.4
5	11	11629704.2	10259838.9	8572777.7	8947044.3
5	12	12585293.5	.0	8965275.1	.0
6	8	.0	2941e06.4	5170713.5	3578435.4
6	9	5177744.2	7852563.0	9818696.3	10907725.6
6	10	6439467.2	9521725.3	11300546.9	10805365.9
6	11	10028962.0	10463194.6	12085743.1	11434302.8
6	12	10708321.1	.0	12295022.4	.0
7	7	.0	.0	.0	.0
7	8	3060047.5	1233462.7	1204587.0	1950319.6
7	9	8440182.6	8440182.6	6219241.2	7591835.9
7	10	10097860.5	10033773.9	8721913.9	9289683.9
7	11	10909225.3	10931272.4	9836543.7	1028e777.3
7	12	11157851.9	.0	10250862.6	.0
8	7	.0	.0	.0	.0
8	8	.0	1701531.2	2280529.2	1837755.9
8	9	6832156.1	7216624.5	5668207.2	6094277.0
8	10	8566692.9	7850621.5	7871794.6	6518558.9
8	11	9e50392.7	9823466.2	9004428.3	90e9144.8
8	12	9963776.2	.0	9117803.9	.0
9	7	.0	.0	.0	.0
9	8	2547196.8	1304760.3	2682418.6	2530272.7
9	9	6271491.5	6257008.9	6610959.0	7143103.9
9	10	7948150.0	7679621.9	8170073.9	8476779.9
9	11	8e37864.4	8516467.2	8954747.4	9304566.2
9	12	9120909.8	.0	9185307.4	.0
10	7	.0	.0	.0	.0
10	8	2151269.4	2434040.7	4020171.4	2644772.7
10	9	6136842.7	5485921.0	7055205.4	6308733.7
10	10	7740825.4	6945025.6	8430411.9	6629249.3
10	11	8e.1818.4	7939525.6	9274803.1	9112794.1
10	12	8040151.0	.0	9278764.2	.0
11	7	.0	.0	.0	.0
11	8	1246672.4	1395099.5	1510930.2	1196887.0
11	9	4190391.1	4748551.3	4832524.7	3913047.2
11	10	6472921.2	5511139.8	6380684.3	5781035.2
11	11	8287477.5	6466294.3	6979573.1	7010891.0
11	12	8712092.8	.0	7309243.7	.0
12	7	.0	.0	.0	.0
12	8	0552797.4	.0	2504851.1	1302150.3
12	9	5417275.9	2766216.0	5435580.1	4e12648.2
12	10	6458274.7	5429921.4	6776052.5	5845358.2
12	11	8e99111.7	6139765.1	6937929.7	6583929.7
12	12	8422716.0	.0	7118182.1	.0
13	7	.0	.0	.0	.0
13	8	902114e.0	1396425.6	.0	.0
13	9	4452710.7	4334570.5	.0	.0
13	10	7254593.5	5577145.8	.0	.0
13	11	8160681.5	6289900.5	.0	.0
13	12	8373953.9	.0	.0	.0

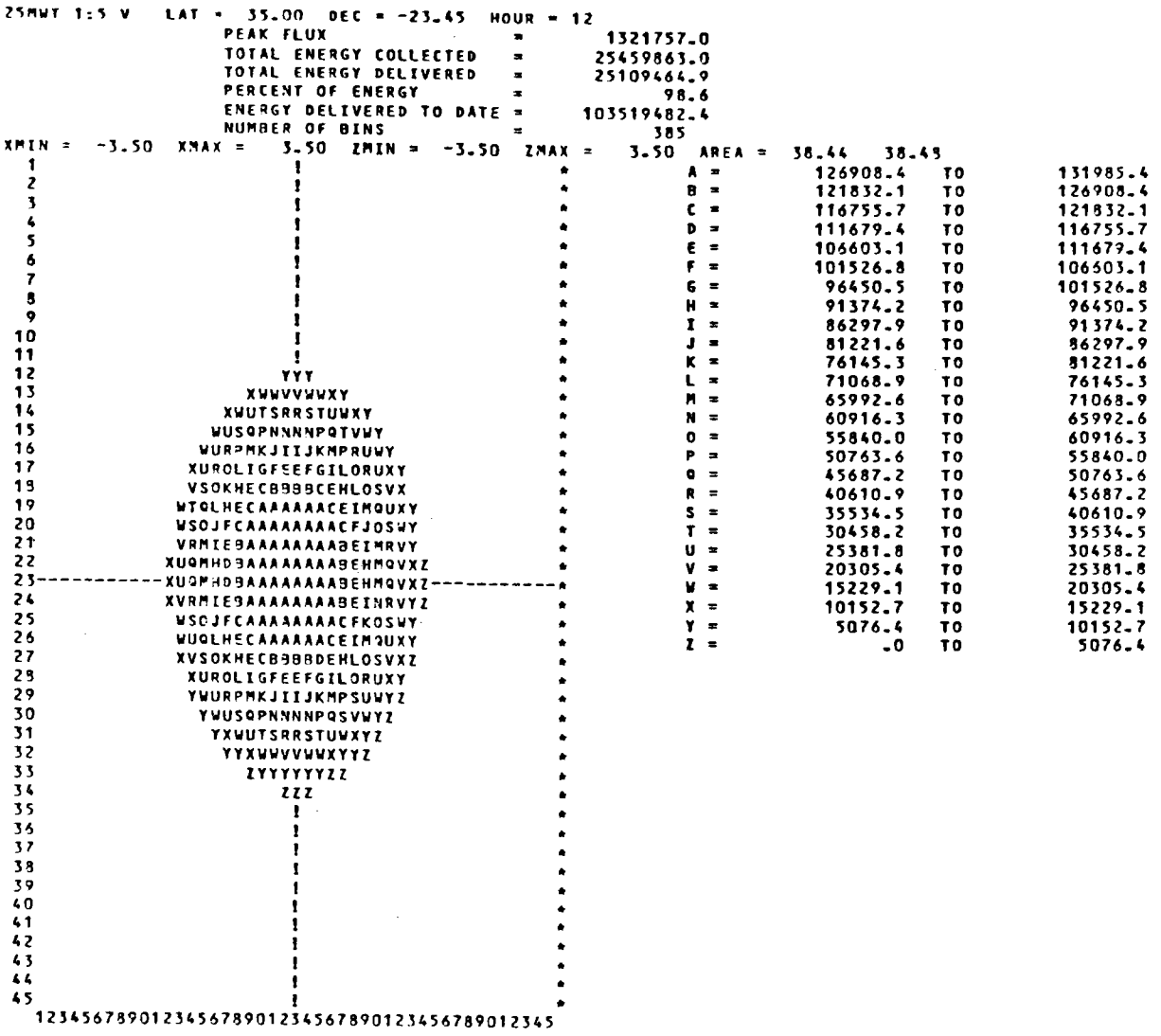

Figure D-4-4. 25 MWt VIH Design Point Round Aperture Characteristics.

Table D-4-4. 25 MWt VIH Power Through the Round Aperture.

DAY	HR	ER1	ER2	ER3	ER4
1	8	14679993.6	13139364.2	.0	.0
1	9	15308178.4	20303846.0	.0	.0
1	10	23552394.6	23384668.2	.0	.0
1	11	24869450.8	24821133.3	.0	.0
1	12	25109464.9	.0	.0	.0
2	8	13125984.2	12826591.9	16353920.9	12335051.3
2	9	18784842.5	13071727.8	20978672.2	19287664.6
2	10	22266686.6	22748087.9	23509120.2	22867776.0
2	11	24174375.9	24029279.5	24464820.4	24174375.9
2	12	23909224.3	.0	24638924.9	.0
3	8	10953435.1	15444920.7	15593164.2	11419374.1
3	9	19344979.6	19912754.2	20139819.2	18459460.3
3	10	22379026.0	22900388.2	22781979.5	21904885.6
3	11	23636077.2	24068843.2	24572549.1	23443763.8
3	12	23835371.7	.0	23907901.1	.0
4	8	15376259.6	17228882.2	17352305.5	12041717.7
4	9	21027900.3	21274816.2	21409760.9	19699306.0
4	10	22307473.8	24109836.1	23571373.2	22705339.8
4	11	25087249.4	25039680.2	24303423.6	23590689.1
4	12	25350439.6	.0	24538720.9	.0
5	8	13770722.2	16604294.7	12641344.6	12126242.3
5	9	18846267.1	19689025.2	17250004.2	18314258.3
5	10	22118407.4	23589797.1	19451340.2	20209931.4
5	11	23855938.9	22251571.2	20567126.9	20940813.2
5	12	24578979.6	.0	20963759.9	.0
6	8	7405700.9	14942451.7	17167766.1	15578197.5
6	9	15180484.2	19848077.4	21811143.3	22899484.7
6	10	18460324.5	21518332.0	23294701.9	22800203.4
6	11	22021909.6	22455485.5	24075579.9	23824519.8
6	12	22702153.4	.0	24286054.1	.0
7	7	5847687.7	6013264.8	4915195.1	3834570.9
7	8	15061599.9	15234730.6	13209183.8	13953692.8
7	9	20435997.4	20435997.4	18318216.0	19588884.8
7	10	22093292.5	22027795.7	20719170.5	21286145.6
7	11	22903978.5	22926195.2	21882894.6	22282581.2
7	12	23167743.6	.0	22251702.8	.0
8	7	6294153.8	5692780.7	7065886.6	3728438.8
8	8	10440987.4	13705867.7	14283939.0	13841874.3
8	9	18831974.1	19016183.4	18668255.5	18095131.4
8	10	20568589.3	19850475.0	19871619.9	18520185.1
8	11	21649520.6	21821873.8	21003881.7	21068515.5
8	12	21966828.4	.0	21121947.8	.0
9	7	8860993.6	8074674.0	9410063.1	8923332.8
9	8	14549276.8	13907908.3	14684273.8	14532380.8
9	9	18377970.3	18061863.1	18615156.1	19148667.3
9	10	19943535.9	19637436.4	20168105.5	20474422.6
9	11	20936415.0	20519975.8	20957274.3	21207315.4
9	12	21105177.8	.0	21189187.6	.0
10	7	8760203.2	8066617.5	9397907.1	8323868.6
10	8	15151922.3	14437807.3	16019250.2	14845845.9
10	9	18141159.4	17491308.9	19058718.7	18313188.7
10	10	19364621.6	18949207.1	20432861.2	18632800.3
10	11	20147613.6	19945526.4	21279446.0	21117601.8
10	12	20245465.9	.0	21283003.4	.0
11	7	6807805.4	6620350.4	6936106.0	7261633.1
11	8	13351877.6	13401269.5	13516926.3	13203354.3
11	9	16199693.1	16255617.1	16888809.8	15920480.2
11	10	17480358.6	17518785.7	18387142.9	17788989.4
11	11	18397845.8	18476598.3	18989432.9	19020723.7
11	12	18715462.9	.0	19310886.4	.0
12	7	7648352.9	4270206.7	7743247.6	6936683.9
12	8	14560986.6	11296752.1	14513099.9	13312892.4
12	9	17425006.0	14776568.8	17443290.0	16621234.5
12	10	18458239.1	17434778.0	18382352.1	17851749.7
12	11	18907245.7	18148628.2	18946035.4	18597361.5
12	12	18926807.6	.0	19121933.5	.0
13	7	7679191.3	6764828.8	.0	.0
13	8	15032504.1	13309499.0	.0	.0
13	9	18161954.1	16347518.9	.0	.0
13	10	19257622.8	17582200.2	.0	.0
13	11	20162856.9	20028237.0	.0	.0
13	12	20340253.7	.0	.0	.0

Table D-4-5. 25 MWt VIH Usable Power at 1000°K, Round Aperture.

TEMPERATURE (KELVIN) = 1000.
AREA (SQ. M.) = 39.7

DAY	HOUR	ER1	ER2	ER3	ER4
1	8	12497193.8	10956564.4	.0	.0
1	9	13125373.6	11121046.2	.0	.0
1	10	21786594.7	21201848.4	.0	.0
1	11	22622693.3	22639333.4	.0	.0
1	12	23136857.0	.0	.0	.0
2	8	17[illegible]84.4	10643792.1	14171121.1	10152251.5
2	9	18[illegible]43.7	12889626.0	18795872.4	17104864.8
2	10	20[illegible]04.3	20565288.1	21326320.4	20704976.2
2	11	21991576.0	21846479.7	22282020.5	21991576.0
2	12	22726424.4	.0	22456125.1	.0
3	8	9770635.3	13262120.9	13410364.4	9236574.3
3	9	17[illegible]79.3	17729954.4	17957019.4	16276650.5
3	10	20[illegible]24.2	20717588.4	20599179.7	19722095.8
3	11	21453277.4	21866043.4	22399749.3	21260963.9
3	12	21[illegible]71.9	.0	21725101.2	.0
4	8	17[illegible]59.8	15046052.4	15169505.7	9858917.9
4	9	18[illegible]44.4	18092016.4	19226361.1	17516506.2
4	10	20[illegible]73.9	21927036.2	21388573.4	20522539.9
4	11	22504449.5	22356880.4	22120623.7	21407889.2
4	12	22[illegible]39.7	.0	22355921.1	.0
5	8	11587722.4	14421494.9	10458544.8	9943442.5
5	9	13[illegible]67.7	17506235.4	15067204.4	16131458.5
5	10	19[illegible]07.6	21406997.2	17268540.4	18027131.6
5	11	21[illegible]29.2	20068771.4	18394327.1	18758013.4
5	12	23[illegible]79.9	.0	18780960.1	.0
6	8	[illegible]01.1	12759651.9	14954966.3	13395397.7
6	9	12937684.4	17665277.6	19628343.4	20715654.9
6	10	16277[illegible]7	19355532.2	21111902.1	20617403.6
6	11	19834[illegible]7	20272635.7	21892780.1	21641719.9
6	12	20516[illegible]6	.0	22103254.3	.0
7	7	[illegible]83.9	3830445.0	2732395.3	1651771.1
7	8	10[illegible]3.1	13051930.8	11026384.0	11770893.0
7	9	10[illegible]7.6	18253197.6	16135416.2	17406094.9
7	10	14[illegible]2.7	19844995.9	18536370.7	19103345.8
7	11	20[illegible]3.7	20743395.4	19700394.7	20399781.4
7	12	20[illegible]3.6	.0	20068902.9	.0
8	7	4[illegible]6.3	3509980.9	4883086.8	1545639.0
8	8	8[illegible]7.6	11523067.9	12101139.2	11659074.5
8	9	14[illegible]3.3	16833283.5	16485455.7	15912331.6
8	10	18[illegible]3.4	17667675.2	17688220.1	16337385.3
8	11	19[illegible]3.8	19639073.9	18821081.9	18885715.7
8	12	19[illegible]3.5	.0	18939147.9	.0
9	7	[illegible]81.8	5991874.2	7227263.3	6740533.0
9	8	12[illegible]7.2	11725108.5	12501474.0	12349531.0
9	9	16[illegible]2.5	15379063.3	16432356.3	16965867.4
9	10	17[illegible]6.9	17454636.6	17985305.7	18291622.7
9	11	19[illegible]5.3	19337176.0	18774474.4	19024515.5
9	12	19[illegible]7.9	.0	19006387.7	.0
10	7	[illegible]03.4	5583817.7	7215107.3	6141068.8
10	8	12[illegible]2.5	12255007.5	13836450.4	12663046.1
10	9	15[illegible]9.6	15303509.1	16875918.9	16130389.9
10	10	17[illegible]1.7	17[illegible]6407.3	19050261.4	16450000.5
10	11	17[illegible]1.7	17[illegible]2726.6	19096446.2	18934801.9
10	12	18[illegible]6.1	.0	19100203.5	.0
11	7	4[illegible]0.6	4437550.6	4753706.2	5073833.3
11	8	11[illegible]7.1	11213469.7	11334126.5	11020554.5
11	9	14[illegible]3.3	14072617.3	14706010.0	13737690.4
11	10	16[illegible]2.5	15335985.9	16274343.1	15006139.6
11	11	16[illegible]6.0	16[illegible]3798.5	16806633.0	16837923.9
11	12	17[illegible]7.1	.0	17128086.5	.0
12	7	[illegible]63.1	2287406.9	5560447.8	4753884.1
12	8	10[illegible]4.3	9111952.3	12312300.1	11130092.6
12	9	15[illegible]6.3	12597769.0	15[illegible]490.3	14438434.7
12	10	16[illegible]9.2	15231978.2	16199552.3	15468949.9
12	11	16[illegible]5.9	15965828.4	16762275.6	16414561.7
12	12	16[illegible]7.5	.0	16939133.7	.0
13	7	5[illegible]1.5	4583029.0	.0	.0
13	8	13[illegible]4.3	11134649.2	.0	.0
13	9	15[illegible]5.3	14166719.1	.0	.0
13	10	17[illegible]2.9	15339470.4	.0	.0
13	11	17[illegible]7.1	17[illegible]7.2	.0	.0
13	12	18[illegible]3.9	.0	.0	.0

Table D-4-6. 25 MWt VIH Usable Power at 1500^{o}K, Round Aperture.

TEMPERATURE (KELVIN) = 1500.
AREA (SQ. M.) = 78.5

DAY	HOUR	ER1	ER2	ER3	ER4
1	8	3629569.4	2088940.0	.0	.0
1	9	4257754.2	9253421.8	.0	.0
1	10	12501970.4	12334244.0	.0	.0
1	11	13619726.5	13770709.1	.0	.0
1	12	14055040.7	.0	.0	.0
2	8	2075560.0	1776167.7	5303496.7	1284627.1
2	9	7734413.7	2021303.6	9929248.0	8237240.4
2	10	11716262.4	11697663.7	12458696.0	11837351.8
2	11	13123751.7	12978855.3	13414396.2	13123951.7
2	12	12656500.1	.0	13588500.7	.0
3	8	.0	4394496.5	4542740.0	363949.9
3	9	8294555.4	9962330.0	9089395.0	7409036.1
3	10	11325601.9	11849964.0	11731555.3	10854461.4
3	11	12585653.7	13013419.0	13522124.9	12393339.6
3	12	12734947.5	.0	12857476.9	.0
4	8	4325375.4	6179458.0	6321881.3	991293.5
4	9	9977476.1	10224392.0	10359336.7	6648821.8
4	10	11257049.6	13059411.9	12520949.0	11654915.6
4	11	14026325.3	13959256.0	13252999.4	12540264.9
4	12	14300015.4	.0	13498296.7	.0
5	8	3720098.0	5553870.5	1590920.4	1075818.1
5	9	7755842.9	9639601.0	6199580.0	7263834.1
5	10	11067953.0	12539372.9	8400916.0	9159507.2
5	11	12806514.7	11201147.0	9516702.7	9890389.0
5	12	13526555.4	.0	9913335.7	.0
6	8	.0	3892027.5	6117341.9	4527773.3
6	9	4130060.0	8797653.2	10760719.1	11343060.5
6	10	7409900.3	10467907.8	12244277.7	11749779.2
6	11	10971455.4	11405061.3	13025155.7	12774095.6
6	12	11691709.2	.0	13275629.9	.0
7	7	.0	.0	.0	.0
7	8	4011175.7	4184306.4	2158759.6	2903268.6
7	9	8385573.2	9385573.2	7267791.8	8538460.6
7	10	11042363.3	10977371.5	9668746.3	10235721.4
7	11	11852554.3	11375771.0	10832470.4	11232157.0
7	12	12117317.4	.0	11201278.6	.0
8	7	.0	.0	.0	.0
8	8	.0	2655443.5	3233514.8	2791450.1
8	9	7781049.9	7965759.2	7617831.3	7044707.2
8	10	9518165.1	8800050.8	8821155.7	7469760.9
8	11	10599096.4	10771449.6	9953457.5	10018091.3
8	12	10916404.2	.0	10071523.6	.0
9	7	.0	.0	.0	.0
9	8	3498352.6	2357494.1	3633849.6	3481956.6
9	9	7327546.1	7011438.9	7564731.9	8098243.1
9	10	8693111.7	8587012.2	9117681.3	9423998.4
9	11	9885990.8	9469551.6	9906350.1	10156891.2
9	12	10054757.4	.0	10138763.4	.0
10	7	.0	.0	.0	.0
10	8	4101498.1	3387383.1	4968826.0	3795421.7
10	9	7090735.2	6440994.7	8008294.5	7362764.5
10	10	7314197.4	7898732.9	9382437.0	7562376.1
10	11	9097189.4	9395102.2	10229021.8	10067177.6
10	12	9195041.7	.0	10232579.2	.0
11	7	.0	.0	.0	.0
11	8	2201453.4	2350945.3	2466502.1	2152930.1
11	9	5149269.3	5205192.9	5838385.5	4370056.0
11	10	6479934.4	6469361.5	7336713.7	6738565.2
11	11	7347421.6	7426174.1	7939008.7	7970299.5
11	12	7665739.7	.0	8260462.2	.0
12	7	.0	.0	.0	.0
12	8	7510562.4	246377.9	7462675.7	2262468.2
12	9	6374591.3	7724144.6	6397965.9	5570610.3
12	10	7427914.5	6364367.8	7171927.9	6501325.5
12	11	7656621.5	7096704.0	7595611.2	7546937.3
12	12	7976033.4	.0	8071509.7	.0
13	7	.0	.0	.0	.0
13	8	3462079.9	2259074.5	.0	.0
13	9	7111523.9	5297094.7	.0	.0
13	10	8207193.1	6551776.0	.0	.0
13	11	9112132.7	5977812.5	.0	.0
13	12	9234329.5	.0	.0	.0

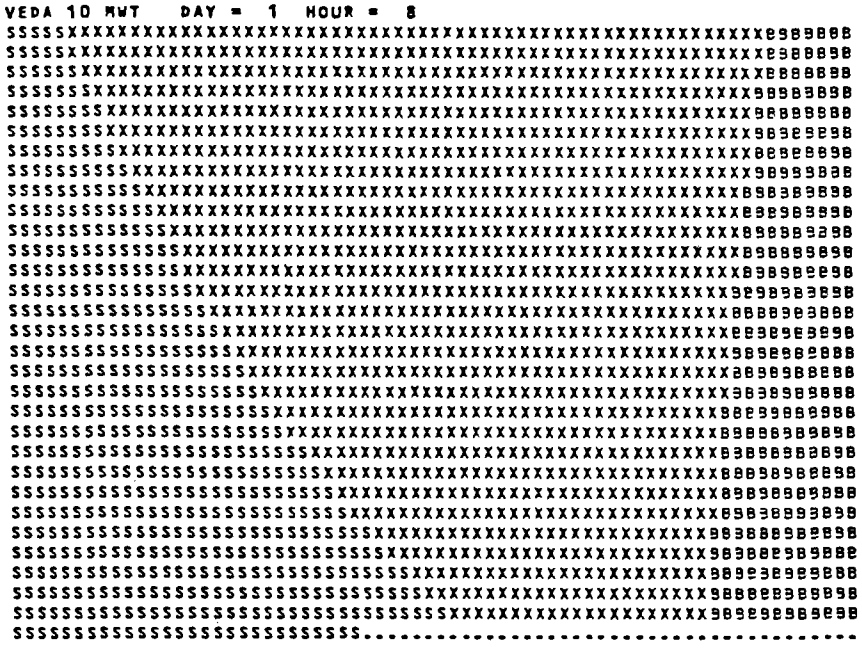

AVERAGE COSINE FACTOR = .878

WEIGHTED SHADING FACTOR = .988

WEIGHTED BLOCKING FACTOR = .948

LEGEND (.) NO SHADING, NO BLOCKING
(S) SHADING, NO BLOCKING
(B) BLOCKING, NO SHADING
(X) SHADING AND BLOCKING

Figure D-5-1. 10 MWt VIH Shading and Blocking Matrix, 0800, Winter Solstice.

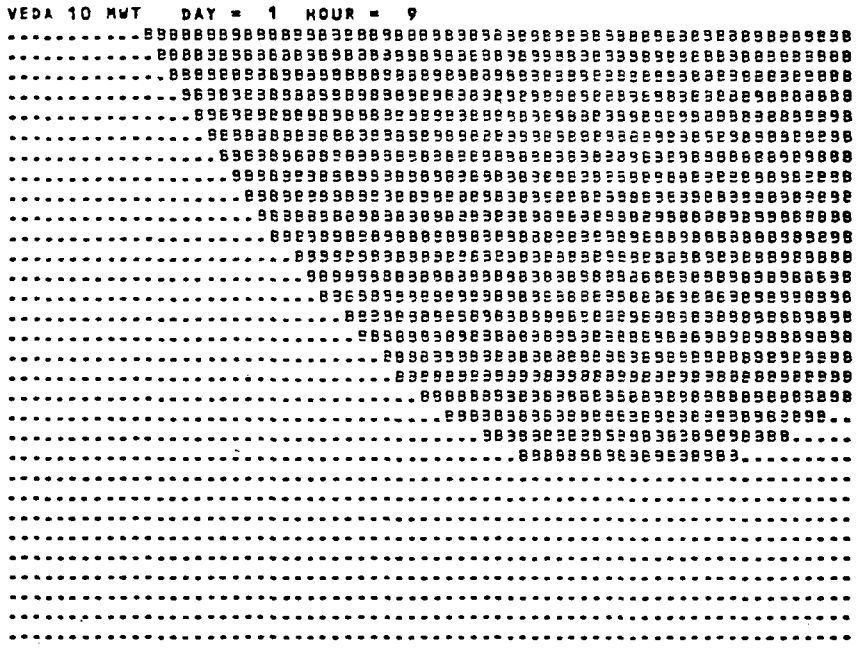

Figure D-5-2. 10 MWt VIH Shading and Blocking Matrix, 0900, Winter Solstice.

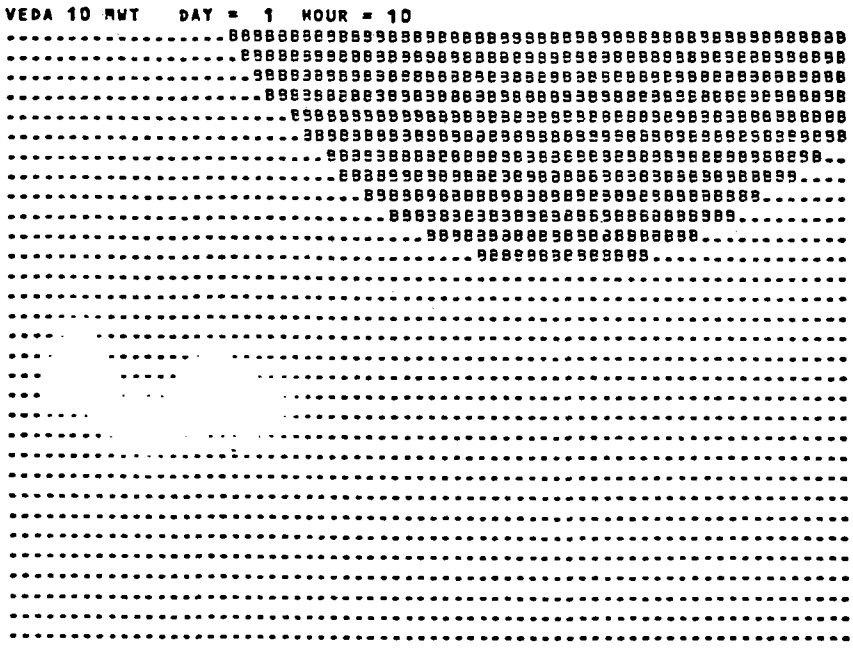

AVERAGE COSINE FACTOR = .925

WEIGHTED SHADING FACTOR = 1.000

WEIGHTED BLOCKING FACTOR = .994

LEGEND (.) NO SHADING, NO BLOCKING
(S) SHADING, NO BLOCKING
(B) BLOCKING, NO SHADING
(X) SHADING AND BLOCKING

Figure D-5-3. 10 MWt VIH Shading and Blocking Matrix, 1000, Winter Solstice.

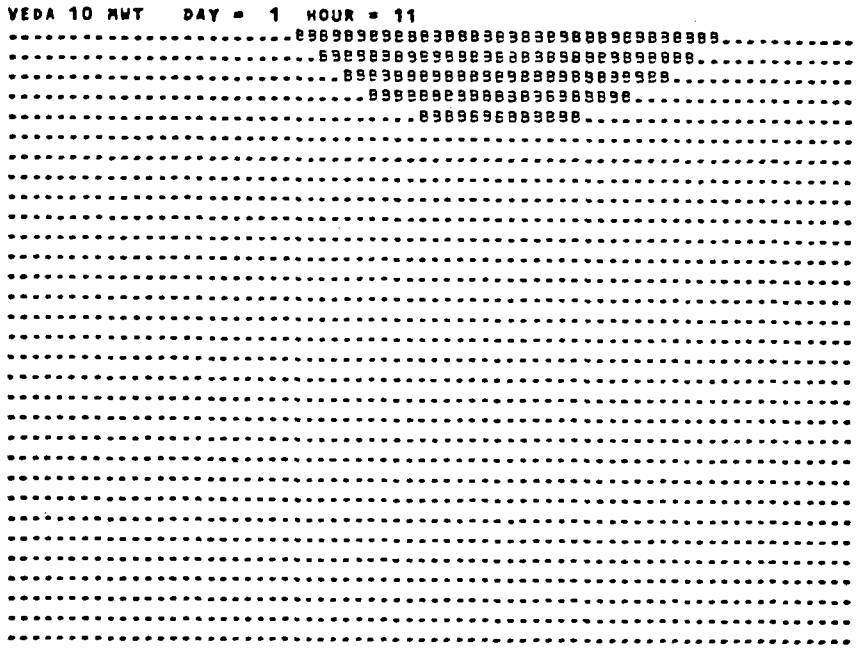

AVERAGE COSINE FACTOR = .938

WEIGHTED SHADING FACTOR = 1.000

WEIGHTED BLOCKING FACTOR = .999

LEGEND (.) NO SHADING, NO BLOCKING
(S) SHADING, NO BLOCKING
(B) BLOCKING, NO SHADING
(X) SHADING AND BLOCKING

Figure D-5-4. 10 MWt VIH Shading and Blocking Matrix, 1100, Winter Solstice.

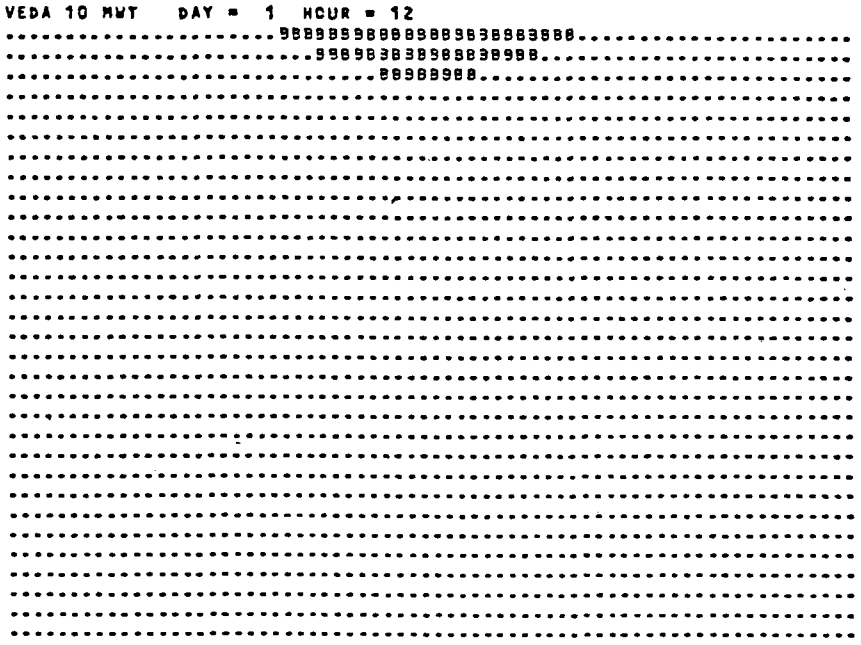

Figure D-5-5. 10 MWt VIH Shading and Blocking Matrix, 1200, Winter Solstice.

43905-80U/P0069

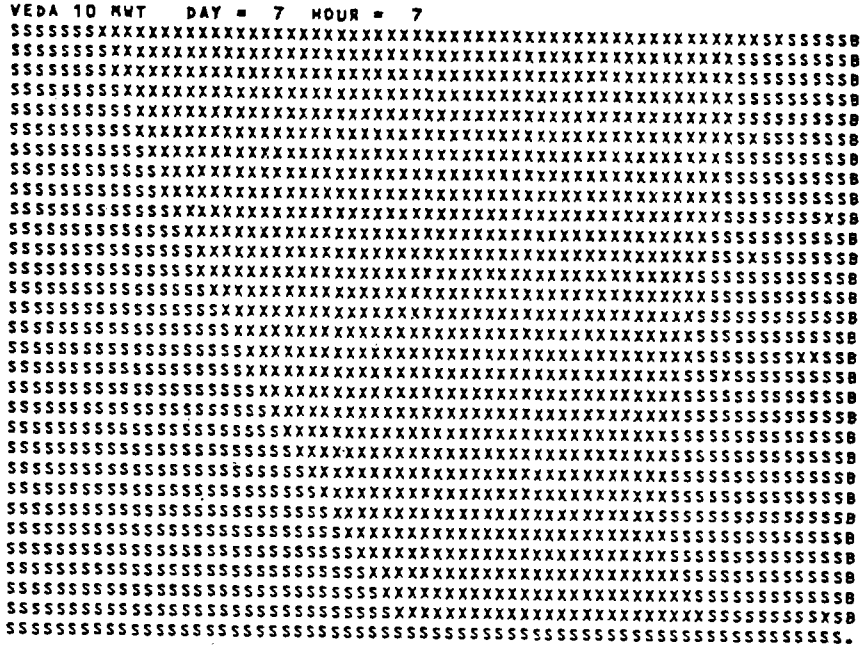

AVERAGE COSINE FACTOR = .745

WEIGHTED SHADING FACTOR = .485

WEIGHTED BLOCKING FACTOR = .994

LEGEND (.) NO SHADING, NO BLOCKING
(S) SHADING, NO BLOCKING
(B) BLOCKING, NO SHADING
(X) SHADING AND BLOCKING

Figure D-5-6. 10 MWt VIH Shading and Blocking Matrix, 0700, Equinox.

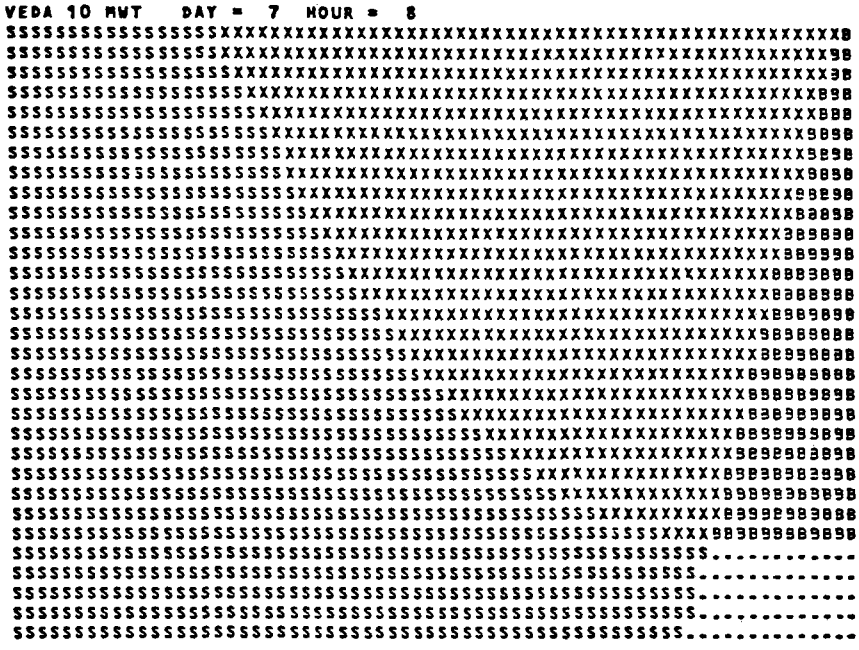

Figure D-5-7. 10 MWt VIH Shading and Blocking Matrix, 0800, Equinox.

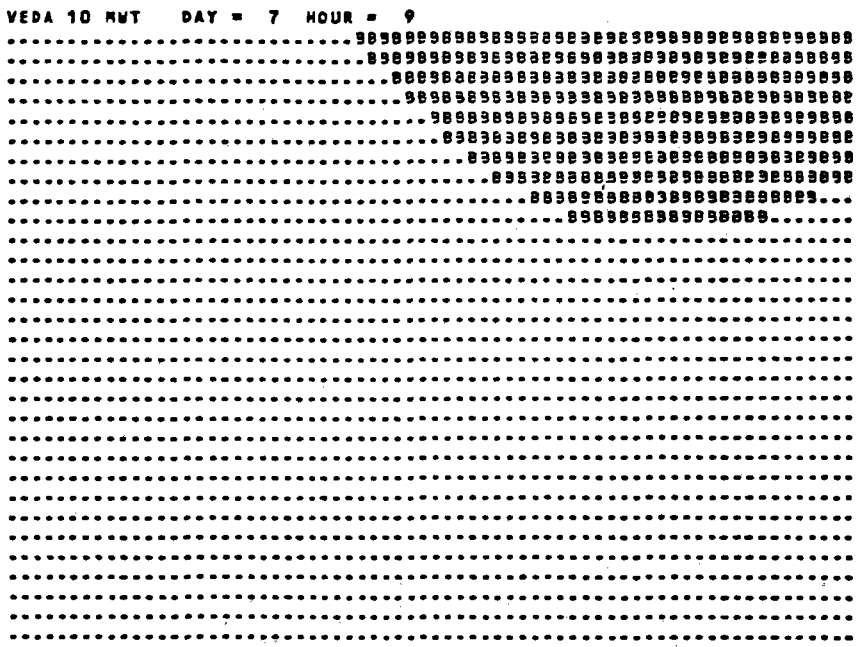

AVERAGE COSINE FACTOR = .818

WEIGHTED SHADING FACTOR = 1.000

WEIGHTED BLOCKING FACTOR = .997

LEGEND (.) NO SHADING, NO BLOCKING
(S) SHADING, NO BLOCKING
(B) BLOCKING, NO SHADING
(X) SHADING AND BLOCKING

Figure D-5-8. 10 MWt VIH Shading and Blocking Matrix, 0900, Equinox.

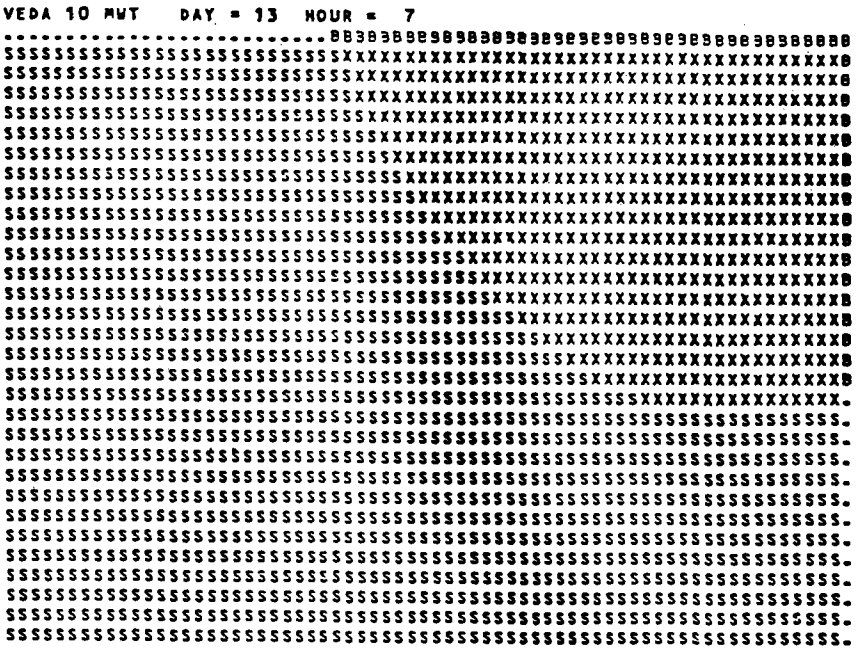

AVERAGE COSINE FACTOR = .619

WEIGHTED SHADING FACTOR = .591

WEIGHTED BLOCKING FACTOR = .991

LEGEND (.) NO SHADING, NO BLOCKING
(S) SHADING, NO BLOCKING
(B) BLOCKING, NO SHADING
(X) SHADING AND BLOCKING

Figure D-5-9. 10 MWt VIH Shading and Blocking Matrix, 0700, Summer Solstice.

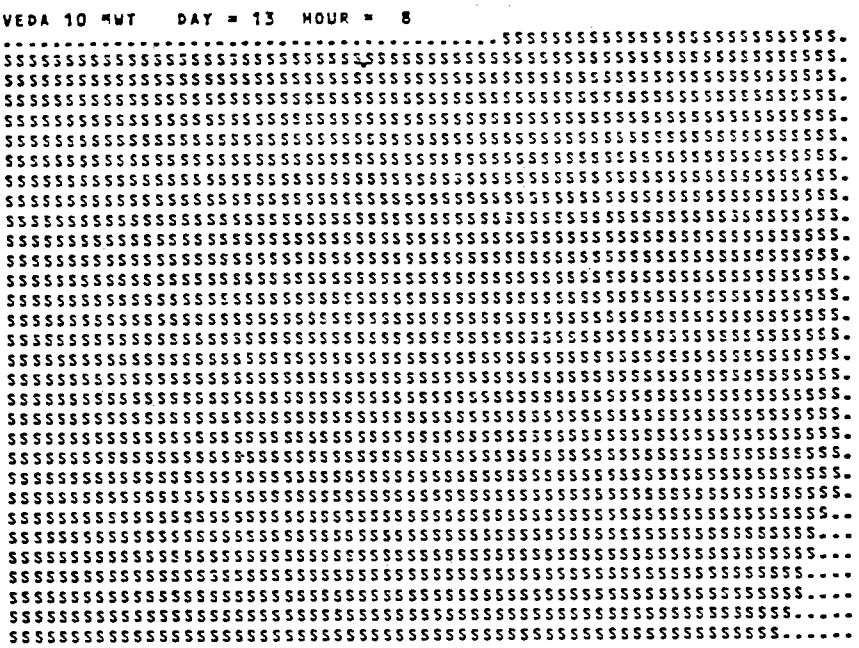

AVERAGE COSINE FACTOR = .664

WEIGHTED SHADING FACTOR = .923

WEIGHTED BLOCKING FACTOR = 1.000

LEGEND (.) NO SHADING, NO BLOCKING
(S) SHADING, NO BLOCKING
(B) BLOCKING, NO SHADING
(X) SHADING AND BLOCKING

Figure D-5-10. 10 MWt VIH Shading and Blocking Matrix, 0800, Summer Solstice.

```
     10 MWT   DAY =  7  HOUR =  7
SSSSSSSSSSSSSSSSSSSSSSSSSSS.
SSSSSSSSSSSSSSSSSSSSSSSSSSS.
SSSSSSSSSSSSSSSSSSSSSSSSSSS.
SSSSSSSSSSSSSSSSSSSSSSSSSSS.
SSSSSSSSSSSSSSSSSSSSSSSSSSS.
SSSSSSSSSSSSSSSSSSSSSSSSSSS.
SSSSSSSSSSSSSSSSSSSSSSSSSSS.
SSSSSSSSSSSSSSSSSSSSSSSSSSS.
SSSSSSSSSSSSSSSSSSSSSSSSSSS.
SSSSSSSSSSSSSSSSSSSSSSSSSSS.
```

AVERAGE COSINE FACTOR	=	.744
WEIGHTED SHADING FACTOR	=	.637
WEIGHTED BLOCKING FACTOR	=	1.000

LEGEND (.) NO SHADING, NO BLOCKING
(S) SHADING, NO BLOCKING
(B) BLOCKING, NO SHADING
(X) SHADING AND BLOCKING

Figure D-6-1. 10 MWt Repowering Heliostat Shading and Blocking Matrix, 0700, Equinox.

```
     10 MWT   DAY =  7  HOUR =  8
SSSSSSSSSSSSSSSSSSSSSS.......
SSSSSSSSSSSSSSSSSSSSSS.......
SSSSSSSSSSSSSSSSSSSSSS........
SSSSSSSSSSSSSSSSSSSSSS........
SSSSSSSSSSSSSSSSSSSSS.........
SSSSSSSSSSSSSSSSSSSSS.........
SSSSSSSSSSSSSSSSSSSSS..........
SSSSSSSSSSSSSSSSSSSSS..........
SSSSSSSSSSSSSSSSSSSSS..........
```

AVERAGE COSINE FACTOR	=	.784
WEIGHTED SHADING FACTOR	=	.947
WEIGHTED BLOCKING FACTOR	=	1.000

LEGEND (.) NO SHADING, NO BLOCKING
(S) SHADING, NO BLOCKING
(B) BLOCKING, NO SHADING
(X) SHADING AND BLOCKING

Figure D-6-2. 10 MWt Repowering Heliostat Shading and Blocking Matrix, 0800, Equinox.

```
     10 MWT   DAY = 13  HOUR =  7
SSSSSSSSSSSSSSSSSSSSSSSSSSSS.
SSSSSSSSSSSSSSSSSSSSSSSSSSSS.
SSSSSSSSSSSSSSSSSSSSSSSSSSSS.
SSSSSSSSSSSSSSSSSSSSSSSSSSSS.
SSSSSSSSSSSSSSSSSSSSSSSSSSSS.
SSSSSSSSSSSSSSSSSSSSSSSSSSSS.
SSSSSSSSSSSSSSSSSSSSSSSSSSSS.
SSSSSSSSSSSSSSSSSSSSSSSSSSSS.
SSSSSSSSSSSSSSSSSSSSSSSSSSSS.
```

AVERAGE COSINE FACTOR = .619

WEIGHTED SHADING FACTOR = .372

WEIGHTED BLOCKING FACTOR = 1.000

LEGEND (.) NO SHADING, NO BLOCKING
(S) SHADING, NO BLOCKING
(B) BLOCKING, NO SHADING
(X) SHADING AND BLOCKING

Figure D-6-3. 10 MWt Repowering Heliostat Shading and Blocking Matrix, 0700, Summer Solstice.

```
     10 MWT   DAY = 13  HOUR =  8
..........................SSSSS.
SSSSSSSSSSSSSSSSSSSSSSSSSSSS.
SSSSSSSSSSSSSSSSSSSSSSSSSSSS.
SSSSSSSSSSSSSSSSSSSSSSSSSSSS.
SSSSSSSSSSSSSSSSSSSSSSSSSSSS.
SSSSSSSSSSSSSSSSSSSSSSSSSSSS.
SSSSSSSSSSSSSSSSSSSSSSSSSSSS.
SSSSSSSSSSSSSSSSSSSSSSSSSSSS.
SSSSSSSSSSSSSSSSSSSSSSSSSSSS.
SSSSSSSSSSSSSSSSSSSSSSSSSSSS..
```

AVERAGE COSINE FACTOR = .664

WEIGHTED SHADING FACTOR = .884

WEIGHTED BLOCKING FACTOR = 1.000

LEGEND (.) NO SHADING, NO BLOCKING
(S) SHADING, NO BLOCKING
(B) BLOCKING, NO SHADING
(X) SHADING AND BLOCKING

Figure D-6-4. 10 MWt Repowering Heliostat Shading and Blocking Matrix, 0800, Summer Solstice.

APPENDIX E

ANNUAL ENERGY SUMMARY TABLES

INDEX

INTRODUCTION

The levelized charge methodology establishes a fixed price per unit of product output for the life span of the project. Entering into the calculation of the levelized charge are capital recovery rate, cost of money, internal rate of return, operating and maintenance expenses, escalation, and tax structure applicable to the energy supplier. The methodology applies to the entire energy supply part of the business.

This study does not directly address the tax structure, since each possible user of this method of solar energy collection may be affected differently from other users. The effect is equivalent to a condition where tax benefits and costs resolve to a net zero charge in the energy cost factor in the operation of the business. Any actual business would need to apply its own operating conditions to the analysis. A G&A factor equal to 50% of direct labor included in the O&M cost structure in this study is expected to absorb the tax effects not addressed directly.

The methodology of ERDA-JPL 1012-76/3, Reference 4-2, assumes that the cost of money is equal to the internal rate of return, and that any retained capital surplus earns at the same rate. Thus, the excess of levelized charge income over expenses during the early years of a project earns at the internal rate of return, thereby contributing to the defrayment of the expenses incurred in excess of the levelized charge in the later years.

The levelized charge per unit of output product varies inversely with total product output. The ratio of capital to O&M costs, when associated with cost of money and escalation, affects the levelized charge in such a way that the levelized charge may decrease as the cost of money increases. This effect

is due to the concept that excess of earnings over expenses earns at the cost of money. This effect can be seen in some of the examples in this Appendix.

The levelized annual charge used in the calculations of unit levelized charges shown in the tables of this Appendix are summarized, from the main body of the report, in Table E-0. Values are in 1000's of dollars which must be earned each year.

Table E-0. Annualized Levelized Charge Summary.

		Annualized Charge 1000's 1980 Dollars			
		UHA SYSTEMS			
COST OF MONEY	ESCALATION RATE	1 MWt VIH	10 MWt VIH	10 MWt Repowering	25 MWt VIH
8%	6%	346.68	2357.05	2163.16	6439.09
	8%	418.78	2512.23	2316.46	6685.82
	10%	521.97	2734.27	2535.76	7038.83
10%	6%	356.98	2715.49	2487.08	7685.57
	8%	417.33	2845.39	2547.36	7892.08
	10%	502.10	3027.89	2701.54	8182.25
15%	6%	400.57	3749.26	3429.11	11301.48
	8%	440.26	3834.64	3513.47	11437.29
	10%	493.42	3939.07	3626.50	11619.33

ARRANGEMENT OF THE TABLES

Each table is arranged in two segments. The upper part of the table lists the annual energy available from the UHA-heliostat-aperture combination, shown in the the title line, as a function of temperature. Since a scaled stairstep for the range of values encountered would be unreadable, the numerical

value of energy is tabulated in the first column and the condition for which this value occurs is identified by an -X- in the appropriate condition column. The condition column continues to the lower portion of the table unless the lower part of the column is otherwise identified. The cost of usable energy is then shown as a matrix in the lower part of the table. It should be noted that the design point apertures were sized such that the annual energy lost due to spillage was approximately 2%. For the other aperture sizes chosen, spillage was allowed to increase in favor of high temperature capability. Thus, for some of the smaller apertures studied, spillage was in excess of 50%.

Tables E-1 through E-8 describe cost of usable energy in terms of dollars per kilowatt hour thermal for design point receiver apertures. Tables E-9 through E-16 express the same data in terms of dollars per million BTU.

In the main body of the report, the optimum aperture as a function of temperature is used as a basis for the efficiency and cost curves. Tables E-17 through E-30 evaluate cost of usable energy for specific apertures, other than design point apertures, over a range of temperatures for each of the UHA-heliostat combinations investigated.

Table E-1., Annual Energy Summary: 1 MWt VIH, 1.85m^2 Round Aperture.

KWHt	DIRECTED TOWARD APERTURE	ENTERING APERTURE	RECOVERABLE AFTER RERADIATION LOSSES AT T°k				
			1000	1250	1500	1750	2000
2 467 082	X						
2 384 708		X					
2 026 262			X				
1 517 137				X			
684 458					X		
NA						X	
NA							X
COST OF RECOVERABLE ENERGY - $/KWHt							
COST OF MONEY	ESCALATION RATE						
8%	6%	0.145	0.171	0.229	0.507		
	8%	0.176	0.207	0.276	0.612		
	10%	0.219	0.258	0.344	0.763		
10%	6%	0.150	0.176	0.235	0.522		
	8%	0.175	0.206	0.275	0.610		
	10%	0.211	0.248	0.331	0.734		
15	6%	0.168	0.198	0.264	0.585		
	8%	0.185	0.217	0.290	0.643		
	10%	0.207	0.244	0.325	0.721		

Table E-2. Annual Energy Summary: 1 MWt VIH, 2.1m^2 Rectangular Aperture.

KWHt	DIRECTED TOWARD APERTURE	ENTERING APERTURE	RECOVERABLE AFTER RERADIATION LOSSES AT T°k				
			1000	1250	1500	1750	2000
2 467 082	X						
2 379 283		X					
1 983 104			X				
1 424 988				X			
534 667					X		
NA						X	
NA							X
COST OF RECOVERABLE ENERGY - $/KWHt							
COST OF MONEY	ESCALATION RATE						
8%	6%	0.146	0.175	0.243	0.648		
	8%	0.176	0.211	0.294	0.783		
	10%	0.219	0.263	0.366	0.976		
10%	6%	0.150	0.180	0.251	0.668		
	8%	0.175	0.210	0.293	0.781		
	10%	0.211	0.253	0.352	0.939		
15%	6%	0.168	0.202	0.281	0.749		
	8%	0.185	0.222	0.309	0.823		
	10%	0.207	0.249	0.346	0.923		

Table E-3. .Annual Energy Summary: 10 MWt VIH, 16.9m^2 Round Aperture.

KWHt	DIRECTED TOWARD APERTURE	ENTERING APERTURE	RECOVERABLE AFTER RERADIATION LOSSES AT T°k				
			1000	1250	1500	1750	2000
24 209 839	X						
23 812 229		X					
20 680 535			X				
16 201 481				X			
8 703 467					X		
434 453						X	
NA							X
COST OF RECOVERABLE ENERGY - $/KWHt							
COST OF MONEY	ESCALATION RATE						
8%	6%	0.099	0.114	0.145	0.271	5.425	
	8%	0.106	0.121	0.155	0.289	5.783	
	10%	0.115	0.132	0.169	0.314	6.294	
10%	6%	0.119	0.138	0.176	0.327	6.549	
	8%	0.114	0.131	0.168	0.312	6.250	
	10%	0.127	0.146	0.187	0.348	6.969	
15%	6%	0.157	0.181	0.231	0.431	8.630	
	8%	0.161	0.185	0.237	0.441	8.826	
	10%	0.165	0.190	0.243	0.453	9.067	

Table E-4. Annual Energy Summary: 10 MWt VIH, 18m^2 Rectangular Aperture.

KWHt	DIRECTED TOWARD APERTURE	ENTERING APERTURE	RECOVERABLE AFTER RERADIATION LOSSES AT T°k				
			1000	1250	1500	1750	2000
24 209 839	X						
23 741 744		X					
20 345 932			X				
15 503 263				X			
7 484 097					X		
56 817						X	
NA							X
COST OF RECOVERABLE ENERGY - $/KWHt							
COST OF MONEY	ESCALATION RATE						
8%	6%	0.099	0.116	0.152	0.315	41.485	
	8%	0.106	0.123	0.162	0.336	44.216	
	10%	0.115	0.134	0.176	0.365	48.124	
10%	6%	0.114	0.133	0.175	0.363	47.794	
	8%	0.120	0.140	0.184	0.380	50.080	
	10%	0.128	0.149	0.195	0.405	53.292	
15%	6%	0.158	0.184	0.242	0.501	65.988	
	8%	0.162	0.188	0.247	0.512	67.491	
	10%	0.166	0.194	0.254	0.526	69.329	

43905-80U/P0069

Table E-5. Annual Energy Summary: 10 MWt Repowering, 21.27m^2 Round Aperture.

KWHt	DIRECTED TOWARD APERTURE	ENTERING APERTURE	RECOVERABLE AFTER RERADIATION LOSSES AT T°k				
			1000	1250	1500	1750	2000
24 814 556	X						
23 640 926		X					
19 645 774			X				
14 150 229				X			
5 157 369					X		
NA						X	
NA							X
COST OF RECOVERABLE ENERGY - $/KWHt							
COST OF MONEY	ESCALATION RATE						
8%	6%	0.092	0.110	0.153	0.419		
	8%	0.098	0.118	0.164	0.449		
	10%	0.107	0.129	0.179	0.492		
10%	6%	0.105	0.127	0.176	0.482		
	8%	0.108	0.130	0.180	0.494		
	10%	0.114	0.138	0.191	0.524		
15%	6%	0.145	0.175	0.242	0.665		
	8%	0.149	0.179	0.248	0.681		
	10%	0.153	0.185	0.256	0.703		

Table E-6. Annual Energy Summary: 10 MWt Repowering, 20.97m^2 Rectangular Aperture.

KWHt	DIRECTED TOWARD APERTURE	ENTERING APERTURE	RECOVERABLE AFTER RERADIATION LOSSES AT T°k				
			1000	1250	1500	1750	2000
24 814 556	X						
23 400 598		X					
19 443 052			X				
13 995 507				X			
5 093 890					X		
NA						X	
NA							X
COST OF RECOVERABLE ENERGY - $/KWHt							
COST OF MONEY	ESCALATION RATE						
8%	6%	0.092	0.111	0.155	0.425		
	8%	0.099	0.119	0.166	0.455		
	10%	0.108	0.130	0.181	0.498		
10%	6%	0.106	0.128	0.178	0.488		
	8%	0.109	0.131	0.182	0.500		
	10%	0.115	0.139	0.193	0.530		
15%	6%	0.147	0.176	0.245	0.673		
	8%	0.150	0.181	0.251	0.690		
	10%	0.155	0.187	0.259	0.712		

Table E-7.. **Annual Energy Summary:** 25 MWt VIH, 38.5m^2 Round Aperture.

KWHt	DIRECTED TOWARD APERTURE	ENTERING APERTURE	RECOVERABLE AFTER RERADIATION LOSSES AT T°k				
			1000	1250	1500	1750	2000
60 198 778	X						
59 429 218		X					
52 165 951			X				
41 759 444				X			
24 168 463					X		
2 591 779						X	
NA							X
COST OF RECOVERABLE ENERGY - $/KWHt							
COST OF MONEY	ESCALATION RATE						
8%	6%	0.108	0.123	0.154	0.266	2.484	
	8%	0.113	0.128	0.160	0.277	2.580	
	10%	0.118	0.135	0.169	0.291	2.716	
10%	6%	0.129	0.147	0.184	0.318	2.965	
	8%	0.133	0.151	0.189	0.327	3.045	
	10%	0.138	0.157	0.196	0.339	3.157	
15%	6%	0.190	0.217	0.271	0.468	4.361	
	8%	0.192	0.219	0.274	0.473	4.413	
	10%	0.196	0.223	0.278	0.481	4.483	

Table E-8. Annual Energy Summary: 25 MWt VIH, 42m^2 Rectangular Aperture.

KWHt	DIRECTED TOWARD APERTURE	ENTERING APERTURE	RECOVERABLE AFTER RERADIATION LOSSES AT T°k				
			1000	1250	1500	1750	2000
60 198 778	X						
59 517 621		X					
51 612 923			X				
40 308 510				X			
21 410 078					X		
967 991						X	
NA							X
COST OF RECOVERABLE ENERGY - $/KWHt							
COST OF MONEY	ESCALATION RATE						
8%	6%	0.108	0.125	0.160	0.301	6.652	
	8%	0.112	0.130	0.166	0.312	6.907	
	10%	0.118	0.136	0.175	0.329	7.272	
10%	6%	0.129	0.149	0.191	0.359	7.940	
	8%	0.133	0.153	0.196	0.369	8.153	
	10%	0.137	0.159	0.203	0.382	8.453	
15%	6%	0.190	0.219	0.280	0.528	11.675	
	8%	0.192	0.222	0.284	0.534	11.815	
	10%	0.195	0.225	0.288	0.543	12.004	

Table E-9. Annual Energy Summary: 1 MWt VIH, 2.1m^2 Rectangular Aperture.

x10^6 BTU	DIRECTED TOWARD APERTURE	ENTERING APERTURE	RECOVERABLE AFTER RERADIATION LOSSES AT T°k				
			1000	1250	1500	1750	2000
8 432	X						
8 130		X					
6 776.3			X				
4 869.2				X			
1 827.0					X		
NA						X	
NA							X
COST OF RECOVERABLE ENERGY - $/10^{6}BTU							
COST OF MONEY	ESCALATION RATE						
8%	6%	42.64	51.16	71.20	189.75		
	8%	51.51	61.80	86.01	229.22		
	10%	64.20	77.03	107.20	285.70		
10%	6%	43.91	52.68	73.31	195.39		
	8%	51.33	61.59	85.71	228.42		
	10%	61.76	74.10	103.12	274.82		
15%	6%	49.27	59.11	82.27	219.25		
	8%	54.15	64.97	90.42	240.97		
	10%	60.69	72.82	101.33	270.07		

Table E-10. Annual Energy Summary: 1 MWt VIH, 1.85m^2 Round Aperture.

x10^6 BTU	DIRECTED TOWARD APERTURE	ENTERING APERTURE	RECOVERABLE AFTER RERADIATION LOSSES AT T°k				
			1000	1250	1500	1750	2000
8 432	X						
8 148.6		X					
6 923.7			X				
5 184.1				X			
2 338.8					X		
0.76						X	
NA							X
COST OF RECOVERABLE ENERGY - $/10^{6}BTU							
COST OF MONEY	ESCALATION RATE						
8%	6%	42.54	50.07	66.87	148.23	456157.9	
	8%	51.39	60.49	80.78	179.06	551026.3	
	10%	64.06	75.39	100.69	223.18	686802.6	
10%	6%	43.81	51.56	68.86	152.63	469710.5	
	8%	51.21	60.28	80.50	178.44	549118.4	
	10%	61.62	72.52	96.85	214.68	660657.9	
15%	6%	49.16	57.85	77.27	171.27	527065.8	
	8%	54.03	63.59	84.93	188.24	579289.5	
	10%	60.55	71.27	95.18	210.97	649236.8	

Table E-11. Annual Energy Summary: 10 MWt VIH, $18m^2$ Rectangular Aperture.

$x10^6$ BTU	DIRECTED TOWARD APERTURE	ENTERING APERTURE	RECOVERABLE AFTER RERADIATION LOSSES AT T°k				
			1000	1250	1500	1750	2000
82 725	X						
81 808.9		X					
69 522			X				
52 974.7				X			
25 573.2					X		
194.14						X	
NA							X
COST OF RECOVERABLE ENERGY - $/10^6BTU							
COST OF MONEY	ESCALATION RATE						
8%	6%	28.81	33.90	44.52	92.17	12141.0	
	8%	30.71	36.14	47.45	98.24	12940.3	
	10%	33.42	39.33	51.64	106.92	14084.0	
10%	6%	33.19	39.06	51.29	106.18	13987.3	
	8%	34.78	40.93	53.74	111.26	14656.4	
	10%	37.01	43.55	57.19	118.40	15596.4	
15%	6%	45.83	53.93	70.81	146.61	19312.2	
	8%	46.87	55.16	72.42	149.95	19751.9	
	10%	48.15	56.66	74.40	154.03	20289.8	

Table E-12. • Annual Energy Summary: 10 MWt VIH, 16.9m^2 Round Aperture.

x10^6 BTU	DIRECTED TOWARD APERTURE	ENTERING APERTURE	RECOVERABLE AFTER RERADIATION LOSSES AT T°k				
			1000	1250	1500	1750	2000
82 725	X						
81 366.4		X					
70 665.4			X				
55 360.25				X			
29 739.8					X		
1 484.5						X	
·NA							X

COST OF RECOVERABLE ENERGY - $/10^{6}BTU							
COST OF MONEY	ESCALATION RATE						
8%	6%	28.97	33.36	42.58	79.26	1587.8	
	8%	30.88	35.55	45.38	84.47	1692.3	
	10%	33.60	38.69	49.39	91.94	1841.9	
10%	6%	33.37	38.43	49.05	91.31	1829.2	
	8%	34.97	40.27	51.40	95.68	1916.7	
	10%	37.21	42.85	54.69	101.81	2039.7	
15%	6%	46.08	53.06	67.72	126.07	2525.6	
	8%	47.13	54.26	69.27	128.94	2583.1	
	10%	48.41	55.74	71.15	132.45	2653.5	

Table E-13. Annual Energy Summary: 10 MWt Repowering, 21.27m^2 Round Aperture.

$x10^6$ BTU	DIRECTED TOWARD APERTURE	ENTERING APERTURE	RECOVERABLE AFTER RERADIATION LOSSES AT T°k				
			1000	1250	1500	1750	2000
84 791	X						
80 781		X					
67 130			X				
48 351				X			
17 635					X		
NA						X	
NA							X
COST OF RECOVERABLE ENERGY - $/$10^6$BTU							
COST OF MONEY	ESCALATION RATE						
8%	6%	26.78	32.22	44.74	126.66		
	8%	28.68	34.51	47.91	131.36		
	10%	31.39	37.77	52.44	143.79		
10%	6%	30.79	37.05	51.44	141.03		
	8%	31.53	37.95	52.68	144.45		
	10%	33.44	40.24	55.87	153.19		
15%	6%	42.45	51.08	70.92	194.45		
	8%	43.49	52.34	72.67	199.23		
	10%	44.89	54.02	75.00	205.64		

Table E-14. Annual Energy Summary: 10 MWt Repowering, 20.99m² Rectangular Aperture.

$x10^6$ BTU	DIRECTED TOWARD APERTURE	ENTERING APERTURE	RECOVERABLE AFTER RERADIATION LOSSES AT T°k				
			1000	1250	1500	1750	2000
84 791	X						
79 959.8		X					
66 437			X				
47 823				X			
17 406					X		
NA						X	
NA							X
COST OF RECOVERABLE ENERGY - $/10^6BTU							
COST OF MONEY	ESCALATION RATE						
8%	6%	27.05	32.56	45.23	124.28		
	8%	28.97	34.87	48.44	133.08		
	10%	31.71	38.17	53.02	145.68		
10%	6%	31.10	37.44	52.01	142.89		
	8%	31.86	38.34	53.27	146.35		
	10%	33.79	40.66	56.49	155.21		
15%	6%	42.89	51.61	71.70	197.01		
	8%	43.94	52.88	73.47	201.85		
	10%	45.35	54.59	75.83	208.35		

Table E-15. Annual Energy Summary: 25 MWt VIH, 42m^2 Rectangular Aperture.

x10^6 BTU	DIRECTED TOWARD APERTURE	ENTERING APERTURE	RECOVERABLE AFTER RERADIATION LOSSES AT T°k				
			1000	1250	1500	1750	2000
205 699	X						
203 372		X					
176 361			X				
137 734				X			
73 158					X		
3 308						X	
NA							X
COST OF RECOVERABLE ENERGY - $/10^{6}BTU							
COST OF MONEY	ESCALATION RATE						
8%	6%	31.66	36.51	46.75	88.02	1946.5	
	8%	32.87	37.91	48.54	91.39	2021.1	
	10%	34.61	39.91	51.10	96.21	2127.8	
10%	6%	37.79	43.58	55.80	105.05	2323.3	
	8%	38.81	44.75	57.30	107.88	2385.8	
	10%	40.23	46.39	59.41	111.84	2473.5	
15%	6%	55.57	64.08	82.05	154.48	3416.4	
	8%	56.24	64.85	83.04	156.34	3457.5	
	10%	57.13	65.88	84.36	158.83	3512.5	

Table E-16. Annual Energy Summary: 25 MWt VIH, 38.5m^2 Round Aperture.

x10^6 BTU	DIRECTED TOWARD APERTURE	ENTERING APERTURE	RECOVERABLE AFTER RERADIATION LOSSES AT T°k				
			1000	1250	1500	1750	2000
205 699	X						
203 069.6		X					
178 251			X				
142 692				X			
82 584					X		
8 856						X	
NA							X
COST OF RECOVERABLE ENERGY - $/10^{6}BTU							
COST OF MONEY	ESCALATION RATE						
8%	6%	31.71	36.12	45.13	77.97	727.09	
	8%	32.92	37.51	46.85	80.96	754.95	
	10%	34.66	39.49	49.33	85.23	794.81	
10%	6%	37.85	43.12	53.86	93.06	867.84	
	8%	38.86	44.28	55.31	95.56	891.16	
	10%	40.29	45.90	57.34	99.08	923.92	
15%	6%	55.65	63.40	79.20	136.85	1276.1	
	8%	56.32	64.16	80.15	138.49	1291.5	
	10%	57.22	65.19	81.43	140.70	1312.0	

Table E-17. Annual Energy Summary: 1 MWt VIH, 0.37m^2 Round Aperture.

x10^6 BTU	DIRECTED TOWARD APERTURE	ENTERING APERTURE	RECOVERABLE AFTER RERADIATION LOSSES AT T°k				
			1000	1250	1500	1750	2000
8 432	X						
3 663		X					
3 405			X				
3 034				X			
2 375					X		
1 384						X	
248							X
COST OF RECOVERABLE ENERGY - $/10^{6}BTU							
COST OF MONEY	ESCALATION RATE						
8%	6%	94.64	101.81	114.26	145.97	250.49	1397.90
	8%	114.33	122.99	138.03	176.33	302.59	1688.63
	10%	142.50	153.30	172.04	219.78	377.15	2104.72
10%	6%	97.46	104.84	117.66	150.31	257.93	1439.44
	8%	113.93	122.56	137.55	175.72	301.54	1682.78
	10%	137.07	147.46	165.49	211.41	362.79	2024.60
15%	6%	109.36	117.64	132.03	168.66	289.43	1615.20
	8%	120.19	129.30	145.11	185.37	318.11	1775.24
	10%	134.70	144.91	162.63	207.76	356.52	1989.60

Table E-18. Annual Energy Summary: 1 MWt VIH, 0.42m^2 Rectangular Aperture.

x10^6 BTU	DIRECTED TOWARD APERTURE	ENTERING APERTURE	RECOVERABLE AFTER RERADIATION LOSSES AT T°k				
			1000	1250	1500	1750	2000
8 432	X						
3 918		X					
3 660			X				
3 288				X			
2 627					X		
1 629						X	
404							X
COST OF RECOVERABLE ENERGY - $/10^{6}BTU							
COST OF MONEY	ESCALATION RATE						
8%	6%	88.48	94.72	105.44	131.97	212.82	858.12
	8%	106.89	114.42	127.37	159.41	257.08	1036.58
	10%	133.22	142.61	158.75	198.69	320.42	1292.00
10%	6%	91.11	97.54	108.57	135.89	219.14	883.61
	8%	106.52	114.02	126.93	158.86	256.19	1033.00
	10%	128.15	137.19	152.71	191.13	308.23	1242.82
15%	6%	102.24	109.45	121.83	152.48	245.90	991.51
	8%	112.37	120.29	133.90	167.59	270.26	1089.75
	10%	125.94	134.81	150.07	187.83	302.90	1221.34

Table E-19. Annual Energy Summary: 10 MWt VIH, 3.7m^2 Round Aperture.

x10^6 BTU	DIRECTED TOWARD APERTURE	ENTERING APERTURE	RECOVERABLE AFTER RERADIATION LOSSES AT T°k				
			1000	1250	1500	1750	2000
82 725	X						
36 902		X					
34 774			X				
31 708				X			
26 169					X		
17 574						X	
6 122							X
COST OF RECOVERABLE ENERGY - $/10^{6}BTU							
COST OF MONEY	ESCALATION RATE						
8%	6%	63.87	67.78	74.34	90.07	134.12	385.01
	8%	68.08	72.24	79.23	96.00	142.95	410.36
	10%	74.10	78.63	86.23	104.49	155.59	446.63
10%	6%	73.59	78.09	85.64	103.77	154.52	443.56
	8%	77.11	81.83	89.74	108.73	161.91	464.78
	10%	82.05	87.07	95.49	115.71	172.29	494.59
15%	6%	101.60	107.82	118.24	143.27	213.34	612.42
	8%	103.91	110.27	120.94	146.53	218.20	626.37
	10%	106.74	113.28	124.23	150.52	224.14	643.43

Table E-20. Annual Energy Summary: 10 MWt VIH, 6.1m^2 Round Aperture.

x10^6 BTU	DIRECTED TOWARD APERTURE	ENTERING APERTURE	RECOVERABLE AFTER RERADIATION LOSSES AT T°k				
			1000	1250	1500	1750	2000
82 725	X						
54 625		X					
50 950			X				
45 654				X			
36 133					X		
21 659						X	
3 975							X
COST OF RECOVERABLE ENERGY - $/10^{6}BTU							
COST OF MONEY	ESCALATION RATE						
8%	6%	43.15	46.26	51.63	65.23	108.83	592.97
	8%	45.99	49.31	55.03	69.53	115.99	632.01
	10%	50.06	53.67	59.89	75.67	126.24	687.87
10%	6%	49.71	53.30	59.48	75.15	125.37	683.14
	8%	52.09	55.85	62.33	78.75	131.37	715.82
	10%	55.43	59.43	66.32	83.80	139.80	761.73
15%	6%	68.64	73.59	82.12	103.76	173.10	943.21
	8%	70.20	75.26	83.99	106.13	177.05	964.69
	10%	72.11	77.31	86.28	109.02	181.87	990.96

Table E-21. Annual Energy Summary: 10 MWt VIH, 7.2m^2 Round Aperture.

x10^6 BTU	DIRECTED TOWARD APERTURE	ENTERING APERTURE	RECOVERABLE AFTER RERADIATION LOSSES AT T°k				
			1000	1250	1500	1750	2000
82 725	X						
60 539		X					
55 898			X				
49 208				X			
37 261					X		
19 363						X	
1 138							X
COST OF RECOVERABLE ENERGY - $/10^{6}BTU							
COST OF MONEY	ESCALATION RATE						
8%	6%	38.93	42.17	47.90	63.26	121.73	2071.22
	8%	41.50	44.94	51.05	67.42	129.74	2207.58
	10%	45.17	48.92	55.57	73.38	141.21	2402.70
10%	6%	44.86	48.58	55.18	72.88	140.24	2386.20
	8%	47.00	50.90	57.82	76.36	146.95	2500.34
	10%	50.02	54.17	61.53	81.26	156.38	2660.71
15%	6%	61.93	67.07	76.19	100.62	193.63	3294.60
	8%	63.34	68.60	77.93	102.91	198.04	3369.63
	10%	65.07	70.47	80.05	105.72	203.43	3461.40

Table E-22. Annual Energy Summary: 10 MWt VIH, 8.9m^2 Round Aperture.

x10^6 BTU	DIRECTED TOWARD APERTURE	ENTERING APERTURE	RECOVERABLE AFTER RERADIATION LOSSES AT T°k				
			1000	1250	1500	1750	2000
82 725	X						
68 296		X					
62 623			X				
54 446				X			
39 966					X		
18 506						X	
203							X
COST OF RECOVERABLE ENERGY - $/10^{6}BTU							
COST OF MONEY	ESCALATION RATE						
8%	6%	34.51	37.64	43.29	58.98	127.37	
	8%	36.78	40.12	46.14	62.86	135.75	
	10%	40.04	43.66	50.22	68.41	147.75	
10%	6%	39.76	43.36	49.87	67.95	146.74	
	8%	41.66	45.44	52.26	71.20	153.75	
	10%	44.33	48.35	55.61	75.76	163.62	
15%	6%	54.90	59.87	68.86	93.81	202.60	
	8%	56.15	61.23	70.43	95.95	207.21	
	10%	57.68	62.90	72.35	98.56	212.85	

Table E-23. Annual Energy Summary: 10 MWt VIH, 12.1m^2 Round Aperture.

$x10^6$ BTU	DIRECTED TOWARD APERTURE	ENTERING APERTURE	RECOVERABLE AFTER RERADIATION LOSSES AT T°k				
			1000	1250	1500	1750	2000
82 725	X						
76 690		X					
69 761			X				
57 363				X			
37 687					X		
10 283						X	
NA							X
COST OF RECOVERABLE ENERGY - $/10^{6}BTU							
COST OF MONEY	ESCALATION RATE						
8%	6%	30.73	33.79	41.09	62.54	229.22	
	8%	32.76	36.01	43.80	66.66	244.31	
	10%	35.65	39.19	47.67	72.55	265.90	
10%	6%	35.41	38.93	47.34	72.05	264.08	
	8%	37.10	40.79	49.60	75.50	276.71	
	10%	39.48	43.40	52.78	80.34	294.46	
15%	6%	48.89	53.74	65.36	99.48	364.61	
	8%	50.00	54.97	66.85	101.75	372.91	
	10%	51.36	56.47	68.67	104.52	383.07	

Table E-24. •Annual Energy Summary: 10 MWt VIH, 12.1m^2 Rectangular Aperture.

x10^6 BTU	DIRECTED TOWARD APERTURE	ENTERING APERTURE	RECOVERABLE AFTER RERADIATION LOSSES AT T°k				
			1000	1250	1500	1750	2000
82 725	X						
75 362		X					
67 832			X				
56 619				X			
37 255					X		
10 260						X	
NA							X

COST OF RECOVERABLE ENERGY - $/10^6 BTU							
COST OF MONEY	ESCALATION RATE						
8%	6%	31.28	34.75	41.63	63.27	229.73	
	8%	33.34	37.04	44.37	67.43	244.86	
	10%	36.28	40.31	48.29	73.39	266.50	
10%	6%	36.03	40.03	47.96	72.89	264.67	
	8%	37.76	41.95	50.26	76.38	277.33	
	10%	40.18	44.64	53.48	81.27	295.12	
15%	6%	49.75	55.27	66.22	100.64	365.42	
	8%	50.88	56.53	67.73	102.93	373.75	
	10%	52.27	58.07	69.57	105.73	383.92	

Table E-25. Annual Energy Summary: 10 MWt Repowering, 10.98m^2 Rectangular Aperture.

x10^6 BTU	DIRECTED TOWARD APERTURE	ENTERING APERTURE	RECOVERABLE AFTER RERADIATION LOSSES AT T°k				
			1000	1250	1500	1750	2000
84 791	X						
60 718		X					
53 630			X				
43 670				X			
26 883					X		
4 905						X	
NA							X
COST OF RECOVERABLE ENERGY - $/10^{6}BTU							
COST OF MONEY	ESCALATION RATE						
8%	6%	35.63	40.33	49.53	80.47	441.01	
	8%	38.15	43.19	53.04	86.17	472.27	
	10%	41.76	47.28	58.07	94.33	516.97	
10%	6%	40.96	46.37	56.95	92.51	507.05	
	8%	41.95	47.50	58.33	94.76	519.34	
	10%	44.49	50.37	61.86	100.49	550.77	
15%	6%	56.48	63.94	78.52	127.56	699.10	
	8%	57.87	65.51	80.46	130.69	716.30	
	10%	59.73	67.62	83.04	134.90	739.35	

Table E-26. Annual Energy Summary: 10 MWt Repowering, 7.19m^2 Rectangular Aperture.

$x10^6$ BTU	DIRECTED TOWARD APERTURE	ENTERING APERTURE	RECOVERABLE AFTER RERADIATION LOSSES AT T°k				
			1000	1250	1500	1750	2000
84 791	X						
45 741		X					
41 099			X				
34 539				X			
23 411					X		
7 270						X	
NA							X
COST OF RECOVERABLE ENERGY - $/$10^6$BTU							
COST OF MONEY	ESCALATION RATE						
8%	6%	47.29	52.63	62.63	92.40	297.55	
	8%	50.64	56.36	67.07	98.95	318.63	
	10%	55.44	61.70	73.42	108.31	348.80	
10%	6%	54.37	60.51	72.01	106.24	342.10	
	8%	55.69	61.98	73.75	108.81	350.39	
	10%	59.06	65.73	78.22	115.40	371.60	
15%	6%	74.97	83.44	99.28	146.47	471.68	
	8%	76.81	85.49	101.72	150.08	483.28	
	10%	79.28	88.24	105.00	154.91	498.83	

Table E.27. Annual Energy Summary: 10 MWt Repowering, 11.28m^2 Round Aperture.

x10^6 BTU	DIRECTED TOWARD APERTURE	ENTERING APERTURE	RECOVERABLE AFTER RERADIATION LOSSES AT T°k				
			1000	1250	1500	1750	2000
84 791	X						
63 644		X					
56 360			X				
46 102				X			
28 797					X		
5 775						X	
NA							X
COST OF RECOVERABLE ENERGY - $/10^{6}BTU							
COST OF MONEY	ESCALATION RATE						
8%	6%	33.99	38.38	46.92	75.12	374.57	
	8%	36.40	41.10	50.25	80.44	401.12	
	10%	39.84	44.99	55.00	88.06	439.09	
10%	6%	39.08	44.13	53.95	86.37	430.66	
	8%	40.03	45.20	55.25	88.46	441.10	
	10%	42.45	47.93	58.60	93.81	467.80	
15%	6%	53.88	60.84	74.38	119.08	593.79	
	8%	55.21	62.34	76.21	122.01	608.39	
	10%	56.98	64.35	78.66	125.93	627.97	

veda

43905-80U/P0069

Table E-28. Annual Energy Summary: 10 MWt Repowering, 8.09 Round Aperture.

$x10^6$ BTU	DIRECTED TOWARD APERTURE	ENTERING APERTURE	RECOVERABLE AFTER RERADIATION LOSSES AT T°k				
			1000	1250	1500	1750	2000
84 791	X						
51 240		X					
46 082			X				
38 774				X			
26 376					X		
8 373						X	
NA							X
COST OF RECOVERABLE ENERGY - $/10^6BTU							
COST OF MONEY	ESCALATION RATE						
8%	6%	42.22	46.94	55.79	82.01	258.35	
	8%	45.21	50.27	59.74	87.82	276.66	
	10%	49.49	55.03	65.40	96.14	302.85	
10%	6%	48.54	53.97	64.14	94.29	297.04	
	8%	49.71	55.28	65.70	96.58	304.24	
	10%	52.72	58.62	69.67	102.42	322.65	
15%	6%	66.92	74.41	88.44	130.01	409.54	
	8%	68.57	76.24	90.61	133.21	419.62	
	10%	70.77	78.70	93.53	137.49	433.12	

Table E-29. Annual Energy Summary: 25 MWt VIH, 16.9m^2 Round Aperture.

$x10^6$ BTU	DIRECTED TOWARD APERTURE	ENTERING APERTURE	RECOVERABLE AFTER RERADIATION LOSSES AT T°k				
			1000	1250	1500	1750	2000
205 699	X						
151 257		X					
140 556			X				
125 132				X			
97 460					X		
55 605						X	
7 358							X
COST OF RECOVERABLE ENERGY - $/$10^6$BTU							
COST OF MONEY	ESCALATION RATE						
8%	6%	42.57	45.81	51.46	66.07	115.80	875.11
	8%	44.20	47.57	53.43	68.60	120.24	908.65
	10%	46.54	50.08	56.25	72.22	126.59	956.62
10%	6%	50.81	54.68	61.42	78.86	138.22	1044.52
	8%	52.18	56.15	63.07	80.98	141.93	1072.58
	10%	54.10	58.21	65.39	83.95	147.15	1112.02
15%	6%	74.72	80.41	90.32	115.96	203.25	1535.94
	8%	75.61	81.37	91.40	117.35	205.69	1554.40
	10%	76.82	82.67	92.86	119.22	209.96	1579.14

Table E-30. Annual Energy Summary: 25 MWt VIH, 26.1m^2 Round Aperture.

x10^6 BTU	DIRECTED TOWARD APERTURE	ENTERING APERTURE	RECOVERABLE AFTER RERADIATION LOSSES AT T°k				
			1000	1250	1500	1750	2000
205 699	X						
187 568		X					
170 550			X				
146 035				X			
103 022					X		
40 355						X	
NA							X
COST OF RECOVERABLE ENERGY - $/10^{6}BTU							
COST OF MONEY	ESCALATION RATE						
8%	6%	34.33	37.75	44.09	62.50	159.56	
	8%	35.64	39.20	45.78	64.90	165.68	
	10%	37.53	41.27	48.20	68.32	174.42	
10%	6%	40.97	45.06	52.63	74.60	190.45	
	8%	42.08	46.27	54.04	76.61	195.57	
	10%	43.62	47.98	56.03	79.42	202.76	
15%	6%	60.25	66.26	77.39	109.70	280.05	
	8%	60.98	67.06	78.32	111.02	283.42	
	10%	61.95	68.13	79.57	112.78	287.93	

☆ U.S. GOVERNMENT PRINTING OFFICE: 1980-740-145/1167

UNITED STATES DEPARTMENT OF ENERGY
P.O. BOX 62
OAK RIDGE, TENNESSEE 37830

OFFICIAL BUSINESS
PENALTY FOR PRIVATE USE $300

POSTAGE AND FEES PAID
UNITED STATES
DEPARTMENT OF ENERGY

FS- 1

SANDIA LABORATORIES
ATTN A. C. SKINROOD
DIVISION 8452
LIVERMORE, CA 94550